ROLES OF A NUCLEAR HORMONE RECEPTOR DURING *C. ELEGANS* GERMLINE DEVELOPMENT

DISSERTATION

A thesis submitted for the degree of
Doctor rerum naturalium
(Dr. rer. nat.)

Max-Planck Institute
of Cell Biology and Genetics (MPI-CBG)
International Max-Planck Research School
&
Faculty of Mathematics and Natural Sciences
Technical University Dresden

XICOTENCATL GRACIDA CANALES
Born on 31st of October 1983 in Acapulco, Mexico

1.Reviewer: Prof. Dr. Günter Vollmer
2.Reviewer: Prof. Dr. Marek Jindra

Date of submission: 24th of October 2011
Date of defense: 7th of February 2012

"*Quien que no busca, no encuentra*"
Mexican saying

ABSTRACT

Two fundamental problems of developmental biology are the understanding of cell fate specification, and the integration of broader environmental contexts into developmental programs. While cell fate specification is largely achieved by differential gene expression programs, environmental integration relies on cellular receptors. A predominant mechanism to mediate both processes utilizes nuclear hormone receptors (NHRs). However, it remains unclear how diverse the NHR's modes of action are in regulating gene expression. This thesis utilizes the development of the *C. elegans* germ line as a model system to study a novel link that integrates cell fate specification and the nutritional environment. In *C. elegans*, germ cell fate specification is chiefly controlled by posttranscriptional mechanisms. Furthermore, overall germline development is influenced by the animal's nutritional status. However, it remains unknown whether germline posttranscriptional control mechanisms and germ cell fate decisions are linked to nutrition, and if so, how this link may operate in molecular terms.

This thesis reports the characterization of the nuclear hormone receptor *nhr-114* and its crucial functions for germline development and fertility. Depending on the tissue of expression, *nhr-114* regulates overall germline organization, germ cell proliferation and oogenesis. Importantly, all aspects of *nhr-114* function are linked to diet. Feeding *nhr-114* mutants with a specific *E. coli* strain, or a tryptophan-supplemented diet significantly reduces germline development defects and sterility. Based on mutant analysis, *nhr-114* was found to have overlapping functions with *gld-4* cytoplasmic poly(A) polymerase (cytoPAP). This thesis provides evidence that *nhr-114* may function in germ cells in a posttranscriptional manner linked to *gld-4* cytoPAP. Further evidence shows that NHR-114 interacts with GLD-4 cytoPAP. Together these findings suggest that NHR-114 may control gene expression by transcriptional and posttranscriptional mechanisms in a tissue-specific manner. This thesis proposes that NHR-114 ensures the input of tryptophan to allow germline development; and that this function integrates nutritional information into the germline gene expression programs according to the environment of the worm. Therefore, NHR-114 potentially provides a direct molecular link to how a developmental program is coordinated with the nutritional status of an animal.

CONTENTS

1. INTRODUCTION

1.1 CONTROL OF GENE EXPRESSION

A fundamental problem of developmental biology is to understand how cell fates are specified and maintained. Cell fate specification and further differentiation generates cellular diversity that enables multicelullarity and ensures the continuity of life from one generation to next (Gilbert S. 2006). All information to specify a single cell or a multicellular organism is contained in the DNA. Although all cells in an organism contain the same DNA, different cell types accumulate different sets of RNAs and proteins that allow them to establish distinct cell fates (Alberts et al. 2008). This differences in gene expression result from many regulatory steps in the pathway from DNA to RNA to protein (Figure 1.1).

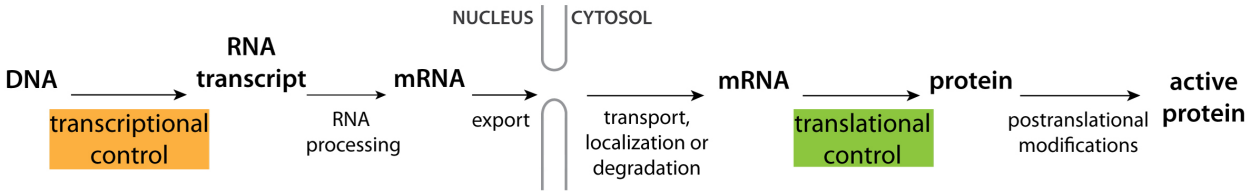

Figure 1.1 Flow of genetic information in eukaryotes
Diagram depicts the flow of genetic information from DNA to RNA to protein. DNA is transcribed into RNA in the nucleus, where the RNA transcript is spliced or processed. Selective export of mRNAs is also regulated. Cytoplasmic mRNAs can be transported and localized to specific compartments, or degraded before they are translated. Translational control refers to the selective translation of mRNAs. Proteins are also targets of regulatory mechanisms; they can be degraded, or covalently modified (posttranslational modifications) before an active protein is produced. Diagram modified from Alberts et al. 2002.

Transcriptional control modulates when and how often a gene is expressed and ensures that no superfluous intermediates are produced. Therefore, it constitutes the principal regulatory mode of gene expression for most genes (Alberts et al. 2008). However, not all mRNAs that reach the cytoplasm are immediately translated, some are degraded, or silenced and localized to specific cellular compartments before their translation (Alberts et al. 2008). Also, during some developmental processes, such as oogenesis and early embryogenesis, different cell fates are specified even when transcription is often absent or little detected (Kuersten and Goodwin, 2003). These differences in gene expression are regulated by posttranscriptional mechanisms that target the mRNA (Figure 1.2). This thesis focuses on a mechanism that influences the translation of specific mRNAs to establish cell fates.

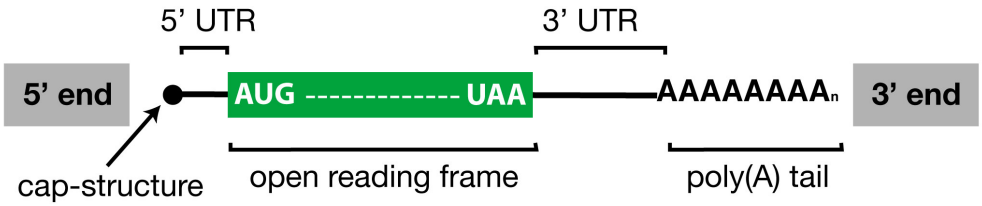

Figure 1.2 Structural elements of an mRNA
Scheme of eukaryotic mRNA containing the structural elements required for translation. The 5' end contains a modified guanine residue (m7GpppN) that prevents mRNA degradation, thus serves as a cap (cap-structure). The sequence within the cap-structure and the initiation codon (AUG) is referred as the 5'UTR (untranslated region). The open reading frame is the coding region and it is defined by initiation codon and the stop codon (UAA). The sequence within the stop codon and the poly (A) tail is referred to the 3'UTR. The poly(A) tails is a stretch of adenine (A) residues of variable length.

1.1.2 TRANSLATIONAL CONTROL OF GENE EXPRESSION

Proteins are essential for life; they catalyze most of the biochemical reactions, and in addition they serve as structural or regulatory components (Mathews et al. 2007; Alberts et al. 2008). Protein synthesis is a biosynthetic step that uses extensive cellular machinery, which consumes large amounts of energetic and nutritional resources. Therefore, protein synthesis is tightly regulated and monitored, and the mechanisms that regulate protein synthesis are collectively referred as translational control. The central concept of translational control is that gene expression is regulated on the basis of the translation efficiency of specific mRNAs. Since translation occurs at final steps of the genetic flow and does not invoke nuclear pathways, translation control offers rapid responses in gene expression changes. Translational control mechanisms regulate protein synthesis in global or selective ways. Global mechanisms affect protein synthesis generically by altering general components of the protein synthesis machinery, thus they affect mRNAs in a non-specific manner (section 1.1.2.2). Selective mechanisms, in contrast, affect the translation of specific mRNAs by exploiting the differential sensitivity of subsets of mRNAs (Mathews et al. 2007).

The process of protein synthesis is divided in three phases: initiation, elongation and termination. Although all three phases are targeted by regulatory mechanisms, translation initiation is the rate-limiting step in protein synthesis, thus it is much more tightly regulated than the elongation and termination phases (Mathews et al. 2007). In fact, most of translational control mechanisms target translation initiation by using *trans*-acting proteins or RNA-binding proteins (RBP), and *cis*-acting structural elements in the mRNA to affect the translational machinery. Two classes of mRNA *cis*-regulatory elements are distinguished: those that interact with the translation machinery, and those that interact with *trans*-acting factors, such as microRNAs or RBPs. On the one hand, the 5' UTR mainly contains elements that interact with the translation machinery. On the other hand, the regulatory elements in the 3' UTR bind *trans*-acting factors that determine mRNA stability, localization and translation initiation (Mathews et al. 2007). Since the 3' UTR can confer spatial and temporal mRNA regulation, translational control through the 3'UTR is highly employed during development (Kuersten et al. 2003, Mathews et al. 2007).

1.1.2.1 Control of translation initiation

Translation initiation involves a series of steps that lead to the positioning of an elongation-competent ribosome (80S) at the initiation codon (AUG) (summarized in Gebauer and Hentze, 2004). The small ribosomal subunit 40S binds translation initiation factors and tRNA-Met to form a 43S pre-initiation complex that associates with the mRNA 5' cap-structure. This 43S complex scans along the 5' UTR until it identifies the initiation codon, to which the tRNA-Met binds to form a stable 48S initiation complex. Subsequently, the hydrolysis of eIF2-bound GTP in the 48S initiation complex allows the joining of the 60S ribosomal subunit to form an elongation-competent ribosome (Figure 1.3) (Gebauer and Hentze, 2004).

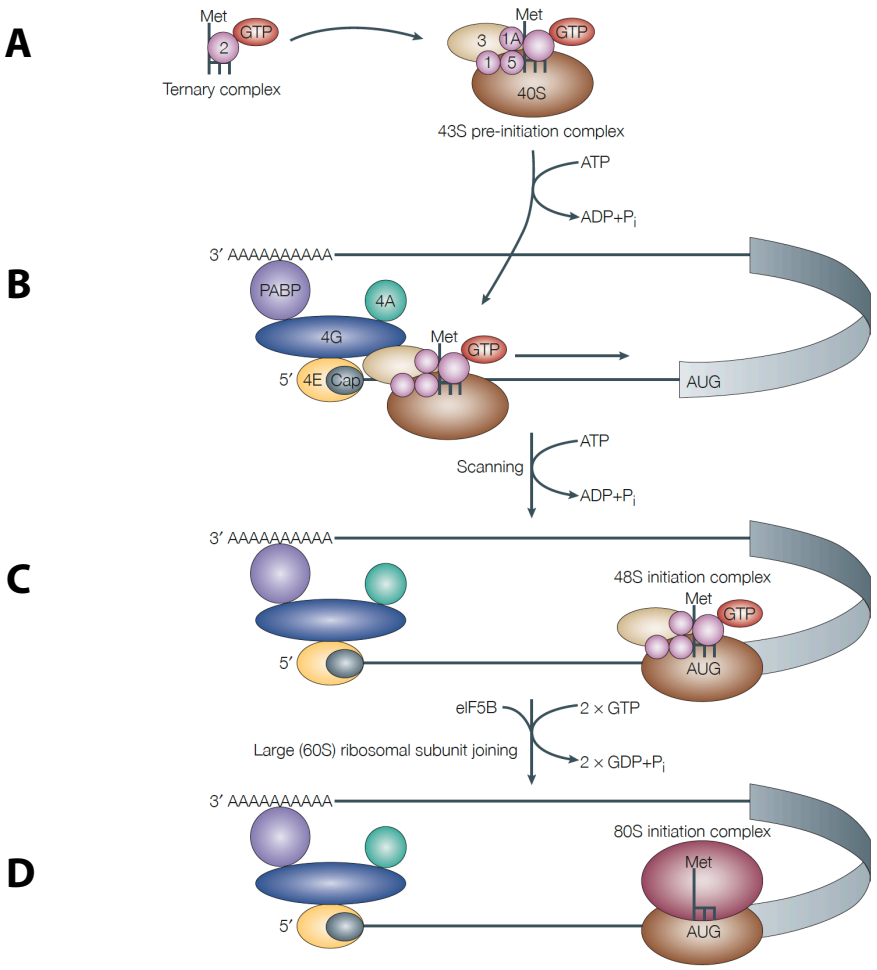

Figure 1.3 Regulation cap-mediated translation initiation
Translation initiation involves a series of steps that lead to the positioning of an elongation-competent ribosome (80S) at an initiation codon (AUG). **A)** The methionine-loaded initiator tRNA (tRNA-Met) binds GTP-coupled initiation factor 2 (eIF2). The small ribosomal subunit 40S binds eIF3, eIF1, eIF1A, eIF5, and the initiator tRNA to form the 43S pre-initiation complex. **B)** The 43S complex recognizes the mRNA 5' end through eIF3, which directly binds eIF4G subunit of the cap-binding complex. The cap-binding complex, in addition, contains eIF4E, which interacts with the 5' cap and eIF4G. The contact of eIF4G and the PABP is thought to circularize the mRNA. **C)** In an ATP-requiring step, the 43S pre-initiation complex moves along the 5'UTR until it identifies the initiation codon, to which the tRNA-Met binds to form a stable 48S initiation complex. This scanning step is assisted by eIF1 and eIF1A. **D)** After tRNA-Met and AUG form base pairs, eIF5B catalyzes the hydrolysis of eIF2-bound GTP, which is a prerequisite for the joining of the 60S ribosomal subunit, releasing most of the initiation factors from the 48S subunit. **E)** The elongation-competent 80S complex is formed. Cartoon was taken from Gebauer and Hentze, 2004.

1.1.2.2 GLOBAL CONTROL OF PROTEIN SYNTHESIS

Mechanisms that control global proteins synthesis generally involve changes in the phosphorylation status of initiation factors or their regulators (summarized in Gebauer and Hentze, 2004). Two well-known examples are the eIF2-alfa kinases and eIF4E-binding proteins, which are introduced in this section. Translation initiation requires continuous recruitment of eIF2-bound GTP (GTP-eIF2) to the initiator tRNA. As mentioned above, when the 43S pre-initiation complex recognizes the AUG initiation codon, this GTP is hydrolyzed and eIF2-bound GDP is produced. Exchange of GDP for GTP is catalyzed by eIF2B, a guanine exchange factor (GEF). Therefore, active translation initiation requires eIF2B to reconstitute functional initiator tRNAs. eIF2 is a trimeric complex composed of the alfa, beta, gamma subunits. Phosphorylation of the alfa subunit (Ser51) increases IF2's affinity for eIF2B, thus reducing their dissociation rate. Therefore, this phosphorylation blocks the GTP-exchange reaction catalyzed by eIF2B and as a consequence global mRNA translation is inhibited (Figure 4A) (Gebauer and Hentze, 2004; Proud 2007).

Different cellular conditions activate specific kinases that phosphorylate eIF2 at Ser51, thus decreasing global translation initiation (Dever and Hinnebusch, 2005, Dey et al. 2005). For example, haem depletion, the presence of viral dsRNA, and endoplasmic reticulum stress activate an eIF2-alfa kinases: HRI, PKR and PERK, respectively (De Haro et al. 1996; Gebauer and Hentze, 2004). GCN2 kinase (general control non-derepressible 2) is an eIF2-alfa kinase activated by amino acid starvation (Kimball and Jefferson, 2000, Dever and Hinnebusch, 2005). Under full nutritional conditions, specific aminoacyl-tRNA synthetases load amino acids residues into corresponding tRNAs. During amino acid starvation, in contrast, unloaded tRNAs accumulate and activate GCN2 kinase, which phosphorylates eIF2-alfa subunit, thus global translation is blocked (Figure 1.5) (Kimball and Jefferson, 2000, Dever et al. 2005).

A second mechanism to regulate general translation rates involves limiting the availability of the cap-binding protein eIF4E (summarized in Gebauer and Hentze, 2004). eIF4G interacts with eIF4E, and both are part of the cap-binding complex that mediates translation initiation. eIF4E-binding proteins (4E-BPs) share domain similarity to eIF4G, thus can bind eIF4E. Hypo-phosphorylated 4E-BPs have more affinity for eIF4E than eIF4G. This competitive displacement of eIF4G inhibits the association of the 43S complex and represses translation. A contrary example is insulin signaling, which promotes protein translation by triggering 4E-BPs hyper-phosphorylation (Figure 1.4B) (Gebauer and Hentze, 2004).

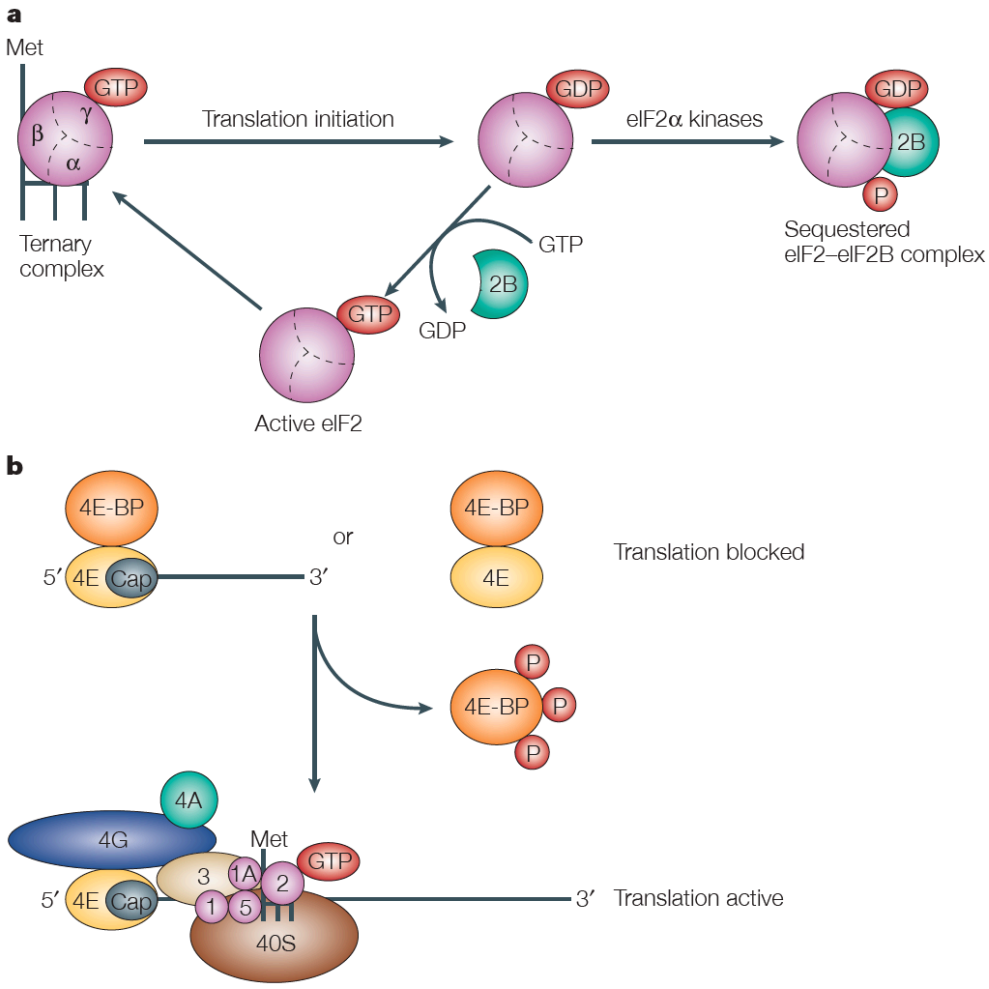

Figure 1.4. Global control of protein synthesis
Mechanisms that control global proteins synthesis generally involve changes in the phosphorylation status of initiation factors or their regulators. **a)** Translation initiation requires continuous recruitment of eIF2-bound GTP (GTP-eIF2) to the initiator tRNA. The exchange of GDP for GTP is catalyzed by eIF2B (green), a guanine exchange factor (GEF). eIF2 is a trimeric complex composed of the alfa (α), beta (β), and gamma (γ) subunits. Phosphorylation of the α subunit (Ser51) increases IF2's affinity for eIF2B and sequesters it, thus blocking the GTP-exchange reaction. As a consequence global mRNA translation is inhibited; see text for details. **b)** The phosphorylation status of eIF4E-binding proteins (4E-BPs) regulates general translation rates. Hypo-phosphorylated 4E-BPs prevent eIF4E interacting with eIF4G and repress translation. Hyper-phosphorylated 4E-BPs release eIF4E, which then binds eIF4G to promote cap-mediated translation initiation, see text for details. Cartoon was taken from Gebauer and Hentze, 2004.

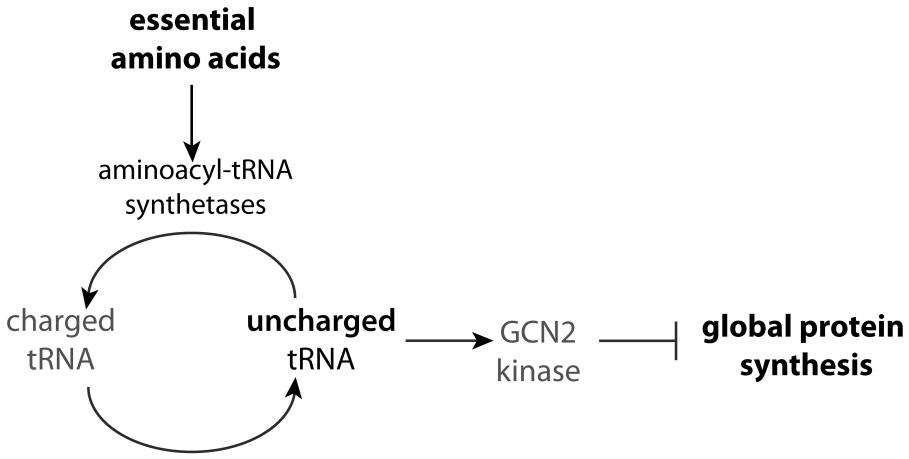

Figure 1.5 Protein synthesis repression induced by amino acid starvation
Scheme depicts the effect of essential amino acids on protein synthesis. Under full nutritional conditions, specific aminoacyl-tRNA synthetases load amino acids residues into corresponding tRNA (charged tRNA). By contrast, unloaded tRNAs accumulate (uncharged tRNA) during amino acid starvation, and activate GCN2 kinase. As a consequence mRNA translation is globally inhibited. Scheme was modified from Kimball and Jefferson, 2000.

1.1.3 POLY(A) TAIL METABOLISM AS A SELECTIVE TRANSLATIONAL CONTROL MECHANISM

The poly(A) tail is a stable 3' modification of eukaryotic mRNAs, and it its addition is catalyzed by poly(A) polymerases (PAPs) during nuclear mRNA processing (summarized in Eckmann et al. 2010). The poly(A) tail facilitates mRNA nuclear export, and prevents the degradation of the mRNA body in the cytoplasm. However, the poly(A) tail is gradually shortened through the cytoplasmic life-time of the mRNA. Another important function of the poly(A) tail is the stimulation of translation initiation. The length of the poly(A) tail correlates with the efficiency of translation. mRNAs with long poly(A) tails are translated more efficiently than those with short poly(A) tails, which translate better than deadenylated mRNAs. The poly(A) tail-mediated stimulation of translation involves de interaction between the poly(A) tail and the cytoplasmic poly(A)-binding protein (PABP) (summarized in Eckmann et al. 2010).

The number of PABP molecules that assemble on a poly(A) tail is proportional to the length of the tail, and multiple PABP copies favor translation (Eckmann et al. 2010). PABP interacts with the 5' cap-bound translation initiation factor eIF4G. The interaction of the PABP and eIF4E is thought to circularize the mRNA, thus the looped mRNA brings the 3' UTR close to the mRNAs 5' end (Figure 6). Although the exact mechanism is not fully understood, the mRNA circularization model provides a conceptual and spatial framework of how the poly(A) tail regulates translation initiation (Gebauer and Hentze, 2004, Eckmann et al. 2010).

On the basis of evolutionary relationships two classes of PAPs are distinguished: canonical PAPs, which contain RNA recognition motifs (RRM); and non-canonical PAPs, which usually lack RRMs. The nuclear canonical PAP catalyzes the poly(A) addition (Wahle and Kehler, 1992); in contrast nuclear non-canonical PAPs, such as Trf4p/Trf5p in yeast, facilitate mRNA turnover of aberrant RNAs (Vanacova et al, 2005). In addition to their nuclear functions, some canonical and non-canonical PAPs localize to the cytoplasm and mediate polyadenylation of specific mRNAs. The mammalian testis-specific PAP, and the *Drosophila* PAP Hiiragi are examples of cytoplasmic canonical PAPs (Kashiwabara et al. 2001; Juge et al. 2002). Although non-canonical cytoplasmic PAPs (cytoPAPs) have being found in many organisms, the best-characterized examples are two cytoPAPs in *C. elegans*, which are called GLD-2 and GLD-4 (*g*erm*l*ine *d*evelopment defective) (Wang et al. 2002, Schmid et al. 2009, Eckmann et al. 2010). I introduce these cytoPAP biological roles in sections below.

1.1.4 DEVELOPMENTALLY CONTROLLED MRNAS

Several mRNAs regulated during development are controlled by translational regulatory mechanisms (summarized in Kuersten and Goodwin 2003; Thompson et al. 2007). The formation of anterior-posterior embryonic axis in *Drosophila* is a classic example of how translational control networks regulate development (Johnstone O., and Lasko P., 2001). Broadly, the anterior development requires translational repression of *caudal* mRNA in the anterior, but not in the posterior; this repression is mediated by bicoid protein. Posterior development requires translational repression of *hunchback* mRNA in the posterior; the repression is mediated by Nanos protein. The *trans*-acting protein Pumilio interacts with *cis*-acting elements in the 3' UTR of *hunchback* mRNA and recruits the translational repressors Nanos and Brat. In addition, the 3'UTR of *nanos* mRNA mediates posterior-restricted Nanos protein expression. This developmental example highlights how cascades of translational repressors allow establishment of complex developmental programs (Kuersten and Goodwin 2003).

Oocyte maturation in *Xenopus laevis* is another paradigm of translational control during development and involves a cytoPAP (Mathews et al. 2007, Radford et al. 2008). As in most female animals, *Xenopus* oocytes are arrested in meiosis I. Progesterone stimulation mediates the completion of meiosis I and progression to meiosis II, and the concomitant translation of specific mRNAs. The information for the translational activation of these mRNAs is encoded in their 3'UTR, which contain sequence elements called cytoplasmic polyadenylation elements (CPE). In the arrested oocyte, the bound CPE-binding protein CPEB is associated with two enzymes of opposite functions: the cytoPAP xGLD-2 that elongates the poly(A) tail, and the poly(A) ribonuclease PARN that deadenylates the poly(A) tail (Figure 1.6). Since PARN is more active than xGLD-2, the targeted mRNAs have short poly(A) tails and they are not translated. However, progesterone stimulation induces CPEB phosphorylation, which displaces PARN, but not xGLD-2 from the complex. Without the repressive action of PARN, the poly(A) tail is elongated and recruits PABP (poly(A) binding proteins) and facilitate translation initiation (Radford et al. 2008).

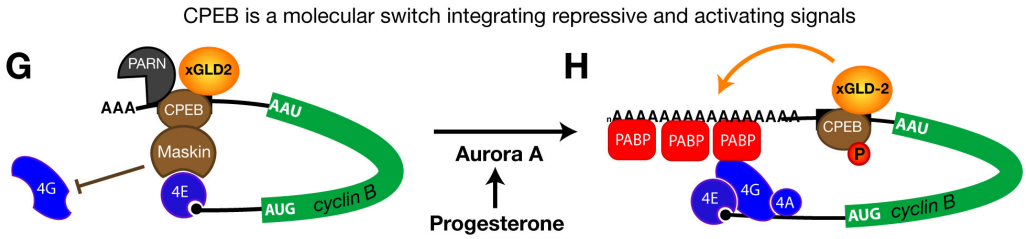

Figure 1.6 Cytoplasmic activation of maternally repressed mRNA in *X. laevis*
Schematic of progesterone stimulated *cyclin B* translation. **(G)** A multi-protein complex consisting of Maskin, CPEB, xGLD-2 and PARN assembles on the cytoplasmic polyadenylation element (CPE). The PARN deadenylase activity trims the poly(A) tail thus preventing mRNA translation. Progesterone stimulation induces Aurora A to phosphorylate CPEB. **(H)** Phosphorylated (P) CPEB displaces PARN and Masking. Without the repressive action of PARN, xGLD-2 elongates the poly(A) tail. A longer poly(A) tail favors the association of PABP (poly(A) binding protein) and its interaction with eIF4G. eIF4G is part of the cap-binding complex (eIF4E, eIF4A) and promotes translation initiation (Radford et al. 2008). Cartoon was taken from Jedamzik B. doctoral thesis (2009).

1.2 *C. ELEGANS* GERMLINE DEVELOPMENT AS A MODEL SYSTEM TO STUDY TRANSLATIONAL CONTROL

Germline developmental programs in different species share fundamental processes, such as: 1) an initial expansion of the pool of germ cells and maintenance of germ cell proliferation, 2) the cell cycle transition from mitosis to meiosis, and 3) the sexual differentiation as sperm or oocyte (Wolpert et al. 1998). In *C. elegans*, these cell fate decisions are controlled by a broadly conserved network of RNA binding proteins that act as activators or repressors of translation (Crittenden and Kimble, 2007). In addition, these different germ cell stages are stereotypically arranged in the gonad, thus it allows the examination of specific cell fates at determined locations. The following sections I introduce in more detail how the *C. elegans* germ line is specified, develops post-embryonically, utilizes gene expression mechanisms that control its development, and how these regulatory mechanisms are influenced by the soma.

1.2.1 THE *C. ELEGANS* GERM LINE IS SPECIFIED DURING EMBRYOGENESIS

The *C. elegans* germ cell lineage is specified early in embryogenesis at the very first zygotic division (Ghosh and Seydoux, 2008). This division produces two asymmetric cells, an anterior one and a posterior one. The posterior cell gives rise to the P-lineage, which establishes the germ cell fate (Sulston et al., 1983). Four consecutive asymmetric divisions set apart a P-lineage cell (P1-P4) from a somatic sister cells at each division. P4 divides again at approximately the 100-cell stage and gives rise to Z2 and Z3, which are the two primordial germ cells (PGC) (Hirsh et al., 1976). The PGCs and the somatic gonad precursors Z1 and Z4 remain quiescent until the first larval stage (Figure 1) (Sulston et al., 1983). The P-lineage, in contrast to embryonic somatic lineages, is maintained transcriptionally silent and inherits cytoplasm that contains germline determinants. The transcriptional repression is partially achieved by the PIE-1 protein, which is an RNA polymerase II inhibitor (Ghosh and Seydoux, 2008).

Gene expression programs in the P-lineage rely on maternally provided mRNAs and posttranscriptional regulatory machinery. Since large cytoplasmic ribonucleoprotein particles, called P granules, co-segregate with the P- lineage it was thought that P-granules specify the germ line fate in *C. elegans,* (Figure 1.7) (Seydoux and Braun, 2006; Strome and Lehmann, 2007). However, now it is known that at least PGL-1 or GLH-1 associated P-granules do not specify the germ line fate (Gallo et al. 2010). This suggests that germ cell specification is achieved by the combination of P-granules germline determinants and other cytoplasmic components present in P-lineage.

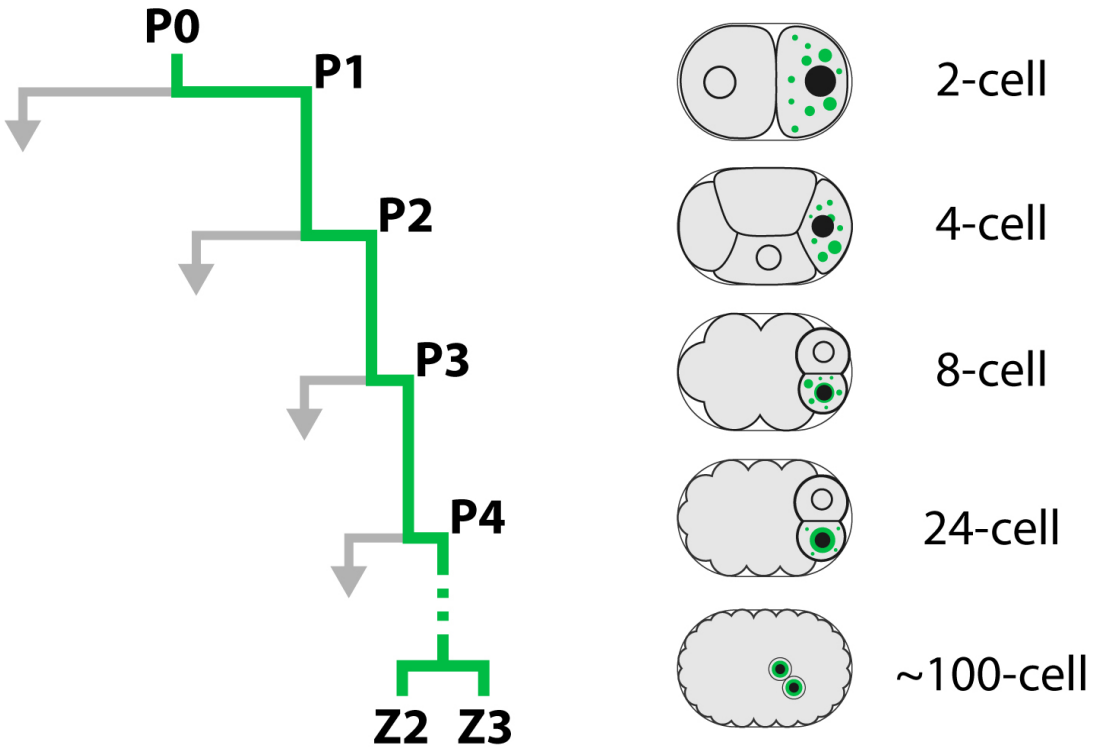

Figure 1.7 The germ cell lineage is set-aside during embryonic development
The *C. elegans* germ line is specified during embryogenesis. The first zygotic division gives rise to two cells, the posterior cell (P1) adopts the germline fate (green) and gives rise to the P-lineage. Three subsequent asymmetric divisions give rise to P2-P4. P4 divides symmetrically around the 100-cell stage to give rise to Z2 and Z3, which become the primordial germ cells. Large maternal ribonucleoprotein particles, called P granules (green), co-segregate with the P-lineage. Left: the P-lineage and corresponding sister blastomeres. Lineage rows correspond to the embryonic cell number at right. Right: embryos at different stages are schematically depicted with their corresponding number of cell (Sulston et al. 1983). Nuclei of the corresponding sister cells are indicated. The cartoon was kindly provided by C.R. Eckmann.

1.2.2 THE *C. ELEGANS* GERM LINE DEVELOPS POST-EMBRYOGENESIS

The *C. elegans* life cycle includes a short interval of embryogenesis (~12h), four larval stages L1, L2, L3 and L4 that take together 3 days until an adult is formed. Adulthood spans for ~17 days. The post-embryonic timing of events during germ line development is similar in males and hermaphrodites. Therefore only hermaphrodite germline development will be described in further detail. The development of the *C. elegans* germ line is coupled to somatic development.

At hatching, the L1 larva contains two primordial germ cells (Z2-Z3) that are quiescent, but start to proliferate when the nutritional environment is favorable (Kimble and Hirsh, 1979). Once proliferation starts, the number of germ cells increases exponentially from L1 to L2 larvae and two germline arms develop, one in the anterior body and the other in the posterior part. In the L3 larvae, proliferation continues distally but the most proximal germ cells enter meiosis, this establishes a polarity in the germ line and removes germ cells from the actively diving pool of mitotic cells. During the L4 larval stage the gonad elongates and germ cells continue to maintain proliferative and differentiating regions. In the hermaphrodite, the germ cells that initially entered meiosis during the L3 larvae differentiate during the L4 stage into sperm, whereas starting from the middle of L4, the germ cells that enter meiosis differentiate into oocytes (Figure 1.8) (Kimble and Crittenden 2007).

The primordial germ cells in the L1 larvae are initially celullarized, but as a result of incomplete cytokinesis germ cell descendants become syncytial. The syncytial germ cells are connected to a common cytoplasm, the rachis, located at the center of the germline arm (Figure 3B). Although germ cells are opened to a common cytoplasm, their nuclei divide independently and their surrounding cytoplasm is distinct, thus germ cell nuclei are not synchronized with other cells. By convention germ cell nuclei are referred to as individual germ cells (Hubbard and Greenstein, 2005). The somatic gonad develops in parallel to the germ line. The Z1 and Z4 somatic precursor cells give rise to the somatic gonad, which consists of the DTC and five pairs of gonadal sheath cells that surround the germ line. The somatic gonad is intimately associated with the germ line; cell ablation experiments have shown that the somatic sheath cells are required for several aspects of germline development (Altun and Hall, 2005).

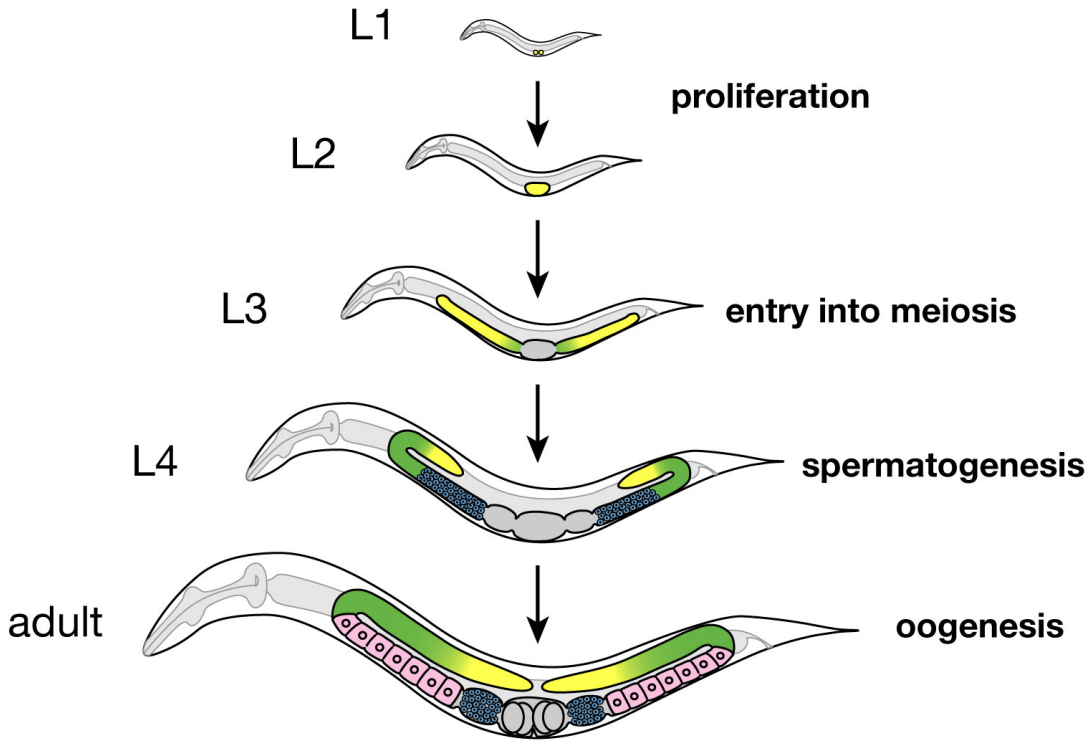

Figure 1.8 Development of the hermaphrodite germ line
Cartoon depicts post-embryonic germline development at each larval stage (L1-L4) and the adult. The four cell fate decisions that shape the germ line are indicated on the right. The L1 larva contains two primordial germ cells that start to proliferate in mitosis (yellow). The number of germ cells increases exponentially from L1 to L3 larvae and two germline arms develop, one at the anterior body and the other at the posterior part. At the L3 larvae, proliferation continues distally but the most proximal germ cells enter meiosis (green). During the L4 larval stage the gonad bends backward and germ cells continue to proliferate and enter meiosis. Those cells that enter meiosis at L3 differentiate into sperm (blue) during L4. Starting from the middle of L4, the germ cells that enter meiosis differentiate into oocytes (pink) in the adult, where germ cells continue proliferation and entry into meiosis (Kimble and Hirsh, 1979; Kimble and Crittenden 2007). The cartoon was kindly provided by C.R. Eckmann.

1.2.3 THE ADULT *C. ELEGANS* GERM LINE

Each of the adult germline arms contains all cell fates organized in a spatial and temporal manner in a distal to proximal fashion. The germline arms have a U-shape and are readily visible using a low magnification microscope. Distinct functional regions in the adult hermaphrodite are identifiable (Figure 1.9 A-B). At the very distal part of the germ line resides the mitotic region. A population of germ cells within the mitotic region is capable of both self-renewal and generating cells that undergo differentiation; hence this population is referred as the germline stem cells (GSC) (Kimble and Crittenden, 2007; Byrd and Kimble, 2009). Therefore, the mitotic region continuously supplies germ cells for gametogenesis in the adult. In the germ line, cell differentiation refers to the execution of a meiotic program, either male meiosis (spermatogenesis) or female meiosis (oogenesis). Germ cells that undergo differentiation locate proximal to the mitotic region and correspond to nuclei in early meiotic stages, leptotene and zygotene, which intermingle with mitotic cells (Kimble and Crittenden, 2007. This region is thus called the transition zone. As cells progress through the meiotic stage of pachytene they locate further proximal in the so-called pachytene region. In the adult hermaphrodite, proximal to the pachytene region and past the bend, meiotic cells mature into a single row of oocytes. Further proximal, larval-produced sperm is stored in the spermatheca (Figure 1.9 B) (Hubbard and Greenstein, 2005, Kimble and Crittenden 2007).

The developmental stage of germ cells is readily distinguished on the basis of its nuclear chromatin configuration (Figure 1.10) (Altun and Hall, 2008). Cells in the mitotic zone are rounded and homogeneous in size. In the transition zone, early meiotic cells start to condense chromatin and form crescent-shaped nuclei; this morphology is typical of leptotene and zygotene stages. During leptotene and zygotene, homologous chromosomes align and a protein complex (synaptonemal complex) is formed in between sister chromatids to allow chromosomal synapsis. The synapsed chromosomes are visible as thread-like chromatin and locate to the pachytene region. After the pachytene stage, during the diplotene stage the synaptonemal complex is destroyed and chromosomes condense again.

At the position right before the germline loops, pachytene cells enter physiological programed cell death to provide cytoplasm for the developing oocytes. Further proximal, chromosomes in the diakinesis stage are observed as six pairs of highly condensed bivalents. Since oocytes arrest in diakinesis, the six pairs of highly condensed chromatin distinguish oocyte nuclei from other germ cell nuclei. At the proximal region mature sperm nuclei areobserved as homogeneous small dots of highly condensed chromatin inside the spermatheca (Altun and Hall, 2008).

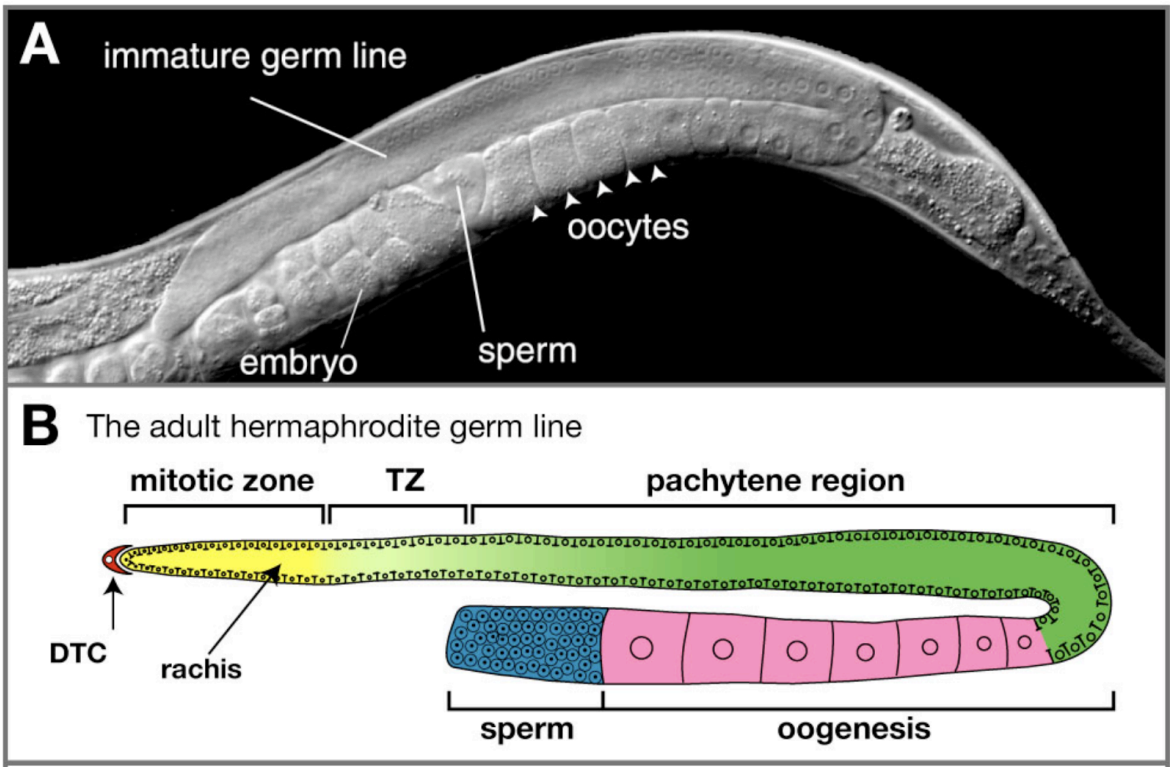

Figure 1.9 Adult hermaphrodite Germ line organization
(A) DIC microscopy image of the anterior part of an adult hermaphrodite focusing the gonadal arm. Arrowheads indicate developing oocytes. **(B)** A schematic representation of an extruded germ line arm indicating the distal tip cell (DTC, red), the rachis, the mitotic zone (yellow), transition zone (yellow-green), meiotic cells in pachytene (green), developing oocytes (oogenesis, pink) and sperm (blue). See text for detailed description. Picture and scheme were kindly provided by C.R. Eckmann.

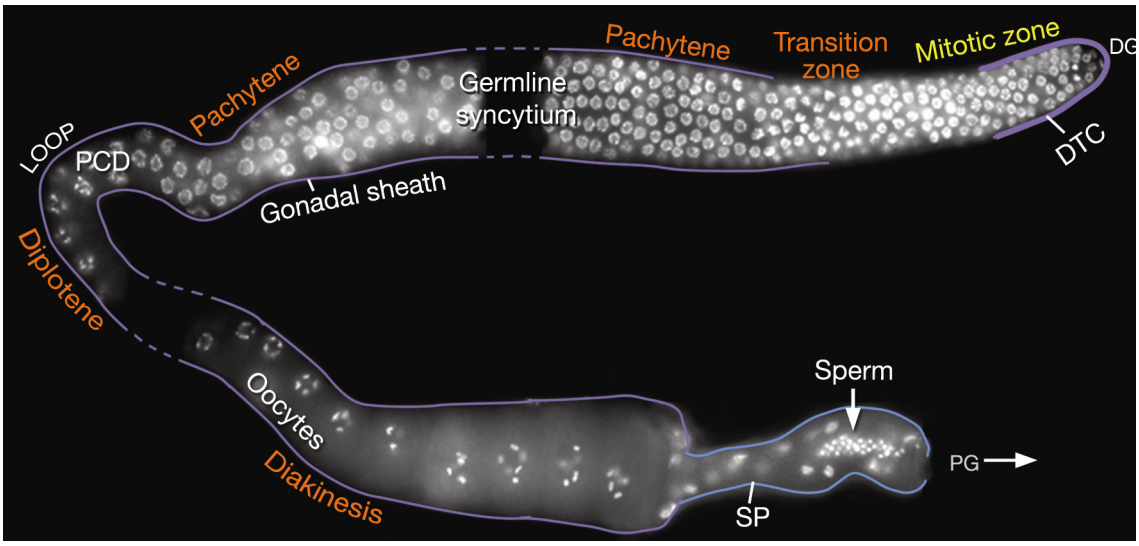

Figure 1.10 Adult hermaphrodite germ cell developmental stages
Composed image shows an extruded adult hermaphrodite germ stained with the nuclear dye DAPI to visualize nuclear morphology. Distal germ line (DG) is at the right. Purple contour indicates somatic gonad: the distal tip cell (DTC) and gonadal sheath. LOOP indicates the position where the germline bends and where programed cell death (PCD) occurs. Spermatheca (SP). Proximal germ line (PG). See text for detailed description. Image was taken from Altun and Hall (2008) in Worm Atlas.

1.2.4 Two major cell fate decisions shape the development of the hermaphrodite germ line

In the hermaphrodite *C. elegans* germ line entry into meiosis and gamete differentiation are regulated as opposing cell fate decisions: proliferation (mitosis) vs. differentiation (meiosis); and spermatogenesis vs. oogenesis . Both cell fate decisions are controlled via posttranscriptional mechanisms and by similar molecular key regulators (Kimble and Crittenden 2007). This section introduces the concept of how posttranscriptional control regulates the mitosis vs. meiosis, and the spermatogenesis vs. oogenesis cell fate decisions.

1.2.4.1 THE MITOSIS VERSUS MEIOSIS DECISION

Germline proliferation is regulated by the somatic DTC, which uses GLP-1/Notch signaling to control a network of RNA regulators (summarized in Kimble and Crittenden 2005; 2007). The DTC expresses on its surface the Delta-ligand LAG-2. Germ cells express the Notch receptor GLP-1, which transduces the DTC signaling to promote mitotic divisions by preventing meiotic entry (Henderson et al. 1994, Tax et al, 1994). Gain-of-function *glp-1* mutants have germ lines containing only mitotic cells, whereas loss of *glp-1* causes complete meiotic differentiation of larval germ cells. Therefore, *glp-1*/Notch signaling is both necessary and sufficient to promote mitotic divisions by preventing the start of meiosis. The DTC promotes mitotic divisions only in those germ cells that are in close contact to it, which correspond to the most distal germ cells. Although *glp-1* mRNA is expressed throughout the germ line, the GLP-1/Notch protein is more abundant in germ cells of the mitotic region and its expression decreases through the transition zone. The translational repressor GLD-1 represses *glp-1* mRNA translation, thus restricts GLP-1/Notch protein expression to the mitotic region. (Kimble and Crittenden 2005; 2007).

The *fbf-2* gene is a direct target of GLP-1/Notch signaling, and FBF-2 protein expression depends on GLP-1 signaling (Lamont et al. 2004). *fbf-2* and the highly similar *fbf-1* gene encode translational repressors of the PUF family (Pumilio and FBF), collectively called FBFs (Zhang et al. 1997). The PUF family comprises RNA-binding proteins essential for GSC maintenance. Consistent with a role in maintaining GSC, loss of both *fbf-1* and *fbf-2* causes all germ cells in the L4 larva to enter meiosis, indicating that the self-renewal GSC capacity is lost. Thus the FBF translational repressors are essential for promoting mitosis in the adult (Crittenden et al. 2002, Kimble and Crittenden 2005; 2007). FBFs control proliferation by repressing the translation of proteins that promote meiosis (Crittenden et al. 2002, Eckmann et al. 2004).

In summary, mitotic proliferation occurs as long as the entry in meiosis is repressed. Four translational regulators are key for the entry into meiosis. Three GLD proteins (germline development defective -1, -2, and -3), and the Nanos/NOS-3 protein control entry into meiosis via two regulatory pathways influenced by FBF. *gld-1* and *nos-3* constitute one branch, whereas *gld-2* and *gld-3* constitute the other branch. Meiosis entry is blocked in double mutants in one gene of each branch, for example in a *gld-1; gld-2* (Figure 1.11) (Kimble and Crittenden 2005; 2007).

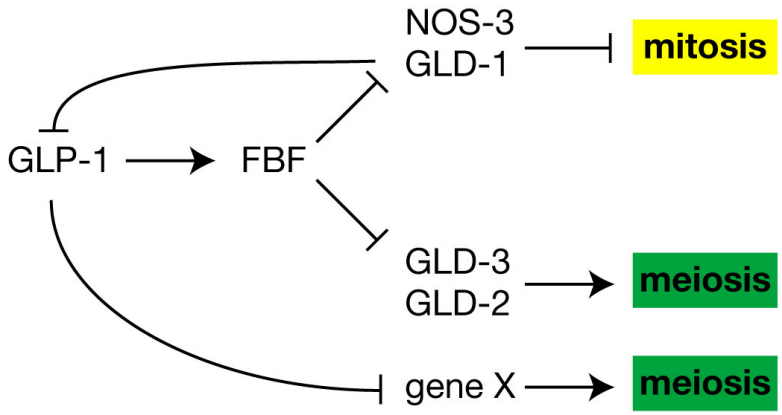

Figure 1.11 Regulation of the decision between mitosis and meiosis
GLP-1/Notch signaling influences a network of RNA binding proteins through FBF proteins (FBF-1 and FBF-2). GLP-1 transcriptionally activates *fbf-2*. FBF-2 and FBF-1redundantly promote mitotic proliferation by: a) repressing the translation of factors that block mitosis (GLD-1) and b) repressing the translation of factors that promote meiosis (GLD-3). Two regulatory pathways influence the entry into meiosis. GLD-1 and NOS-3 constitute one branch, GLD-3 and GLD-2 the second branch. Gene x represents an uncharacterized minor branch that promotes meiotic entry. GLD-1 and GLD-3 are translational repressors, whereas GLD-2 and GLD-3 form an active poly(A) polymerase and act as translational activators.

1.2.4.2 The sperm-to-oocyte switch

Global regulators specify somatic sexual identity, and germline-specific regulators control the decision from sperm-to-oocyte production (Hodking J. and Brenner S., 1977; summarized in Ellis and Schedl 2007, and Kimble and Crittenden, 2007). Although, hermaphrodites have a female identity they transiently produce sperm, and switch later to oogenesis.The global sex determination regulators TRA-2 and FEM-3 proteins promote oogenesis and spermatogenesis, respectively.

Germ line-specific regulators of the sperm-to-oocyte switch are also involved in the mitosis vs. meiosis decision. The translational repressor GLD-1 directly binds to *tra-2* 3'UTR and represses its translation during the L4 larval stage. This temporal repression allows the FEM-3 protein to promote spermatogenesis (Figure 7A). However, in order to stop spermatogenesis, the translational repressor FBF binds *fem-3* 3'UTR and represses its translation thus spermatogenesis stops. Since at this point *tra-2* mRNA is not repressed anymore by GLD-1, TRA-2 protein can promote oogenesis throughout adulthood (Figure 7B) (Ellis and Schedl 2007, Kimble and Crittenden, 2007). In addition to GLD-1 and FBF, GLD-3 and NOS-3 proteins are also involved in the sperm-to-oocyte switch. For example, GLD-3 promotes hermaphrodite spermatogenesis by de-repressing *fem-3* mRNA from FBF (Eckmann et al. 2002). A controlled switch from spermatogenesis to oogenesis leaves hermaphrodites with ~320 sperm that is used for self-fertilization hence ensures hermaphrodites fertility.

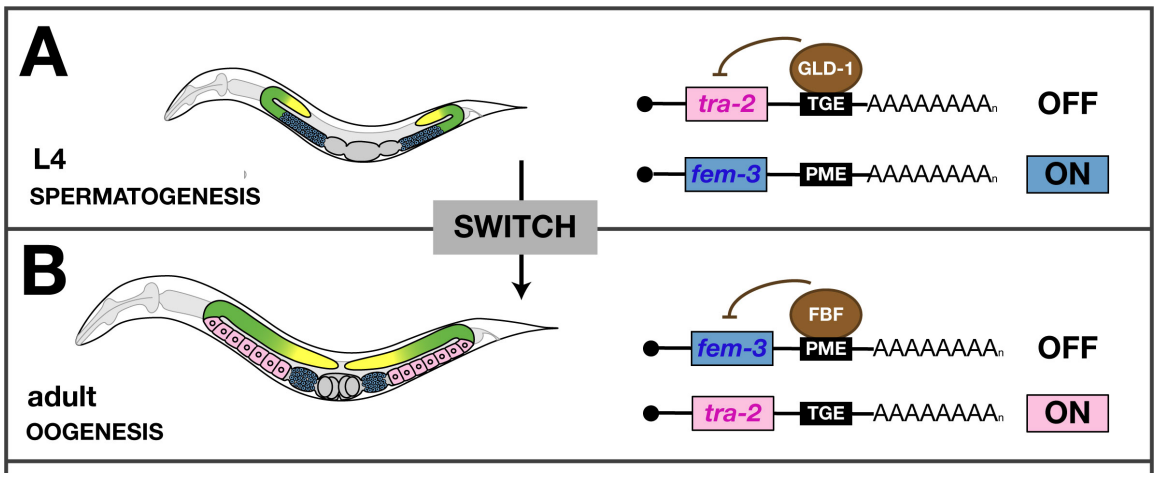

Figure 1.12 Regulation of the sperm-to-oocyte switch
The switch from spermatogenesis to oogenesis is controlled by global sex determination regulators (*tra-2* and *fem-3* in this cartoon) and germline-specific regulators (GLD-1, FBFs and GLD-3 in this cartoon). *tra-2* promotes oogenesis (pink), *fem-3* promotes spermatogenesis (blue). **(A)** The translational repressor GLD-1 directly binds to *tra-2* 3'UTR and represses its translation during the L4 larval stage. This temporal repression allows the FEM-3 protein to promote spermatogenesis. **(B)** In order to stop spermatogenesis and switch to oogenesis, the translational repressor FBF binds *fem-3* 3'UTR and represses its translation thus spermatogenesis stops. Since at this point *tra-2* mRNA is not repressed TRA-2 protein promotes oogenesis throughout adulthood. Cartoon was taken from Jedamzik B. doctoral thesis.

1.2.5 Novel regulators of germ line development

Additional proteins required for *C. elegans* germ line development have being identified by yeast two-hybrid screens. For example, the novel protein GLS-1 (germline survival defective) is a modulator of the network of RNA regulators that control germ cell fate decisions (Rybarska et al. 2009). Aditionally, the GLD-4 protein was recovered as a GLS-1 binding protein (Schimd et al. 2009). GLD-4 is a non-canonical cytoPAP (cytoplasmic poly (A) polymerase) similar to GLD-2 cytoPAP. *In vitro* experiments showed that GLS-1 binding enhances GLD-4 PAP enzymatic activities, suggesting that GLD-4 in vivo functions may be stimulated and regulated by GLS-1. Both germline cytoPAPs *gld-4* and *gld-2* have a redundant function in promoting female meiotic progression (Schimd et al. 2009).

Also, GLD-4 and GLS-1 are required for the sperm-to-oocyte switch (Rbyarska et al. 2009). However, other aspects of GLD-4 function are less understood. First, *gld-4* mutants have a small pool of mitotic cells giving rise to underproliferated germ lines (Schmid M. PhD thesis, 2009). It is currently not know whether *gld-4* is required to establish or to maintain the pool of mitotic cells. Second, *gld-4* mutant hermaphrodites produce sperm but no oocytes. Currently it remains unknown what aspect of oogenesis is promoted by *gld-4* (Schmid M. PhD thesis, 2009).

1.2.6 Germline development is coupled to the nutritional status of the animal

During *C. elegans* embryogenesis, the PGCs Z2 and Z3 protrude large lobes into two instestinal cells; presumably this contact nurtures the germ cells until they attach to the somatic gonadal cells (Sulston et al. 1983). However, it is not know what is the long-term impact of early contact. Later, germ cell proliferation responds dynamically to external signals such as the nutritional status. This dependency is first observed in the Z2 and Z3, which start proliferation only when the hatched larvae encounter enough nutrients (Kimble and White, 1981). In contrast, if larvae hatch in a nutritional limited medium the PGC do not start proliferation until the larvae is fed, suggesting that a signal derived from food triggers the initial germ cell proliferation (Figure 1.13) (Kimble and White, 1981).

PGC are transcriptionally quiescent during embryogenesis and remains so at hatching in the absence of food. Therefore, it is expected that the food-related signal that triggers proliferation induces chromatin changes that allow transcriptional activation (Schaner et al. 2003). *C. elegans* larvae develop into dauer instead of L3 larvae when environmental conditions are harsh, such as low food supply. Dauer larvae are stress-resistant, non-feeding, and arrests somatic and germline development (Hu, 2007). In fact, dauer larvae germ lines contain about 35 germ cells that are arrested in mitotic interphase and do not enter meiosis (Narbonne and Roy, 2006). Dauer development is chiefly controlled by the nuclear receptor VitD/DAF-12, and constitutes a paradigm of the integration of environmental conditions into the whole organism and not only the germ line (Antebi et al. 2000, Hu et al. 2007).

Another example of the influence of external signals is larval germ cell proliferation. Although germ cell proliferation is chiefly controlled by GLP-1/Notch signaling, the robust proliferation of the larval mitotic pool requires local signals from the Sh1 sheath cell and insulin-IFG-like receptor (IIR) signaling (Killian and Hubbard, 2005; Michaelson et al. 2010). The direct molecular link between the Sh1 sheath cell and the germ line is unknown, but genetic evidence suggests optimal ribosomal biogenesis is involved (Killian and Hubbard 2004). On the other hand, IIR signaling is activated in response to full nutritional conditions and activates the PI3K pathway that promotes nuclear exclusion of the transcription factor DAF-16/FOXO (Michaelson et al. 2010). Nuclear DAF-16/FOXO antagonizes cell cycle progression (Henderson and Johnson, 2001); therefore impaired DAF-2/IIR signaling reduces cell cycle progression and leads to germline underproliferation. DAF-2/IIR signaling in the larvae responds to two insulin-like peptides *ins-3* and *ins-33* produced in the somatic tissues (Figure 1.13) (Michaelson et al. 2010). This study on DAF-2/IIR conveys a direct case on how germ cells respond to a diet-related signaling pathway.

Starvation provides a clear example on how the germ line is sensitive to nutrition. Starved L4 hermaphrodites loose a substantial number of germ cells; however, a small population of germ cells remains present (Angelo and Van Gilst, 2009). These starved animals proceed to adulthood as a diapause stage that extends life span. Importantly, when full nutritional conditions are restored, the adult diapause animals develop a fertile germ line from the population of protected germ cells. Optimal entry into adult diapause and exit from it require an worm HNF4 ortholog, the nuclear hormone receptor *nhr-49*, which mediates the physiological starvation response, but not the protection of the germ cell population (Figure 8) (Angelo and Van Gilst, 2009). Similarly, the *Drosophila* HNF4 (hepatocyte nuclear factor - 4) mediates an starvation response (Palanker et al. 2009). The response to starvation in *C. elegans* highlights how the germ line can dynamically respond to varying nutritional conditions. Moreover, the regeneration of a functional germ line after food restriction strongly suggests that germline development is coordinated to mechanisms that sense nutritional conditions.

In summary, germ line development requires three major components: 1) a germline posttranscriptional network of translational regulators that controls gene expression, 2) several germ cell fate decisions that shape the germ line architecture, and 3) the animal's overall nutritional status. However, it remains largely unknown whether nutrition is molecularly linked to the germline posttranscriptional control mechanisms and the cell fate decisions, and if so, how they are linked.

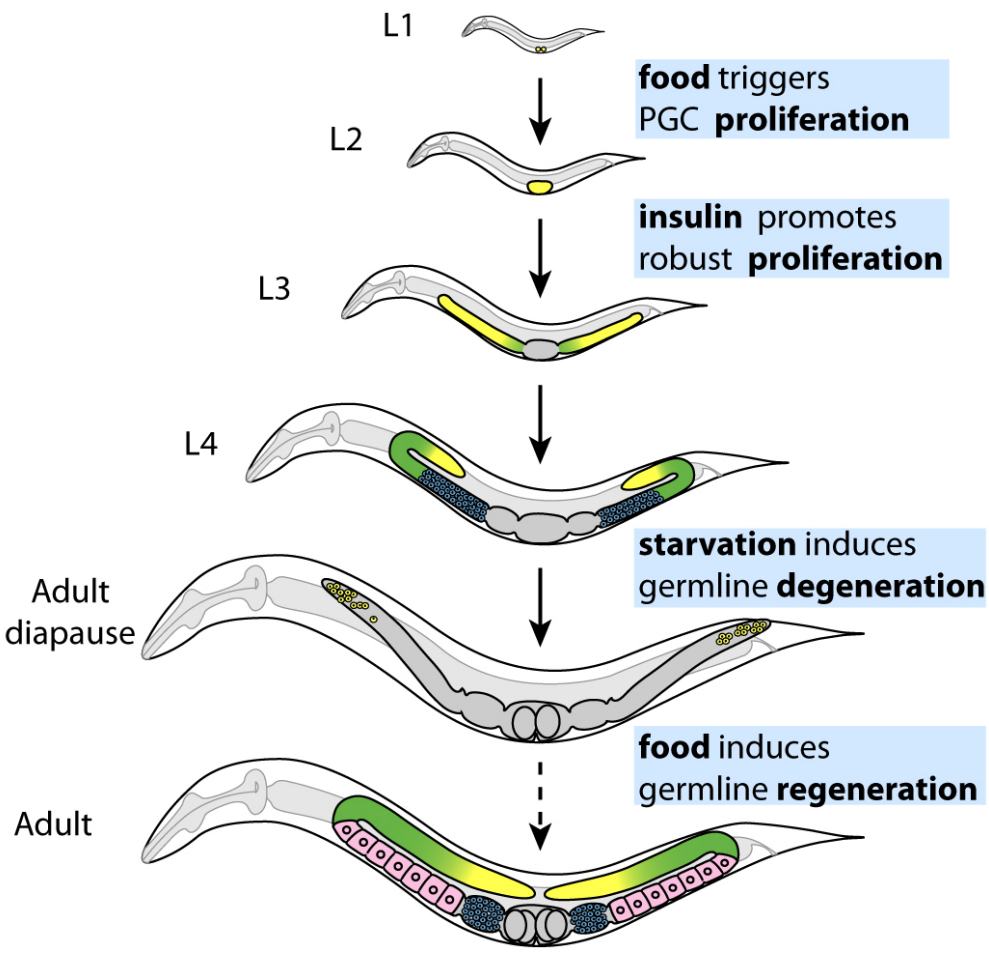

Figure 1.13 Germline development is sensitive to nutrition
Scheme shows three examples of how nutrition influences germline development at different stages of life. An unknown food-related signal triggers initial proliferation of the primordial germ cells (PGC). Insulin signaling promotes robust larval proliferation under full nutrient conditions. Starvation of L4 larvae induces and adult diapause stage, and germline degeneration of most, but not all germ cells (yellow circles). Food restoration induces germline regeneration. Dotted line indicates intermediate steps.

1.3 NUCLEAR RECEPTORS ARE CELLULAR SENSORY ELEMENTS

The development, growth, metabolism and reproduction in multicellular organisms largely depend on the ability to send and receive information among tissues to coordinate their functions (Alberts et al. 2008). Several biomolecules act as signals, some at the cell surface, and some directly enter the cell and bind intracellular receptors (Bunce and Campbell, 2010. Signaling biomolecules, such as hormones, transduce the external environment to influence cellular decisions by eliciting physiological and transcriptional responses. Metazoans evolved a way to coordinate theses processes by using nuclear receptors (NR) (Mangelsdorf et al., 1995; Bunce and Campbell, 2010). NRs or nuclear hormone receptors (NHRs) are a family of receptors that commonly function within transcriptional complexes to selectively regulate gene expression (Bunce and Campbell, 2010). Since the study of NHRs has advanced the understanding of gene transcription, NRs are mostly considered as transcription factors rather than receptors. However, NRs are both cellular sensory elements and transcription factors (Bunce and Campbell, 2010). The NR primary structure allows them to bind ligands and interact with DNA (Figure 1.14), thus NRs are involved in a diversity of physiological processes.

1.3.1 NRS REGULATE DIVERSE DEVELOPMENTAL, METABOLIC AND PHYSIOLOGICAL ASPECTS

Nuclear hormone receptors have a similar structural organization. Nevertheless, NRs are implicated in many different biological processes and are regulated by diverse compounds (Bunce and Campbell, 2010). Several small lipophilic molecules that modulate development, cell differentiation and physiological processes were isolated before the discovery of NRs. Steroids, retinoids, thyroid hormones and vitamin D3 (Figure 1.15) were later found to bind NRs, establishing this class of transcription factors. Overall, NRs are regulators of development, cell differentiation, organ physiology and metabolism. Based on their ability to dimerize and DNA-binding properties, NR family can be broadly divided into four classes: I-IV (Table 1.1) (Mangelsdorf et al. 1995; Bunce and Campbell, 2010).

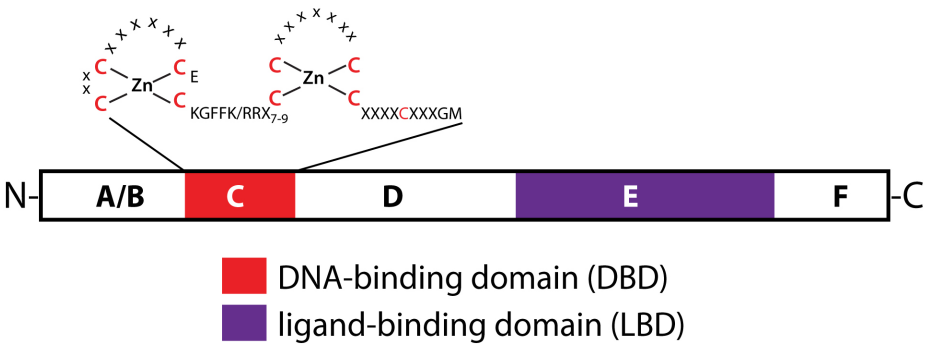

Figure 1.14 Nuclear receptor structure is modular
The NR primary structure comprises five or six contiguous regions nominated A/B, C, D, E and F. These regions have different degrees of homology among interspecies. A, C and E regions are best conserved whereas B and D regions are less conserved. This structural classification corresponds to the functional compartmentalization of NR proteins. The C region encodes a highly conserved DNA-binding domain (DBD) made of two stereotyped cysteine-4 (C) zinc fingers characteristic for NRs, but not found in other DNA-binding proteins. The consensus sequence between the zinc fingers is given as single amino acid letter. KGFFK/RRX, X corresponds to any amino acid. The E region is second best conserved among NRs, and it encodes the ligand-binding domain (LBD). The variable D region separates the DBD and the LBD and acts as a hinge region that confers structural flexibility of the receptor. Both the A/B and F regions are variable and encode no protein structural domains, but effector functions that influence gene transcription (Bunce and Campbell, 2010).

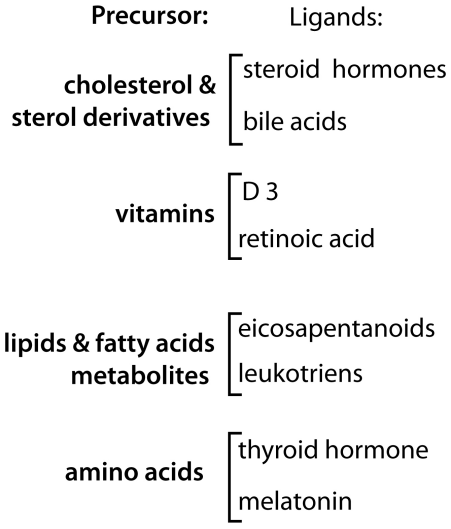

Figure 1.15 Common signaling molecules that bind NRs
Figure shows the most common precursor molecules of NR ligands. Most of the NRs have being named after their ligand, for example the bile acids receptor or the vitamin D receptor. See text for details.

Class	Ligand			DNA binding		Receptors
	Precursor	Source	Affinity	Dimerization	RE	
I	steroids	endocrine	nM	homodimer	inverted repeated	AR, ER, GR, PR
II	dietary lipids, bile acids, xenobiotics	diet	μM	heterodimers with RXR	direct repeat	PPAR, FXR, PXR, CAR, LXR, HNF4
III	dietary compounds	endocrine	nM	homodimers	direct repeat	RAR, VDR, TR
IV		unknown		monomer	extended RE	NGF1-B

Table 1.1 NRs classes based on type of ligand bound and DNA-binding modes
NR ligands are synthetized from different compounds that server as precursors. The actual ligand is synthetized by endocrine tissues, or is used directly from the dietary compounds. The affinity for a ligand to bind a receptor correlates with the source: endocrine-produced ligands bind their receptors with high affinity (nM range); dietary ligand bind receptors with low affinity (μM range). Endocrine receptors bind DNA as homodimers; class II receptors and also RAR; VDR and TR form heterodimers with RXR. NRs bind specific DNA sequences called response elements (RE) to regulate gene expression in a selective fashion. AGGTCA is the RE consensus sequence (extended). Depending on the dimerization, NRs bind direct repeats AGGTCA…AGGTCA; or inverted repeats AGGTCA…ACTGGA. (Bunce and Campbell, 2010). Only some examples of NRs of each class are given: Androgen (AR), estrogen (ER), glucocorticoid (GR) and progesterone (PR) receptors. Peroxisome-proliferator activated (PPAR), retinoic X (RXR), farnesoid X (FXR, bile acid receptor) pregnane X (PXR), constitutive androstane (CAR), liver X (LXR) retinoic acid (RAR), vitamin D (VDR), thyroid receptors (TR). Nerve growth factor (NGF1-B). (Mangelsdorf et al. 1995, Schmidt and Mangelsdorf 2008).

The classification of NRs into classes is arbitrary and does neither reflect phylogenetic relationships, nor functional output (Mangelsdorf et al, 1995). However, this classification helps to understand the functions of two classes of nuclear receptors, those that bind endocrine ligands, and those binding physiological ligands (dietary) (Chawla et al. 2001). Endocrine ligands, such as sterol hormones, and their NRs are regulated by negative-feedback control; and they are key in controlling development, growth and reproduction. In contrast, physiological ligands, such as bile acids, bound to NRs activate feed-forward metabolic cascades to maintain dietary lipid homeostasis. Therefore, physiological ligands and their NRs are emerging as key regulators of nutrient uptake, metabolism and excretion (Chawla et al. 2001, Schmidt and Mangelsdorf 2008).

1.3.2 Coregulators mediate mechanistic aspects of NR function

NRs bind specific DNA sequences called response elements (RE) to trans-activate or trans-repress gene transcription. Whether an NR activates or represses transcription depends on its association with coregulators. In the canonical model of NR function, ligand binding to a NR renders a conformational change that favors the recruitment of enzymatic coactivator complexes that bridge RE to the basal transcriptional machinery. Whereas a ligand-unbound NR recruits corepressors complexes that locally modify histones to allow structural chromatin changes that repress gene expression. Corepressors and coregulators typically bind the LBD, and they are both targets and transmitters of posttranslational modifications (Lonard and O'Malley 2006, 2007, Bunce and Campbell, 2010). Common coregulators are kinases, acetylases, methylases, histone deacetylases, ubiquitin ligases, sumoylases, and other enzymatic functions yet uncharacterized (Jung et al. 2005) (Figure 1.16).

1.3.3 Extranuclear activities of NRs

NRs also function out of the nucleus; these functions are referred as non-genomic or extranuclear (Bunce and Campbell. 2010). For example, the orphan NR Nur77, which functions elicit contrary phenotypes depending on subcellular localization. Nuclear Nur77 is an oncogene, while cytoplasmic Nur77 binds Bcl-2 in the mitochondria and releases cytochrome *c* to trigger apoptosis (Zhang XK, 2007). On the other hand, the TR-beta, ER-alfa, RAR-alfa, and GR can bind the phosphoinositide 3-kinase (PI3K) and stimulate PI3K downstream signaling. The accumulating evidence of NRs interacting with PI3K has suggested that this kinase may represent an interface between surface receptor signaling and extranuclear NR mediated signaling (Bunce and Campbell. 2010).

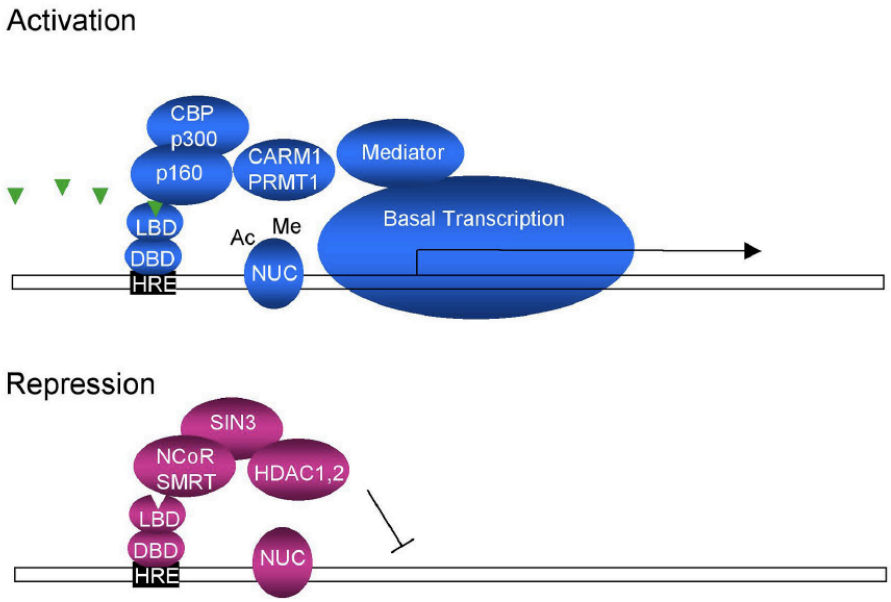

Figure 1.16 Model of NR-mediated transcriptional activation and repression
Cartoon depicts the general model of ligand-dependent NR-mediated transcription based on vertebrate NRs. In blue, an activation complex is depicted: in the presence of ligand (green triangles) the NR binds the DNA hormone response elements (HRE) and assembles coactivator complexes. p160 and CREB-binding protein (CBP/p300), or CARM1, PRMT1 complexes acetylate (Ac) or methylate (Me) nucleosomes (NUC), respectively. The mediator complex facilitates the recruitment of the basal transcription machinery. Arrow indicates active transcription from DNA template (open bar). In purple, a repression complex: in the absence of ligand the NR assembles corepressor complexes, such as NCoR, SMRT, SIN3, which in turn recruit histone deacetylases complexes (HDAC1,2). The change in the nucleosome status blocks transcription. The assembly of both classes of coregulators is specific for NRs and the promoter context. Image was taken from Antebi et al. 2006.

1.3.4 NRs ARE PHYLOGENETICALLY CONSERVED IN METAZOANS

The presence of two functionally conserved domains, the DBD and LBD has been exploited to establish robust phylogenies within NHRs (Markov et al. 2010). The NR family is divided into six monophyletic subfamilies: NR1 to NR6. All receptors within a subfamily originate from a single ancestor (Figure 1.17). The ligand-binding ability of NRs is not linked to its phylogeny. The exact origin of NRs is still unknown, however it is clear that NHRs are a metazoan specific protein family. Fungi and plants have no NRs, but different types of proteins that combine a DNA-binding domain and a ligand-binding domain that are non-homologous to NRs (Markov et al. 2010).

Although NRs share a similar structural organization, the analysis of *nhr* genes in different metazoan phyla has revealed an enormous diversity of NRs. The *Drosophila melanogaster* genome encodes 21 NR genes (Adams et al. 2000). Mammalian model organisms like rat, mouse and human have 47, 49 and 48 NR genes, respectively (Zhang et al. 2004). The most dramatic example of NR diversity is found in *C. elegans*, which encodes approximately 280 NR genes (Sluder et al. 1999).

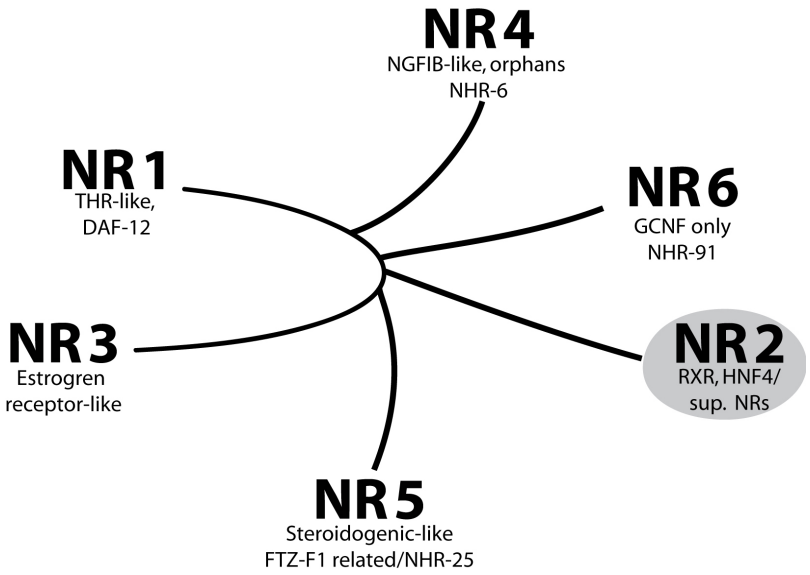

Figure 1.17 The NR super family comprises six monophyletic subfamilies
Diagram shows the six NR subfamilies: NR1-NR6 and the representative example in humans and the corresponding *C. elegans* ortholog (bottom row). The NR1 subfamily comprises THR-like receptors. The NR2 subfamily comprises RXR-like receptors, the *C. elegans* supplementary NRs (sup. NRs) such as *nhr-114* belong to this subfamily. The NR3 subfamily comprises ER-like receptors, with no obvious ortholog in *C. elegans*. The NR4 subfamily comprises nerve growth factor like IB-like receptors (NGFIB) and orphan receptors. The NR5 subfamily comprises steroidogenic receptors, such as steroidogenic factor 1 (SF-1) or the *Drosophila* Ftz-F1 (fushi tarazu-F1). The NR6 subfamily comprises the germ cell nuclear factor (GCNF) as the only single member. Proteins that contain a DBD without a LBD or vice verse are grouped in the NR0 subfamily, not shown. (Robinson-Rechavi and Laudet M. 2003, Antebi et al. 2006, Markov et al. 2010).

1.3.4.1 *C. ELEGANS* NR FAMILY IS EXTENDED AND DIVERSIFIED

The 280 NR genes in *C. elegans* constitute the largest number of NR genes described from a single species (Sluder et al. 1999). Out of this expanded NR family in *C. elegans*, only 15 have orthologs found in arthropods or vertebrates, the remaining majority is highly divergent and rapidly evolving. These divergent NRs have being termed supplementary NRs. Supplementary NRs diverge mostly at the DBD region, and the change in some highly conserved amino acids may render a non-functional DBD or DNA-binding specificities distinctive from NRs. In addition, the LBD of supplementary NRs is also variable. Two groups can be separated within supplementary NRs: group I is less divergent, group II is more divergent (Robinson-Rechavi et al, 2005). Supplementary NRs originated from lineage-specific expansion of the HNF4 (hepatocyte nuclear factor 4, NR2A) (Figure 1.18).

Importantly, most of the supplementary NRs genes are found on *C. elegans* chromosome V (Robinson-Rechavi et al, 2005), of which substitution and duplication rates are highly increased. The expansion of the NR family is also observed in *Caenorhabditis briggsae,* which encodes 230 predicted NR DBD sequences that are HNF4-derived. Only half of the *C. briggsae* NRs have clear *C. elegans* orthologs, indicating independent ongoing diversification of their NR genes (Robinson-Rechavi et al, 2005). As their mammalian orthologs, conserved NRs in *C. elegans* have broad functions, and affect developmental, metabolic and homeostatic processes. Some of these functions are summarized in Table 1.2. Experimental characterization has demonstrated that supplementary NRs are not pseudogenes. In contrast, the presence of such a large number of functional NRs suggests that they have been maintained and amplified as a result of having important roles in the organism (Robinson-Rechavi et al, 2005).

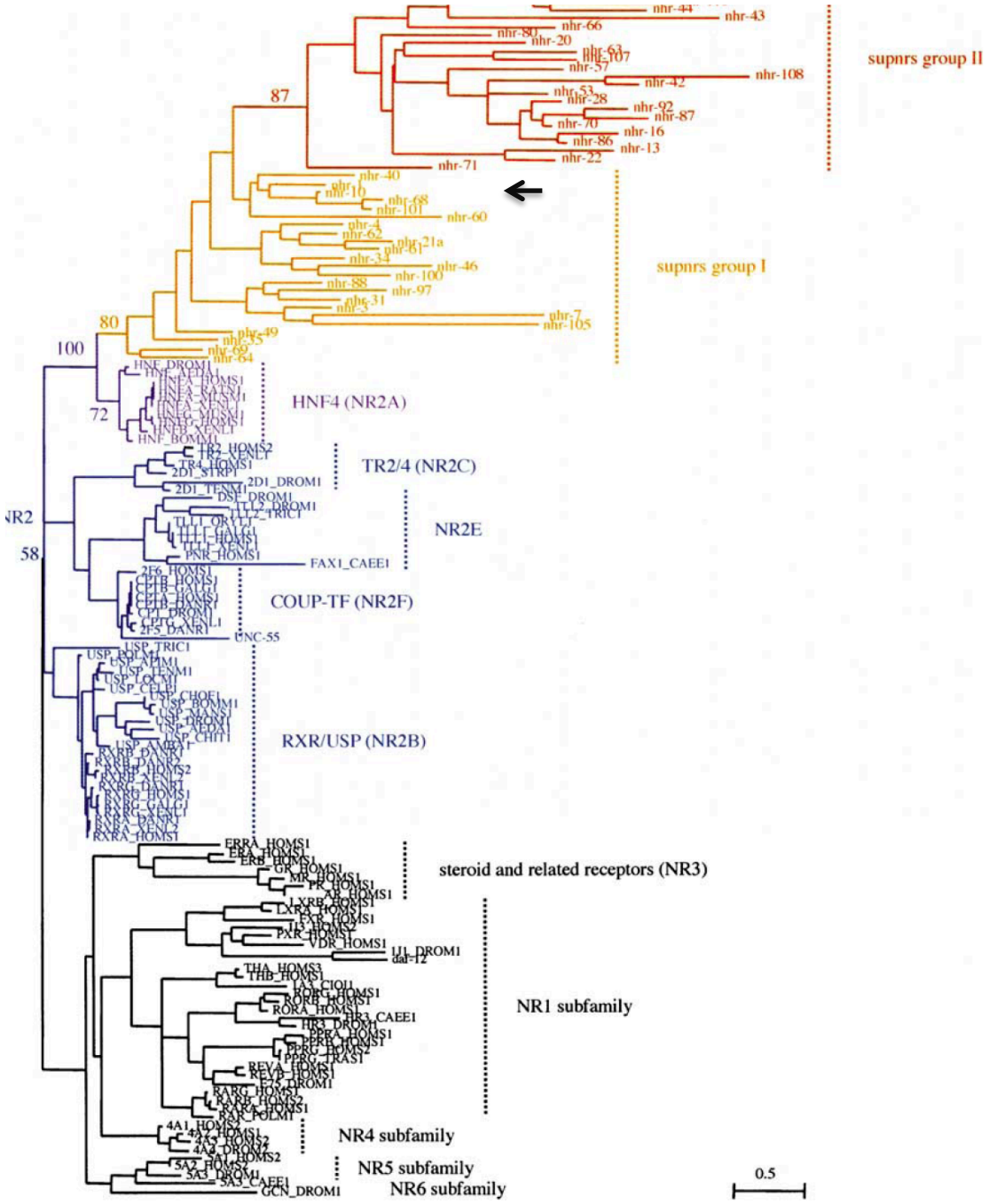

Figure 1.18 Phylogenetic relationships of *C. elegans* supplementary NRs
Supplementary NRs (supnrs) are a monophyletic group derived from HNF4, and they belong to the NR2A subfamily. Group II (orange) is more divergent that group I (yellow). Arrow indicates the *nhr-114* clade. In purple the HNF4s, in blue other members of the NR2 subfamily. The tree was constructed using complete amino acid sequence and maximum likelihood. The length of the branch is proportional to the estimated evolutionary change. Scale bar represents substitution per site. Image was taken from Robinson-Rechavi et al. (2005).

C. elegans	Functions	Mouse or human	Functions
DAF-12	Dauer formation, lipid metabolism, stage specification, life span	VDR	Bone differentiation, bile acid metabolism
NHR-8	Xenobiotic metabolism	CAR, PXR	Xenobiotic and bile acid metabolism
NHR-48	Unknown		
FAX-1	Neural differentiation	PNR	Photoreceptor fate
NHR-23	Molting, epidermal differentiation, dauer formation	ROR-α ROR-β ROR- γ	Cerebellar differentiation Circadian clock Thymopoiesis
NHR-25	Ventral closure, epidermal differentiation, molting, dauer formation	SF1 LHR	Steroidogenesis Cholesterol homeostasis, bile acid metabolism
NHR-41	Dauer formation	TR2/TR4	Unknown
NHR-49	Fatty acid metabolism	HNF4	Glucose homeostasis, liver metabolism
NHR-6	Ovulation	Nurr1 NGFI-B	Dopaminergic differentiation Apoptotic and non-apoptotic programmed cell death
NHR-67	Molting, growth, vulval formation	TLX	Forebrain development, neural stem cell maintenance
NHR-91	No obvious function	GCNF	Germ cell differentiation, embryogenesis
SEX-1 NHR-85	Sex determination Egg laying, molting?	revERB C	Circadian clock, transcriptional repression
UNC-55	Neural differentiation	COUPTF1 COUPTF2	Neural development

Table. 1.2 Some functionally described *C. elegans* NRs and their orthologs
Known functions of NRs are given for *C. elegans* and mammalian ortholgs (mouse or human). Table was taken and modified from Antebi 2006. Original evolutionary comparison is found in Robinson-Rechavi et al. 2005.

1.3.5 THE INTESTINAL NR CLADE

Using similarities in anatomical expression patterns, the NR family can be clustered in two broad groups (Bookout et al. 2006). One group is composed by NRs that regulate development, growth and reproduction; the other is composed by NRs that regulate nutrient uptake, metabolism and excretion of nutrients. The NR members of the latter group are expressed in the gastrointestinal tract and have being referred as the enteric or intestinal NR clade (Bookout et al. 2006, Schmidt and Mangelsdorf 2008). Specific intestinal NRs regulate nutrition by three major functional aspects: intestinal microbial community regulation, xenobiotic neutralization, or nutrient absorption. HNF4, the bile acid receptor FXR, the xenobiotic receptors PXR and CAR, the vitamin D receptor VDR and other NRs belong to the intestinal clade (Schmidt and Mangelsdorf 2008).

Bile acids and the activation of the bile acid receptor (FXR) prevent bacterial overgrowth in the intestine (Inagaki et al. 2006). This antimicrobial activity is mediated by bile acids detergent properties, and in part by activation of gene expression programs mediated by FXR. On the other hand, the xenobiotic receptors modulate the three phases of detoxifying pathways to eliminate toxic compounds and xenobiotics that are absorbed by the intestine. Detoxifying pathways chemically transform xenobiotics into less toxic (phase I) and more hydrophilic compounds (phase II) that can be transported out of the cell (phase III) (Schmidt and Mangelsdorf 2008).

1.4 AIMS OF THE THESIS

In *C. elegans,* germ cell fate specification is chiefly controlled by posttranscriptional mechanisms; and the overall germline development is influenced by the animal's nutritional status (Crittenden and Kimble, 2007; Korta and Hubbard, 2010). However, it remains unknown whether the germline-specific posttranscriptional gene expression mechanisms and germ cell fate decisions are molecularly linked nutrition, and if so, how they are linked. Metazoans evolved a way to coordinate development, metabolism and reproduction by using nuclear hormone receptors (NHRs) to regulate gene expression. NHRs comprise a family of transcription factors regulated by lipophilic signaling molecules (Mangelsdorf et al. 1995). The NHR family is highly expanded and diversified in *C. elegans* in comparison to other metazoans (Robinson-Rechavi et al. 2005). This raises the possibility that NHRs have being coopted during evolution to fulfill different roles and novel functional niches.

The NHR-114 was found in a screen for additional proteins that regulate *C. elegans* germline development. Thus, the central question posed in this thesis is: does NHR-114 integrate nutritional cues into posttranscriptional mechanisms and germ cell fate decisions? To address this question, this thesis aimed to characterize the *nhr-114* gene and to identify the germ line cell fate decisions that require *nhr-114* function. Furthermore, this thesis set to identify a nutritional cue linked to NHR-114 function; and to investigate whether *nhr-114* roles may be linked to germ cell fate decisions through a specific posttranscriptional regulator, the GLD-4 cytoplasmic poly(A) polymerase. By elucidating the functions of NHR-114, this thesis aims to provide a molecularly link between germline posttranscriptional mechanisms and a nutritional cue.

2. RESULTS

SECTION I: *NHR-114* IS REQUIRED FOR GERMLINE DEVELOPMENT AND FERTILITY

2.1 IDENTIFICATION OF NHR-114 AS A GLD-4 BINDING PROTEIN

The NHR-114 protein was a found as an interactor of GLD-4 full-length protein in a yeast-to-hybrid screen performed by Schmidt et al. (2008) (Table 2.1). Preliminary *nhr-114* RNAi knockdown experiments suggested germ line development defects (Schmid, 2008). In order to find NHR-114'S most closely related NHRs, a phylogenetic distance tree was constructed using the DNA-binding domain sequence of all NRs (Habermann B. and Eckmann CR, personal communication). NHR-114 was found to cluster with NHR-101, NHR-68 and NHR-10 (Figure 2.1 A). For some experiments in this thesis, NHR-68 and NHR-17 were chosen to serve for controls as closely related and less related NRs, respectively. Functional domains in the NHR-114 clade were predicted using the Pfam protein families database at http://pfam.sanger.ac.uk/ (Figure 2.1 B) (Finn et al. 2010). All NHRs in the NHR-114 clade have predicted standard NHR domains: DNA- binding and ligand-binding domains. In addition, NHR-114 has a predicted domain of unknown function, which is also present in some bacterial proteins. Similar to NHR-114, NHR-10 has a predicted ATP-binding domain, and a serum amyloid protein domain. The relevance and functionality of the non-standard NHR domains is unknown.

Gene	Name	Clones	Unique	Function
C36B1.8	*gls-1*	16	5	Unique to *C. elegans*
F14F3.1a	*vab-3*	16	8	Transcription factor
ZC123.3	-	12	4	Transcription factor
Y45G5AM.1a	***nhr-114***	7	2	Nuclear hormone receptor
ZK270.2b	*frm-1*	11	4	Transmembrane protein
F33G12.5	-	5	5	DNA-binding protein
W04D2.1a	*atn-1*	3	3	Actin binding protein
Y105E8B.4	*bath-40*	2	1	DNA-binding protein
C04F6.1	*vit-5*	2	1	Lipoprotein
T04C12.4	*act-3*	1	1	Structural muscle protein

Table 2.1 Top ten proteins recovered from a yeast two-hybrid screen using GLD-4 as a bait

20 Proteins were recovered as interactors of full-length GLD-4. Their protein function was predicted on the basis of protein family motifs (Screen was conducted by Schmid M., Stamford J., and Eckmann CR.)

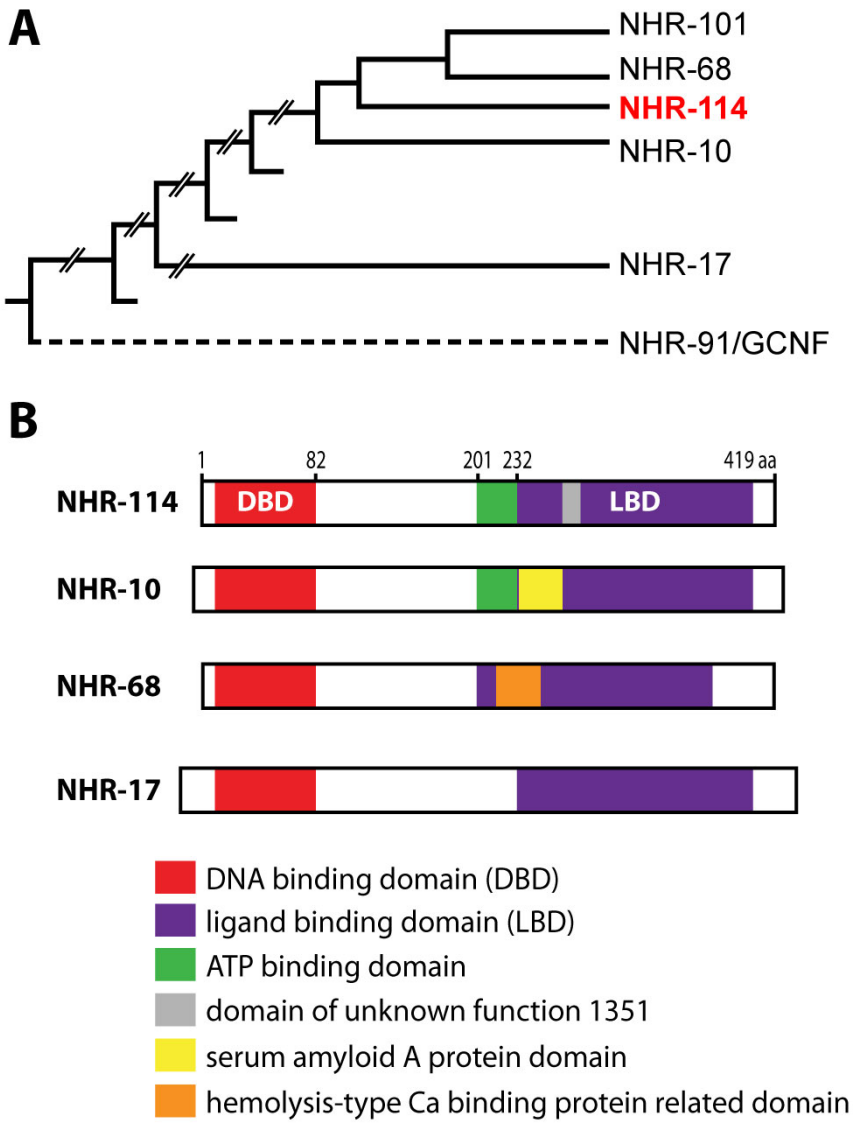

Figure 2.1 Phylogenetic relationship and proteins domains of the NHR-114 clade

(A) The phylogenic tree is based on the DNA-binding domain sequence. The terminal branches in the NHR-114 clade are proportional to evolutionary distance. Only a portion of tree is shown. **(B)** Stick diagrams represent protein domains (color coded), see main text for further description.

2.2 THE *NHR-114* GENE AND MRNA EXPRESSION

To study *nhr-114* functions *in vivo*, I generated a deletion mutation (Materials and Methods 4.1). I sibling screened mutated animals by PCR with different primers covering the *nhr-114* gene (see section in Materials and Methods). I isolated the *nhr-114(ef24)* mutant allele, which is a 1400 bp deletion that removes the last intron and the 3' UTR of *nhr-114* genomic region (Figure 2.2). Additionally, at later stage of the project *nhr-114(gk849)* and *nhr-114(tm3755)* mutant alleles were obtained from the *C. elegans* Gene Knockout Consortium and the National Bioresource Project (http://www.shigen.nig.ac.jp/c.elegans/index.jsp), respectively. *nhr-114(gk849)* mutant allele is a 1744 bp deletion with 11 bp inserted that removes the 5' UTR and initial exons. All alleles are homozygote viable. The *nhr-114(tm3755)* deletion is included within *nhr-114(gk849)* mutant allele, hence only *nhr-114(ef24)* and *nhr-114(gk849)* were chosen for characterization, see 2.2 A.

2.2.1 *NHR-114* MRNA IS A SINGLE SPLICE PRODUCT EXPRESSED IN GERM CELLS AND SOMA

The *nhr-114* gene was uncharacterized. Although bioinformatics predictions at the Wormbase database (www.wormbase.org) predicted two *nhr-114* mRNA isoforms only one isoform was recovered in the original yeast two-hybrid screen. I conducted RT-PCR analysis on wild-type cDNA to determine how many *nhr-114* mRNA isoforms are expressed, see Materials and Methods 4.2.7. Sequencing analysis revealed that *nhr-114* is expressed as a single mRNA, indicating that no alternative *nhr-114* splice variants exist. In addition, *nhr-114*'s 3'UTR is 120 nt long and 83% of its sequence is composed by AU nucleotides, see fig. 2.2 C. AU-rich sequences in 3'UTRs are correlated with increased mRNA instability (Barreau et al. 2005), suggesting that *nhr-114* mRNA may be unstable and NHR-114 protein may not be abundant.

To characterize *nhr-114* mRNA expression, I conducted Northern blot analysis on total RNA extracted from wild-type adult hermaphrodites or *nhr-114* hermaphrodites (Materials and Methods 4.2.6). In order to be able to detect any potential mutant *nhr-114* mRNA, the hybridization probe was designed to span exons that are not deleted in any of the *nhr-114* deletion alleles, see fig. 2.2 A. Since the *nhr-114(gk849)* allele deletes potential promoter regions, I expected that no *nhr-114* mRNA would be present. In contrast, since the *nhr-114(ef24)* allele deletes the AAUAAA sequence that precedes poly(A) tail addition in *nhr-114* mRNA (see RT-PCR analysis) I expected that a non-wild-type size mRNA may also be present.

Northern blot experiments detected *nhr-114* mRNA in wild-type animals as a single product of the predicted size by the RT-PCR analysis (Figure 2.3 A). *nhr-114* mRNA was not detected in *nhr-114(gk849)* mutants; two *nhr-114* mRNA transcripts of different size than wild type were detected in *nhr-114(ef24)* mutants, see fig. 2.3 A. This analysis confirmed the RT-PCR results that *nhr-114* mRNA is single product, and the lack of *nhr-114* mRNA expression in *nhr-114(gk849)* animals indicated this allele is likely to be a molecular null. As described in the following sections, *nhr-114(ef24)* animals show similar germline phenotypes to *nhr-114(gk849)* animals, suggesting that either *nhr-114* mRNA in *nhr-114(ef24)* mutants is not translated or the mutant NHR-114^{ef24} protein may not be functional.

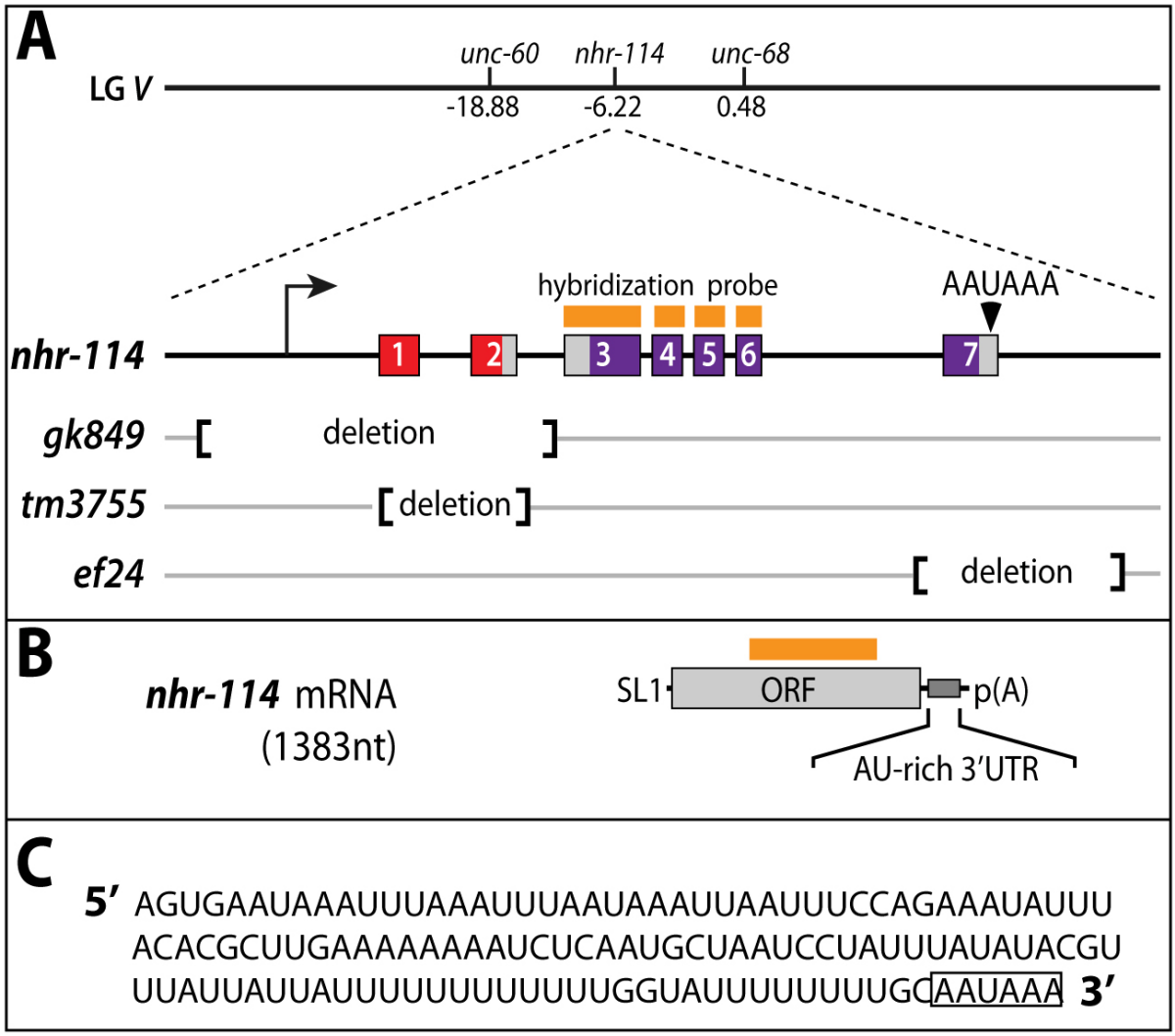

Figure 2.2 The *nhr-114* genomic locus

(A) *nhr-114* locus maps to position -6.22 on linkage group V (LG V). Arrow indicates the direction of transcription. Exons are shown as open boxes, in red those encoding the DNA binding domain, in purple those encoding the ligand-binding domain. AAUAAA sequence indicates the site of poly(A) tail addition. Genomic deletions in three *nhr-114* alleles are indicated in brackets. Yellow bars indicate the region used to synthesize a complementary hybridization probe. Note that the probe hybridizes to a region that is not comprised in any of the deletions, hence it can hybridize to any mutant *nhr-114* mRNA. **(B)** *nhr-114* locus produces a single SL1 *trans*-spliced mRNA, with a 6 nt long 5'UTR, a 1257 nt long open reading frame (ORF) and a 120 nt long 3'UTR, rich in AU nucleotides. **(C)** *nhr-114* mRNA 3'UTR contains AU-rich sequences. Box: denotes cleavage and polyadenylation signal.

To investigate whether *nhr-114* mRNA expression is restricted to hermaphrodites, Northern blot analyses were conducted on total RNA extracted from young *him-8(e1489)* adult males, *fog-1(253ts)* females, wild-type hermaphrodites with germ lines, or *glp-1(q224)* hermaphrodites that lack germ lines (Kimble and Austin, 1987). The expectation was that *nhr-114* mRNA would be mostly expressed in germ lines, however several indications suggested that somatic tissues would also express *nhr-114* mRNA (see below).

nhr-114 mRNA was detected in adult males, females, and wild-type hermaphrodites; in contrast, *nhr-114* mRNA detection was reduced in *glp-1(q224)* adult hermaphrodites that lack germ cells. Consistently, detection of a known germline-enriched mRNA, *inf-1* mRNA, is reduced in *glp-1(q224)* adult hermaphrodites that lack germ cells, see fig. 2.3 B. These results show that *nhr-114* mRNA is expressed in male, female and hermaphrodite animals. In addition, the reduction of *nhr-114* mRNA detection in hermaphrodites that a lack germ line clearly indicates that *nhr-114* mRNA is abundantly expressed in the germ line.

Germline genes required for germline development such as *gld-2* (Wang et al. 2002) or *gld-4* (work from this thesis, not shown) mRNA expression sharply increases at the L4 larval stage and adulthood, reflecting the sharp increase in germ cells number (for example the germline volume). To investigate whether *nhr-114* mRNA follows a similar pattern, Northern blot analysis was conducted on poly(A) selected RNA from wild-type animals of different developmental stages. *nhr-114* polyadenylated mRNA was equally detected throughout development with no apparent differences in detection levels in a specific stage, see fig. 2.3 C. This indicated that polyadenylated *nhr-114* mRNA is constantly expressed throughout development. Since constant mRNA levels throughout development do not reflect a germline-enriched gene, this data is therefore inconsistent with the interpretation that that *nhr-114* is mostly germline expressed. However, it remains possible that bulk *nhr-114* mRNA may increase with germ line volume, but a proportion of polyadenylated mRNA is kept constant throughout development. This suggests that polyadenylation may play a regulatory role in *nhr-114* mRNA expression.

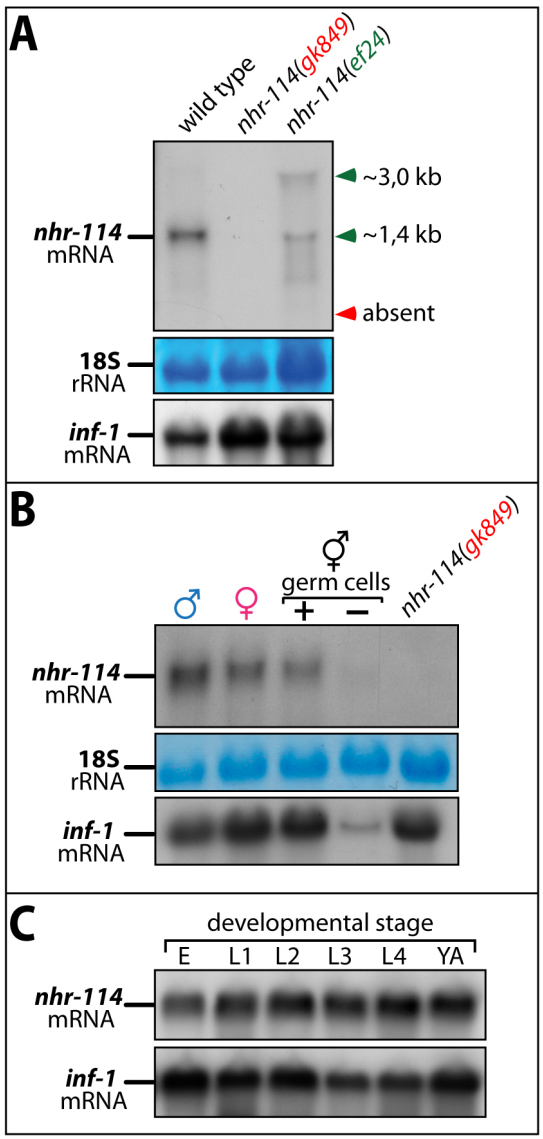

Figure 2.3 Analysis of *nhr-114* mRNA expression
Northern blot analysis of *nhr-114* mRNA using anti-sense *nhr-114* probe described in figure 4.2. **(A)** Total RNA from mixed-stage wild-type or mutant *nhr-114* hermaphrodites. Anti-sense *nhr-114* hybridizes to a single product in the wild type but not in *nhr-114(gk849)* mutants (red triangle indicates absence of predicted truncated mRNA). In *nhr-114(ef24)* mutants two different products are present (green triangles, kb: kilobases). 18S rRNA serves as loading control, *inf-1* mRNA is an internal control for a germline-enriched gene. **(B)** Total RNA from young *him-8(e1489)* adult males (blue male symbol), *fog-1(253ts)* females (pink female symbol), wildtype hermaphrodites (black symbol) with germ lines (+), *glp-1(q224)* hermaphrodites that lack germlines (-). RNA extracted from *nhr-114(gk849)* hermaphrodites serves as a negative control for the anti-sense *nhr-114* probe. **(C)** Developmental expression of *nhr-114* mRNA using poly(A)$^+$ selected mRNA. E: embryos, L1-L4: larval stages, YA: young adults. Note that the translation initiation factor *inf-1* mRNA also follows a similar expression pattern that *nhr-114* mRNA.

2.2.2 *NHR-114* mRNA IS EXPRESSED IN THE GERMLINE AND SOMA

To investigate *nhr-114* mRNA expression pattern in the germ line, *in situ* hybridizations were conducted on extruded gonads from wild-type hermaphrodite or *nhr-114(gk849)* hermaphrodites (Materials and Methods 4.2.3). Anti-sense *nhr-114* hybridization probe was generated using *nhr-114* mRNA sequence described in figure 2.2 A, which is the same used for Northern blots. Since *nhr-114(gk849)* animals express no *nhr-114* mRNA these germ lines serve as a specificity control for the hybridization. As expected, only background signal was detected in *nhr-114(gk849)* germ lines, indicating that the anti-sense *nhr-114* probe is specific (Figure 2.4). In contrast to *nhr-114(gk849)* germ lines, a specific signal was detected in the wild type throughout the germ line, indicating that *nhr-114* mRNA expression is not restricted to a specific germ line region but rather present in the cytoplasm of all germ cells, see fig. 2.4 A.

The Northern blot analysis indicated *nhr-114* mRNA is also expressed in somatic tissues. Taking advantage of the fact that the intestine may remain attached to the germ line during material preparation, *in situ* hybridization was conducted on intestines of wild-type hermaphrodites or *nhr-114(gk849)* hermaphrodites. Consistent with the specificity of the hybridization probe only background signal was detected in *nhr-114(gk849)* intestines. In contrast, in wild-type intestines a clear signal was detected within the nucleoplasm of all intestinal cells, indicating that *nhr-114* mRNA is abundantly expressed in the intestine, see fig. 2.4 C-E. Although the expression of *nhr-114* mRNA in a somatic tissue was expected, the relative abundance of mRNA in the nucleoplasm versus to the cytoplasm, inverse to the expression pattern of germ cells, was highly unexpected.

To investigate whether the nucleoplasmic localization is a common feature among *nhr* mRNAs in *C. elegans,* I examined the expression of all *nhr* mRNAs reported in the *in situ* hybridization database of the Nematode Expression Pattern Data Base (http://nematode.lab.nig.ac.jp/). Out of eight reported *nhr* mRNAs with expression in intestines (*nhr-6, -23, -25, -45 -49, -53, -55* and *-90*) only *nhr-6* and *nhr-45* mRNAs show nucleoplasmic localization, indicating that nuclear localization is not a common feature of *nhr* mRNAs but some have nuclear enrichment. Therefore, *nhr-114* mRNA nuclear localization may suggest a regulatory mode for *nhr-114* mRNA translation in the intestine.

Taken together, the *in situ* hybridization analysis confirmed that *nhr-114* mRNA is expressed in germ cells. In addition this analysis identified the intestine as at least one somatic tissue that expresses *nhr-114* mRNA. Therefore, these experiments conclusively addressed that *nhr-114* is expressed in the germ cells and put forward the hypothesis that an NHR-114 and GLD-4 complex exist in the germ line. In addition, the finding of *nhr-114* mRNA in the intestine suggested that *nhr-114* function is linked to diet.

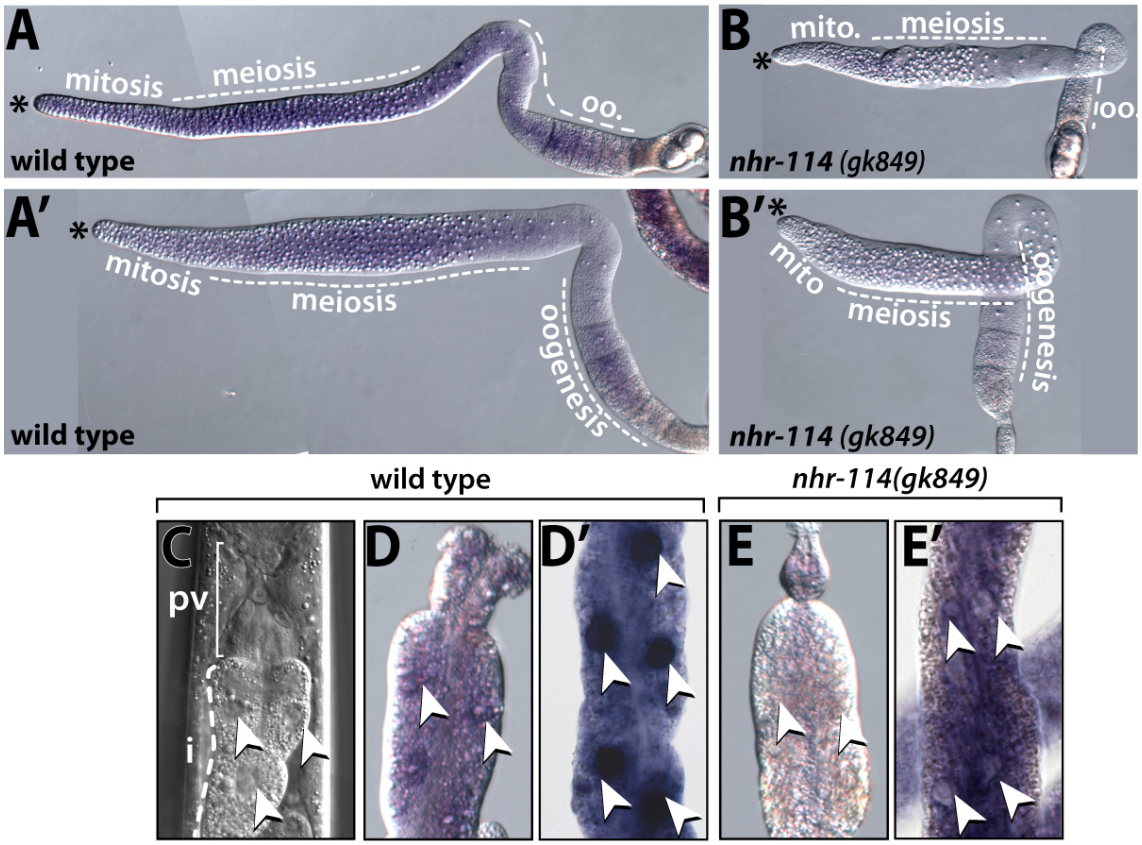

Figure 2.4. *nhr-114* mRNA localization
In situ hybridizations using anti-sense *nhr-114* mRNA probe, described in Fig.1A. **(A-A')** Two representative wild-type germ lines show *nhr-114* mRNA present throughout the germ line (purple staining). **(B-B')** *nhr-114(gk849)* germ lines serve as a negative control and show no *nhr-114* mRNA expression after same time of color development. Asterisk indicates the position of the distal tip cell, and the distal gonad. **(C)** DIC microscopy image of intact animal focusing on the most anterior part of the intestine. pv: pharyngeal valve (bracket), i: intestine (dotted line). Arrowheads indicate intestinal nuclei. **(D-D')** Two wildtype extruded intestines show *nhr-114* mRNA localized to intestinal nucleoplasm. (E-E') Two *nhr-114(gk849)* intestines show no *nhr-114* mRNA. D' and E' are longer incubation times with the color-developing substrate.

2.3 GERMLINE DEVELOPMENT AND FERTILITY REQUIRE THE FUNCTION OF *NHR-114*

Once *nhr-114* mRNA expression in germ cells was confirmed, I set to investigate whether *nhr-114* is required for germ line development in hermaphrodites. To address this question, the reproductive fitness of *nhr-114* homozygote mutants was evaluated by counting the number of fertile and sterile animals within a population, and the number of embryos sired by fertile *nhr-114* homozygote mutants, see Materials and Methods 4.1.2. In this thesis, sterile animals are defined as those that contain no embryos; hence sterile animals are easily discernable from fertile animals using a dissecting scope.

In the wild-type strain, all hermaphrodites scored were self-fertile, and no sterile animals were found. Furthermore, wild-type hermaphrodites lay on average 300 embryos which virtually all develop into adults (no embryonic lethality) hence hermaphrodites have an effective brood of ~300 animals. In contrast to the wild type, both *nhr-114(gk849)* and *nhr-114(ef24)* mutants have high penetrance of sterility and a reduced brood size that is partially explained by an uncharacterized embryonic lethality. Table 2.2 summarizes the data. This analysis indicated that *nhr-114* function is required for hermaphrodite fertility.

	Wild type	***nhr-114(gk849)***	***nhr-114(ef24)***
Penetrance of sterility:			
Fertile adults	100%	55%	9%
Sterile adults	0%	45%	91%
Scored animals, n=	>2000	3400	3158
Brood analysis:			
Embryonic lethality[4]	<1%	7.2%	6.4%
Embryos n=	>100	306	637
Effective brood size[5]	~300	141	191
Mothers, n =	9	94	17

Table 2.2 Reproductive fitness in *nhr-114* mutant hermaphrodites
Analysis of homozygote young adults grown at 20°C. Fertile animals contain at least one embryo in uterus. Embryonic lethality indicates the percentage of embryos that do not develop further. Animals that reach adulthood represent the effective brood. The number of mother used for brood analyses is indicated.

2.3.1 *NHR-114* MUTANTS ARE GERMLINE DEVELOPMENT DEFECTIVE

To investigate whether defective germ line development was the cause of impaired fertility in *nhr-114* mutants, live *nhr-114* adult hermaphrodites were analyzed by DIC microscopy. The *C. elegans* germ line has a stereo typical spatiotemporal organization, see wild-type hermaphrodite in figure 2.5 A. Different cell types within the germline, such as mitotic cells, meiotic cells, oocytes and mature sperm are easily recognized by its their cellular morphology and arrangement using DIC microscopy. Considering that NHR-114 protein is a potential GLD-4 protein interactor, it was antcipated that *nhr-114* sterile hermaphrodites would show similar phenotypes to *gld-4* sterile hermaphrodites: small germ lines that contain sperm but lack oocytes (Schmid et. al 2009).

In contrast to wild-type hermaphrodites, both *nhr-114(ef24)* and *nhr-114(gk849)* sterile animals have small germ lines that contain sperm and lack oocytes, similar to *gld-4* sterile germ lines. Contrary to wild type, in which germ cells are mononucleated and syncytial, *nhr-114* sterile germ lines have a grape-like morphology and multinucleated germ cells indicative of cellularization defects combined with an overall germline disorganization, see fig. 2.5 B. This analysis indicated that *nhr-114* function promotes germline proliferation and oogenesis, two aspects of *gld-4* function. In addition, *nhr-114* function promotes germ line organization, an unknown function of *gld-4*.

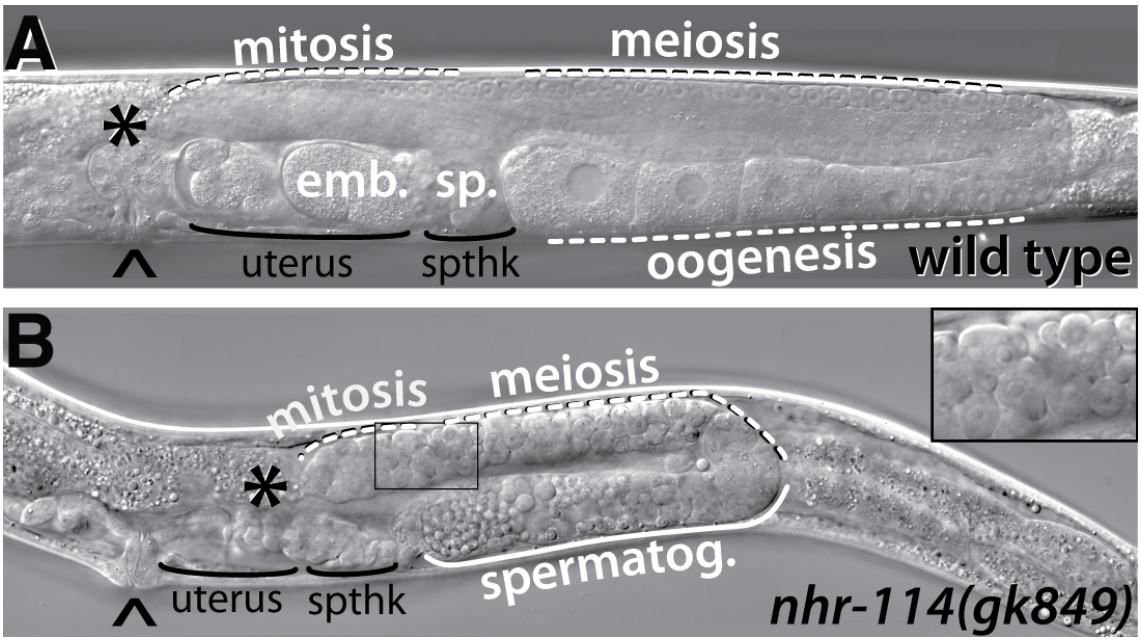

Figure 2.5 Morphological defects in *nhr-114* sterile germ lines
DIC microscopy images of adult hermaphrodites of similar age. Asterisk indicates the position of the distal tip cell, marks the distal end of the gonad. Caret indicates the position of the vulva. **(A)** Cell types within the wild type germline: mitotic cells (mitosis), early meiotic cells (meiosis), oocytes (oogenesis) and mature sperm (sp.) stored in the spermatheca. Presence of embryos (emb.) in uterus indicate fertile animal. **(B)** A typical *nhr-114(gk849)* adult hermaphrodite contains a small germ line of fewer mitotic and meiotic cells than in wild type, it lacks oocytes, but contains mature sperm and residual bodies that indicate spermatogenesis (spermatog.). Germ cells have grape-like morphology and some are multinucleated. Inset image is scaled two times and highlights distal germ cell nuclei.

To characterize in further detail the unexpected germline disorganization phenotype, wild-type and *nhr-114(gk849)* hermaphrodite gonads were extruded and immunostained with markers for cell cortex (anti-anillin) and the nuclear pore complex (anti-NPC) (Materials and Methods 4.3.2). These cellular markers clearly delimit the nuclear (NPC) and germ cell boundaries (cortex) to allow an assessment on germ cell multinucleation and cellularization. As expected, in wild-type hermaphrodite germ lines each nucleus (NPC staining) is surrounded by a cell membrane (cortex staining) that is not fully enclosed, thus forming a syncytium with a wide rachis at center of the germ line (Figure 2.6 A).

In contrast to wild type, *nhr-114(gk849)* hermaphrodite germ lines show one or more nuclei (NPC staining) surrounded by an irregular cell membrane (cortex staining) that appears fully enclosed, as in the distal end of the gonad in fig. 2.6 B. The presence of a syncytium is not apparent but only a collapsed rachis, see fig. 2.6 B. Furthermore, analysis of germ cell chromatin stained with the nucleic acid dye DAPI, confirmed that *nhr-114* germ lines have multinucleated cells, and in addition chromatin aberrations (Figure 2.7).

Figure 2.6 Germline organization defects in *nhr-114* sterile germ lines
Immunostaining of extruded gonads from adult hermaphrodites to visualize cellular organization. Cell cortex is visualized using anti-anillin, the nuclear pore complex using anti-NPC antibodies **(A)** Wild-type germ line shows a syncytium with a wide rachis at center of the germ line. Note that one nucleus (NPC staining) is surrounded by a cell boundary (cortex staining) that is not fully enclosed. **(B)** *nhr-114(gk849)* germ line shows irregular cell boundaries (cortex staining) and the presence of a syncytium is not apparent but only a collapsed rachis. Note that one or more nuclei (NPC staining) appear fully enclosed by a cell boundary. Asterisk marks the distal gonadal end.

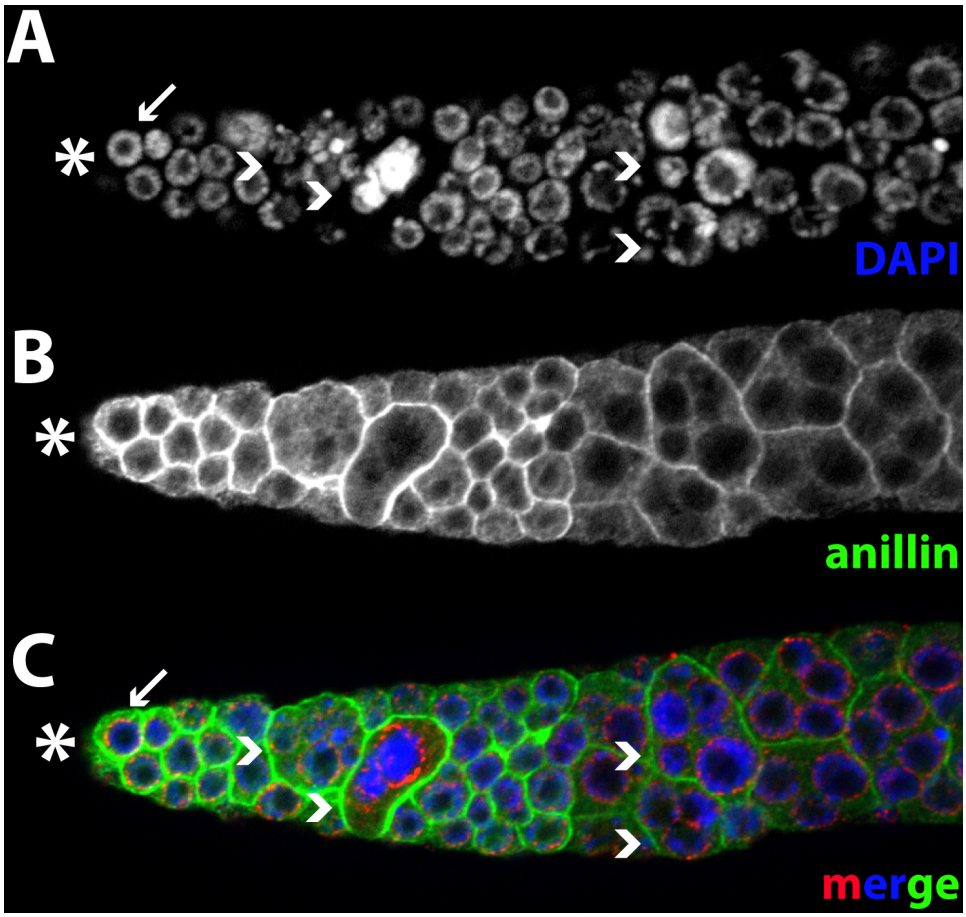

Figure 2.7 Germ cell multinucleation defect in *nhr-114(gk849)* germ lines
Immunostaining on extruded gonad from adult hermaphrodite to visualize cellular organization in the distal end of the gonad. Cell cortex is visualized using anti-anillin, the nuclear pore complex using anti-NPC antibodies, and chromatin is stained with DAPI. **(A)** DAPI staining shows chromatin morphology. Arrow indicates wild-type-looking chromatin. Arrowheads indicate aberrant chromatin. **(B)** Cell cortex staining highlights germ cell boundary organization. **(C)** Merged image from cell cortex (green), NPC (red) and chromatin (blue). Arrow indicates a wild-type-looking germ cell containing one nucleus surrounded by a cell membrane. Arrowheads indicate multinucleated germ cells containing more than one nucleus surrounded by a cell membrane. Note that all aberrant nuclei are found within multinucleated cells. Asterisk indicates the position of the distal tip cell and distal gonad.

2.3.2 *NHR-114* STERILE GERM LINES ACCUMULATE LOW LEVELS OF THE OOGENIC MARKER GLD-1

In wildtype adult hermaphrodites, meiotic cells committed to oogenesis accumulate the oogenic protein GLD-1 at early meiotic stages (Jones et al. 1996); hence GLD-1 can be used as an oogenesis marker (Figure 2.8 C). To investigate whether *nhr-114(gk849)* sterile germ lines have an oogenic identity, wild type and *nhr-114(gk849)* adult hermaphrodite gonads were extruded and immunostained with markers for meiosis (anti-HIM-3) and the oogenic marker (anti-GLD-1). HIM-3 is a lateral element component of the synaptonemal complex, a proteinaceous structure that forms during meiotic recombination (Zetka et al. 1999).

In the adult wild type hermaphrodite germ line, HIM-3 was localized on chromosomes that initiated meiosis, as judged by the typical crescent-shape nuclei. GLD-1 was localized to the cytoplasm of the same cells, indicating that meiotic cells had oogenic identity, see fig. 2.8 A-C. Similar to wild type, in *nhr-114(gk849)* sterile germ lines HIM-3 was localized on in nuclei chromosomes located further proximally of the distal end of the germ line. However, in 7 out of 10 cases (n=10) GLD-1 was weakly detected and no oocytes were present, indicating that these meiotic cells do not have an oogenic identity, see fig 2.8 B-D. In the remaining 3 germ lines, GLD-1 levels were high, but only two germ lines contain oocytes, suggesting that GLD-1 levels correlate with germ line sexual fate, and that GLD-1 is not a direct target of *nhr-114* regulation. This result suggests that *nhr-114(gk849)* meiotic cells in the adult fail to adopt an oogenic identity. Two simple explanations are that NHR-114 may indirectly promote GLD-1 protein accumulation, or that the obligatory sperm-to-oocyte switch does not occur in *nhr-114* mutants.

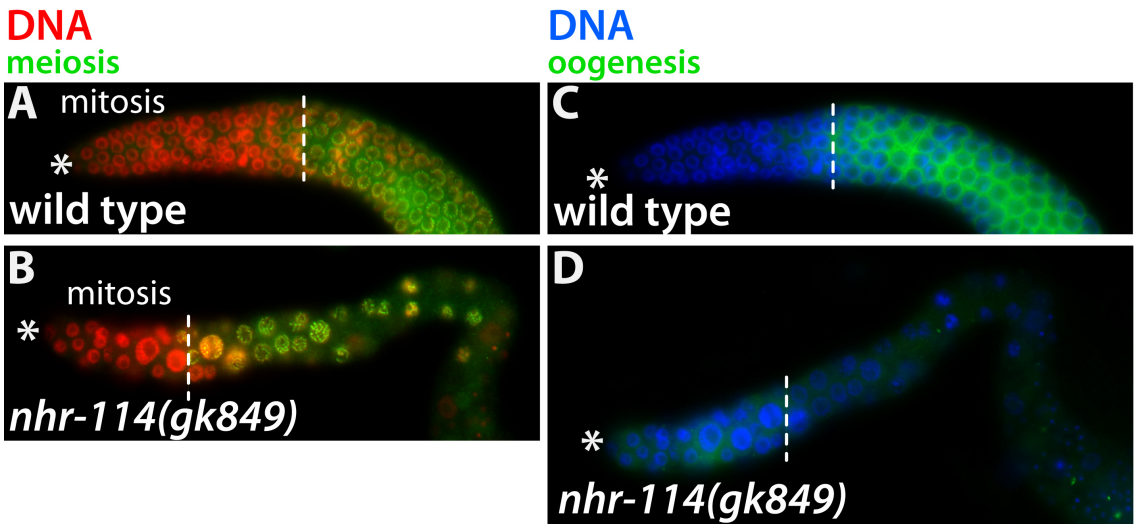

Figure 2.8 Germ cell fates in *nhr-114* distal germ lines
Immunostaining on extruded germ lines from adult hermaphrodites to visualize the oogenic fate. Meiotic cells are visualized using anti-HIM-3, oogenesis is visualized using anti-GLD-1, and DNA is stained with DAPI. **(A-B)** Anti-HIM-3 staining (green) on chromosomes is used in combination with DNA morphology to set the boundary between mitosis and meiosis (dotted line). Meiotic nuclei show anti-HIM-3 staining; mitotic nuclei lack HIM-3 staining. Note that *nhr-114* germline in B has a smaller mitotic region than wild type in A, and irregularly enlarged nuclei. **(C-D)** Anti-GLD-1 staining (green) accumulates in the cytoplasm of wild type meiotic cells, but not in sterile *nhr-114(gk849)* meiotic germ cells. Asterisk indicates the position of the distal tip cell.

2.3.3 *NHR-114* GERM LINES EXPRESS GERM CELL MARKERS

nhr-114 germ lines have a unique combination of defects that are complex. In particular, the syncytial disorganization and chromatin aberrations were clearly distinctive from mutants of germline mutants in posttranscriptional control machinery components. Germ cells are totipotent and can be induced to differentiate into somatic cell types. Also, extremely low GLD-1 levels can cause loss of the germ cell identity (Ciosk et al. 2006, Tursun et al. 2011). To investigate whether *nhr-114* germ lines contained only germ cells, but no somatic cells, wild-type and *nhr-114(gk849)* hermaphrodite gonads were extruded and immunostained with germ cells fate markers of the germline exclusively expressed proteins GLH-1/2 and NOS-3. GLH-1 is a P-granule component (Gruidl et al. 1998) and NOS-3 is a cytoplasmic diffusely expressed protein (Kraemer et al. 1999).

In wild-type germ lines, perinuclear GLH-1/2 localized to P granules in all germ cells except mature spermatocytes; cytoplasmic NOS-3 staining was detected in all germ cells except primary and mature sperm (Figure 2.9 A-C). In *nhr-114(gk849)* germ lines, similar to wild type, perinuclear GLH-1/2 staining was also detected in all germ cells except mature sperm; cytoplasmic NOS-3 staining was detected in all germ cells except primary and mature sperm, see fig. 2.9 D-F. Therefore this immunostaining conclusively showed that despite the abnormal chromatin morphology, *nhr-114* germ lines contain only cells with germ cell identity. From here on, sterile germ lines with the combination of underproliferation, germline disorganization and lack of oocytes will be referred to as Nhr-114 phenotypes, and the sterility upon *nhr-114*-loss will be referred to as Nhr-114 sterility.

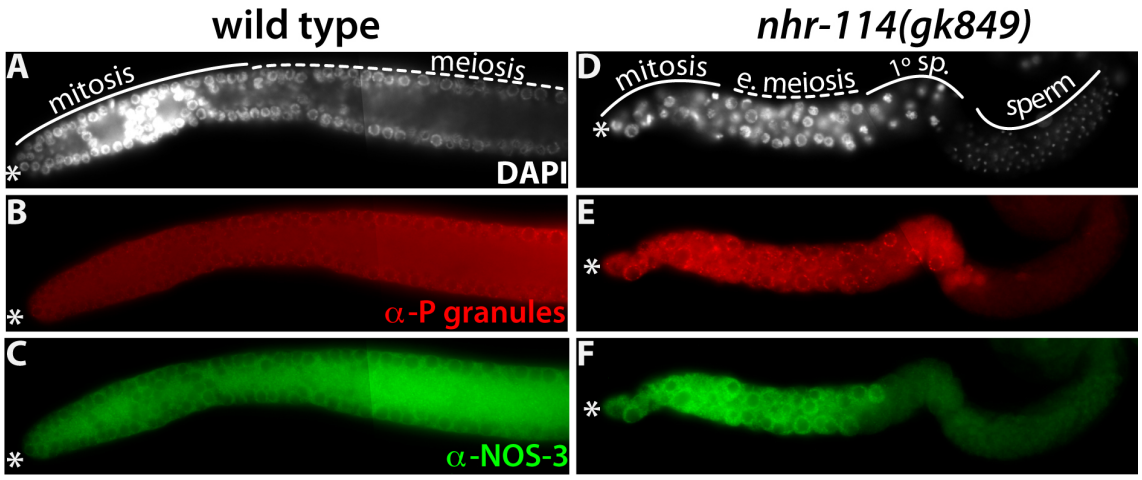

Figure 2.9 *nhr-114* germ lines express germ cell fate markers
Immunostaining of extruded gonads from adult hermaphrodites to visualize germ cell fate identity using anti-GLH-1/2 and anti-NOS-3 antibodies. DAPI stains chromatin. Asterisk indicates the position of the distal gonadal end. **(A-C)** Distal fragment of wild type adult hermaphrodite shows perinuclear GLH-1/2 staining (anti-P granules) in mitotic, meiotic cells and primary sperm (not shown), but not in mature sperm (not shown). Cytoplasmic NOS-3 is present in mitotic and meiotic cells, but not in primary nor in mature sperm (not shown) **(D-F)** *nhr-114(gk849)* complete germ line shows perinuclear GLH-1/2 staining in mitotic and early meiotic cells (e. meiosis) and primary sperm (1° sp.), but not in mature sperm. Cytoplasmic NOS-3 is observed in mitotic, early meiotic cells (e. meiosis), but not in primary spermatocytes neither in mature sperm.

Although the sterility phenotype is always similar among *nhr-114* mutants, its penetrance and the fecundity levels are highly variable among *nhr-114* homozygote mutant batches. For example, the penetrance of sterility within the brood of one *nhr-114(gk849)* mother could be on average 80%; however, in a different brood from another *nhr-114(gk849)* mother the penetrance could be on average 20%. Therefore, I set to investigate whether delivering *nhr-114* dsRNA by injection (RNAi knockdown) yields a consistently high percentage of sterile *nhr-114*(RNAi) animals to reliably study *nhr-114* loss-of-function. First, to validate the specificity of *nhr-114* RNAi knockdown effects, and rule out possible RNAi off-target effects, *nhr-114* dsRNA was injected into wild type and *nhr-114(gk849)* adult fertile hermaphrodites (Materials and Methods 4.1.5.1). *nhr-114* RNAi knockdown in the wild type strain was expected to yield highly sterile *nhr-114*(RNAi) progeny. In contrast, if the *nhr-114* RNAi knockdown were specific, the penetrance of sterility in the progeny of injected *nhr-114(gk849)* mothers should remain similar to that of the uninjected *nhr-114(gk849)* mothers.

~80% of *nhr-114*(RNAi) progeny hermaphrodites were sterile, the remaining 20% was fertile (n>3000). In contrast to *nhr-114* knockdown effect in the wild type strain, the penetrance of sterility among *nhr-114(gk849); nhr-114*(RNAi) remained similar to that of uninjected *nhr-114(gk849)* mothers (<1% steriles, n>1400). This indicates that *nhr-114* RNAi knockdown specifically affects *nhr-114* mRNA and has no off-target effects. Since *nhr-114* RNAi knockdown is highly specific, and penetrance of 80% sterility is highly reproducible, most of the following analyses were conducted using *nhr-114* RNAi knockdown by microinjection. In all upcoming experiments, more than or equal to 80% sterility was set as the base line of Nhr-114 sterilty.

2.3.4 VALIDATION OF RNAI KNOCKDOWN TO STUDY *NHR-114* LOSS

Due to the highly expanded NHR family in *C. elegans*, it is likely that some of *nhr* functions are redundant among closely related members. NHR-68 is part of the NHR-114 clade, and *nhr-68* mRNA is expressed in the germline cytoplasm (The Nematode Expression Pattern Data Base, http://nematode.lab.nig.ac.jp/). Therefore, I investigated if Nhr-114 defects are specific upon *nhr-114* loss, or can be caused by the loss of *nhr-68*. To address this point, *nhr-114* and *nhr-68* RNAi knockdown experiments were conducted in parallel, and their adult progeny was scored for sterility. In contrast to *nhr-114*(RNAi), less than 1% of *nhr-68*(RNAi) animals were sterile, the remaining 99% was fertile (n>1300), indicating that *nhr-68* is not required for fertility. This suggested that *nhr-114* but not the closely related and germline-expressed *nhr-68,* is specifically required for fertility.

2.4. *NHR-114* PROMOTES GERMLINE ORGANIZATION, PROLIFERATION AND OOGENESIS

To characterize in better detail how the loss of *nhr-114* affects germ line fates, *nhr-114*(RNAi) and *nhr-68*(RNAi) animals were fixed and stained with the nuclear dye DAPI to visualize chromatin. This allows distinguishing practically all germ cell stages based on their stereotyped chromosomal architectures (Figure 2.10 A). This morphological analysis categorized the three major defects observed in *nhr-114* mutant germ lines: underproliferation, germline disorganization and defective oogenesis.

In the wild-type strain, all adult hermaphrodites contain mitotic and meiotic chromatin of homogeneous size without chromatin aberrations. In addition, all germ lines contained diakinesis arrested oogenic chromatin, condensed mature sperm, and chromatin of dividing cells in embryos, supporting full fertility (Table 2.3, first column). In contrast to wild type, *nhr-114*(RNAi) sterile germlines fall in two categories of underproliferation: a Glp-like germ line (Germ line proliferation defective), or an underproliferated germ line with abnormal chromatin, see fig. 2.10 B. The abnormal chromatin is of two sorts: fragmented chromatin figures, as in fig. 2.10 B; or enlarged or shrunk but complete chromatin figures, as in fig. 2.10 C. Although no formal assessment of the nuclei ploidy was carried out, the level of chromatin compaction is apparently variable. Most of *nhr-114* sterile germ lines contain sperm chromatin, a third of the sterile germ lines contain chromatin in early meiotic stages, but lack differentiated gamete chromatin, see table 2.3. These analyses indicated that *nhr-114* function is necessary for germ cell proliferation, germline organization, genomic stability and oogenesis, hence implies that loss of *nhr-114* impairs several aspects of germline development. In contrast to sterile *nhr-114*(RNAi) germ lines, *nhr-68*(RNAi) germ lines have no chromatin aberrations and the very low sterility arises from a single cause: lack of oocytes, see figure 2.11 and third column in table 2.3.

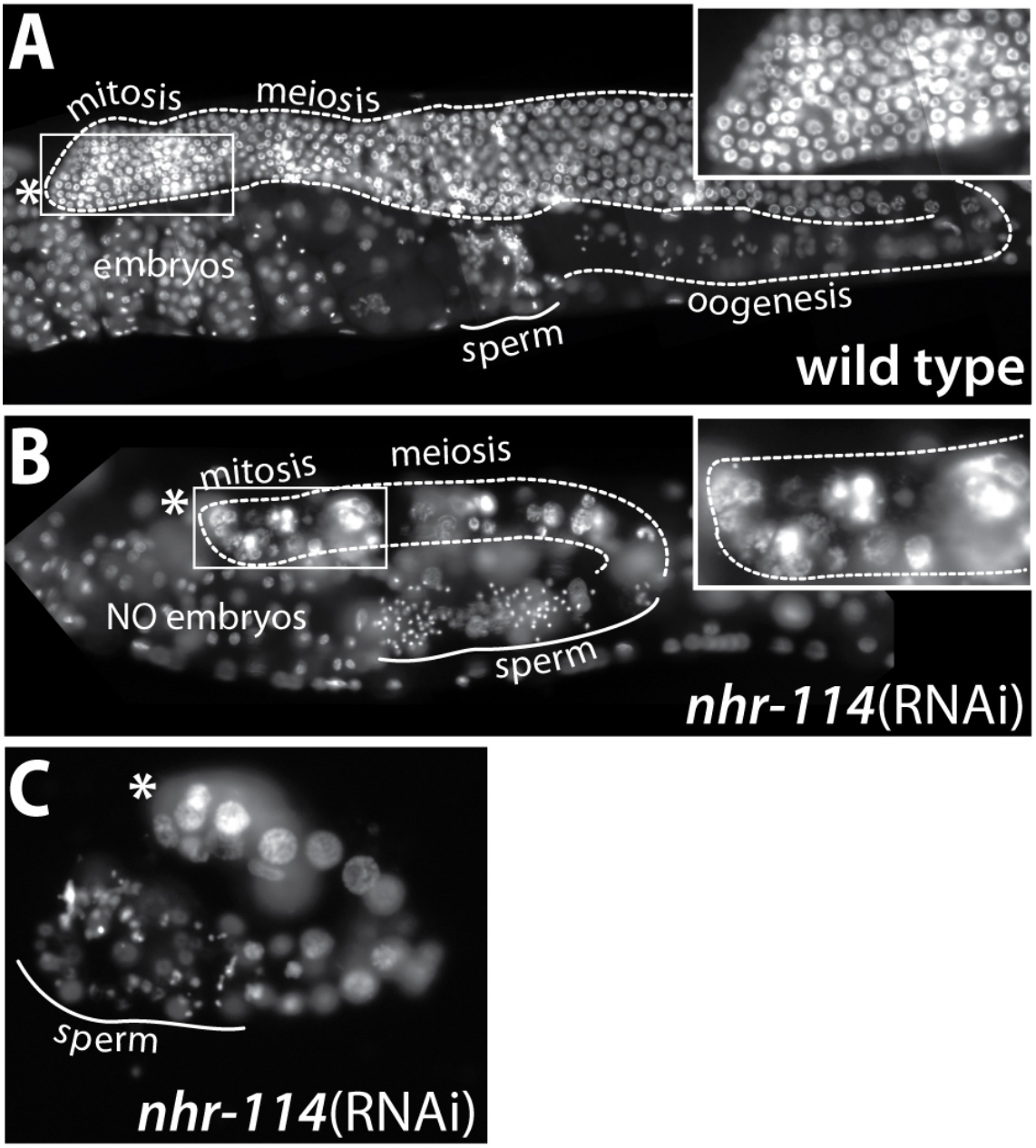

Figure 2.10 *nhr-114* is required for proper germ line development
Germ cell chromatin is visualized with the nucleic acid dye DAPI. Germ lines are delineated by a dotted or continuous line (sperm). **(A)** Adult wild type animal shows germ line with mitotic, meiotic, oocyte and sperm nuclei. Inset: highlights distal mitotic chromatin of homogeneous size. **(B)** Adult *nhr-114*(RNAi) animal with typical sterile germ line shows aberrant mitotic and meiotic nuclei, and only sperm, but not oocyte nuclei. Inset: highlights abnormal distal mitotic chromatin condensation and size heterogeneity (arrows). Compare the reduced density of mitotic nuclei with in A. **(C)** Extruded adult hermaphrodite germ line shows enlarged distal nuclei and aberrant spermatogenesis with chromatin bridges (arrows). Insets and image in C are scaled two times. Asterisk indicates the position of the distal gonadal end.

	Wild type Steriles: 0%	***nhr-114*(RNAi)** Steriles: ~80%	*nhr-68*(RNAi) Steriles: <3%
Scored germ lines:	>200	178	198
Proliferative phenotypes:			
Glp-like	0%	6%	0%
Underproliferation and multinucleation	0%	**88%**	0%
Wild-type like	100%	6%	100%
Gametes produced:			
Sperm and oocytes	100%	3%[1]	0%
Sperm only	0%	**65%**	100%
No differentiated gametes	0%	35%	0%

Table 2.3 Germ line defects in *nhr-114* and *nhr-68* sterile germ lines
Analysis of adult wild type and *nhr-114*(RNAi) hermaphrodites grown at 20°C; *nhr-68*(RNAi) were grown at 25°C. On the basis of the overall germline size, three classes of germ lines are distinguished. First, Glp-like (Germ line proliferative defective phenotype) gonads have less than 10 germ cells or no germ cells, presence of mature sperm is not strictly correlated. Second, germ line underproliferation and germ cell multinucleation phenotypes refer to small gonads with more than 10 germ cells, the syncytium is disorganized and contains multinucleated cells and chromatin aberrations. Third, germ lines appear of wild type size; however, exact number of germ cells was not counted. Germ lines with no differentiated gametes have germ cell nuclear morphology that resembles pachytene, but not gametes can be identified by nuclear morphology (DAPI staining) or cellular morphological features (DIC microscopy). n.a.: not applicable because these categories apply to sterile germ lines.
[1] Despite having sperm and oocytes these germ lines lack embryos.

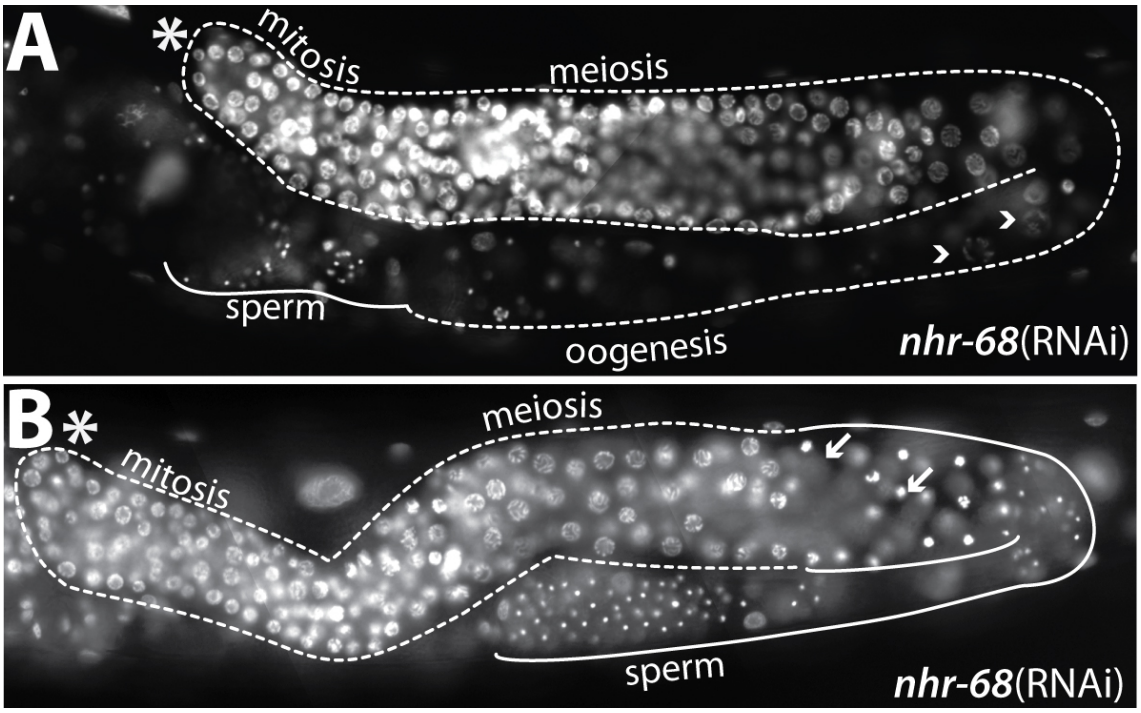

Figure 2.11 *nhr-68*(RNAi) phenotype is different from Nhr-114 phenotypes
Germ cell chromatin is visualized with the nucleic acid dye DAPI. Germ lines are delineated by dotted or continuous lines (sperm) **(A)** Fertile adult shows germ line with, mitotic, meiotic, oocyte (arrowhead) and sperm nuclei. **(B)** Adult *nhr-68*(RNAi) animals show typical sterile germ lines with mitotic, meiotic, and only sperm but not oocytes nuclei. Distal primary sperm (arrows) is indicative of active spermatogenesis at a place and time where oogenesis should be occurring. Asterisk indicates the distal gonadal end.

2.4.1 *NHR-114* FUNCTION IS REQUIRED FOR MALE GERMLINE DEVELOPMENT

The *nhr-114*(RNAi) germ line analysis indicated that in most cases *nhr-114* sterile germ lines contain sperm but lacked oocytes, suggesting that *nhr-114* function is essential for oogenesis, but not for spermatogenesis, hence *nhr-114* function may be restricted to female germ lines. Since wild-type hermaphrodites only occasionally sire males, the *him-8* mutant background (*h*igh *i*ncidence of *m*ales) was used to generate large numbers of males. Therefore, to investigate if *nhr-114* function is required for male germline development, *nhr-114* function was knocked-down in *him-8(e1489)* hermaphrodites by RNAi.

The adult male germline has a topologically similar organization to the hermaphrodite germline: germ cells proliferate distally and form a pool of mitotic cells that proximally enter meiosis and differentiate into sperm (Figure 2.12 A). In contrast to hermaphrodites, spermatogenesis stays active in adult males and no switch to oogenesis occurs). Male germline development in *him-8(e1489)* males is not different from wild type males (n>30), see fig. 2.12 B. In contrast to *him-8(e1489)* males, the majority of *him-8(e1489)*; *nhr-114*(RNAi) males (81%, n=59) have underproliferated germ lines without apparent germ cell multinucleation, and lack obvious chromatin aberrations in the mitotic region, see 4.12 C-D.. The process of spermatogenesis appears normal, however the quality of this sperm to produce viable progeny was not tested. A minority of 19% of *him-8(e1489)*; *nhr-114*(RNAi) (n=59) males have underproliferated germ lines and multinucleated germ cells with chromatin aberrations, restricted to the mitotic region; spermatogenesis appears normal, see fig. 2.12 E. Therefore, the presence of *nhr-114* phenotypes in *him-8(e1489)*;*nhr-114*(RNAi) male germ lines indicated that *nhr-114* is also required for male germ line proliferation. Hence *nhr-114* functions are not restricted to the female sex or female germ lines.

Unexpectedly, more than half of the *him-8(e1489)*; *nhr-114*(RNAi) males (n=59) have abnormal accessory copulatory organs, such as fused or heterogeneous tail rays (not shown). Several abnormalities in tail ray formation (Male Abnormal tail phenotypes or Mab) are genetically linked to Sma/Mab TGF-ß signaling pathways (Savage-Dunn, 2005). TGF-ß ligands are a large family of secreted growth factors involved in different developmental and physiological process in animals. In *C. elegans,* the Sma/Mab signaling pathway regulates, body size, the patterning of male tail and germline integrity (Savage-Dunn, 2005, Luo et al. 2010). In addition, the Sma/Mab signaling maintains the germline syncytium, germ cell morphology and proper chromosomal segregation, and its up-regulation is presumed to reduce germline integrity (Luo et al. 2010). Based on that, the germline syncytial defects and the defective male tail phenotype suggest that *nhr-114* function may be linked to the TGF-B pathway. An experimental setup to test this hypothesis is explained in Future directions section.

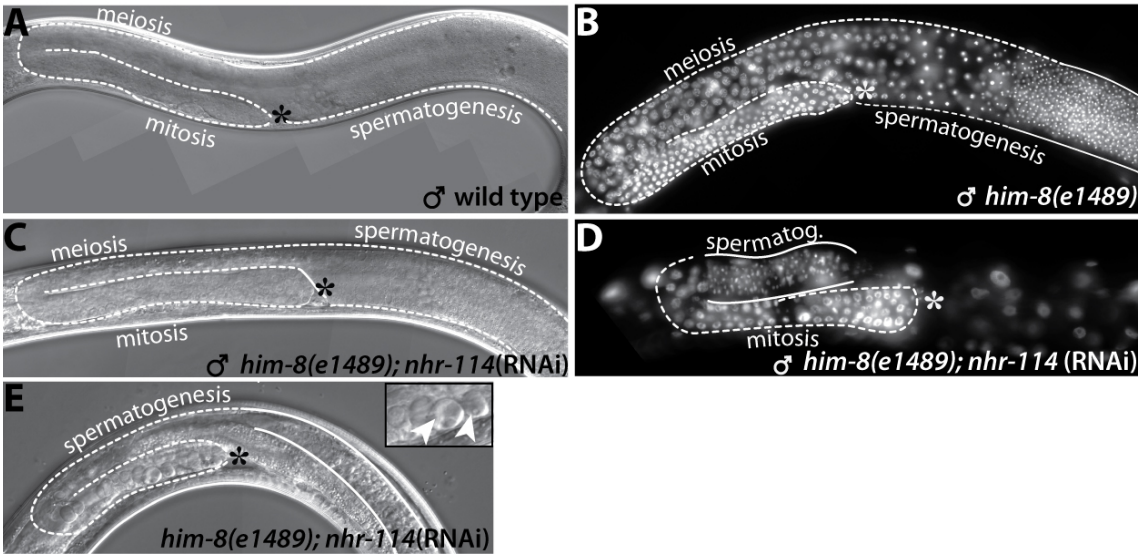

Figure 2.12 *nhr-114* is required for male germline development
(A,C,E) DIC microscopy of adult males germ lines. **(B,D,F)** Germ cell chromatin is visualized with the nucleic acid dye DAPI. Germ lines are delineated by dotted lines. Asterisk indicates the position of the distal tip cell and distal gonad. **(A)** Wild type adult male shows mitotic cells (mitosis), meiotic cells (meiosis), and different stages of spermatogenesis readily recognized by its cellular morphology. **(B)** Chromatin morphology in *him-8(e1489)* male adult shows similar germ cell distribution as in wild type male in A. **(C-D)** The majority of adult *him-8(e1489)*; *nhr-114*(RNAi) males have underproliferated germ lines with wild-type like organization and no chromatin aberrations (n=59). **(E)** The minority of adult *him-8(e1489)*; *nhr-114*(RNAi) males have underproliferated germ lines and germ cell multinucleation (n=59). Inset: highlights distal multinucleated germ cells (arrowhead).

2.4.2 NHR-114 DEFECTS AFFECT GERMLINE STEM CELLS AND APPEAR AT L3 LARVAL STAGE

In *C. elegans,* a population of germline stem cells (GSC) maintains germ cell proliferation throughout the life cycle. GSC are located distally in close contact to the somatic distal tip cell (DTC), which uses Notch/GLP-1 signaling to promote both self-renewal and prevent differentiation of the GSC population (Crittenden et al. 2006, Kimble and Crittenden 2007, Cinquin et al. 2009, Byrd and Kimble 2009). The severe underproliferation in *nhr-114*(RNAi) germ lines suggested that the population of GSC may be affected and as a consequence is unable to maintain germ cell proliferation.

To investigate this hypothesis, wild type and *nhr-114*(RNAi) hermaphrodites were synchronized and their germ lines were analyzed live at each larval stage using DIC microscopy (Materials and Methods 4.1.1). The analysis aimed to quantify total germ cell number throughout larval development, and to identify whether *nhr-114* multinucleation defects arise during larval development and whether the most distal germ cells (GSC) show multinucleation defects. The variability of the *nhr-114* phenotype led me to predict that the appearance of underproliferation and multinucleation defects in *nhr-114*(RNAi) germ lines would occur at random from the first until the last larval stage.

In wild type, the early L1 germ line contains two primordial germ cells, which start to proliferate and duplicate the number of germ cells in L1 and through subsequent larval stages. Starting at L3 larval stage the germ cell number increases sharply, and by the late L4 larval stage wild type germ lines contain on average 330 germ cells (Figure 2.13 A, black lane). Similar to wild type, *nhr-114*(RNAi) L1 germ lines also contain two primordial germ cells, and through the L2 larval stage the germ cell number remains similar to wild type. However, from L3 onwards *nhr-114*(RNAi) germ lines contain consistently less cells than wild-type germ lines, and by the late L4 larval stage *nhr-114*(RNAi) germ lines contain on average only 80 germ cells, a quarter of the wild type number (Figure 2.13 A, red line), indicating that the underproliferation defect is specifically evident starting at the L3 larval stage, and not randomly during larval development.

In addition to underproliferation, the first multinucleated germ cells in *nhr-114*(RNAi) germ lines are also detected starting at L3 larval stage, compare fig. 2.13 B and C. The first multinucleated germ cells are found at the most distal position. At later stages, multinucleated germ cells are found throughout the germ line, and they constitute no more than tenth of the total germ cell number (Figure 2.13 A, blue bars). The presence of aberrant germ cells at the distal germ line, the location where GSC reside, suggests that these cells have a compromised GSC capacity. Taken together, these data indicated that two *nhr-114* major defects, underproliferation and germ cell multinucleation arise at L3 larval stage, and the origin of these defects is consistent with a view that mitotic GSC are affected by the loss *nhr-114*.

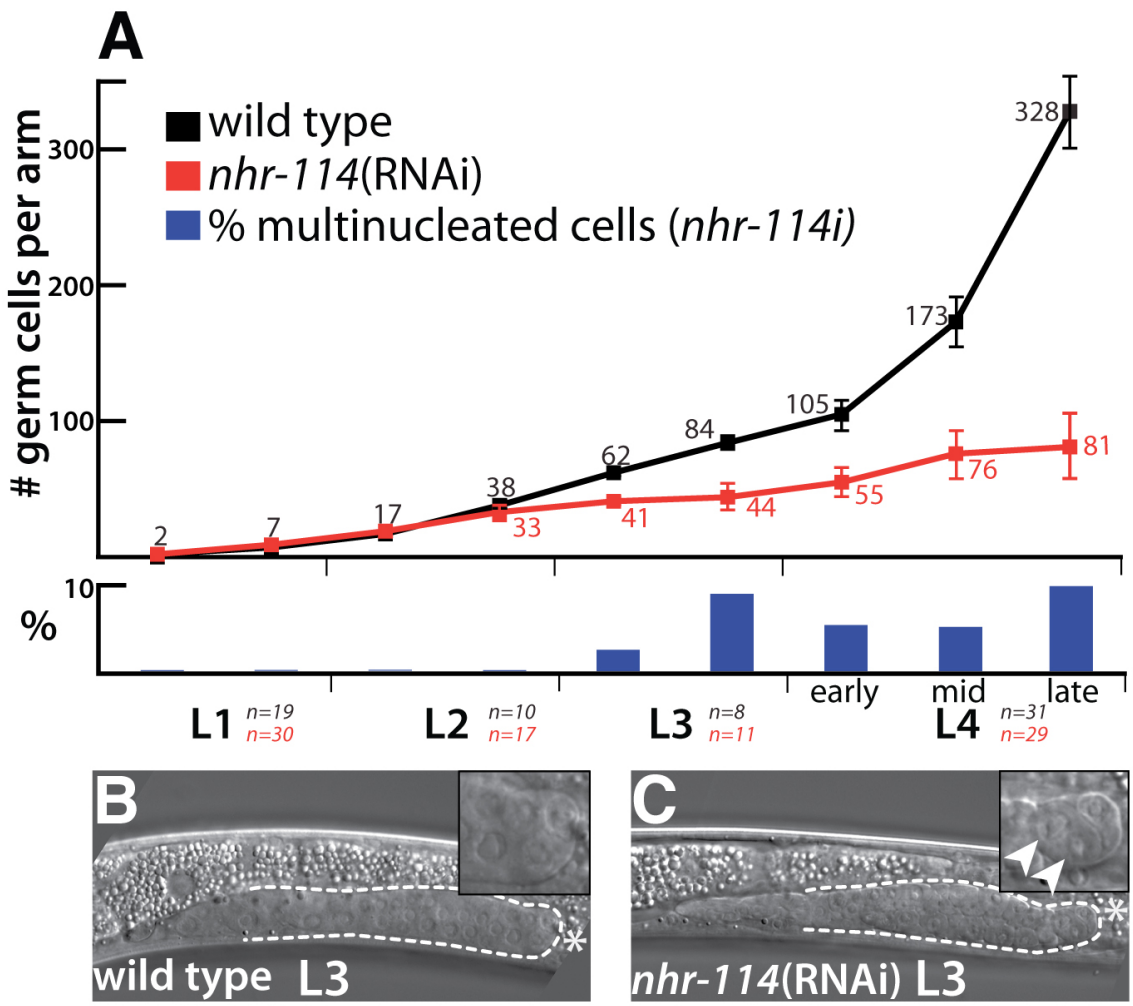

Figure 2.13 Developmental analysis of Nhr-114 defects

Appearance of Nhr-114 phenotypes coincides with L3 larval stage. **(A)** Quantification of total germ cell number throughout larval development in wild type (black line) and *nhr-114*(RNAi) larvae (red line) using DIC microscopy on synchronized live animals. Horizontal axes indicate larval stages from L1-L4. Germ cell number was quantified at two different time points in L1-L3, and three time points at L4: early-L4, mid-L4 and late-L4. (n=) indicates total germ lines quantified per developmental stage, wild type (black), *nhr-114*(RNAi) (red). Top vertical axis indicates number of germ cells per germ line arm. Error bars indicate standard deviation. Bottom vertical axis indicates the average percentage (blue bars) of multinucleated cells per germ line at a given time point. Note that multinucleated germ cells first appear at L3. **(B-C)** DIC microscopy images of L3 larvae showing representative germ lines (dotted line). **(B)** Wild-type hermaphrodite. Inset highlights distal germ cell nuclei and the distal tip cell (asterisk). **(C)** *nhr-114*(RNAi) hermaphrodite. Inset highlights distal germ cell multinucleation (arrowhead) and the distal tip cell (asterisk). Insets are scaled two times.

2.5 SOMATIC *NHR-114* PROMOTES PROPER GERM CELL DIVISIONS

The Northern blot and *in situ* hybridization analyses showed that *nhr-114* mRNA is expressed in germ cells and soma. However it remained unclear to which extent a germline or a somatic function of *nhr-114* is required for germ line development. Duet to the lack of anti-NHR-114 antibodies it was unknown whether NHR-114 protein is expressed in germ cells. To investigate whether germline expressed *nhr-114* is required for germ line development, germline *nhr-114* function was specifically knocked down by RNAi. In an *rrf-1(pk1417)* mutant background, RNAi amplification and knockdown occurs only in the germline; thus the function of the targeted gene remains intact in the soma (Sijen et al. 2001). *nhr-68* RNAi knockdown was conducted in parallel to control for the RNAi knockdown effect in the *rrf-1(pk1417)* mutant background. Considering the complexity of Nhr-114 phenotypes, and the *nhr-114* mRNA expression, it was surmised that *nhr-114* influences different aspects of germline development depending on the tissue of its function. Therefore, I expected that *rrf-1(pk1417); nhr-114*(RNAi) sterile hermaphrodites might show a deviation from the Nhr-114 phenotype.

All *rrf-1(pk1417)* mutant hermaphrodites are self-fertile (n>500) and their germ lines have a wild-type-like organization (n=135) (Figure 4.14). Similarly, all *rrf-1(pk1417); nhr-68*(RNAi) hermaphrodites are self-fertile (n=1609), and their germ lines have a wild-type-like organization (n=87), indicating that RNAi knockdown in the *rrf-1(pk1417)* strain does not affect germ line development, see 2.14 B and table 4.4. As described before, ~80% of *nhr-114*(RNAi) hermaphrodites are sterile (n>3000). Unexpectedly, only ~40% *rrf-1(pk1417); nhr-114*(RNAi) hermaphrodites are sterile (n>2150). The remaining 60% are fertile (n>2150), indicating that the penetrance of Nhr-114 sterility is reduced in a *rrf-1(pk1417)* background. Therefore, this result implies that *nhr-114* somatic function promotes fertility.

To investigate whether the reduction in *nhr-114* sterility was associated with amelioration of Nhr-114 phenotypes, *rrf-1(pk1417); nhr-114*(RNAi) hermaphrodites were fixed and stained with DAPI to visualize chromatin. In contrast to *nhr-114*(RNAi) germ lines (see fig. 2.14 C), the majority of *rrf-1(pk1417); nhr-114*(RNAi) sterile germ lines (64%, n=240) are bigger than *nhr-114*(RNAi), albeit smaller than wild type, see fig. 2.14 D and table 2.4.

rrf-1(pk1417); nhr-114(RNAi) sterile germ lines contain wild-type-like mitotic and meiotic nuclear morphology, no multinucleation or chromatin aberrations, and more sperm; yet they lack oocytes, see fig. 2.14 D and table 2.4. This genetic and morphological analysis highlighted that somatic *nhr-114* prevents germ cell multinucleation and chromatin aberrations. Thus in the wild type, the somatic NHR-114 likely promotes proper germ cells divisions. Concomitantly, the germ cell underproliferation and the lack of oocytes must be a consequence of the germline *nhr-114* knockdown, which implies that germline *nhr-114* function promotes proliferation and oogenesis. Importantly, the *rrf-1(pk1417); nhr-114*(RNAi) sterile germ lines (as in fig. 2.14 D) are reminiscent of *gld-4(ef15)* germ lines, which are underproliferated, contain sperm, but and lack oocytes. Therefore this phenotypic resemblance suggests that both germline NHR-114 and GLD-4 share common functions: germ cell proliferation and oogenesis.

Considering that a somatic function of *nhr-114* promotes proper germ cell divisions, I anticipated that knock down of *nhr-114's* somatic function would specifically impair germ cell divisions and increase chromatin aberrations. To confirm this hypothesis, *nhr-114* RNAi knockdown was conducted in an *rrf-3(pk1426)* mutant background, in which somatic tissues are hypersensitive to RNAi knockdown (Sijen et al. 2001). To control for the RNAi knockdown effect in the *rrf-3(pk1426)* mutant background, *nhr-68* RNAi knockdowns were conducted in parallel.

All *rrf-3(pk1426)* mutant hermaphrodites are self-fertile (n>50) and their germ lines have a wild-type-like organization (n=14). Similarly, all *rrf-3(pk1426); nhr-68*(RNAi) hermaphrodites are self-fertile (n=121), and their germ lines have a wild-type-like organization (n=86) (Table 2.4). As anticipated, the majority of *rrf-3(pk1426); nhr-114*(RNAi) animals are sterile (~90%, n=249), the minority is fertile (10%, n=249) (Table 2.4). Almost all *rrf-3(pk1426); nhr-114*(RNAi) sterile germ lines are multinucleated, contain aberrant chromatin, and lack both sperm and oocytes, see fig. 2.14 E. This indicated that germ cell divisions are more susceptible to a further knockdown of somatic *nhr-114* function. Taken together, these analyses imply that germline *nhr-114* and somatic *nhr-114* functions are required for germline development. In addition, these results put forward the hypothesis that *nhr-114* affects different germline development aspects depending on the tissue where *nhr-114* is expressed.

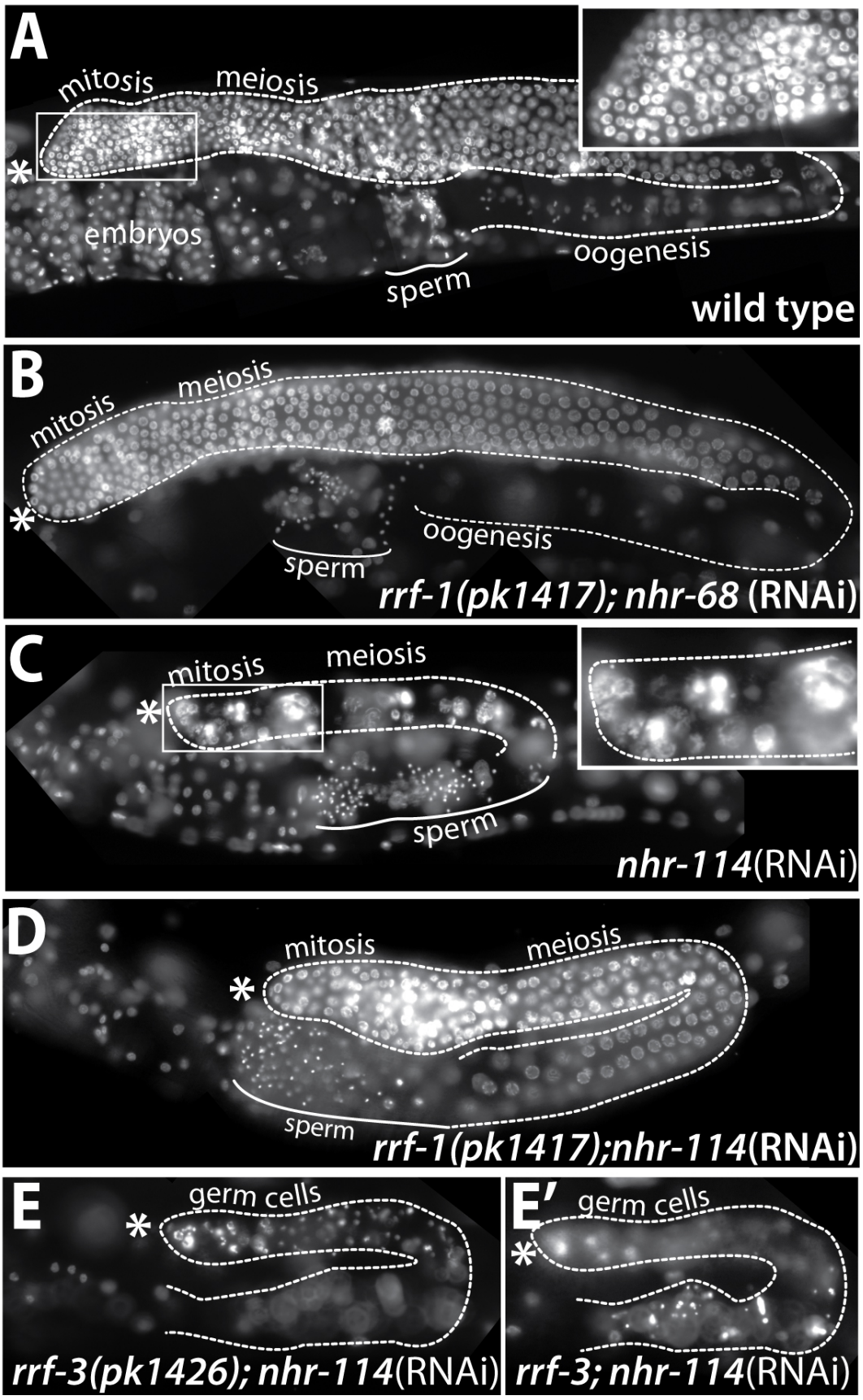
A
mitosis
meiosis
*
embryos
sperm
oogenesis
wild type
B
mitosis
meiosis
*
sperm
oogenesis
rrf-1(pk1417); nhr-68 (RNAi)
C
mitosis
meiosis
*
sperm
nhr-114(RNAi)
D
mitosis
meiosis
*
sperm
rrf-1(pk1417);nhr-114(RNAi)
E
germ cells
*
rrf-3(pk1426); nhr-114(RNAi)
E′
germ cells
*
rrf-3; nhr-114(RNAi)

Figure 2.14 Nuclear morphology in different *nhr-114*(RNAi) sterile germ lines
Germ cell chromatin is visualized with the nucleic acid dye DAPI. Germ lines are delineated by dotted or continuous line (sperm). **(A)** Adult wild type hermaphrodite shows germ line with mitotic, meiotic, oocyte and sperm nuclei. Inset highlights distal mitotic chromatin of homogeneous size. **(B)** Adult *rrf-1(pk1417); nhr-68*(RNAi) hermaphrodite shows germline organization and chromatin morphology no different from wild type. Oocytes are out of focus so not visible in this image. **(C)** Adult *nhr-114*(RNAi) animal shows typical sterile germ line with aberrant mitotic and meiotic nuclei, only sperm, but no oocyte nuclei. Inset highlights abnormal distal mitotic chromatin condensation and heterogeneity in nuclei size (arrows). Compare the reduced density of mitotic nuclei with in A. **(D)** Adult *rrf-1(pk1417); nhr-114*(RNAi) hermaphrodite shows typical sterile germ line with normal mitotic and meiotic nuclei, only sperm, but no oocyte nuclei. Inset highlights distal mitotic chromatin of homogeneous size as in wild type. **(E-E')** Two different focal planes of same adult *rrf-3(pk1426); nhr-114*(RNAi) hermaphrodite show a small germ line with highly aberrant germ cell chromatin and sperm. Insets are two-times scaled. Asterisk indicates the position of the distal tip cell and distal gonadal end.

Strain:	N2 (wild type)		*rrf-1(pk1417)*		*rrf-3(pk1426)*	
RNAi knockdown:	germline, soma		germline		mainly soma	
nhr- dsRNA:	***-114***	*-68*	***-114***	*-68*	***-114***	*-68*
Steriles:	80%	<1%	36%	0%	89%	0%
Scored germ lines:	178	97	240	87	121	86
Proliferative phenotypes:						
Glp-like	6%	0%	2%	NA	11%	n.a.
Underproliferation and chromatin aberrations	**88%**	0%	**18%**	NA	**89%**	n.a.
Underproliferation	0%	0%	80%	NA	0%	n.a.
Wild-type like	8%	100%	0%	100%[1]	0%	100%[1]
Gametes produced:						
Sperm and oocytes	3%[2]	0%	5%	100%[1]	1%	100%[1]
Sperm only	**62%**	100%	**92%**	NA	**15%**	n.a.
No differentiated gametes	35%	0%	3%	NA	84%	n.a.

Table 2.4 Germline defects upon tissue-specific *nhr-114* RNAi knockdowns
Analysis of sterile adult hermaphrodites grown at 20°C. On the basis of the overall germline size, four classes of germ lines are distinguished. First, Glp-like (Germ line proliferative defective phenotype) gonads have less than 10 germ cells or no germ cells, presence of mature sperm is not strictly correlated. Second, germ line underproliferation and chromatin aberration phenotypes refers to small gonads with more than 10 germ cells, the syncytium is disorganized and contains chromatin aberrations. Third, underproliferated germ lines are smaller than wild type, but bigger than *nhr-114*(RNAi) germ lines, and lack chromatin aberrations. Fourth, germ lines appear of wild type size; however, exact number of germ cells was not counted. Germ lines with no differentiated gametes have germ cell nuclear morphology that resembles pachytene, but not gametes can be identified by nuclear morphology (DAPI staining) or cellular morphological features (DIC microscopy). n.a.: not applicable, category only applies to sterile germ lines.
[1]Refers to fertile germ lines.
[2]Despite having sperm and oocytes these germ lines lack embryos.

2.6 GERMLINE *NHR-114* PROMOTES PROLIFERATION AND OOGENESIS

The genetic analysis using tissue-specific *nhr-114* knockdown shows that if only germline *nhr-114* is knocked-down, as in *rrf1(pk1417)*; *nhr-114*(RNAi), the germ cell number in sterile germ increases drastically, in comparison to total *nhr-114* knocked-down (Table 2.5). However, the increment does no reach wild-type levels (Table 2.5). Therefore, this reduced number of mitotic cells suggests that *nhr-114* is cell-autonomously (NHR-114 in germ cells) and cell-non-autonomously (NHR-114 in somatic cells) required to promote germ cell divisions.

	Mitotic region:		
	Density (range)	Extension (range)	n=
Wild type	204 (157-243)	20 (16-27)	>10
nhr-114(RNAi)	5 (4-9)	n.a.	9
rrf1(pk1417); *nhr-114*(RNAi)	116 (52-215)	17 (11-22)	7
gld-4(ef15)[1]	93 (n.d)	12 (n.d)	>5

Table 2.5 Analysis of *nhr-114* impact on germ cell proliferation
By definition, the mitotic region spans all germline distal nuclei until the zone where 60% of nuclei have crescent-shaped morphology typical of early meiotic prophase (transition zone) (Crittenden and Kimble, 2007). The germ line mitotic region was determined using chromosomal morphology (DAPI staining). Density corresponds to the total nuclei number in the mitotic region counted from stack series. The mitotic extend was resolved by counting the rows of cells from the transition zone to the distal tip cell. Number is given as cell diameter divided by two. Not determined (n.d.)
[1] Data taken from Schmid M. 2008.

2.6.1 *NHR-114* INFLUENCES THE SPERM-TO-OOCYTE SWITCH

C. elegans hermaphrodite fertility is ensured by stopping spermatogenesis and switching to oogenesis. Thus, a failure to switch to oogenesis could be a simple explanation why *nhr-114* mutants lack oocytes and are sterile. To investigate this hypothesis, genetic interactions of *nhr-114* with *fbf-1* were probed for and analyzed in the *fbf-1(ok91)* mutant, which is a sperm-to-oocyte switch defective background. In contrast to wild type, *fbf-1(ok91)* mutants switch late to oogenesis and accumulate twice more sperm than wild type (Crittenden et al. 2002). Therefore, a loss-of genes that are involved in the sperm-to-oocyte switch may enhance the sperm-to-oocyte switch defect of the *fbf-1(ok91)* mutant background, resulting in either increased sperm number or even a complete block of oocyte production (Schmid M., 2008; Rybarska et al. 2009). *fbf-1* is highly redundant to the *fbf-2* gene (Crittenden et al. 2002); however, the sperm-to-oocyte synergistic effect is not seen in an *fbf-2(q738)* mutant background, hence this mutant serves as a control for the genetic analysis (Rybarska et al. 2009). Based on the resemblance of *nhr-114* and *gld-4* phenoytpes, and since *gld-4(ef15); fbf-1(ok91)* mutants are fully sterile and produce only sperm (Schmid M., 2008), I anticipated that *fbf-1(ok91);nhr-114*(RNAi) germlines would show similar phenotypes.

Wild-type hermaphrodites produce ~160 sperm per germ line, by contrast, *fbf-1(ok91)* hermaphrodites produce ~300 sperm (Crittenden et al. 2002). Consistent with previous *nhr-114* knockdowns, *fbf-1(ok91); nhr-114*(RNAi) sterile germ lines show Nhr-114 phenotypes, and the total sperm number is higher than in *nhr-114*(RNAi) germ lines, but lower than in *fbf-1(ok91)* (Table 2.6 and Figure 2.15). However, contrary to a full oogenesis block, about 3% of *fbf-1(ok91); nhr-114*(RNAi) sterile germ lines contain oocytes, indicating that the switch to oogenesis occasionally happens, see table 2.6. Similarly, *fbf-2(q738); nhr-114*(RNAi) sterile germ lines show Nhr-114 phenotypes too, but less sperm than wild type and than *nhr-114*(RNAi) germ lines, see table 2.6 and fig. 2.15 C-D. In summary, these results suggests that *nhr-114* is not synergistic with *fbf-1(ok91)* and that *nhr-114* does not work in a parallel with *fbf-1* pathway to assist the sperm-to-oocyte switch. Further, the switch to oogenesis appears not to be a common function between *nhr-114* and *gld-4*.

Genotype:	**Sperm** (range)	Germ lines, n=
Wild type[1]	170 (n.d.)	13
nhr-68(RNAi)	248 (105-456)	9
nhr-114(RNAi)	90 (31-182)	16
rrf-1(pk1417); nhr-114(RNAi)	185 (51-308)	12
fbf-1(ok91)[2]	285 (225-380)	3
fbf-1(ok91); nhr-114(RNAi)	178 (11-337)	18
fbf-2(q739); nhr-114 (RNAi)	76 (60-84)	6

Table 2.6 Analysis of sperm production in *nhr-114*(RNAi) hermaphrodites
Analysis of average number of sperm per germ line in adult hermaphrodites. Animals were grown at 20ºC; *nhr-68*(RNAi) were grown at 25ºC. Sperm was identified using chromosomal morphology (DAPI staining) and counted from stacks series. Not determined (n.d.).
[1] Taken from Rybarska et al. 2009.
[2] Taken from Crittenden et al. 2002.

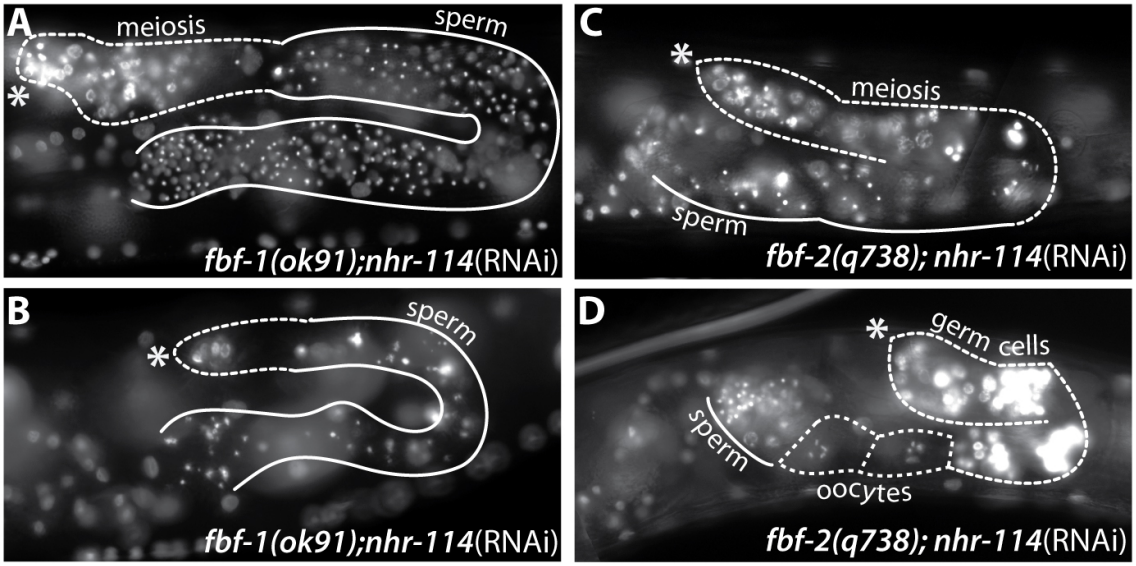

Figure 2.15 *nhr-114* influences the sperm-to-oocyte switch
Germ cell chromatin is visualized with the nucleic acid dye DAPI. Germ lines are delineated by dotted or continuous line (sperm). **(A-B)** Adult *fbf-1(ok91); nhr-114*(RNAi) hermaphrodites with excess of sperm in (A), or very few germ cells and sperm in (B). **(C-D)** Adult *fbf-2(q738); nhr-114*(RNAi) hermaphrodites with very few sperm in (C), or few sperm and two oogenic nuclei together with few immature germ cells in (D). Note that oogenic nuclei are only occasionally present in *nhr-114* germ lines. Asterisk indicates the position of the distal tip cell and distal gonad.

The increase in sperm number in *fbf-1(ok91); nhr-114*(RNAi) germ lines with respect to *nhr-114*(RNAi) germ lines apparently indicates a synergistic effect in the sperm-to-oocyte switch defect. However, *nhr-114*(RNAi) aberrations may limit the starting pool of mitotic germ cells that enter meiosis and differentiate as sperm. Thus, it is likely that the total sperm produced upon *nhr-114* RNAi rather reflects the total number of sperm that each mutant background produces. Consistent with this idea, *rrf-1(pk1417)*; *nhr-114*(RNAi) germ lines, which have a bigger pool of mitotic cells and no aberrant nuclei, produce more sperm than *nhr-114*(RNAi) and slightly more than wild type, see table 4.6. This slight increase, in the sperm number indicates that the sperm-to-oocyte switch is not robust when *nhr-114* is absent, but does eventually happen, suggesting that *nhr-114* germline function is involved in the sperm to oocyte switch.

fbf-1 and *fbf-2* are both essential to maintain the mitotic fate, and to promote stem cells (Crittenden et al. 2002). For example in *fbf-1; fbf-2* double mutants, the germline stem cells are not maintained, and eventually all germ cells prematurely differentiate into sperm. However, this effect is not seen in single mutants of either *fbf* gene (Crittenden et al. 2002). In contrast to *nhr-114*(RNAi) sterile germ lines, *fbf-1; nhr-114*(RNAi) and of *fbf-2; nhr-114*(RNAi) sterile germ lines are more likely to contain differentiated gametes (Table 4.7). This suggests that in the absence of *nhr-114* premature differentiation favors spermatogenesis. This observation is consistent with a view that the stem cell capacity degenerates upon loss of *nhr-114*.

Strain:	wild type	***fbf-1(ok91)***[1]		***fbf-2(q738)***[2]	
RNAi:	*nhr-114*	-	*nhr-114*	-	*nhr-114*
Sperm and oocytes	3%	99%	3%	99%	14%
Oocytes only	0%	0%	0%	1%	5%
Sperm only	62%	<1%	87%	0%	73%
No differentiated gametes	35%	0%	10%	0%	7%
Scored germ lines:	178	1141	146	2201	81

Table 2.7 Gamete production in *nhr-114*(RNAi) sterile germ lines in different genetic backgrounds
Analysis of adult hermaphrodites grown at 20ºC. *fbf-1(ok91)* hermaphrodites represent a sensitized background for oogenesis defects. *fbf-2(q738)* represent a sensitized background for spermatogenesis defects. Germ lines with no differentiated gametes have germ cell nuclear morphology that resembles pachytene, but not gamete can be identified by nuclear morphology (DAPI staining) or cellular morphological features (DIC microscopy).
[1] Taken from Crittenden et al. 2002
[2] Taken from Lamont et al. 2004

2.6.2 *NHR-114* AND THE OOGENIC PROGRESSION

Taking into account that *nhr-114* sterile germlines switch from spermatogenesis to oogenesis, an alternative explanation to why *nhr-114* germ lines still fail to produce oocytes is that *nhr-114* germ cells are arrested in early stages of female meiosis, such as pachytene, and do not progress further throughout oogenesis. In addition to promoting the sperm-to-oocyte switch, *gld-4* promotes female meiosis progression along with *gld-2*. For instance, all *gld-2 gld-4* double mutants are sterile and ~70% of their germ lines enter female meiosis but return to mitosis, the remaining ~30% arrests in late pachytene I (Schmid et. al 2009). In a further attempt to identify if oogenesis defects in *nhr-114* germlines were similar to the oogenesis defects in *gld-4* germ lines, *nhr-114* epistatic interaction was analyzed in a *gld-2* mutant background. If *nhr-114* function also promotes oogenic meiotic commitment then a high percentage of *gld-2(q497)*; *nhr-114(gk849)* germ lines were expected to enter meiosis and return to mitosis. Contrary to the expectation, only one out of 17 *gld-2(q497);nhr-114(gk849)* germ lines show entry into meiosis and return to mitosis, the remaining 16 show post-pachytene arrest, typical of *gld-2* germ lines. This result indicated that *nhr-114* function does not promote oogenic progression in parallel to *gld-2*, as *gld-4* does.

2.7 *NHR-114* DEFECTS ARE INDEPENDENT OF MEIOTIC ONSET

In the adult *C. elegans* germ line, Notch/*glp-1* signaling controls most germ cell proliferation and maintains stem cells by promoting mitosis, and restricting their differentiation to meiosis. Therefore, germline underproliferation can arise if the balance between proliferation and differentiation is shifted towards differentiation (Reviewed in Kimble and Crittenden 2005). To investigate whether *nhr-114* underproliferation and germ cell defects were a consequence of unbalanced germ cell differentiation into meiosis, *nhr-114* RNAi knockdown was conducted in a *nos-3(q650) gld-3(q730)* mutant background. In this mutant background, germ cells stay in mitosis, but never enter meiosis hence give rise to a mitotic tumor (Eckmann et al. 2004). Considering that *nhr-114* RNAi knockdown always affected mitotic cells, it was expected that *nos-3(q650) gld-3(q730); nhr-114*(RNAi) germ lines would be underproliferated and contain chromatin aberrations.

All *nos-3(q650) gld-3(q730)* germ lines are mitotic tumors with wild-type mitotic nuclear morphology (n>14, Figure 2.16 A) (Eckmann et al. 2004). As expected, the majority of *nos-3(q650) gld-3(q730); nhr-114*(RNAi) germ lines have reduced tumor size and aberrant chromatin (72%, n=50), see fig. 2.16 B. Additionally, 24% have reduced tumor size with normal nuclei, see fig. 2.16 C. The remaining 4% are indistinguishable from *nos-3(q650) gld-3(q730)* tumors (n=50). The tumor size reduction and the presence of aberrant chromatin indicate that *nhr-114* knockdown impairs tumorous proliferation. Hence, this implies that *nhr-114* defects are not linked to the meiotic onset. Importantly, the relatively big size of the *nos-3(q650) gld-3(q730); nhr-114*(RNAi) tumor suggests that the severe underproliferation observed in *nhr-114*(RNAi) germline results from both impaired proliferation and meiotic progression defects.

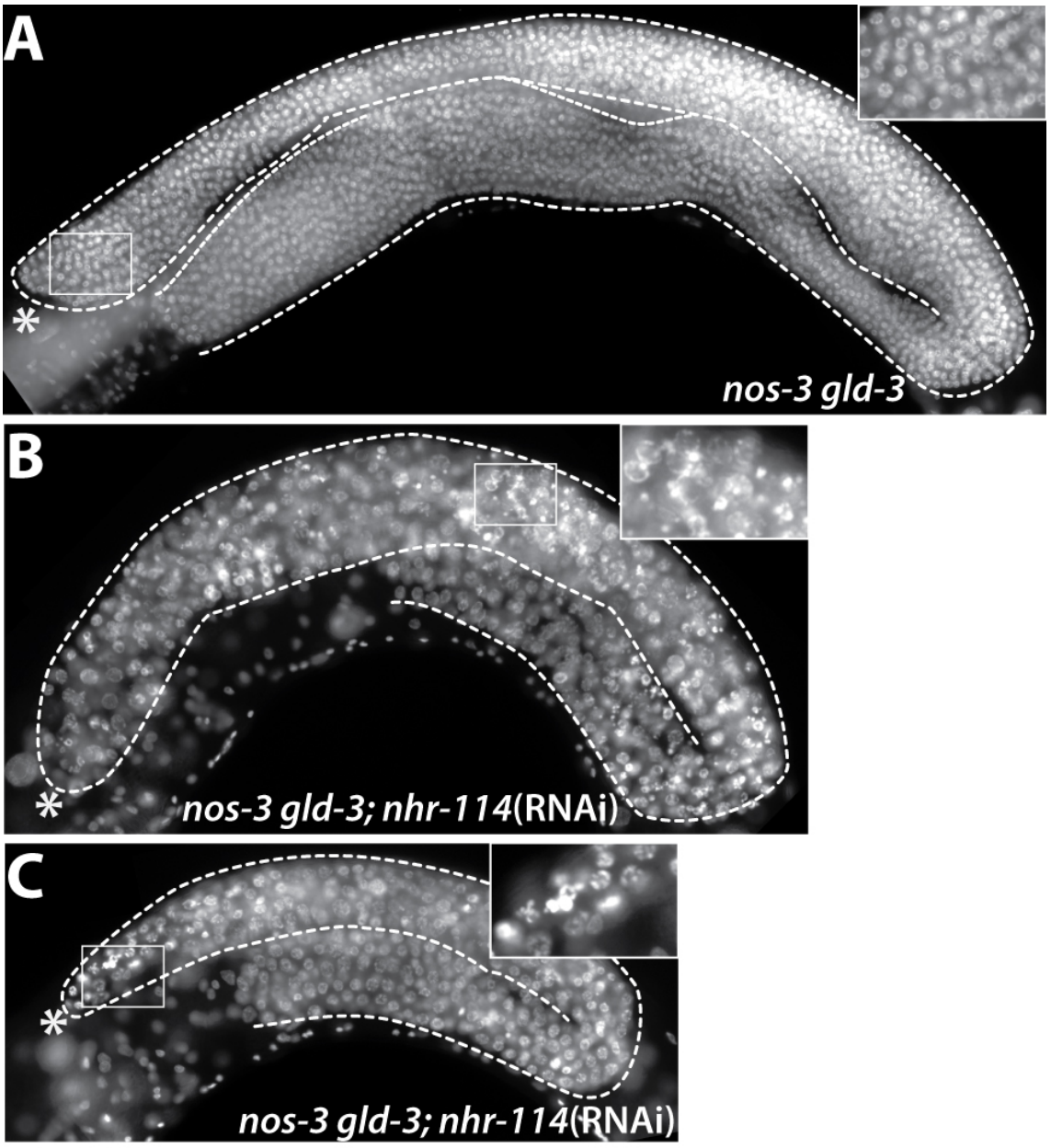

Figure 2.16 *nhr-114* defects occur independently of meiotic onset
Whole adult fixed hermaphrodites stained with DAPI. Germ lines are delineated by dotted lines. **(A)** Adult *nos-3(q650) gld-3(q730)* germ line shows a mitotic tumor. Inset highlights homogeneous chromatin size of mitotic nuclei. **(B)** Adult *nos-3(q650) gld-3(q730)*; *nhr-114*(RNAi) germ line shows a smaller tumor than (A), with chromatin of heterogeneous size and configurations. Inset highlights heterogeneous chromatin and loose chromatin. **(C)** Adult *nos-3(q650) gld-3(q730)*; *nhr-114*(RNAi) germ line shows a small tumor with apparently normal chromatin. Inset highlights loose chromatin. Insets are scaled two times. Asterisk indicates the position of the distal tip cell and distal gonad.

2.8 PREFACE TO SECTION II

In the previous chapter, genetic and molecular experimental data show that *nhr-114* promotes proper germ cell divisions, mitotic proliferation and female meiotic progression. Especially, mitosis appears to depend on somatic expression of *nhr-114*. In addition, the data indicates that *nhr-114* function may prevent a reduction of germline stem cell capacity. As a next step, I set to investigate if NHR-114 could integrate external cues to influence germline development. One key observation prompted the investigation on this regard: the penetrance of sterility of *nhr-114* homozygous mutants ranges from 10% to 90% of sterile animals among different batches. This suggested that germline development could be influenced differently within individuals of the same mutant genetic background, and that Nhr-114 sterility may be influenced by an environmental factor.

2.9 *NHR-114* STERILITY IS ABOLISHED BY FEEDING A DIFFERENT BACTERIUM

In an attempt to investigate whether oogenesis *per se* requires *nhr-114,* oogenic *nhr-114* germ lines were generated by feeding *fog-1* dsRNA (in the experiments I introduce before, I delivered dsRNA by microinjection). In the *fog-1* background spermatogenesis is absent (Luitjens et al. 2000), therefore *fog-1*(RNAi) mutants only produce oocytes, leading to a *f*eminization *o*f *g*erm line phenotype (Fog phenotype) (Luitjens et al. 2000). *fog-1*RNA was induced by feeding dsRNA-expressing bacteria to wild type, *nhr-114(gk849)* and *nhr-114(ef24)* mutants. Based on a presumed *nhr-114* oogenic role, I anticipated that *fog-1*(RNAi); *nhr-114* feminized germlines would have *nhr-114* defects and would fail to produce oocytes.

Feeding *fog-1* dsRNA to wild-type animals abolished spermatogenesis, >90% (n=46) of *fog-1*(RNAi) germ lines contained only oocytes, indicating that RNAi knockdown was effective (Figure 2.17 A). Unexpectedly, >95% of *fog-1*(RNAi); *nhr-114(gk849)* or *fog-1*(RNAi); *nhr-114(ef24)* germ lines (n=75) had wild-type size and normal oocytes, see fig. 2.17 B-C. Surprisingly, almost all *nhr-114(gk849)* or *nhr-114(ef24)* animals fed with control-RNAi were fertile too, and had germ lines of a wild-type organization and were wild type sized (n=796). This indicated that a component in the RNAi-feeding setup was abolishing Nhr-114 phenotypes.

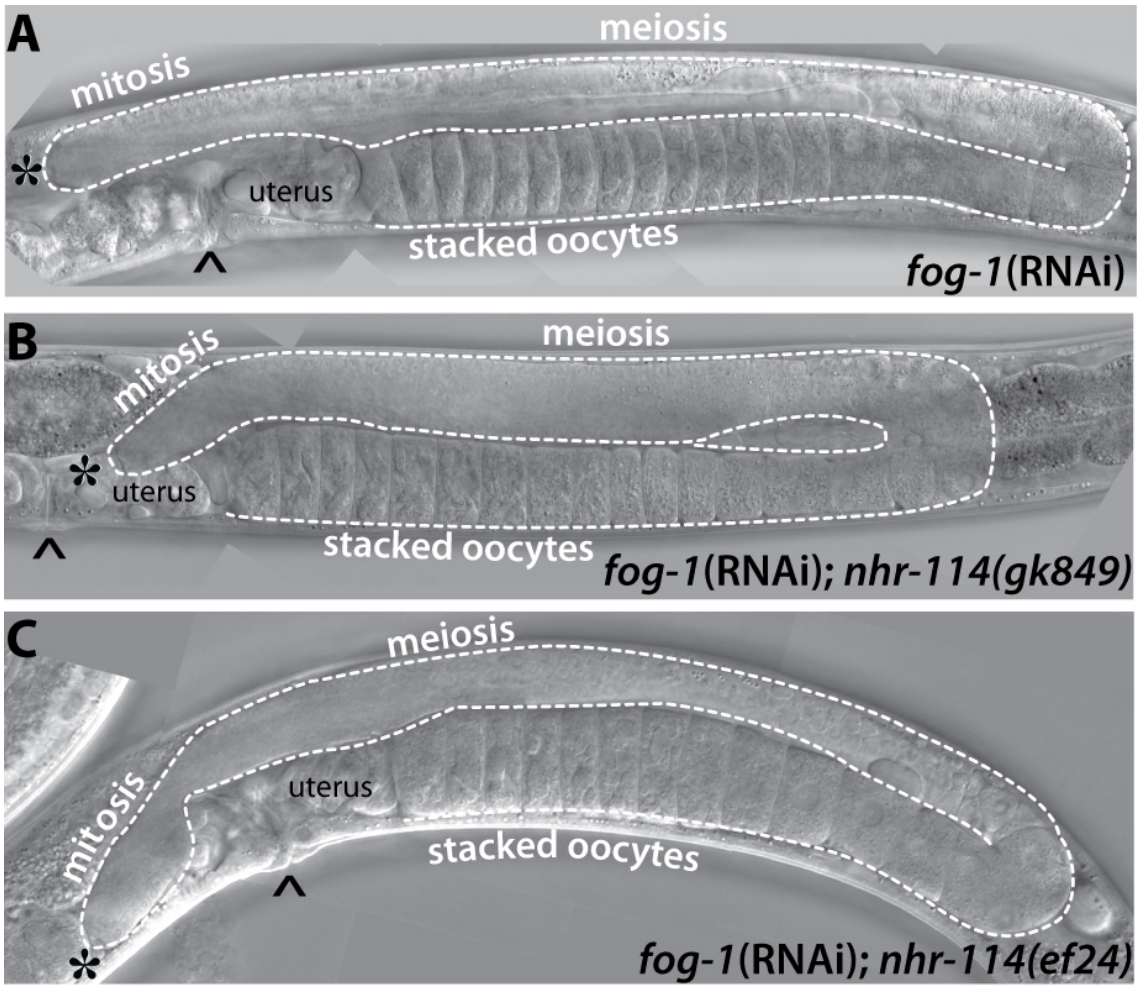

Figure 2.17 Bacteria used for feeding-RNAi abolishes Nhr-114 sterility
DIC microscopy images. Asterisk indicates the position of the distal gonadal end. Caret indicates the position of the vulva. **(A)** *fog-1*(RNAi) feminized adults have a germ line with oocytes only. Oocytes stack proximally due to the lack of sperm. Mitotic and meiotic regions are indicated. (**B)** *fog-1*(RNAi);*nhr-114(gk849)* and **(C)** *fog-1*(RNAi);*nhr-114(ef24)* adult animal shows a germ line of wild-type organization, with multiple oocytes that stack proximally. Germ lines lack any multinucleation or syncytial disorganization.

The standard laboratory food of *C. elegans* is *E. coli* strain OP50. In contrast, RNAi-feeding experiments use the *E. coli* strain HT115(DE3), which contains an IPTG inducible T7 RNA polymerase and is RNAseIII-deficient. This strain allows stable dsRNA expression from a pL4440 plasmid (Sijen et al. 2001). For brevity reasons, HT115(DE3) will be referred as HT115. Since control RNAi-feeding was sufficient to abolish Nhr-114 sterility, three presumed candidates were thought to be responsible of the effect: IPTG induction, the dsRNA expression or the bacteria by itself. To identify which component was sufficient to suppress sterility, the progeny of *nhr-114(gk849)* animals was scored for sterility when fed with different HT115 or OP50 conditions.

In this experiment, 20% of *nhr-114(gk849)* animals fed OP50 were sterile, the remaining 80% was fertile (Figure 2.18 A). Similarly, 24% of *nhr-114(gk849)* animals fed OP50+IPTG were sterile, the remaining 76% was fertile. The unchanged penetrance of sterility upon IPTG addition, showed that IPTG itself does not have any effect on *nhr-114* sterility, see fig. 2.18 A, white bars. In contrast, less than 0.1% of *nhr-114(gk849)* animals were sterile when fed with HT115+IPTG or HT115/pL4440+IPTG, the remaining 99.9% was fertile. This abolishment of sterility with HT115+IPTG in the absence of pL4440 plasmid indicated that the induction of dsRNA itself was not required to abolish *nhr-114* sterility. Moreover, only 10% of *nhr-114(gk849)* animals fed HT115 were sterile, the remaining 90% was fertile, see fig. 2.18 A black bars. This result therefore shows that HT115 bacteria itself is sufficient to reduce *nhr-114* sterility.

To challenge the observation that HT115 reduces *nhr-114* sterility further and to rule out the possibility that this phenomenon was an artifact mediated by the genetic background in *nhr-114* deletion alleles, *nhr-114*(RNAi) animals were fed with HT115. Note that *nhr-114* dsRNA was always delivered by microinjection, and *nhr-114*(RNAi) knockdown yields a consistently high penetrance of sterility. In this experiment, more than 90% of *nhr-114*(RNAi) animals fed OP50 or OP50+IPTG were sterile, the remaining 10% was fertile. In contrast, only 2% of *nhr-114*(RNAi) animals fed HT115+IPTG were sterile, the remaining 98% was fertile, see 2.18 B.

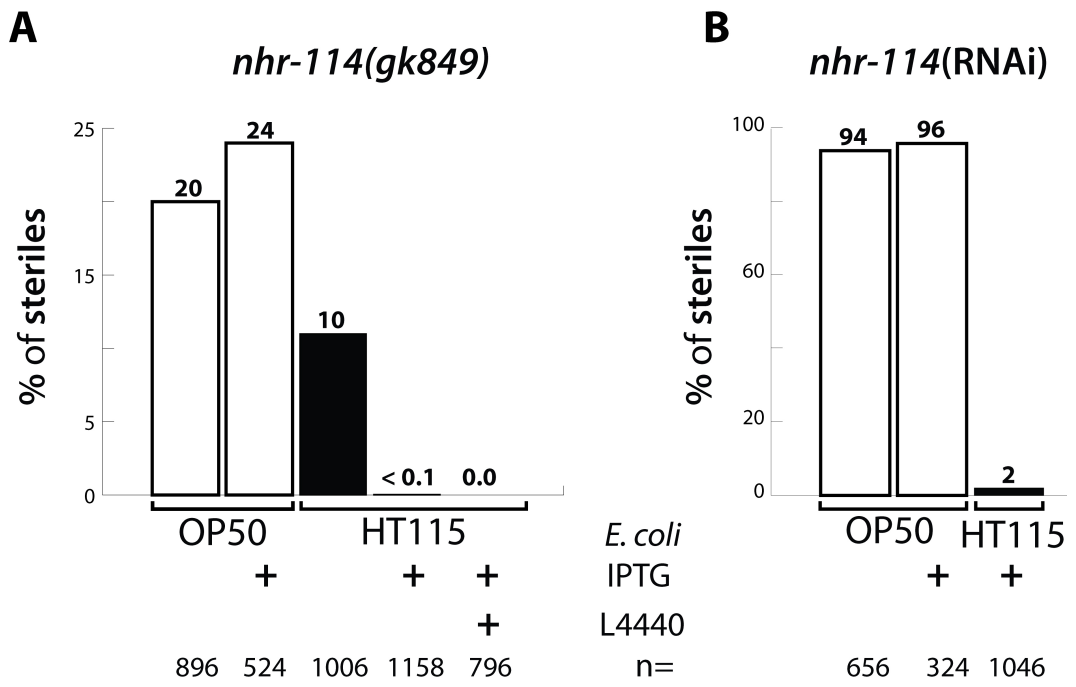

Figure 2.18 Penetrance of Nhr-114 sterility using two *E. coli* strains as diet
Percentage (%) of sterile adult animals with respect to the total number of animals analyzed (n=). **(A)** *nhr-114(gk849)* mutants are sterile when fed OP50 (white bars), sterility is reduced or abolished when fed HT115 (black bars). IPTG is used to induce T7 RNA polymerase in HT115. pL4440 plasmid is used as a transcription template for dsRNA production. (**B)** *nhr-114*(RNAi) animals are sterile when fed OP50 (white bars). The sterility is strongly reduced when fed HT115 (black bars).

To visualize the HT115 effect on germ line organization and germ cell nuclear morphology, *nhr-114(gk849)* adults and *nhr-114*(RNAi) adults were stained with DAPI. As expected from the reduced sterility penetrance, *nhr-114(gk849)* and *nhr-114*(RNAi) animals fed HT115 develop germ lines that have wild-type looking mitotic, meiotic, oogenic and sperm nuclei (Figure 2.19 A-D). Although the total number of germ cells was not quantified, the germ line size suggests the number is similar to wild-type germ lines. Taken together these results indicated that HT115 is sufficient to abolish sterility in any situation of *nhr-114* loss, deletion mutants or RNAi knockdown. Therefore these results confirmed that abolishment of sterility by HT115 is specifically linked to *nhr-114* function and that *nhr-114* germ line defects depend on the food source. The initial question could not be addressed in this experiment; however these experiments hinted that Nhr-114 phenotypes were triggered by an exogenous factor.

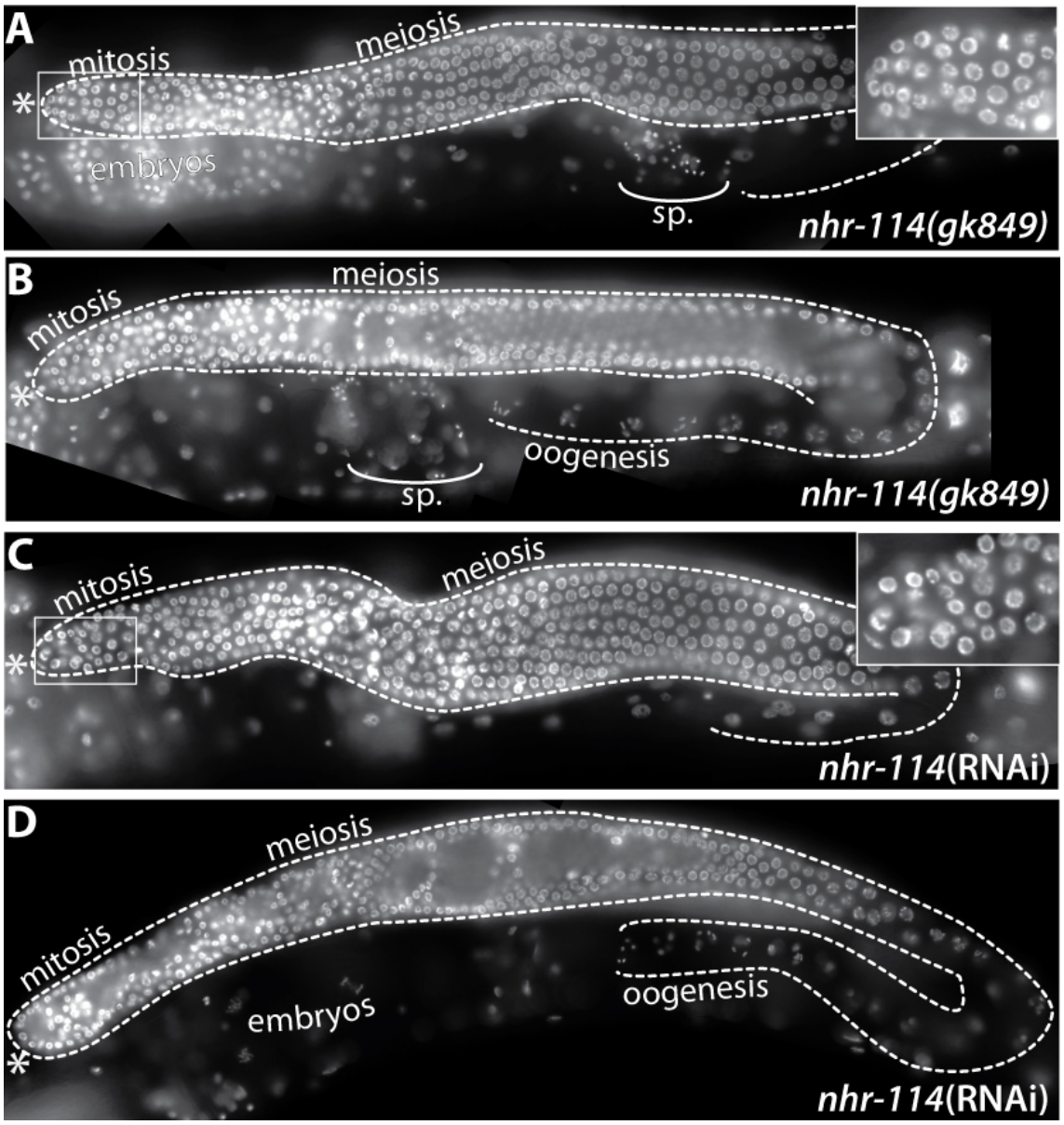

Figure 2.19 *E. coli* HT115 abolish Nhr-114 germline defects
Whole adult hermaphrodites stained with DAPI to visualize nuclei morphology. Two different germ line focal planes are outlined in each genetic background. **(A-B)** Adult *nhr-114(gk849)* animals fed HT115+IPTG show wild-type looking mitotic, meiotic, oogenic, sperm and embryonic nuclei (in A) without chromatin aberrations. Inset in A shows distal wild-type mitotic nuclei. **(C-D)** Adult *nhr-114*(RNAi) animals fed HT115+IPTG have wild-type looking germ lines with mitotic, meiotic, oogenic, and embryos without chromatin aberrations. Inset in C shows distal wild-type mitotic nuclei. **(B-D)** wild-type looking oogenic nuclei are present . Insets are scaled two times. Asterisk indicates the position of the distal tip.

2.10 IDENTIFICATION OF A NUTRIENT THAT ABOLISH *NHR-114* STERILITY

Why does HT115 abolish *nhr-114* sterility? One simple explanation is that *nhr-114* function ensures optimal levels of nutrients required for germline development that are less abundant in OP50, and more abundant in HT115. The OP50 strain is an *E. coli* B derivative and HT115 is an *E. coli* K12 derivative. In terms of macronutrient composition, the main difference between these two strains is that HT115 contains almost five times more carbohydrates than OP50 (Brooks et al. 2009). Although both *E. coli* strains have similar fatty acid composition and amounts, animals fed OP50 accumulate significantly more storage lipids (triacylglycerides) than those fed HT115 (Brooks et al. 2009). In addition, the most obvious difference between OP50 and HT115 is that OP50 is uracil-auxotroph (Brenner 1974).

2.10.1 URACIL-SUPPLEMENTED DIET DOES NOT ABOLISH NHR-114 STERILITY

E. coli OP50 was established as the standard laboratory food for *C. elegans* because it forms thin bacterial lawns on agar that facilitate microscopy (Brenner 1974). In contrast to HT115, OP50's growth depend on the available uracil in medium. To investigate whether *nhr-114* phenotypes arise from limited uracil levels in OP50, *nhr-114*(RNAi) animals were fed standard OP50 or 2 mg/l uracil-supplemented OP50 ($OP50^{Ura}$). As previous experiments, 95% of *nhr-114*(RNAi) animals (n>100) fed OP50 were sterile. Similarly, >95% of *nhr-114*(RNAi) animals (n=538) fed $OP50^{Ura}$ were sterile indicating that uracil-supplementation does not reduce Nhr-114 sterility. Therefore, limited uracil levels in OP50 are unlikely to trigger Nhr-114 sterility.

2.10.2 STEROL-DEPLETED DIET DOES NOT ENHANCE NHR-114 STERILITY

C. elegans cannot synthesize sterols *de novo*, hence it depends on exogenous sterol sources (Hieb and Rothstein 1968; Chitwood 1999). Following the reasoning that HT115 could provide nutrients that are scarce in OP50, and considering that *C. elegans* reproductive growth and fertility require a sterol-derived hormone (Matyash and Entchev et. al 2004), it was surmised that Nhr-114 sterility may be sensitive to sterols. To test this idea, wild-type or *nhr-114(gk849)* animals were grown on normal conditions or sterol-free conditions (Materials and Methods 4.1.4). If *nhr-114* sterility is triggered by a deficiency of a sterol-derived signal, it would expected that sterol-free conditions would raise the otherwise low penetrance of sterility in *nhr-114(gk849)* mutants. In contrast, if *nhr-114* sterility is independent of a sterol-derived signal, the penetrance of sterility in *nhr-114(gk849)* mutants on sterol-free conditions would remain similar to that on normal conditions.

Similar to was reported by Matyash and Entchev (2004), ~75% of wild type animals (n=553) grown on sterol-free conditions arrest as young larvae (L1-L3), the remaining 25 % reached adulthood (n=553). This larval arrest indicated that sterol depletion is effective. Similarly to the effect in wild type, the majority *nhr-114(gk849)* mutants (85%, n=797) grown on sterol-free conditions arrest as young larvae, the remaining 15% reached adulthood. The penetrance of sterility in these animals (n=123) that reached adulthood remained similar to those *nhr-114(gk849)* grown on standard conditions (n=1433). Therefore, these results indicate that sterol-depletion does not trigger *nhr-114* sterility and that *nhr-114* sterility is independent of a sterol-derived signal.

2.10.3 L-TRYPTOPHAN-SUPPLEMENTED DIET PREVENTS NHR-114 STERILITY

In *Drosophila*, oogenic germ line stem cells and their progeny respond to protein changes in diet: protein-rich diet promote robust germ cell proliferation, protein-poor diet impairs germ cell proliferation and fertility (Drummond-Barbosa and Spradling, 2001). This germ cell response to diet is mediated by insulin-dependent and insulin-independent mechanisms that regulate the cell cycle (La-Fever et al. 2005, Hsu et al. 2007). *C. elegans*, insulin signaling promotes robust larval germ cell proliferation too (Michaelson et al. 2010). However, Michaelson et al. (2010) assumed that the effect on germ cell proliferation is triggered by nutrient-rich diets in a similar way to *Drosophila*, but is was not experimentally confirmed. The documented connection between protein-rich diet and germ line proliferation in *Drosophila* raised questions whether the HT115 effect on Nhr-114 sterility was reflecting a protein-driven effect. Brooks and colleagues (2009) reported that both OP50 and HT115 show no apparent differences in bulk protein amounts, albeit the composition of individual amino acids in each strain remains unknown. Nevertheless, even small differences in essential amino acids in both *E. coli* strains may be relevant when considering that general protein synthesis is very sensitive to variations in essential amino acids supply (Jefferson and Kimball, 2000).

Under laboratory conditions, *C. elegans* laboratory diet is spotted on agar, which provides additional nutritional support for the bacteria. Therefore, *C. elegans* nutrition may ultimately be influenced by the macronutrients present in the supporting medium such as salts, cholesterol, and peptone, which serve as the source for amino acids. However, the proportion of individual amino acid varies among peptone batches because it is an enzymatic product of animal proteins (Loginova et al. 1974). Based on these observations, I set to investigate whether amino acid supplementation on standard OP50 food plates could prevent Nhr-114 sterility. To test this idea, *nhr-114*(RNAi) animals were fed OP50 or OP50 supplemented with all L-amino acids (OP50^{+all}) or specific L-amino acids (OP50$^{a.a}$) (Materials and Methods 4.1.3).

I reasoned that if Nhr-114 sterility were triggered by a deficiency in amino acids, the OP50 bacteria supplemented with all amino acids would reduce the penetrance of sterility in *nhr-114*(RNAi) animals. In contrast, if *nhr-114* sterility is triggered by a deficiency in essential amino acids (arginine, histidine, isoleucine, leucine, lysine, methionine, phenylalanine, threonine, tryptophan and valine) it would be expected that OP50 supplemented with only essential amino acids would be sufficient to reduce the penetrance of sterility in *nhr-114*(RNAi) animals.

Almost all *nhr-114*(RNAi) animals fed OP50 were sterile (n=228) (Figure 2.20, white bars). Similarly, 90% of *nhr-114*(RNAi) animals fed OP50 supplemented with all amino acids except tyrosine and tryptophan (OP50$^{+\text{all-TYR-TRP}}$) were sterile, the remaining 10% was fertile (n=601), see fig. 2.20. However, this mixture lacked tyrosine and the essential amino acid tryptophan. When tyrosine but not tryptophan was added to the amino acid mixture (OP50$^{+\text{all-TRP}}$) 60% of *nhr-114*(RNAi) animals were sterile, the remaining 40% was fertile (n=361), indicating that bulk amino acid supplementation has a mild effect in reducing Nhr-114 sterility. Unexpectedly, when tryptophan, but not tyrosine, was added to the amino acid mixture (OP50$^{+\text{all-TYR}}$) sterility was reduced to 15% (n=443), suggesting that tryptophan itself could be the key essential amino acid that reduces Nhr-114 sterility, see fig. 2.20.

To test if tryptophan itself was sufficient to reduce sterility, *nhr-114*(RNAi) animals were fed OP50 supplemented with tryptophan itself or in combination with other amino acid. Less than 8% of *nhr-114*(RNAi) animals fed OP50 supplemented with tryptophan in combination with tyrosine (OP50$^{+\text{TRP+TYR}}$), see fig. 2.20, or with lysine (OP50$^{+\text{TRP+LYS}}$, not shown) were sterile, the remaining 92 % was fertile (n=276, n=204, respectively). However, almost all *nhr-114*(RNAi) animals fed OP50 supplemented with only tyrosine (n=332), lysine (OP50$^{+\text{LYS}}$), alanine (OP50$^{+\text{ALA}}$), or glycine (OP50$^{+\text{GLY}}$) (n>500 in each condition, not shown) were sterile. In contrast, 5% of *nhr-114*(RNAi) animals were sterile when fed OP50 supplemented with only tryptophan (OP50$^{+\text{TRP}}$), the remaining 95% was fertile (n>600), see fig. 2.20 This result indicated that tryptophan, but no other amino acid is sufficient to reduce *nhr-114* sterility.

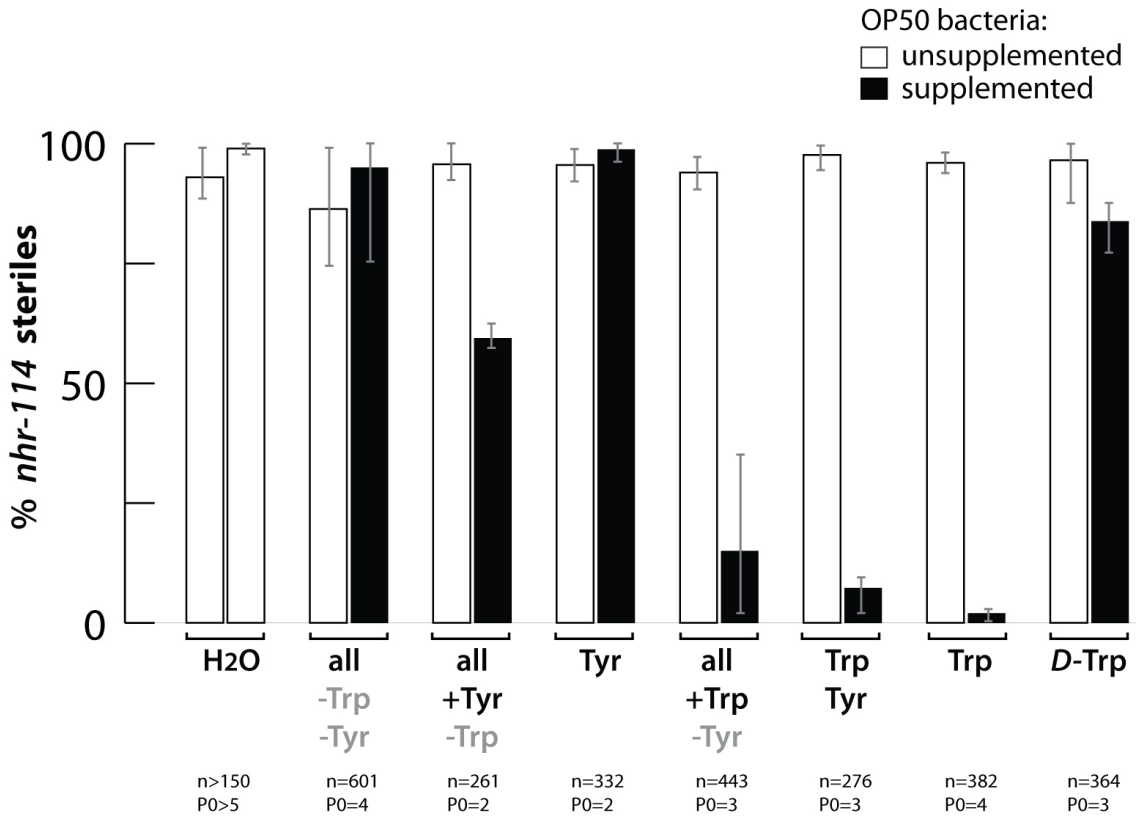

Figure 2.20 L-tryptophan-supplemented diet prevents Nhr-114 sterility
Percentage (%) of sterile adult animals with respect to the total number of animals analyzed, n> 200 in each condition, see main text for exact number. To ensure that *nhr-114* RNAi knockdown was effective, injected mothers were first OP50 fed for 24h (white bars), and then transferred to an amino acid supplemented OP50 plate (black bars). H_20 was used to dissolve all amino acids. Note that the effectiveness of RNAi knockdown is increased after 24 h post injection (second white bar in H20 treatment). All amino acids (all) as described in Materials and Methods, (-) indicates missing amino acids, (+) indicates added amino acid. Trp: tryptophan, Tyr: tyrosine. L-amino acids were used in all cases; except for D-Trp. Error bars indicate the range of sterility among independent experiments. (n=) corresponds to the total number of animals per corresponding supplementation (black bar). n>100 for each other corresponding unsupplemented condition.

Amino acids are chiral compounds therefore exists as D- or L-stereoisomers (Nelson and Cox, 2005). Virtually all amino acid residues in proteins are L-stereoisomers, and the asymmetric active sites of enzymes catalyze L-sterospecific reactions. Thus, D-amino acid residues are practically excluded from biological compounds, yet rarely present in bacteria (Nelson and Cox, 2005).

To investigate if Nhr-114 sterility was reduced by a biologically active tryptophan form, *nhr-114*(RNAi) animals were fed with OP50 supplemented with L-tryptophan or D-tryptophan. If supplemented L-tryptophan were biologically active, D-tryptophan would not be expected to reduce Nhr-114 sterility. On the contrary, if the tryptophan effect on Nhr-114 sterility were mediated by another compound that co-purifies with tryptophan, D-tryptophan would also reduce Nhr-114 sterility. Contrary to L-tryptophan-supplementation, the majority of *nhr-114*(RNAi) animals (80%, n=364) were sterile when fed D-tryptophan-supplemented OP50, indicating that the reduction of Nhr-114 sterility is specific to biologically active tryptophan, see fig. 2.20. This results shows that specifically L-tryptophan, but not D-tryptophan, or any other amino acid, is sufficient to reduce Nhr-114 sterility. Taken together, these results suggest that L-tryptophan is compensating the absence of *nhr-114*, and that Nhr-114 sterility is triggered by tryptophan deficiency.

2.10.4 Exogenous serotonin does not prevent Nhr-114 sterility

As a further step, I set to investigative the possible mechanisms by which tryptophan prevents Nhr-114 sterility. A simple explanation is that tryptophan is metabolized into a compound that promotes fertility. Serotonin (5-hydroxytriptamine, 5-HT) is a tryptophan derivative (Figure 2.21 A). In *C. elegans*, exogenous serotonin induces pharyngeal pumping; therefore it is a potent modulator of the feeding rate (Avery and Horvitz, 1990). Hence, it raised the question whether supplemented tryptophan was metabolized to serotonin, which promotes higher food consumption that allows proper germline development in *nhr-114* animals. To test this hypothesis, *nhr-114*(RNAi) animals were fed with OP50 or OP50 supplemented with serotonin. Two different serotonin concentrations were chosen: 0.3 mM serotonin is the equivalent molar concentration as tryptophan supplementation. 5 mM serotonin elicits behavioral responses in *C. elegans*: depresses locomotion, stimulates pharyngeal pumping and stimulates egg laying (Horvitz et al. 1982). I reasoned that if supplemented tryptophan were metabolized into serotonin, then exogenous serotonin would be sufficient to reduce Nhr-114 sterility. In contrast, if Nhr-114 sterility were independent of a serotonergic pathway, serotonin supplementation would not reduce it.

As in previous experiments, more than 80% of *nhr-114*(RNAi) animals fed OP50 were sterile (n=69) (Figure 2.21 B, white bar). Similarly, more than 90% of *nhr-114*(RNAi) animals were sterile when OP50 supplemented with two different concentration of serotonin (0.3mM, n=333; 0.5 mM, n=64) see fig. 2.21 B, black bars). The high percentage of sterility upon serotonin supplementation indicated that exogenous serotonin does not prevent Nhr-114 sterility; therefore these data strongly suggests that the tryptophan effect in reducing *nhr-114* sterility is independent of serotonin.

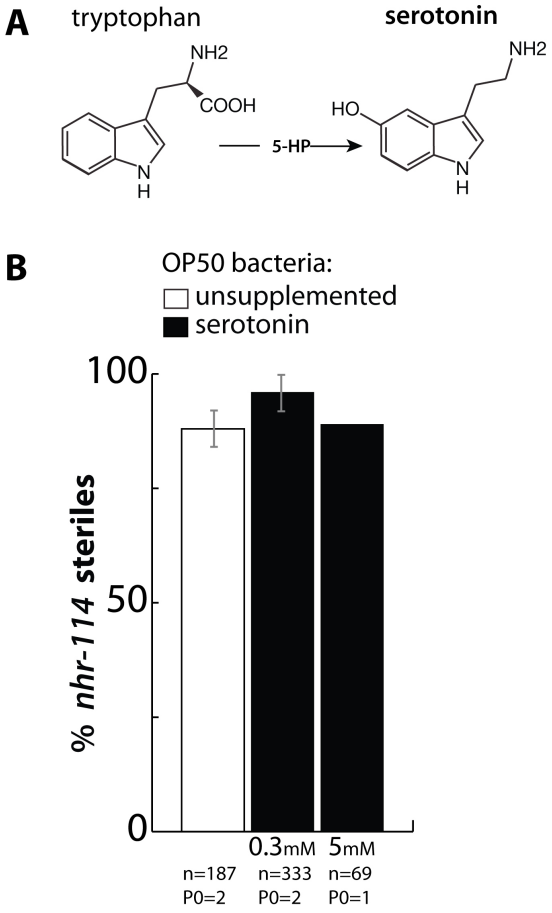

Figure 2.21 Exogenous serotonin does not prevent Nhr-114 sterility
A) Chemical structures of tryptophan and serotonin. Tryptophan is serotonin precursor; serotonin is synthetized in two chemical reactions. The first reaction is the rate-limiting step and produces 5-hydroxytryptophan (5-HP), this reaction is catalyzed by tryptophan hydroxylase (TPH). The second step is catalyzed by 5-HTP/L-dopa decarboxylase and matures 5-HP to serotonin (Sze et al. 2000). **B)** Percentage (%) of sterile adult animals with respect to the total number of animals analyzed per set. To ensure that *nhr-114* RNAi knockdown was effective, injected mothers were first OP50 fed for 24h (white bars), and then transferred to a serotonin supplemented OP50 plates (black bars). Error bars indicate the range of sterility among independent experiments.

2.11 TRYPTOPHAN PROMOTES PROLIFERATION AND OOGENESIS IN *NHR-114* GERM LINES

As shown in the previous section, loss of *nhr-114* leads to three major germ line defects that lead to sterility: underproliferation of the mitotic cells, lack of oocytes, and syncytial disorganization characterized by germ cell multinucleation. Tryptophan abolishes *nhr-114* sterility. What is the positive effect of tryptophan on germ line development? To address this question, *nhr-114* (RNAi) animals fed tryptophan-supplemented diets were analyzed by DIC microscopy. Considering that *nhr-114* animals develop wild-type looking germ lines when fed HT115 bacteria, it was expected that *nhr-114*(RNAi) animals would also develop wild-type looking germ lines when fed OP50 tryptophan-supplemented diet (OP50^{+TRP}). As expected, almost all *nhr-114*(RNAi) animals fed OP50^{+TRP} (n=128) developed fertile germ lines with normal syncytia; however, germ cell proliferation was not wild-type-like (Figure 2.22 A-C). Also, 48% of these fertile germ lines still contained germ cell multinucleation, see fig. 2.22 A-B; the remaining 52% lacked multinucleated germ cells (n=128).

Importantly, if tryptophan is supplemented in combination with all amino acids (OP50$^{+all-TYR}$), 75% of *nhr-114*(RNAi) animals develop wild-type-like germ lines, the remaining 15% contained multinucleated germ cells (n=73), see fig. 2.22 D. In a similar way, if tryptophan is supplemented in combination with tyrosine (OP50$^{+TRP+TYR}$) or lysine (OP50$^{+TRP+LYS}$), 90% of *nhr-114*(RNAi) animals develop wild-type-like germ lines, and only the remaining 10% contained multinucleated germ cells (n=48 and 108, respectively), see fig. 2.22 E-F. Since neither OP5O^{+TYR} nor OP5O^{+LYS} ameliorate of *nhr-114* phenotypes (images not shown), the germline effect of OP50$^{+TRP+TYR}$ and OP50$^{+TRP+LYS}$ is specific for tryptophan. These results therefore indicate that in the loss of *nhr-114*, tryptophan is sufficient to restore fertility by promoting mitotic proliferation, proper germline organization and oogenesis. In addition, if tryptophan is combined with other amino acids, tryptophan is able to reduce germ cell multinucleation defects. Therefore, the data suggest that tryptophan supplementation bypasses *nhr-114* germline functions (proliferation and oogenesis), and that tryptophan combined with other amino acids bypasses *nhr-114* somatic functions and indirectly proper germ cell divisions.

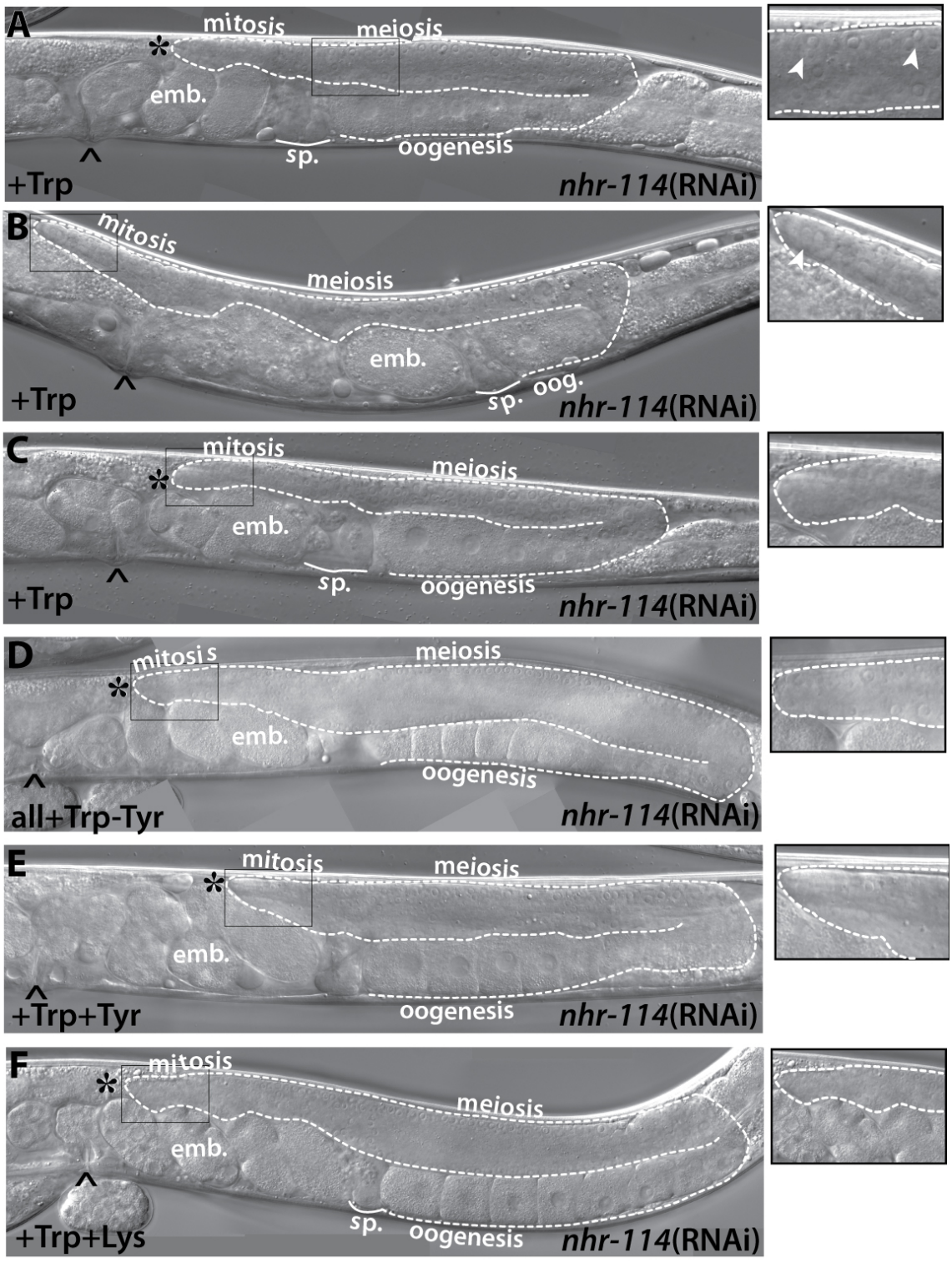
A
mitosis
meiosis
emb.
sp.
oogenesis
+Trp
nhr-114(RNAi)
B
mitosis
meiosis
emb.
sp.
oog.
+Trp
nhr-114(RNAi)
C
mitosis
meiosis
emb.
sp.
oogenesis
+Trp
nhr-114(RNAi)
D
mitosis
meiosis
emb.
oogenesis
all+Trp-Tyr
nhr-114(RNAi)
E
mitosis
meiosis
emb.
oogenesis
+Trp+Tyr
nhr-114(RNAi)
F
mitosis
meiosis
emb.
sp.
oogenesis
+Trp+Lys
nhr-114(RNAi)

Figure 2.22 L-Trp restores proliferation and oogenesis in *nhr-114* germ lines
DIC microscopy images of adult *nhr-114*(RNAi) animals fed with amino acid-supplemented OP50. Mitotic and meiotic regions, oogenesis, sperm (sp.) and embryos (emb.) are indicated. Asterisk indicates the position of the distal tip cell, and the distal gonad. Caret indicates the position of the vulva. Insets are scaled two times. **(A-C)** Animals fed tryptophan-supplemented diet (+Trp), show germ lines with wild-type-like organization and oocytes, but also proliferation defects. Insets highlight germ cell nuclei, arrowheads indicate multinucleated cells. **(D)** Animal fed a diet supplemented with all amino acids except tyrosine (all+Trp-Tyr) shows a typical wild-type-like germ line. **(E)** Animal fed diet supplemented with tryptophan and tyrosine (+Trp+Tyr) shows a wild-type-like germ. **(F)** Animal fed a diet supplemented with tryptophan and lysine (+Trp+Lys) shows a typical wild-type-like germ line.

SECTION III: *NHR*-114 FUNCTION IS LINKED TO POSTTRANSCRIPTIONAL CONTROL

2.12 PREFACE TO SECTION III

Previous chapters in this thesis show that *nhr-114* function is essential for germ line development and its functions are linked to a dietary input. In addition, this thesis identified that *nhr-114* function, similar to *gld-4* function, is involved in mitotic proliferation and oogenesis. However, it remains unknown whether *nhr-114* functions are linked to posttranscriptional programs that control gene expression in the germ line. The interaction between NHR-114 and GLD-4 proteins in the yeast-two-hybrid screen, and the overlapping phenotypes between *nhr-114* and *gld-4* mutants, suggested that GLD-4 cytoPAP may link NHR-114 function to germline posttranscriptional programs. In order to validate this hypothesis, I set to validate and characterize the interaction between NHR-114 and GLD-4 proteins in further detail, and to investigate how *nhr-114* and *gld-4* are genetically linked. In an attempt to study NHR-114 protein dynamics *in vivo,* different anti-NHR-114 polyclonal and monoclonal antibodies were generated. Although anti-NHR-114 antibodies specifically recognize recombinant NHR-114 protein they failed to recognize endogenous NHR-114 protein (Appendix 1). Therefore, validation of NHR-114 protein complexes *in vivo* remains elusive. Nevertheless, directed yeast-two-hybrid assays provided a powerful tool to investigate in further detail the interaction between NHR-114 and GLD-4 proteins in a heterologous system.

2.13 NHR-114 SPECIFICALLY BINDS GLD-4 CYTOPAP IN YEAST

To test if GLD-4 binds specifically to NHR-114, a directed yeast-two-hybrid assay was performed (Materials and Methods 4.4) To this end, GLD-4 and NHR-114 proteins were fused N-terminally to either LexA or Gal4 activation domain reporter protein domains (hybrids), and co-expressed in yeast. If the two testing fusion proteins form a complex, LexA and Gal4 domains come in close proximity of each other and activate the transcription of the reporter gene ß-galactosidase (ß-gal). Upon addition of a substrate that turns blue in the presence of ß-gal, one infers that the testing proteins interact. To validate a specific interaction between NHR-114 and GLD-4, NHRs -17, -68 and -114 were fused to Gal4 and tested for interaction with GLD-4 hybrid. Since LexA::NHR-114 hybrid protein interacts non-specifically with any GAL4 fusion, only NHR-114:GAL4 protein interactions were investigated. To validate the assay and as a control for a positive interaction, LexA::GLD-4 was co-expressed with Gal4::GLS-1 (Schmid et al. 2009). As negative control LexA::GLD-4 was coexpressed with Gal4 domain or germ line protein FOG-1, a presumed RNA binding protein (Luitjens et al. 2000).

Consistent with previous yeast two-hybrid assays, LexA::GLD-4 does not bind Gal4 domain, neither the germline protein Gal4::FOG-1, but binds Gal4:GLS-1 and Gal4::NHR-114 (Figure 2.23). Moreover, LexA::GLD-4 does not bind NHR-17 nor NHR-68 hybrids. To test if NHR-114 interaction was specific to GLD-4 cytoPAP, the LexA::GLD-2 cytoPAP was co expressed with Gal4::NHR-114. As expected, GLD-2:LexA cytoPAP does not bind NHR-114:Gal4, see fig. 2.23 Fusion protein expression was validated by immunoblotting. These results indicated that GLD-4 cytoPAP binds specifically NHR-114 in yeast.

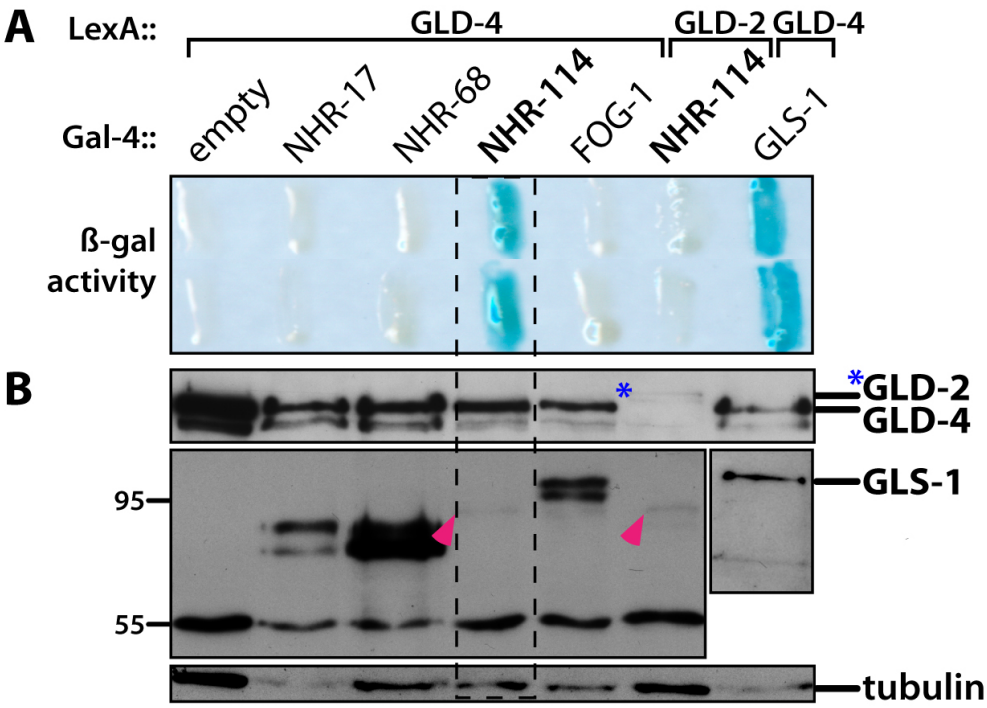

Figure 2.23 NHR-114 specifically binds GLD-4 cytoPAP in yeast
(A) Panel shows ß-galactosidase activity (ß-gal) on X-gal substrate from two yeast colonies co-expressing two hybrid proteins. White colonies indicate no hybrid interaction; blue colonies indicate hybrid interaction, as in GLD-4/NHR-114 (dotted box) and GLD-4/GLS-1. **(B)** Immunoblots for detection of hybrid protein expression. Top blot: anti-LexA antibody. LexA::GLD-2 (asterisk). Middle blot: anti-HA antibody. Low levels of NHR-114 hybrid proteins (pink triangles). Note that this level of NHR-114 protein are sufficient to activate the reporter, suggesting that NHR-114 may bind GLD-4 effectively. Band at 55kDA is background. Left blot: anti-GLS-1 antibody. Bottom blot: loading control using anti-tubulin antibody.

2.13.1 NHR-114 LIGAND-BINDING DOMAIN BINDS GLD-4

In order to obtain some mechanistic insight into the NHR-114 and GLD-4 interaction, I set to identify the NHR-114 protein domain(s) required for binding GLD-4 protein. To identify such NHR-114 domain(s), truncated NHR-114 hybrids were produced, Δ1 to Δ11 (Figure 2.24 A). The resulting hybrid proteins were assayed for interaction with GLD-4 protein as described above. Since NHR-17 and NHR-68 proteins are closely related to NHR-114, but do not bind GLD-4, I reasoned that NHR-114's most distinct region, the area surrounding DUF1351, would bind GLD-4.

Consistent with the previous yeast two-hybrid result, this assay demonstrates that LexA::GLD-4: does not bind GAL4 domain, but binds full-length Gal4::NHR-114 protein (Figure 2.24 B). However, although all NHR-114 protein truncations were expressed, only NHR-114-Δ3 recapitulated the interaction with GLD-4 (Figure 2.24 B). This indicated that the LBD and the hinge region of NHR-114 are sufficient to bind GLD-4. In an attempt to identify NHR-114-Δ3's minimal region necessary to bind GLD-4, additional amino (N-) terminal and carboxy (C-) terminal protein truncations were generated respecting predicted helical conformations (Δ8-Δ11). However, none of these truncations recapitulated the interaction with GLD-4, see 2.24 B, Δ10-Δ11 are not shown. This result indicated that an intact hinge region and the LBD of NHR-114 are both necessary and sufficient to bind GLD-4 in yeast.

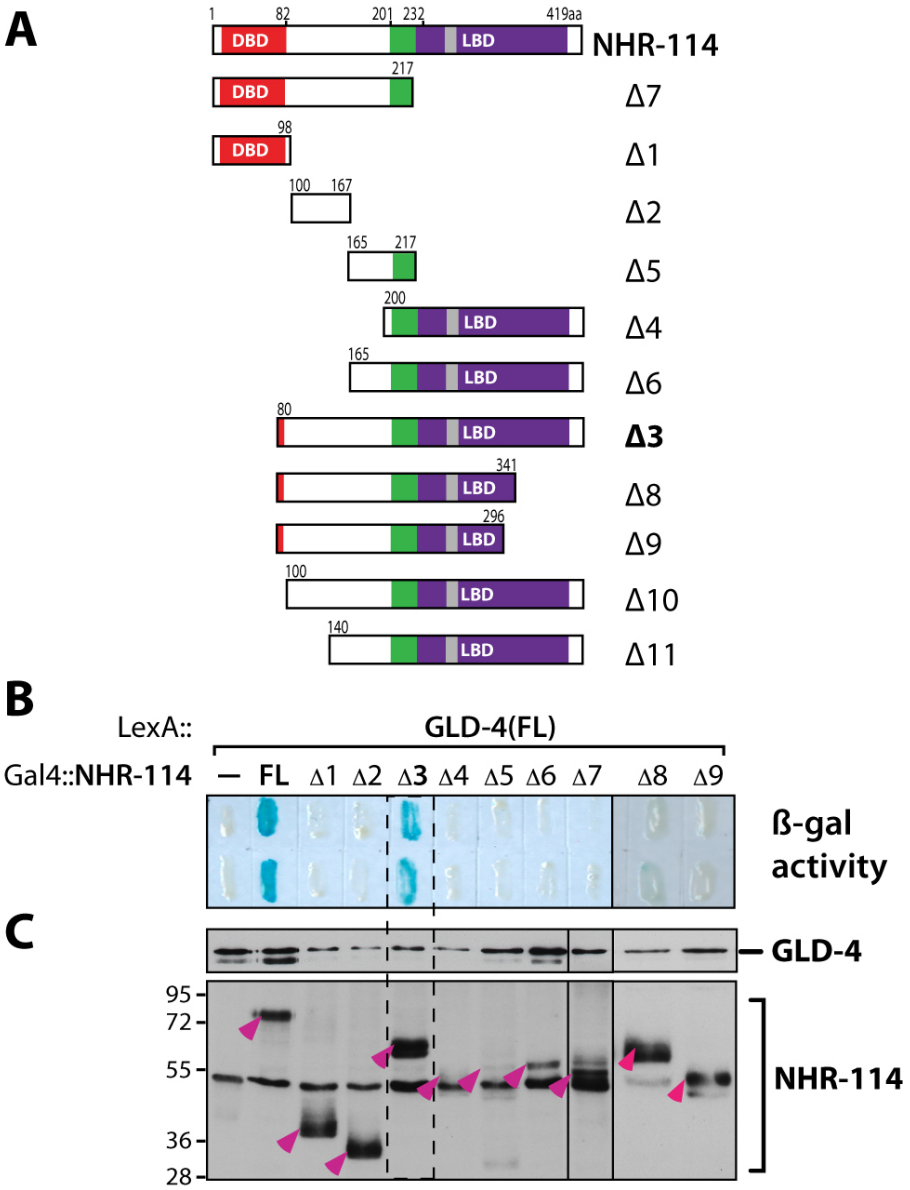

Figure 2.24 NHR-114's hinge region and LBD domain bind GLD-4
(A) Protein domains in different NHR-114 protein truncations. Full-length NHR-114 contains: DNA-binding domain (DBD, red), the ATP-binding domain (green), the domain of unknown function DUF1351 (gray), and the ligand-binding domain (LBD, purple). Numbers on top of the diagram indicate the amino acid residue with respect of NHR-114 full-length protein sequence. **(B-C)** Directed yeast two-hybrid assays. **(B)** Gal-4 protein itself (-) or fused to the indicated NHR-114 truncated proteins. Interaction with LexA::GLD-4 measured in a ß-galactosidase assay (ß-gal). White colonies indicate no hybrid interaction; blue colonies indicate hybrid interaction, as in GLD-4/NHR-114-full length and GLD-4/NHR-114-Δ3 (dotted box). **(C)** Immunoblots to visualize hybrid protein expression. Top blot: anti-Lex-A antibody. Lower blot: anti-HA antibody to detect Gal4 domain. NHR-114 truncated hybrid proteins (pink triangles). Background band at 55kDA serves as loading control.

2.13.2 GLD-4 CATALYTIC REGION BINDS NHR-114

GLD-4 cytoPAP is predicted to contain two conserved domains, a catalytic nucleotydiltransferase domain (NTD) and a poly(A) polymerase associated domain (PAD). In addition to these domains, a poly(A) polymerase central domain is also located at GLD-4's N-terminal region, the rest of GLD-4 C-terminal region lacks predictable sequence motifs (Schmid et al. 2009). In order to identify the GLD-4 protein domain(s) required for binding NHR-114 protein, GLD-4 protein truncations hybrids were produced: N-term, middle and C-term (Figure 2.25 A), and assayed for interaction with NHR-114 full-length protein. Since GLS-1 protein interacts with the N-terminal region (N-term) of GLD-4 in the in yeast (Botti V. and Eckmann CR., unpublished results); and GLS-1stimulates GLD-4 cytoPAP function (Schmid et al. 2009), the expectation was that NHR-114 would bind a different region from the N-terminal one of GLD-4.

Consistent with the previous assays, Gal4::NHR-114 binds full-length LexA::GLD-4 protein, and serves as a positive control, see fig. 2.25 B. Only a GLD-4 N-terminal fragment containing the entire NTD and PAD regions binds NHR-114, but not a middle or C-terminal GLD-4 fragment, see 6.3 B. This indicated that GLD-4's functional domains mediate the interaction with NHR-114. In an attempt to identify GLD-4's minimal region necessary to bind NHR-114, additional protein N-terminal truncations of GLD-4 were tested (Δ1-Δ4) (Figure 2.26 A). However, none of these truncations recapitulated the interaction with GLD-4, see fig. 2.26 B. This result indicated that the complete catalytic region of GLD-4 is both necessary and sufficient to bind NHR-114 in yeast. Taken together, this analyses show that NHR-114 binds GLD-4 in a specific manner. In addition, NHR-114 protein binds to a GLD-4 fragment that is also the minimal interacting region required for GLS-1 binding. Therefore, this finding suggests that NHR-114 binding could also play a regulatory role on GLD-4 cytoPAP activity, similar or opposite to GLS-1.

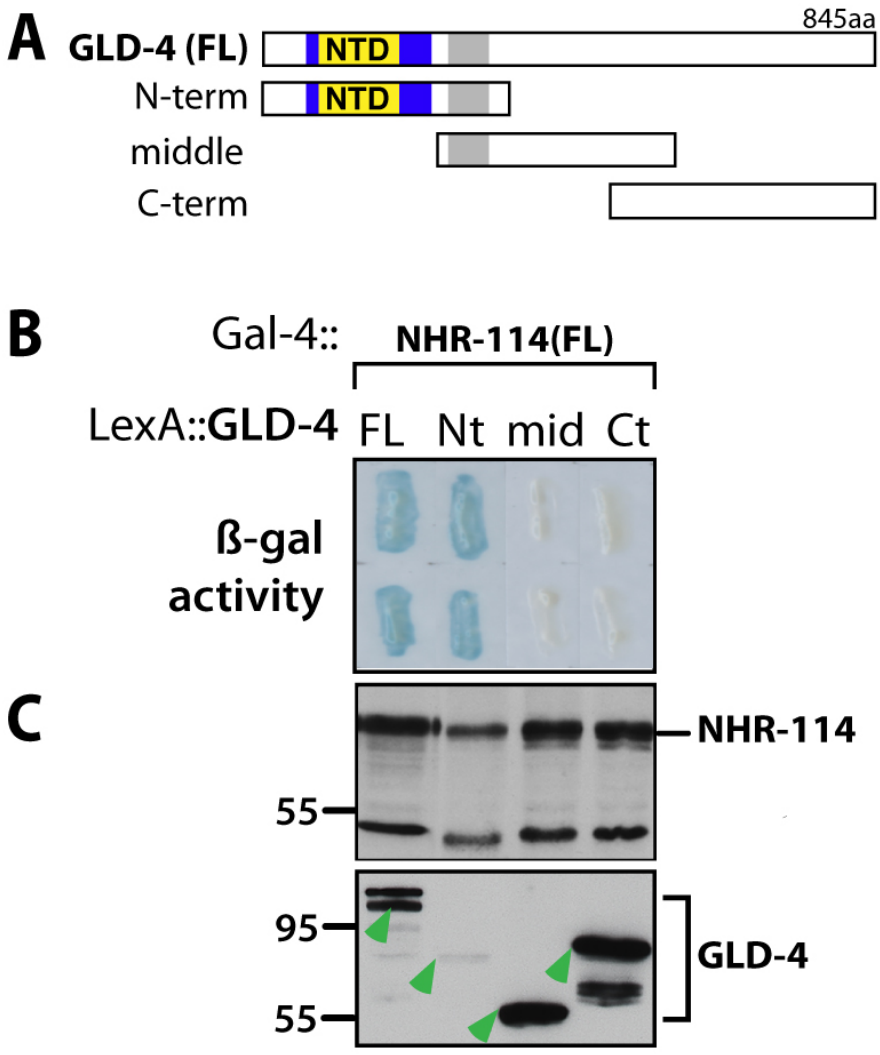

Figure 2.25 GLD-4 catalytic region binds GLD-4
A) Diagrams show protein domains of GLD-4 full-length protein: the nucleotydiltransferase domain (NTD, yellow), the poly(A) polymerase central domain (blue) and the poly(A) polymerase associated domain (gray). **(B)** Directed yeast two-hybrid assays. White colonies indicate no hybrid interaction; blue colonies indicate hybrid interaction, as in NHR-114(FL)/GLD-4(FL) and NHR-114/GLD-4-Nter (dotted box). **(C)** Immunoblots for detection of hybrid protein expression. Top blot: anti-HA antibody detects Gal4::NHR-114 protein. Background band at 55kDA serves as loading control. Lower blot: anti-Lex-A antibody detects LexA::GLD-4 truncated hybrid proteins (green triangles).

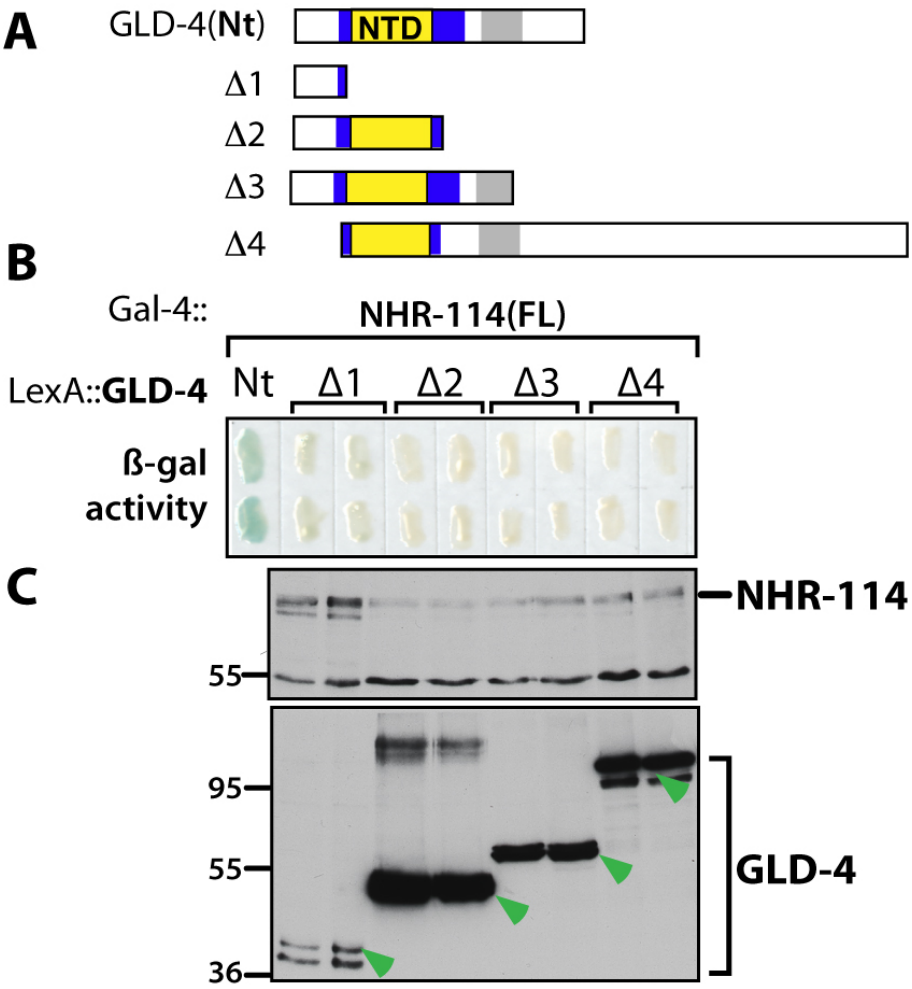

Figure 2.26 Truncations of GLD-4 catalytic region abolish NHR-114 binding
A) Diagrams show protein domains of GLD-4 full-length protein: the nucleotydiltransferase domain (NTD, yellow), the poly(A) polymerase central domain (blue) and the poly(A) polymerase associated domain (gray). **(B)** Directed yeast two-hybrid assays. White colonies indicate no hybrid interaction; blue colonies indicate hybrid interaction, as in NHR-114/GLD-4-Nter only. **(C)** Immunoblots for detection of hybrid protein expression. Top blot: anti-HA antibody detects Gal4::NHR-114 protein. Background band at 55kDA serves as loading control. Lower blot: anti-Lex-A antibody detects LexA::GLD-4 truncated hybrid proteins (green triangles). Δ1-Δ4 constructs were provided by V. Botti.

2.14 NHR-114 GERM CELL MULTINUCLEATION DEFECTS REQUIRE *GLD-4* AND *GLS-1*

The specific interaction of NHR-114 protein with GLD-4's catalytic region suggested that a GLD-4/NHR-114 cytoPAP complex may exists *in vivo*. In addition, the overlapping phenotypes between *nhr-114* and *gld-4* mutant suggested that both genes are required for mitotic proliferation and oogenesis. Therefore, it was intriguing to know how germ lines that lack both *gld-4* and *nhr-114* look. To address this point, *nhr-114* was knocked down by RNAi in heterozygote *gld-4(ef15)* mothers. Considering the *nhr-114* RNAi knockdown effect observed in other genetic backgrounds, I anticipated that *gld-4(ef15)*; *nhr-114*(RNAi) animals would show Nhr-114 defects: severe underproliferation, lack of oocytes and syncytial defects. Since *gld-4(ef15)* germ lines also show underproliferation and lack of oocytes, I focused my analysis on the germ cell multinucleation defect, an Nhr-114 conspicuous syncytial defect, as a read-out of the genetic interactions.

The majority of *nhr-114*(RNAi) germ lines (80%, n>170) have germ cell multinucleation, the remaining 20% has wild-type-like mononucleation (Figure 2.27, first black bar, and fig. 2.28 A). The majority of *gld-4(ef15)* germ lines has wild-type-like mononucleation (95%, n=109), only a minority show multinucleation defects (5%, n=109), see fig. 2.27 and fig. 2.28 B. Unexpectedly, the majority of *gld-4(ef15); nhr-114*(RNAi) germ lines lacked Nhr-114 multinucleation defects (78%, n=150). Only a fraction of these germ lines had multinucleation defects (22%, n=150), see Fig. 2.28 C-D, Fig. 2.28 C-D. This analysis indicated that the penetrance of the Nhr-114 multinucleation defect is significantly reduced in a *gld-4(ef15)* mutant background, suggesting that this defect requires *gld-4* activity. This result implies that in *nhr-114*(RNAi) germ lines germ cell division defects (multinucleation) arise as a consequence of GLD-4 activity, which may be mis-regulated in the absence of NHR-114.

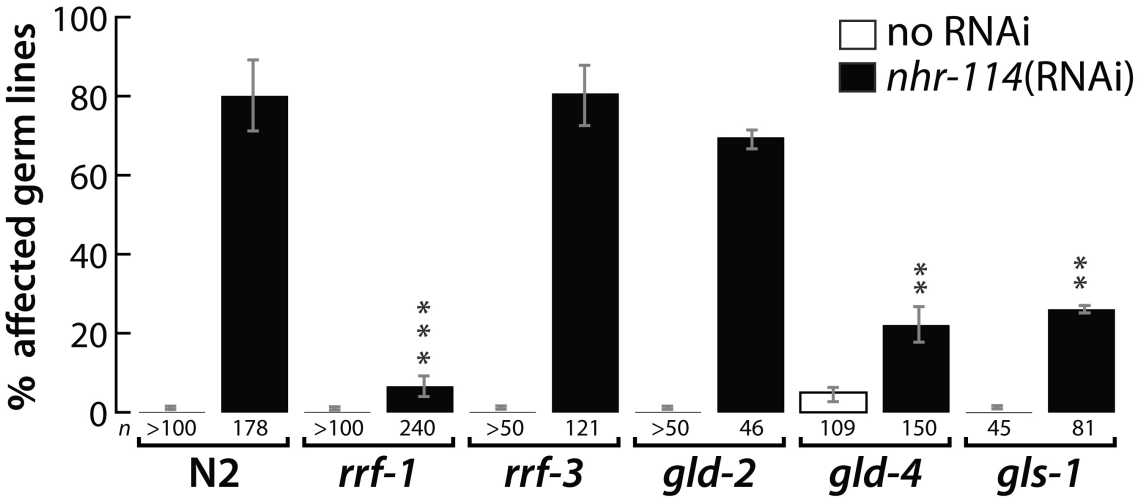

Figure 2.27 Nhr-114 multinucleation defects in different genetic backgrounds
Percentage (%) of germ lines with multinucleation defects in respect to the total number of germ lines analyzed per set (n). Low row indicates the strain genotype. Multinucleated germ lines are defined as those that contain at least one germ cell with more than one nucleus. No RNAi knockdown control, white bar. *nhr-114* RNAi, black bars. Error bars indicate range among independent experiments. **N2** is the wild type reference strain and has no multinucleation, but high penetrance of multinucleation (~80%) upon *nhr-114*(RNAi) knockdown. ***rrf-1*** Illustrates the reduction of multinucleation defects when only germline *nhr-114* is knocked-down, as in *rrf-1(pk1417)*; *nhr-114*(RNAi). ***rrf-3*** Increased multinucleation defects are apparent in *rrf-3(pk1426)*; *nhr-114*(RNAi) germ lines, in which the soma is hypersensitive for RNAi. ***gld-2*** Multinucleation is absent in *gld-2*; upon *nhr-114* RNAi knockdown multinucleation is present to a similar penetrance as in N2 or *rrf-3*. ***gld-4*** shows a low penetrance of multinucleation (~5%), which increases (22%) upon *nhr-114* RNAi knockdown. Note that despite the increase, the penetrance is significantly lower than in *nhr-114* RNAi knockdown in N2. ***gls-1*** shows no multinucleation itself, but a reduced penetrance of multinucleation (24%) upon *nhr-114* RNAi knockdown, in respect to N2 or the *rrf-3* background. Significance values with respect to *nhr-114* (RNAi). *P* values, *t*-test, ** p=0.01, *** p<0.01.

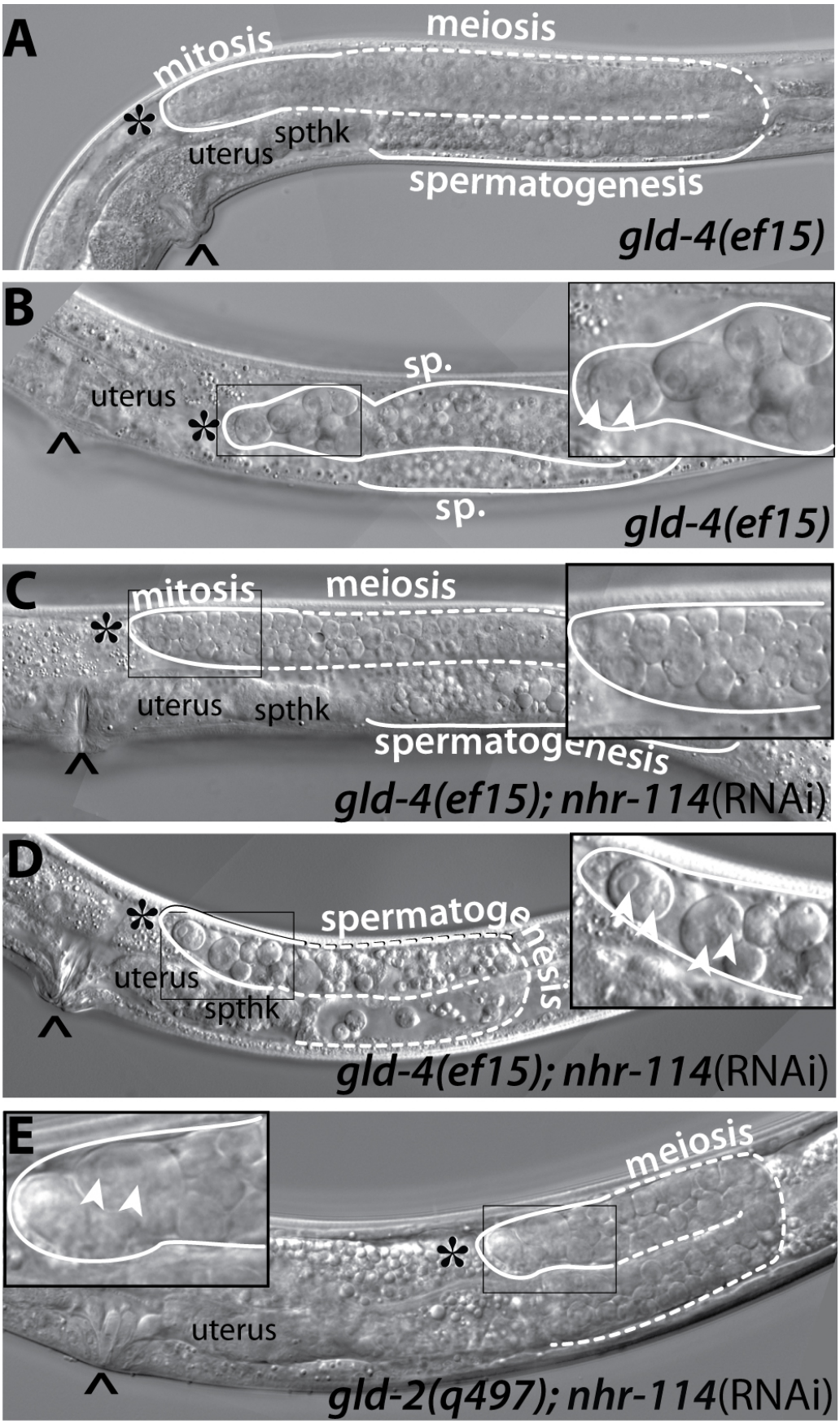
A
mitosis
meiosis
spthk
uterus
spermatogenesis
gld-4(ef15)
B
sp.
uterus
sp.
gld-4(ef15)
C
mitosis
meiosis
uterus
spthk
spermatogenesis
gld-4(ef15); nhr-114(RNAi)
D
spermatogenesis
uterus
spthk
gld-4(ef15); nhr-114(RNAi)
E
meiosis
uterus
gld-2(q497); nhr-114(RNAi)

Figure 2.28 Nhr-114 multinucleation defects in germline cytoPAP mutants
DIC microscopy images of adult animals. Mitotic and meiotic regions, and spermatogenesis are indicated. Asterisk indicates the position of the distal tip cell, and the distal gonad. Caret indicates the position of the vulva. Inset images are scaled two times and highlight multinucleation (arrowhead). **(A-B)** *gld-4(ef15)* animals show two different classes of *gld-4* sterile germ lines (n=109). (A) ~95 % show underproliferated germ lines with meiotic cells and sperm, they lack both oocytes and germ cell multinucleation. (B) The remaining 5% are severely underproliferated, contain only sperm, and have multinucleated germ cells. **(C-D)** *gld-4(ef15); nhr-114*(RNAi) animals show two different classes of sterile germ lines (n=150). (C) ~78% show underproliferated germ lines with meiotic cells and sperm, they lack both oocytes and germ cell multinucleation. (D) The remaining 22% are severely underproliferated, contain only sperm, and have multinucleated germ cells. **(E)** ~76% of *gld-2(q497); nhr-114*(RNAi) germ lines show underproliferation and germ cell multinucleation (n=46).

The germline cytoPAPs *gld-4* and *gld-2* have a redundant function in promoting meiotic progression (Schmid et al. 2009); however, it is not know if they have other redundant functions. To investigate weather *nhr-114* multinucleation also requires *gld-2* function, genetic epistatic interactions between *nhr-114* and *gld-2* were analyzed by *nhr-114* RNAi knockdown in heterozygote *gld-2(q497)* mothers. The resulting homozygote *gld-2(q497)*;*nhr-114*(RNAi) progeny was scored for germline defects. Since *gld-2(q497)* germ lines contain no proliferation or apparent germ cell division defects (multinucleation), it was envisioned that *gld-2* function may not to be linked to germ cell divisions. Hence, *gld-2(q497)*; *nhr-114*(RNAi) germ lines were expected to show a high penetrance of multinucleation defects in contrast to *gld-4(ef15)*; *nhr-114*(RNAi).

All *gld-2(q497)* germ cells arrest at early meiotic stages and do not produce gametes (Kadyk et al.1998). Further, *gld-2(q497)* germ lines do not contain multinucleated germ cells (n>50). As expected, the majority of *gld-2(q497)*; *nhr-114*(RNAi) germ lines (76%, n=46) show multinucleated germ cells, see Fig. 2.28 and 2.28 E. The high penetrance of *nhr-114* multinucleation in the *gld-2(q497)* mutant background indicated that *nhr-114* multinucleation defect does not require *gld-2* function. This result supports the notion that it is the specific activity of *gld-4* function that elicits germ cell division defects in *nhr-114*(RNAi) germ lines.

Considering that *gld-4* activity is required for Nhr-114 multinucleation defects, I set to establish, at the genetic level, whether *gld-4* cytoPAP function is specifically linked to the multinucleation defects. GLD-4 cytoPAP activity is stimulated by its allosteric co-factor GLS-1 (Schmid et al. 2009, Eckmann et al. 2010). Hence elimination of GLS-1 is expected to reduce GLD-4 cytoPAP activity. To test this hypothesis, *nhr-114*(RNAi) knockdown was conducted in heterozygote *gls-1(ef8)* mothers, and their progeny was scored for germline defects. Theoretically, if Nhr-114 multinucleation defects were mediated by misregulated GLD-4/GLS-1 cytoPAP activity, loss of *gls-1* is expected to reduce the penetrance of Nhr-114 multinucleation. Hence, *gls-1(ef8)*; *nhr-114*(RNAi) germ lines were expected to show a low penetrance of multinucleation defects.

Similar to reported in Rybarska et al. (2009), 44% of *gls-1(ef8)* animals contain gonads (n=45) that lack germ cells (*G*erm*l*ine *s*urvival defect: Gls phenotype), see figure 2.29 A. However, 32% have germ lines that contain germ cells and sperm, but fail to produce oocytes. The remaining 24% have fertile germ lines with sperm and oocytes (n=45), see fig. 2.29 B. Therefore, only *gls-1(ef8)* animals that contain germ cells (non-Gls) can be assessed in the epistatic analysis. Similar to *gls-1(ef8)*, 44% of *gls-1(ef8); nhr-114*(RNAi) animals contained gonads that lacked germ cells, *i.e.* show the Gls phenotype (n=183). However, 46% have germ lines that contain germ cells and sperm, but fail to produce oocytes, thus were sterile; the remaining 10% have germ lines with sperm and oocytes (n=183), see fig. 2.29 C. In these non-Gls germ lines (n=81), the majority showed wild-type-like germ cell mononucleation (74%), see fig. 2.29 and 2.29 B; a minority shows germ cell multinucleation defects 26% (not shown).

Importantly, more than 70% of *gls-1* heterozygote siblings (*gls-1(ef8)/hT2g)* show germ cell multinucleation defects upon *nhr-114* RNAi knock-down, the remaining 30% show wild-type-like germ cell mononucleation (n=104). This indicated that the presence of one copy of *gls-1* is sufficient to promote *nhr-114* multinucleation defects. Taken together, these epistatic analyses indicate that the penetrance of the Nhr-114 multinucleation defect is significantly reduced in a *gls-1(ef8)* mutant background. Hence the multinucleation defect requires *gls-1* function. Therefore, this result is consistent with the idea that in *gls-1(ef8)*; *nhr-114*(RNAi) germ lines germ cell division defects (multinucleation) are reduced because GLD-4 cytoPAP function lacks GLS-1 stimulation.

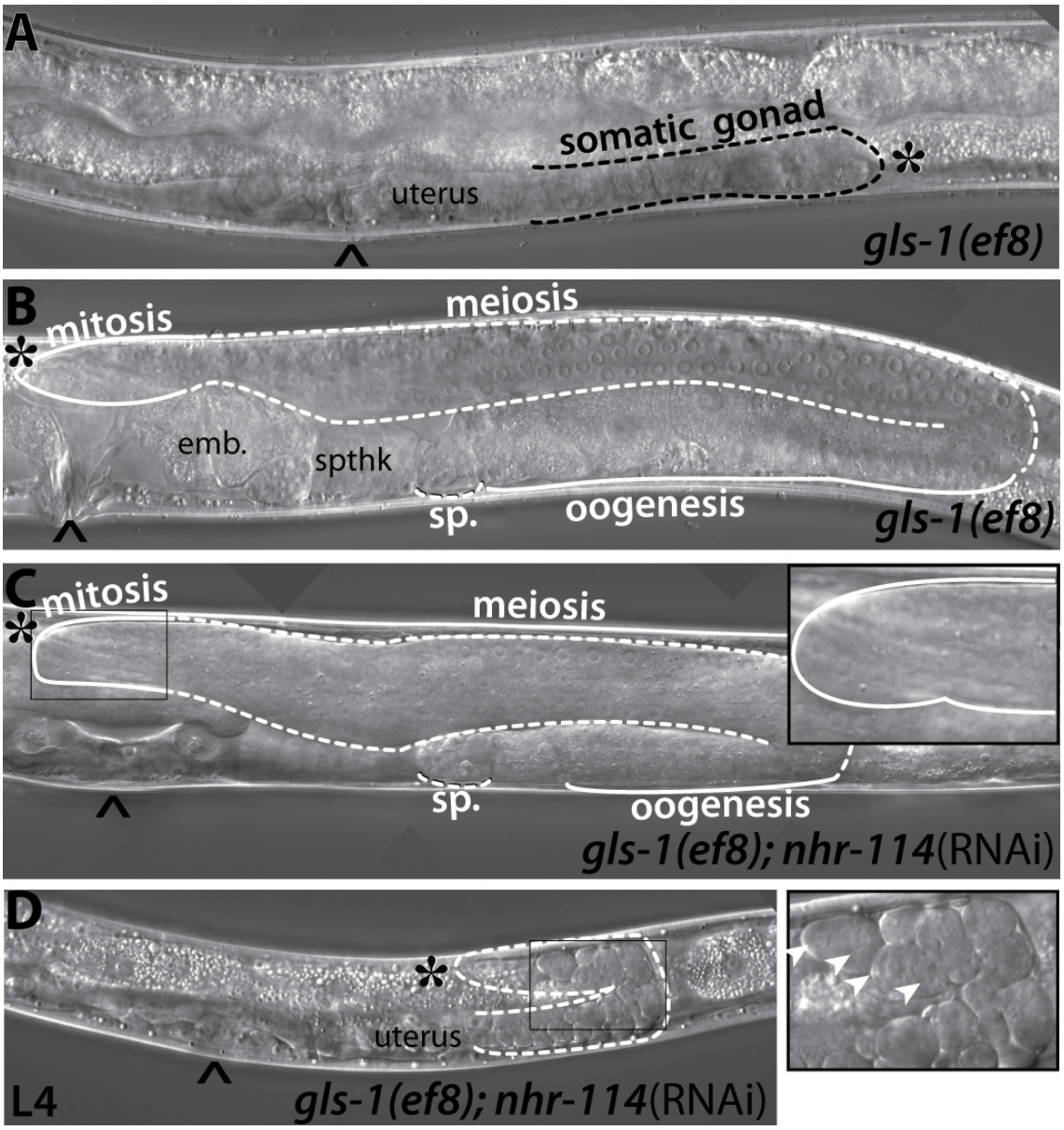

Figure 2.29 Multinucleation defects in *gls-1(ef8)* mutants
DIC microscopy images of adult animals, except D. Mitotic and meiotic regions, oogenesis and spermatogenesis (sp.) are indicated. Asterisk indicates the position of the distal tip cell, and the distal gonad. Caret indicates the position of the vulva. Inset images are scaled two times and highlights distal germ cell nuclei. **(A)** 44% of *gls-1(ef8)* animals show Gls phenotype: no germ lines and only the somatic gonad (n=45). **(B)** 24% of *gls-1(ef8)* animals have fertile germ lines with sperm and oocytes and wild-type-like germ cell mononucleation. **(C)** The majority of *gls-1(ef8);nhr-114*(RNAi) animals have no-Gls germ lines without multinucleation defects (76%, of n=81). **D)** The remaining 24% has under proliferation and multinucleation defects (arrow heads). Image of an L4 larva.

2.15 *GLD-4* STERILITY IS SENSITIVE TO DIET

Molecular and genetic evidence reported in this thesis are consistent with the hypothesis that *nhr-114* and *gld-4* together regulate similar aspects of germ line development. However, the most remarkable and novel aspect of *nhr-114* function is that it links germ line development to diet, specifically to tryptophan input. Previous characterizations of gld-4 focused on its roles on meiotic progression (Schimd et al. 2009). However, it remains unknown if *gld-4* function also links germ line development to diet. To address this question, *gld-4(ef15)* heterozygote mothers and their progeny were fed either OP50 or HT115 bacteria, and *gld-4(ef15)* homozygote animals were scored for the penetrance of sterility. Considering the increasing evidence of common functions between *nhr-114* and *gld-4*, it was suspected that feeding HT115 bacteria may reduce the penetrance of sterility in *gld-4(ef15)* mutants.

On average, 60% of OP50 fed *gld-4(ef15)* animals are sterile (Figure 2.30); the remaining 30% are fertile (n=190). As suspected, less than 20% of HT115 fed *gld-4(ef15)* animals fed are sterile, the remaining 80% are fertile (n=65), indicating that feeding HT115 bacteria also reduces *gld-4* germline defects (Figure 2.30). To test if tryptophan is sufficient to reduce *gld-4* sterility, OP50 plates were supplemented with tryptophan. Similar to *nhr-114* mutants, 94% of *gld-4(ef15)* animals fed OP50^{+TRP} were fertile (n=53), the remaining 6% were sterile, see fig. 2.30. This indicates that tryptophan is also sufficient to reduce *gld-4* sterility.

Most of OP50 fed *gld-4(ef15)* adult sterile hermaphrodites produce only sperm (n=48). Whereas, most OP50^{+TRP} fed *gld-4(ef15)* adult sterile hermaphrodites produce sperm and oocytes (n=62). This suggest that the reduction of sterility in *gld-4(ef15)* hermaphrodites upon tryptophan supplementation results from restored oogenesis. These results indicate that a link between germline development and diet may depend on *gld-4* function. This is consistent with the idea that together *nhr-114* and *gld-4* link nutritional inputs to direct germline development and fertility in *C. elegans*.

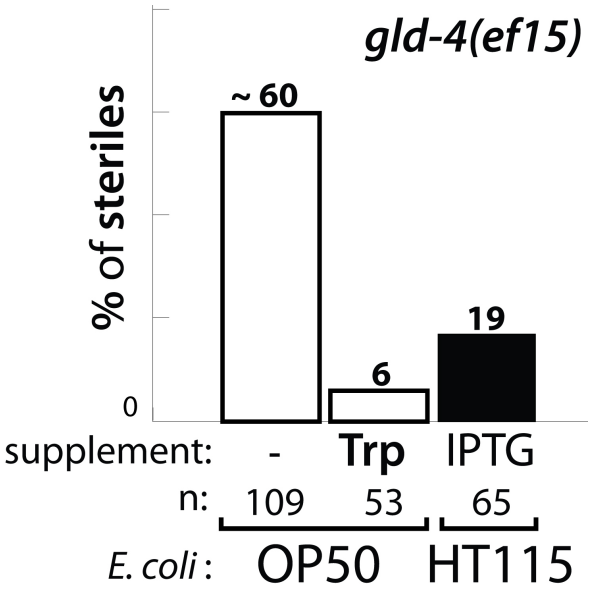

Figure 2.30 *gld-4* sterility is sensitive to diet
Adult animals were scored using DIC microscopy. Percentage (%) of sterile animals is given in respect to the total number of adult *gld-4(ef5)* homozygote animals analyzed per set (n). ~60% of *gld-4(ef15)* fed OP50 (first white bar) are sterile. Sterility is reduced to ~6% by supplementing L-tryptophan or to 19% by feeding induced HT115(DE3) bacteria (black bar).

3. Discussion

3.1 On the Nhr-114 phenotypes

3.1.1 Nhr-114 sterility is of variable penetrance

A key observation in this thesis is that the penetrance of sterility and the fecundity levels vary among *nhr-114* mutant individuals. The presence of fertile animals among an *nhr-114* mutant progeny correlates, to a large extent, with the fecundity of their mother: the bigger the brood, the less likely that brood members will become sterile. This suggests that *nhr-114* sterility is linked to a maternal influence. In *C. elegans*, *mes* genes (maternal-effect sterile) are required to establish epigenetic patterns of gene expression, and ensure the fertility of the next generation (Capowski et al. 1991, Strome S. 2005). The Mes phenotype may be similar to the sterility observed in *nhr-114* mutants. However, the Mes phenotype is fully penetrant (Capowski et al. 1991), but not the Nhr-114 sterility penetrance. This suggests that the maternal influence in *nhr-114* mutants may not be linked to an epigenetic effect. The finding of diet-conditional sterility in *nhr-114* mutants suggests that the incomplete sterility penetrance in the *nhr-114* progeny is triggered by diet. One possibility is that the incomplete sterility penetrance in *nhr-114* mutants arises from variable tryptophan levels among individuals; this idea is further expanded at the end of the section.

3.1.2 Nhr-114 defects appear at the L3 stage

During harsh environmental conditions, such as low food, the dauer program is executed at the L3 stage (Hu et al. 2007). *C. elegans* dauer development is chiefly controlled by the nuclear receptor VitD/DAF-12 (Antebi et al. 2000). The fact that Nhr-114 defects are linked to diet raises questions about similarities or overlapping processes between germline development in dauer and *nhr-114* mutants. If *nhr-114* were necessary to prevent dauer entry under full nutritional conditions, this would imply that loss-of *nhr-114* would render, at least, a germline dauer like status.

Dauer larvae germ lines contain about 35 germ cells that are arrested in mitotic interphase and do not enter meiosis (Narbonne and Roy, 2006). However, if this arrest is alleviated by mutations in AMP-activated protein kinase (AMPK) signaling, germ cells proceed to meiosis and produce sperm (Narbonne and Roy, 2006). In contrast to dauer germ lines, *nhr-114*(RNAi) germ lines do not arrest, and the germ cell number increases further. Also, in *nhr-114* germ cells, chromatin defects are apparent, which are lacking in the dauer. A comparison of *nhr-114* defects with dauer germ lines highlights clear differences between Nhr-114 phenotypes and the dauer phenotypes. Therefore, Nhr-114 defects appear not related to dauer programs, thus *nhr-114* function is likely to be independent of dauer development.

During the L3 larval stage, germ cells initiate meiosis proximally (Kimble and Crittenden, 2005); and start robust proliferative cycles that expand the pool of mitotic cells distally (Korta and Hubbard, 2010). This thesis provides evidence that Nhr-114 defects can occur in mitotic germ lines in which germ cells never enter meiosis, such as in *nos-3 gld-3* double mutants (Section 2.7). Therefore, the onset of meiosis is not required to trigger Nhr-114 defects, hence *nhr-114* function is not linked to entry into meiosis. Could Nhr-114 defects be linked to the start of robust proliferation? Germline proliferation and germ cell survival depend on constant nutritional supply. For example, insulin signaling transduces a food-related cue that promotes robust germ cells proliferation (Michaelson et al. 2010). Also, starvation at the L4 larva induces germ line degeneration (Angelo and Van Gilst 2009). These two examples imply that the developing germ lines rely on and utilize considerable macronutrients amounts. Analysis of this thesis shows that *nhr-114*(RNAi) germ cells at L3 stage do not proliferate robustly and additionally they start to accumulate cell division defects. However, these defects can be prevented with tryptophan supplementation. Based on these observations, this thesis proposes that Nhr-114 defects appear at the L3 stage as a consequence of the depletion of a scarce nutrient that is consumed during robust germ cell proliferation. Therefore, one might infer that that NHR-114 ensures sufficient tryptophan input under poor-tryptophan nutritional conditions.

3.1.3 SOMATIC *NHR-114* FUNCTION PROMOTES PROPER GERM CELL DIVISIONS

Cytokinesis is the last step in cell division and ensures that each daughter cell contains one single nucleus surrounded by a single plasma membrane. A peculiarity of the germ line is the formation of a syncytium, which arises from incomplete germ cell cytokinesis. The *C. elegans* germline syncytium consists of nuclei that are partially enclosed by a single cell membrane connected to a central cytoplasm, the rachis. (Hubbard and Greenstein, 2005). However, defective cytokinesis leads to cell multinucleation. Loss of *nhr-114* leads to germ cell multinucleation, therefore NHR-114 activity is required for proper cytokinesis of mitotic germ cells. In general, cytokinesis is regulated both at a cell autonomous and cell non-autonomous level. At the cell autonomous level, RhoA kinase triggers the formation of an actin-myosin II contractile ring at the equator of the dividing cell. As the nuclei of the two daughter cells start to reform, the contractile ring constricts and a cleavage furrow is formed (Lodish, 2000, Alberts et al. 2002). At the cell-non-autonomous level, extracellular matrix components, such as hemicentin, prevent premature cleavage furrow retraction and cleavage furrow maturation (Xu and Vogel, 2011).

What aspect of cytokinesis requires NHR-114 function? Genetic analysis in this thesis indicates that somatic, but not germline function of *nhr-114* is required for cytokinesis. Although this result suggests that *nhr-114* regulates a cell non-autonomous process similar to extracellular matrix proteins, it is also possible that nhr-*114* regulates a cell autonomous process of cytokinesis. For example the functional output of somatic NHR-114 may influence a germline complex that drives cytokinesis. It is unclear why Nhr-114 multinucleation defects require *gld-4* and *gls-1* activities. One explanation to this dependency is that multinucleation defects arise from imbalanced GLD-4/GLS-1 cytoPAP activity. This implies that NHR-114 somatic function indirectly regulates germline GLD-4/GLS-1 cytoPAP activity to control cytokinesis. Furthermore, the finding that tryptophan supplementation reduces Nhr-114 multinucleation suggests a connection of tryptophan with GLD-4/GLS-1 cytoPAP complex, likely at the level of protein synthesis; this idea is expanded at the end of the section.

3.1.3.1 ON THE GERM CELL CHROMATIN ABNORMALITIES UPON NHR-114-LOSS

The cell cycle is divided in interphase and mitosis (M). During interphase the cell undergoes growth (G1), divides its DNA (S) and prepares for mitosis (G2). During mitosis, accurate chromosome segregation ensures the survival of the next generation by preventing aneuploidies (Verdassdonk and Bloom 2011). Chromosome segregation is facilitated by the kinetochore, a proteinaceous structure, and the chromosomal locus that links the kinetochore, the centromere (Verdassdonk and Bloom 2011). Impaired chromosomal segregation leads to abnormalities that reflect in chromatin figures. Abnormal chromatin is a conspicuous phenotype of *nhr-114* sterile germ cells. These abnormal chromatin figures are of two sorts. First, a category of enlarged or shrunk, but otherwise complete chromatin figures. These *nhr-114* germ cells that have enlarged chromatin that resembles germ cells that arrest in the G2 phase as a consequence of activated DNA replication checkpoints (Merlet et al, 2010). This G2 arrest impacts overall germline proliferation and fertility (Merlet et al, 2010). Based on this phenotypic resemblance, it is likely that Nhr-114 underproliferation may in part arise from cell cycle arrest.

The second category of Nhr-114 abnormal chromatin corresponds to fragmented chromatin figures. Although is not clear how this fragmentation arises, this chromatin morphology is also observed in *chk-1*(RNAi) germ cell nuclei (Kalogeropoulus et al. 2004). CHK-1 protein controls an S-to-M phase checkpoint that prevents the start of a new round of cell division until DNA replication is completed and mistakes are repaired. Therefore, loss of a CHK-1 mediated checkpoint causes a new cell division to start while the DNA is still replicating, or while replication mistakes are not yet repaired. This increases the transmission of defective and aneuploid DNA (Kalogeropoulus et al. 2004). *C. elegans* germ cells have rapid and continuous cell cycles and a short G1 phase, hence they are particularly sensitive to the loss of a CHK-1 mediated checkpoint (Jaramillo-Lambert, 2007, Fox et al. 2011, Kalogeropoulus et al. 2004). Since aneuploidies can be lethal (Verdassdonk and Bloom 2011), it is likely that abnormal chromosome segregation is the major cause of the underproliferation in *nhr-114* germ lines.

The phenotypic resemblance of *nhr-114*(RNAi) to *chk-1*(RNAi) germ lines raises the question if *nhr-114* function is required to maintain sufficient CHK-1 protein or other proteins that prevent premature entry into mitotic M phase. Alternatively, the fragmented nuclei in *nhr-114*(RNAi) may result from DNA damage induced by genotoxic insults. The regulation of various aspects of cell cycle by NHRs has being reported for mammalian intestinal nuclear receptors that metabolize bile acids (FXR) and xenobiotics (PXR and CAR) (Schmidt and Mangelsdorf 2008.). These three NHRs may directly affect the transcription of cell cycle regulators, or indirectly eliminate genotoxic agents. The vitamin D receptor is implicated in promoting both functions (Schmidt and Mangelsdorf 2008.) Although the chromatin abnormalities in *nhr-114*(RNAi) germ cells are pleiotropic, the fact that tryptophan is sufficient to overcome them supports a single common defect triggering those these chromating abnormalities.

3.1.4 GERMLINE *NHR-114* FUNCTION PROMOTES GERM CELL PROLIFERATION

Genetic analysis presented in this thesis shows that animals lacking *nhr-114* function in the germline, such as in *rrf-1(pk1417); nhr-114*(RNAi), have normal germ cell morphology but are underproliferated (section 2.6). In the adult *C. elegans* germ line, Notch signaling controls germ cell proliferation and maintains germline stem cells in the distal most part of the germ line. This regulation is achieved using a network of RNA-binding proteins (RBPs) that promotes germ cell mitoses and restricts germ cell differentiation to a further proximal part of the germ line (Kimble and Crittenden 2005). Since ultimately proliferation is a consequence of cell cycle progression, Notch signaling and the RBP network must therefore control components of the cell cycle regulatory machinery. How does underproliferation arise in germ lines that lack *nhr-114*? A simple explanation is that loss of germline *nhr-114* function causes germ cells to slow down or arrest in the cell cycle, as a consequence germ cells divide less often.

Based on nuclear morphology, germ cells lacking *nhr-114* do not resemble G2 phase arrested enlarged nuclei. Therefore loss of germline *nhr-114* is less likely to arrest germ cells in G2 phase, but yet another cell cycle phase. For example, a general G1 phase arrest is induced by the checkpoint protein controlled by p53/CEP-1, which promotes accumulation of the cyclinE-CDK inhibitor p21 to prevent cell cycle progression into S phase (Nelson and Cox, 2005). In order to test if germline *nhr-114* function stimulates proliferation by promoting G1 to S phase progression, p21, cyclinE-Cdk-1 levels and G2 phase markers could be investigated. Nevertheless, since germline underproliferation is also seen in the absence of *gld-4*, it may potential be that GLD-4/NHR-114 cytoPAP complex in the germ line regulate the translation of a mitogen-like protein required for constant germ cell cycle progression.

3.1.5 GERMLINE *NHR-114* FUNCTION PROMOTES OOGENESIS

Genetic analysis shows that germline *nhr-114* activity promotes also oogenesis. Germ lines that lack *nhr-114,* such as in *rrf-1(pk1417); nhr-114*(RNAi), have early prophase and pachytene nuclei and differentiated sperm. Although no differentiating oocytes are apparent, late meiotic stages of spermatogenesis are lacking. The additional lack of continued spermatogenesis suggests that pachytene nuclei of *nhr-114* sterile germ lines may have switched to the oocyte fate, but do not proceed further than the pachytene stage. Thus, one possible explanation for *nhr-114* oogenic defects is that germline *nhr-114* function promotes the female pachytene to diplotene transition.

In *C. elegans*, the transition from pachytene to diplotene stage in female and male germ lines is regulated by MAPK signaling (Greenstein, 2005). Therefore, MAPK signaling-defective mutants have conspicuous pachytene nuclei that clump together and produce no sperm (Church et al. 1995). Germ lines that lack *nhr-114* produce sperm and do not have clumping nuclei phenotype as in MAPK mutants. Therefore, *nhr-114* oogenic defects are presumably not linked to defective MAPK signaling. However, other genes exist that are specifically required for the female pachytene to diplotene transition.

Hermaphrodite mutants of these genes have germ lines containing pachytene nuclei next to mature sperm. Example of these genes are the RNA-binding protein DAZ-1 (Deleted in Azoospermia homolog -1), or two regulators of a ubiquitin-mediated protein degradation system *skr-1* and *skr-2* (Karashima et al. 2000, Greenstein, 2005). This arrested pachytene transition phenotype in *daz-1* germ lines resembles the phenotype upon loss of germline *nhr-114* activity. This offers the possibility that germ line localized NHR-114 promotes oogenesis by regulating a protein required for the female pachytene-to-diplotene transition, such as DAZ-1.

gld-4 is also important for oocyte production, and loss of *gld-4* causes meiotic cells to arrest in early meiotic stages. However, it is not known how *gld-4* affects oogenesis (Schmid M, doctoral thesis 2008, Schmid et al. 2009). Functional analysis using tryptophan supplementation shows that this amino acid stimulates the production of oocytes in *gld-4(ef15)* germ lines similar to *nhr-114*(RNAi). This restored oogenesis strongly suggests that *nhr-114* and *gld-4* may regulate a common oogenic process that requires dietary tryptophan. Based on this observation and the arrested pachytene shared phenotype of both mutants, a common function of *nhr-114* and *gld-4* appears to be the female pachytene-to-diplotene transition. If this were the case, it would imply that NHR-114 and GLD-4 promote oogenesis in a nutrient-dependent manner, thus they may ensure the presence of key nutrients needed to meet the nutritional demands of oocyte production.

3.2 On the effect of diet for germline development

nhr-114 is a supplementary NR that evolutionary derived from HNF4. This phylogenetic origin casts important implications for predicting supplementary NR's functional roles (Robinson-Rechavi et al, 2005). First, HNF4 is important for the development of the digestive tract, mainly the liver and intestine; and it regulates metabolic energy stores (Chen et al, 1994, Shih et al 2000). Second, HNF4 binds a small lipid that may play a structural rather than a regulatory role (Wisely et al. 2002). Since supplementary NRs have divergent LBDs it remains to be determined what kind of signaling molecules supplementary NRs could bind (Robinson-Rechavi et al, 2005).

Considering HNF4's functional and structural aspects, one of the consequences of the HNF4-linage expansion could be a diversification of metabolic pathways adapted to the ecology of a soil-dwelling nematode (Robinson-Rechavi et al, 2005). Characterization of *nhr-114* in this thesis is consistent with functional expectations for an HNF4 derivative. First, *nhr-114* is expressed in the intestines; second, *nhr-114* activity likely provides nutritional homeostasis under different diets. However, instead of being involved in global nutritional homeostasis, *nhr-114* functions are specifically required for the germ line to support reproduction under different food conditions.

3.2.1 HT115 bacteria abolishes Nhr-114 phenotypes

Feeding *E. coli* HT115 instead of *E. coli* OP50 abolishes Nhr-114 sterility and reduces germline development defects of *gld-4* mutants. Although *E. coli* OP50 is used as the standard laboratory food for *C. elegans*, OP50 is a pathogen for *C. elegans* (Darby 2005, Kim 2008). If Nhr-114 defects arise from OP50 pathogenic effect, then one could reason that *nhr-114* function may protect the germ line from pathogens. However, different models of *C. elegans* pathogenic infections show a down-regulation of *nhr-114* expression upon bacterial infection (Troemel et al. 2006, Wong et al. 2007, Bolz et al. 2010, Irazoqui et al. 2010). Therefore, this implies that *nhr-114* function is not likely to protect the germ line from pathogens. On the contrary, *nhr-114* down-regulation and consequent germline degeneration may save resources during infection.

The *C. elegans* metabolome is significantly affected by the bacterial diet. Overall, animals fed HT115 have slightly increased lifespan and brood size compared to animals fed OP50, showing that HT115 has positive effects on fecundity (Brooks et al. 2009, Reinke et al. 2010). In comparison to OP50-fed animals, HT115-fed animals have significantly higher levels of lysine, aspartate and glutamate; and elevated levels of glucose, betaine, lactate and O-phoshocholine (Reinke et al. 2010). Importantly, irrespective of the bacterial diet, tryptophan levels are the lowest of all the amino acids in the *C. elegans* metabolome (Reinke et al. 2010). This fact may reflect that tryptophan use is tightly rationed (Nelson and Cox, 2005), thus it may render tryptophan a sensitive proxy for assessing subtle changes in the worm's nutritional environment.

3.2.3 Tryptophan-supplemented diet prevents Nhr-114 sterility

A key observation of this work is that tryptophan supplemented to OP50 food is sufficient to promote germ line proliferation and oogenesis in *nhr-114*(RNAi) animals and mutants. A combined supplement of tryptophan with another amino acid, such as lysine, further promotes proper germ cell divisions and restores a fully functional germ line. There are many models that can explain how HT115 bacteria suppress Nhr-114 phenotypes. The idea of limiting tryptophan amounts in OP50, but not in HT115 bacteria is a simple yet intuitive way to explain this suppression; and the fact that tryptophan suppresses Nhr-114 sterility supports this idea. Moreover, since a HT115 diet yields higher lysine levels than an OP50 diet (Reinke et al. 2010), high lysine levels may synergize with the available tryptophan to potentiate its sterility suppressive effect. Such a tryptophan/lysine potentiation effect is a well-documented phenomenom; diets with a ratio of six-times more lysine than tryptophan are optimal for infant growth (Albanese et al. 1955, 1956). In this thesis, a different kind of potentiation effect was discovered upon the addition of IPTG. Although it is unclear why IPTG-induction potentiates the HT115 protective effect, it may reflect an indirect increment of tryptophan or lysine levels. Direct examination of tryptophan amounts under different feeding regimes awaits further characterization.

How does tryptophan prevent Nhr-114 germline development defects? One possibility is that tryptophan is metabolized in a biologically active compound such as a neuropeptide or biogenic amine, that promotes germ line development. Data in this thesis indicates that serotonin, a tryptophan derivative, is ineffective in preventing Nhr-114 defects. However, this does not exclude the possibility that another tryptophan metabolite promotes germline development. Nevertheless, a simpler idea is that tryptophan residues are directly used for protein translation (see end of this section).

3.2.4 Additional implications of diet-dependent sterility

Aside from the focus of this thesis, its findings have direct implications in respect to the interpretations derived from feeding RNAi experiments in *C. elegans*. Since all large-scale RNAi knockdown screens use HT115 bacteria, the question arises whether some phenotypes in RNAi-feeding screens have remained undiscovered because diet masks them. For instance, Green et al. (2011) reported feeding screen focusing on gonad phenotypes. Several genes were identified as important for germline organization, yet *nhr-114*, which clearly affects germline organization, was not reported. Moreover, the *C. elegans* database Wormbase (www.wormbase.org) reports no obvious *nhr-114* phenotypes using RNAi-feeding knockdown (Cuppen et al. 2003). The *nhr-114* and *gld-4* examples illustrate that at least two of maybe many other genes have no apparent phenotypes when feeding HT115 bacteria. This may also explain some differences that others sometimes have being observed by comparing RNAi-feeding with RNAi-injection knockdown experiments.

3.3 On the physiology and mechanisms of NHR-114 function

A clear example of how nutrient absorption is mediated by an intestinal NR is the mammalian vitamin D receptor (VDR) (Schmidt and Mangelsdorf, 2008). NHR-114 functions in *C. elegans* may be analogous to VDR function. In mammals, vitamin D deficiency impairs dietary calcium absorption and causes bone softening. VDR functions in the kidney, bone, and more importantly in the intestine where it regulates transcriptionally calcium transporters and calcium-binding proteins that are essential for calcium uptake. Moreover, intestinal VDR also regulates calcium intracellular trafficking and local efflux (Bouillon et al. 2003, Schmidt and Mangelsdorf 2008). In mice VDR-knockout causes bone softening, a phenotype that is prevented with a high calcium/phosphorous and high lactose diet (Amling et al. 1999). In *C. elegans*, *nhr-114* RNAi knockdown leads to sterility, which is prevented by dietary tryptophan. Thus by analogy, intestinal NHR-114 may transcriptionally regulate tryptophan absorption and further efflux to other tissues, such as the germ line.

It remains unknown why intestinal *nhr-114* mRNA is more abundant in the nucleoplasm than in the cytoplasm, and how NHR-114 protein is distributed in the intestine. Interestingly, the CTN-RNA (Cationic amino acid transporter 2 Transcribed Nuclear-RNA), an inosine-containing RNA, is normally retained in the nucleus, but it is exported to the cytoplasm for translation upon cellular stress (Prasanth et al. 2005). Since *nhr-114* mutants fed HT115 have no apparent defects, one could speculate that NHR-114 expression is induced by a negative-feed loop by certain nutritional circumstances, such as reduced tryptophan levels. For example, low tryptophan dietary levels may induce intestinal *nhr-114* mRNA nuclear export and its consequent translation to promote tryptophan uptake.

3.3.1 MECHANISTIC ASPECTS OF THE TRYPTOPHAN EFFECT AND *NHR-114* FUNCTION

The requirement of *nhr-114* and *gld-4* for oogenesis and germ cell proliferation and their shared tryptophan suppressed sterility phenotype suggest that both genes have common functions. Consequently, NHR-114 function is expected to intersect with posttranscriptional pathways that control these germline processes. GLD-4 is a cytoPAP that functions to positively influence poly(A) tail metabolism. Cytoplasmic polyadenylation enhances the stability, or the translation initiation of targeted mRNAs (Eckmann et al. 2010). Which posttranscriptional processes could NHR-114 intersect to? One major observation suggests that *nhr-114* function is linked to translational initiation. The sedimentation profile of polysomes, ribosomes associated to mRNAs, serves as indicator of efficient translation initiation (in Mathews et al. 2007). *nhr-114(gk849)* hermaphrodites have reduced polysomal fractions, suggesting that loss of *nhr-114* impairs mRNA translation initiation (Nousch M. and Eckmann CR., unpublished results).

Since mRNA poly(A) tail metabolism affects translation initiation, it is likely that NHR-114 affects poly(A) tail regulation through a direct interaction with GLD-4. The formation of a NHR-114/GLD-4 cytoPAP may target many mRNAs to obtain longer poly(A) tails, which enhances their translation re-initiation rate thus more polyribosomes would be formed. In addition to poly(A) tail metabolism, protein translation relies on amino acid input, thus translational control mechanisms are very sensitive to essential amino acid supply (Kimball and Jefferson, 2000). Amino acid levels are sensed and linked to the translational machinery through different signaling pathways that impinge on the initiation step in translation (Kimball and Jefferson, 2000, Proud 2007). For example, amino acid input stimulates the kinase mTOR activity (mammalian targert of rapamycin) to positively regulate protein synthesis (Hara et al. 1998). In *C. elegans*, disruption of *let-363*/mTOR or general translation initiation factors arrests larval development, induces germline degeneration and dilates the intestinal lumen (Long et al. 2002). Also, impaired peptide-bound amino acid uptake retards larval development and induces intestinal lumen dilation (Meissner et al 2004). *nhr-114* mutant hermaphrodites have dilated intestinal lumens, but show no developmental arrest, suggesting that *nhr-114* affect more likely a specific step during the translation of certain mRNAs rather than global mRNA translation.

How could impaired translation initiation and the tryptophan effect on Nhr-114 phenotypes be reconciled? The simplest explanation is that tryptophan residues are used for translation, thus its supplementation may alleviate impaired initiation in *nhr-114* animals. For instance, under full amino acid supply, specific aminoacyl-tRNA synthetases load amino acids into corresponding tRNAs. Constant tRNA aminoacylation maintains acylated-tRNA (loaded) levels available for translation, while preventing accumulation of deacylated-tRNAs (unloaded) (Kimball and Jefferson, 2000). During amino acid starvation deacylated-tRNAs accumulate, which in turn activate a signaling pathway that regulates translation initiation. The activation of GCN2, a key kinase in this pathway, causes the phosphorylation of a translation initiation factor eIF2 subunit. Phosphorylated status of eIF2-α prevents eIF2 from promoting new rounds of translation initiation so general translation initiation is stopped (Kimball and Jefferson, 2000, Proud 2007). I propose that in *nhr-114* animals low tryptophan levels induce unloaded tryptophanil-tRNA accumulation, which activates the GCN2 kinase to stall translation initiation. To test this hypothesis, the phosphorylation status of eIF2-α could be investigated in *nhr-114* animals.

3.3.2 Significance of the NHR-114 and GLD-4 protein interaction

Directed yeast two-hybrid tests confirmed that NHR-114 protein specifically binds GLD-4 protein. Although this physical interaction has not being verified *in vitro*, further genetic interactions between *nhr-114* and *gld-4* exist. What could be the significance of the interaction between NHR-114 and GLD-4 cytoPAP? Firstly, I focus on how GLD-4 may impact NHR-114 function, and secondly on how NHR-114 binding may impact GLD-4 enzymatic activities.

In general, the transcriptional functions of NRs are extended and regulated by corepressors and coactivators, which bind NRs directly. Both classes of coregulators are themselves targets and transmitters of posttranslational modifications (Lonard and O'Malley 2006, 2007). The finding of GLD-4 binding NHR-114's ligand-binding domain (LBD) is intriguing, as it may uncouple NHR-114 from DNA-associated acitivities.

The LBD in NRs serves as interface for binding to coregulators, ligands, as well as other NRs modifications (Jung et al. 2005, Lonard and O'Malley 2006, 2007). Therefore this domain is important for regulating NR's transcriptional activities (Chawla et al. 2001, Benoit et al. 2004, Traubert et al. 2011). GLD-4 binding to NHR-114's requires an intact LBD, suggesting that GLD-4 interferes with other potential NHR-114 interaction partners, and a dimerization of itself. At the same time, since GLD-4 binding does not block NHR-114's DNA-binding domain, this suggest that NHR-114 transcriptional activities may not be interfered by GLD-4. Since GLD-4 protein distribution is predominantly cytoplasmic, and GLD-4's enzymatic activity is posttranscriptional rather than posttranslational (Schmid et al. 2009) thus it is unlikely that GLD-4 is a coregulator of NHR-114 transcriptional activities in the nucleus.

Preliminary analysis of a germline expressed NHR-114::GFP fusion protein shows that NHR-114 is at steady state predominantly cytoplasmic (Appendix 2). Nevertheless, it is possible that NHR-114 is transcriptionally active as it may shuttle in and out of the nucleus depending on ligand binding, as the case of other NRs (Bunce and Campbell, 2010). Consequently, it is likely that GLD-4 influences the cytoplasmic-to-nuclear localization of NHR-114, but not directly its transcriptional activities.

This thesis also established that NHR-114 binds to the catalytic region of GLD-4. Importantly, GLS-1 stimulates GLD-4 enzymatic activities; to do so GLS-1 binds the catalytic region of GLD-4, the same that NHR-114 binds, to form a GLD-4/GLS-1 cytoPAP complex (Botti V. and Eckmann CR., unpublished results; Schmid et al. 2009,). Yet there is no experimental validation that documents the presence of a GLD-4/NHR-114 complex *in vivo*. However, the binding of NHR-114 to GLD-4 is mechanistically interesting and highly intriguing. The formation of a NHR-114/GLD-4 cytoPAP complex would expand the regulatory potential of GLD-4 cytoPAP activity. A hypothesis is that this protein complex may be analogous to the protein complex formed between the second poly (A) polymerase GLD-2 and its protein cofactors in the *C. elegans* germ line. For example, the RNA-associated regulators GLD-3 and RNP-8 bind to the catalytic region of GLD-2 in a mutually exclusive manner, forming a GLD-3/GLD-2 and RNP-8/GLD-2 complex (Wang et al. 2002, Kim et al. 2009).

The formation of either GLD-2 cytoPAP complex determines antagonistic outputs of GLD-2; GLD-2/GLD-3 promotes spermatogenesis (Eckmann et al. 2002), while GLD-2/RNP-8 promotes oogenesis (Kim et al. 2009). It was previously reported that the GLS-1/GLD-4 cytoPAP complex promotes the sperm-to-oocyte switch and meiotic progression (Rybarska et al. 2009, Schmid et al. 2009). My discovery of the tryptophan effect on germ cell proliferation and oogenesis in *nhr-114*(RNAi) and *gld-4* mutants may suggest that a NHR-114/GLD-4 cytoPAP complex promotes robust mitotic proliferation and oogenesis. While it is not clear how GLS-1, GLD-4 and NHR-114 proteins interact among each other, the genetic interactions may be indicative of functional regulation. Further experimental assays are required to determine if NHR-114 and GLS-1 bind GLD-4 in a mutually exclusive manner, competing for GLD-4 binding, or if they form a trimeric protein complex.

3.3.3 Working model for NHR-114 function

The expression and function of *nhr-114* in soma and germ cells, combined with the effect of tryptophan on germ cells, and the interaction of NHR-114 with GLD-4, lead to the following working model of tissue-specific functions of NHR-114 (Figure 3.1). In the intestine, NHR-114 may localize to the nucleus to act as a transcription factor to promote the uptake of dietary tryptophan (L-Trp) or its efflux to other tissues, such as the germ line. In germ cells, cytoplasmic NHR-114 may form a protein complex with GLD-4 cytoPAP. The formation of this complex may regulate NHR-114 subcellular localization; and influence the enzymatic activity of the GLD-4/GLS-1 cytoPAP. A putative GLD-4/NHR-114 may regulate the translation of specific mRNAs via poly(A) tail length control. In addition, the translation of certain germ cells mRNAs may be sensitive to the availability of tryptophanyl-tRNAs. Presumably, the putative protein products of translation activation are responsible for promoting mitosis and oogenesis.

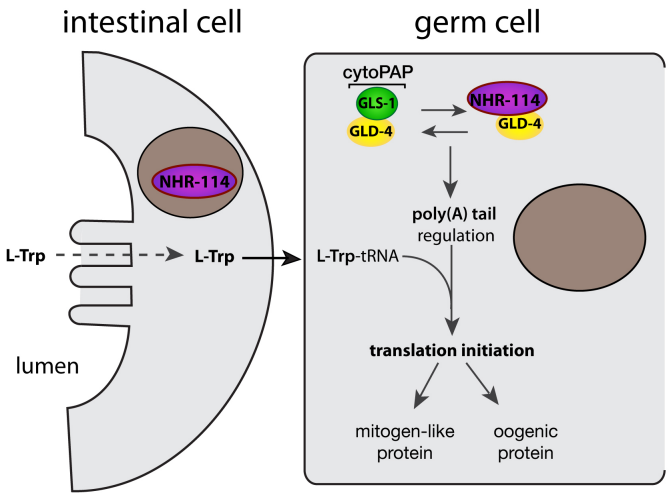

Figure 3.1 Tissue-specific NHR-114 functions promote germline development
A somatic cell and a germ cell are depicted in close proximity to each other, with cytoplasm (gray) and nucleus (brown circles). NHR-114, GLD-4 and GLS-1 proteins are shown as colored ovals. The intestinal cell is depicted with the microvilli facing the intestinal lumen at left (lumen), where tryptophan residues (L-Trp) are present. In the intestines, NHR-114 may localize to the nucleus to promote L-Trp uptake (dotted arrow), or its efflux to the germ line (arrow). In germ cells, NHR-114 may form a complex with GLD-4 cytoPAP. Poly(A) tail regulation, and the availability of tryptophanyl-tRNAs (L-Trp-tRNA) may control the translation of mRNAs encoding proteins responsible for promoting mitosis and oogenesis.

3.3.4 Concluding remarks

NRs are intracellular sensory elements that communicate the status of the external environment to elicit physiological changes inside the cell. NRs nuclear functions are well documented; however, their non-genomic functions are less understood (Bunce and Cambpell, 2010). Cytoplasmic regulation of gene expression provides an economical and fast alternative to regulate gene expression without invoking nuclear programs. Non-canonical poly(A) polymerases are cytoplasmic regulators and translational activators. The potential regulation of a cytoplasmic PAP complex by a NR opens a ground for studying and understanding the further potential of NRs as intracellular sensory elements. NHR-114 may serve as an example for many other supplementary NRs. It holds great potential to expand our understanding and to discover novel paradigms of nuclear receptor functions and their influence on diverse modes of gene expression.

4. MATERIALS AND METHODS

4.1 WORM HANDLING AND STRAINS

All strains were grown on 6 cm Nematode Growth Medium (NGM) agar plates, and fed with E. coli strain OP50, (Brenner, 1974). All strains were grown at 20ºC (except indicated in the text). Strains containing more than deletion were generate by chromosomal segregation. Chromosomal segregation was determined by using gene specific PCR. *nhr-114(ef24)* was isolated in a PCR-based screen for deletion mutants induced by ethyl methane sulfonate (EMS) (Kraemer et al., 1999) using the following nested PCR primers: 1º PCR: CE1689 ACCTTGGGTTCCGGAATATC and CE1870 TGGGACTGTTATTGCGGCAT. 2ºA PCR: oligos prime out of the deletion: CE1995 TGTTATGCAATACGCATTCTCAG and CE1692 GAACCAGTCTCTCTCGTGCC 2ºB PCR: oligos prime inside the deletion: CE778 CAAGACAGTTCGATCTTCACG and CE1641 TGTGTATCCGATAGGGTCACG.

The *nhr-114(gk849)* and *nhr-114(tm3755)* mutant alleles were obtained from the C. elegans Gene Knockout Consortium and the National Bioresource Project. Both *nhr-114(ef24)* and *nhr-114(gk849)* deletion mutants were outcrossed at least 10 times against wild type (Bristol, N2). At the 6th backcross the strains were balanced with nT1g (*wnk-1(tm487) IV/ nT1[qIs51] (IV;V)).* Normally, balanced mutant strains segregate 50% of heterozygote progeny (they contain one copy of *nT1g*, thus are GFP positive), 25 % of homozygote progeny (they lack nT1g, thus are GFP negative), and the remaining 25% is lethal. Within the progeny of *nhr-114* balanced strains, all GFP positive animals were heterozygotes for nhr-114. However, most of GFP negative animals were heterozygotes for nhr-114, instead of homozygotes. To rule out that this abnormal segregation pattern was associated with the genetic background of the strain that donated the *nT1g*, I used the nT1g balancer from the another strain: *mep-1(ok421) IV / nT1[qIs51] (IV;V).*

The segregation behavior in the new nhr-114 balanced strain was similar to the previous case: all GFP positive animals were heterozygotes, but not all GPP negative animals were homozygotes. This behavior was observed in both *nhr-114(gk849)* and *nhr-114(ef24)* deletion alleles. To overcome the segregation problem, both mutant strains were kept as homozygotes. The following strains were generated or used in this thesis:

Genotype	**LG**	**Strain number**	**Primers:**
nhr-114(gk849)	V	EV250	1. 1689/18702 2.a 1995/1692 2.b 778/1641
nhr-114(ef24)	V	EV245-249	1.1689/1870 2.a1995/1692 2.b 778/1641
gld-4(ef15)	I	EV 97	
gls-1(ef8)	I	EV52	
gld-2(q497)		JK 2497	1. 82/80
fbf-1(ok91)	I	JK3022	1. 431/432 2a.433/434 2b 433/439
fbf-2(q738)	I	JK3101	
rrf-1(pk1417)	I	NL2098	1. 2804/2809 2.a 2805/2808 2.b 2806/2807
rrf-3(pk1426)	I	NL2099	
nhr-114(ef24) V/nT1[qIs51] (IV;V)	V	EV203, 204, 207, 209,	
nhr-114(ef24) V/nT1[qIs51] (IV;V)	V	EV208, 210	
him-8(e1489) IV; nhr-114(gk849) V		EV298	
gld-2(q497)/hT2g(I;III)I; him-8(e1489)IV;nhr-114(gk849)V		EV306-307	
rrf-1(pk1417) I; gld-3(q730) nos-3(q650)/ mIn1[mIs14 dpy-10(e128)] II		EV357-358	
gld-3(q730) nos-3(q650)/ mIn1[mIs14 dpy-10(e128)] II		EV359-360	
fbf-1(ok91)/mIn1g II; him-8(e1489)IV; nhr-114(gk849)/+		EV315	

Table 4.1 List of strains generated or used in this thesis
All strains used in this thesis are listed with their genotype. The EV number of each strain is unique and corresponds to the indicated genotype. The primers used to detect the deletions are given. Double, and triple mutants were created by chromosomal segregation. LG (linkage group).

4.1.1 Larval germ cell count

To synchronize the F1, wild type or *nhr-114*(RNAi) hermaphrodites were singled on NGM plates without food over night (O/N) (~12 h). Next day, the hatched larvae were arrested as L1 and food was spotted on the plate. The larval stage was determined by matching the developmental time at 25ºC with vulva morphology as in Johnson et al. (2009). Two developmental time points were score for each larval stage, and three for L4 larval stage.

Larval stage:	**L1**		**L2**		**L3**		**L4**		
	early	late	early	late	early	late	early	mid	late
h past L1:	0	<11	>12	<20	>21	<25	>26	30	<35

4.1.2 Brood size analysis

Late L4 mothers were placed on a plate for 8-12h, then the mother is transferred to a new plate. The number of laid embryos from the previous plate is counted, then the plate was incubated for 72h until embryos develop into adults. Adults were countet. The percentage of embryonic lethality was calculated by dividing the total number of hatched adults between the total number of laid embryos.

4.1.3 Supplementation of OP50 plates

12.5 mg of each amino acid, individual amino acids, uracil or serotonin were dissolved in 1 ml of H20 in a 1.5 ml tube and mixtures were incubated for 30- 60 min at 30ºC in a thermo shaker at maximum shaking. 100 µl of the solution were spotted on top of the OP50 bacterial spot on a 6 cm plate. Plates were let to dry for 5 min before using. Spotting was done under laminar flow hood. Supplementation was done always fresh, and plates were never stored for further use.

Supplement	Brand	Number
Uracil	Calbiochem	6630
Serotonin, creatinine sulfate	Sigma	H-7752
Arginine	Merk	731 K2320342
Alanine	Merk	721 K2229307
Asparagine	Sigma	A7094
Aspartic acid	Merk	546 K1434126
Cysteine*	Sigma	C7352
Glutamic acid	Merk	708 k3430191
Glutamine*	Merk	632K 1529089
Glycine*	Merk	711 k3305601
Histidine*	Merk	702 k797551
Isoleucine	Merk	721 K4363962
Leucine	Merk	731 K2572660
Lysine	Sigma	L-5626
Methionine	Sigma	M-9625
Phenylalanine	Merk	717 K4208356
Proline*	Sigma	P-0380
Serine*	Merk	723 K4496369
Threonine	Merk	709K 1747411
Tryptophan	Merk	645 K2050174
Tryptophan	Sigma	T9753
D-Tryptophan	Roth	7700.1
Tyrosine	Merk	721 K1221371
Valine	Merk	646 K1494595

Table 4.2 List compounds used to supplement OP50 food plates
See text for description of supplementation. Star indicates essential amino acids. Two different brands and three different batches of L-tryptophan were used, without apparent changes in the tryptophan effect on Nhr-114 sterility.

4.1.4 STEROL FREE CONDITIONS

Chlorophorm extracted NGM agar (sterol free) and *E. coli* NA22 grown on cholesterol free medium were kindly provided by C. Penkov, S. Boland and Teymuras Kurzchalia from the MPI-CBG, Dresden. Further details on the preparation of these reagents is found at Matyash and Entchev et al. (2004). Wild type, *nhr-114(gk849)* or *nhr-114(ef24)* L4 hermaphrodites were seeded on sterol-depleted plates or normal plates, and kept at 20ºC. The founder hermaphrodites were moved to a different plate every morning and evening until no more embryos were laid, ~ 80 h past L4. After each passage, the number of laid embryos per plate was scored at the dissecting scope. A grid was drawn at the back of the plate to facilitate the counting. 48 h after the number of hatched animals was scored by single picking animals away from the plate. Hatched animals were classified as: fertile adult, sterile adult or larval-arrested. The percentage of embryonic lethality was calculated by dividing the total number of hatched adults between the total number of laid embryos.

4.1.5 RNAI KNOCKDOWNS

4.1.5.1 DSRNA DELIVERY BY MICROINJECTION

The *nhr-114* mRNA full-length sequence was uses as a template for dsRNA generation. Young adult hermaphrodites (hermaphrodites containing one single row of oocytes) were single picked and transferred to an NGM plate without food, then animals were let to crawl for ~20 to eliminate the bacteria from the body of the animals. dsRNA was microinjected into each germ line of the P0 hermaphrodite. To eliminate the unaffected F1 progeny, injected P0 of the same genotype were placed into a plate for ~2 hrs, then P0 were singled into a new plate, and P0 were passed to a new plate every 12 or 24 h. Only F1 produced more than ~2 hrs post injection was analyzed. The F1 progeny was analyzed 24 hours past L4, or during larvae, when indicated.

4.1.5.2 dsRNA DELIVERY BY FEEDING

From a bacterial glycerol stock, LB agar containing 50 μg/ml Amp/15 μg/ml Tet (Amp+Tet) was streaked out with *E. coli* HT115 transformed with the feeding vector pL4440, or pL4440 containing *fog-1* open reading frame. A single bacterial colony was used to inoculate 500 μl LB with100 μg/ml ampicillin and grown for four hours at 37°C at 180 rpm. Cells were pelleted by centrifugation at 3000 rpm for 5 minutes and washed twice in LB/Amp and resuspended LB/Amp. 20 ml LB/Amp were inoculated with the pre-culture and grew over night at 37°C and 180 rpm. Culture was spun for 7 minutes at 4,400 rpm and washed twice in LB/ampicillin. Cell pellet was resuspended in 1 ml LB/ampicillin. Feeding plates were seeded with 4 x 100 μl drops in a laminar flow hood. To induce dsRNA expression plates were dried upright O/N in dark at RT and stored at 4°C covered in aluminum foil. Two adult hermaphrodites were placed on each plate and after 3 days at 20°C L4 larvae were collected for analysis. Feeding plates: NGM agar plates containing 1 mM IPTG and 25 μg/ml carbenicillin.

4.2 WORK WITH NUCLEIC ACIDS

4.2.1 IN VITRO TRANSCRIPTION AND DIOXIGENIN LABELING OF RNA PROBES FOR NORTHERN BLOTS

For the Northern blot probe, DNA template was cleaned with phenol:chlorophorm, or column purified and resuspended in DEPC-H20 if RNAse inhibitors were used. Before starting the transcription, 10x DTT and 5X transcription buffer (Epicenter BP1001) were warmed up at 37°. The DNA template and DEPC-H20 were kept at RT. Dioxigenin (DIG) RNA labeling mix (Roche 11277073910).

A 20 μl reaction was assembled in the following order:

8.0 μl	H20
2.0 μl	10X DTT
4.0 μl	5X transcription buffer
3.0 μl	DNA template (1 μg)
2.0 μl	10X DIG RNA labeling mix (or 10X NTPs as a control for the transcription)
0.2 μl	RNAsin (RNAse inhibitor)
1.0 μl	T7 or T3 RNA pol (produced at MPI-CBG)

The reaction was incubated at 37ºC for 2 h. The reaction can be frozen down at -80ºC. To test the efficiency of the transcription 2 µl of the reaction were tested in a RNA gel. To eliminate the template plasmid The remaining volume of the reaction was incubated with 1 µl of DNAse I, without RNAses, for 15 min at 37ºC. Since DIG- labeled RNA goes into organic solution, the transcription reaction should never be cleaned with phenol:chlorophorm. The volume was brought up to 200 µl with DEPC-H20, 3 volumes of cold ethanol were added and sodium acetate to 100 mM. Probes were stored in ethanol at -80ºC indefinitely. Prior use, a quarter of the volume was precipitated and resuspended in 15 µl of DEPC-H2O. The standard transcription reaction yielded ~ 10µg of a 1kb transcript in 2h at 37ºC. ~ a quarter of the transcript incorporates DIG-labeled UTP nucleotides. The unlabeled transcript was used to compare the efficiency of transcription, samples were run in a RNA gel.

4.2.1.1 In vitro transcription of dsRNA

Production of template for dsRNA transcription

The pACT vectors containing either *nhr-114* or *nhr-68* were used as PCR templates for generating linear DNA fragments flanked by T7 sites. To visualize the product 2 ul of PCR were run in a 0.8-1.0% agarose gel.

PCR setup:	
Template (20 ng)	1.0 µl
CE1027/T7pACT-fwd primer	0.2 (100uM) µl
CE1028/T7pACT-rev primer	0.2 (100uM) µl
10x PCR Buffer	5 µl
10mM dNTPs	1 µl
HiFi polymerase	0.2 µl
H2O	42.4 µl
Total	50 µl

The in vitro transcription was performed using the MEGAscript® T7 Kit (Ambion #AM1334). The following reaction was assembled at room temperature into PCR tubes:

Template (PCR product)	4 µl	(3-4 µg was optimal)
10x Transcription buffer	2 µl	(thawed at 37°C and mixed)
2.5x rNTP mix	8 µl	
10x T7 RNA polymerase mix		2 µl
DEPC-treated ddH2O	4 µl	

The reaction was incubated at 37°C for 4 hours in a thermocycler. To purify the RNA, the 20 µl in vitro transcription reaction was mixed with 20 µl DEPC-treated ddH_2O, 2 µl Tris (1 M, pH 7.5) and 200 µl Trizol, contents were mixed and the RNA was incubated for 3 minutes at 65°C. 25 µl $CHCl_3$ were added and the tube was shook by hand, then incubated for 3 minutes at room temperature, and spun for 5 minutes at full speed and room temperature. The supernatant was transferred to a new tube, and extracted with 200 µl PCI by mixing and then spinning at maximum speed. Supernatant was saved and the extraction was repeated with 200 µl CI. RNA was precipitated by adding 20 µl NaOAc (3 M, pH 5.2 DEPC-treated) and 500 µl Ethanol. RNA was incubated at -20°C for at least 30 minutes. Then RNA was precipitated by centrifugation for 10 minutes at 4°C and full speed. The pellet was washed with 300 µl 70% ice-cold ethanol, spun down for 5 minutes at full speed and 4°C. Ethanol was removed carefully with a Pasteur pipette. The pellet was air dried and resuspended in 30 µl DEPC-ddH_2O. The concentration was measured using a NanoDrop spectrophotometer and the concentration was adjusted to 2 µg/µl. 1 µg of dsRNA was run in non-dentaturin agarose gel to check the quality of the RNA. When the RNA did not appear as a major single band, the RNA was annealed using the PCR program below. RNA was stored at -20°C until used.

PCR settings:
1) 95°C for 1 minute
2) 85°C for 3 minutes
3) 75°C for 5 minutes
4) 65°C for 5 minutes
5) 45°C for 5 minutes
6) 37°C for 5 minutes
7) 30°C for 15 minutes
8) 20°C forever

4.2.2 Digoxygenin labeling of DNA probes for in situ hybridizations

nhr-114 mid-sequence (HindIII-719 to1335-Acc65I) was cloned within T7 and T3 promoter sequences of the pBKSII(+) vector. To produce the template for generation hybridization

probe: two PCR mixes per probe were prepared, and the EXT35 PCR program was run. Plasmid template was DpnI digested (1µl Dpn I, 1 hr at 37°C). After digestion PCR product was cleaned over a PCR purification column (Wizard SV Gel and PCR clean-up system #A1460, Promega) and eluted in 50 µl H2O. 2ul of the elution were analyzed in an agarose gel.

PCR template preparation:

PCR setup:	(stock conc.)	(1:10 diluted)	
Template (50ng/ml)	2.0	2.0	
T7/T3 primer mix	0.3 (100µM)	3.0	(10µM)
10x PCR Buffer	5.0	5.0	
10mM dNTPs	1.0	1.0	
HiFi polymerase	1.0	1.0	
H2O	40.7	38.0	
total	50µl	50µl	

To produce the DIG-labeled hybridization probe: two PCR mixes per probe were prepared. As a control for the transcription setup, a PCR mix using non-labeled dNTPs was conducted in parallel. The T3-primer was used to generate *sense* probe, the T7-primer was used to generate the *antisense* probe. The EXT35 PCR program was run. Then, 75µl of ddH20 were added each PCR mix, and 95µl were transferred to a fresh tube. To precipitate the DNA, 10µl 1M NaCl or 30 µl 3M Na-Acetate and 3 Vol. (315µl) of ethanol were added and precipitated for 30' at -70C or O/N at -20°C. Tubes were spun down for 10 min at maximum speed, then supernatant was removed, and pellet was washed with 500 µl of 70% ethanol, then spun down for 7.5 min at 10,000 g. Supernatant was removed and pellet was air-dried, then resuspended in 400µl of hybridization buffer. Probe was boiled for 1hr in water bath and then verified by a dot blot assay. Probes were stored at -20C indefinitely. DIG DNA labeling mix (Roche, # 1 277 065).

DIG-probe preparation:

setup:	(stock conc.)	(1:10 diluted)	
Template (200ng/µl)	4.0	4.0	
T7 or T3 primer	0.2 (100µM)	2.0	(10µM)
10x PCR Buffer	2.5	2.5	
10x DIG DNA labeling mix	2.5	2.5	
HiFi polymerase	0.5	0.5	
H2O	15.3	13.5	
total	25µl	25µl	

4.2.2.1 Dot blot analysis of DIG-labeled probes

The purpose of this analysis was to determine the quality and quantity of the DIG-labeled probes, with this information, similar amounts of sense and antisense probes can be estimated. The concentrated DIG-labeled probe was diluted 1:1, 1:3, 1:10, 1:20. In parallel, a proven probe was used as a positive control. From each dilution, 1µl probe was mixed with 5µl of 5xSSC, and boiled for 5min, then cooled down on ice. 1µl probe was spot on nitrocellulose (NC) membrane strip. The membrane was baked for 30 min at 80ºC in an oven, or UV cross-linker (auto-mode in Stratalinker). Membrane was washed once in 2xSSC, twice in PBST, and blocked for 30min in PBST-B. Then the membrane was incubated with anti-DIG antibody (1:2.000)/PBST(-B) for 30-60min, afterward membrane was washed thrice 10min in PBST, twice quickly in staining buffer and then incubated in the dark with NBT/BCIP-containing staining buffer, violet spots show in minutes. Incubation with CDP-star (Roche 1 685 627) increases the sensitive of detection; in this case membranes are exposed to a chemiluminisence film.

4.2.3 In situ hybridizations of dissected gonads

Day 1 (Thursday). Dissections and fixation

I adapted this protocol from the protocols of Min-Ho Lee's and Schedl's lab. Healthy worms were hand picked or wash off with 2 ml M9 into a1.5 ml tube (4 plates with 4 ml of M9 (2x2ml tubes). Worms were washed once in ddH2O and once in PBST (0.1% Tween 20). Worms were added to a baked 10 cm glass dish containing 10 ml PBST/0.02mM levamisole. ~100 worms were cut in 10 minutes using a needle (25G 1" – Nr.18, 0.5 x 25 mm). Carcass-attached gonads were transferred into a baked 15 ml conical glass tube with 3 ml *fixation buffer*, and were incubated for 2hr at RT with occasional gentle mixing (swirl movement, not tapping).

Gonads were settled down by spinning the tube at 2,500 x g for 3 minutes in tabletop swing-out centrifuge. I preferred to only let the tubes stand for 2 min. Most of the fixative was sucked up carefully using a glass Pasteur pipette with a blunted tip, and discarded. Special attention was paid to prevent gonads being sucked up. To wash the gonads, 3 ml PBST was added to the tube, then supernatant was removed. 3 ml of -20ºC pre-chilled methanol (100%) was added. Tubes were incubated over night at -20°C. Tubes with the methanol and gonads can be stored more than one week at -20°C.

Day 2 (Friday). Proteinase K digestion and fixation

2 ml PBST were added to the tubes containing the gonads in methanol. The gonads were let to settle for 5 min and then washed twice in 2 ml PBST and the supernatant was discarded. 400 µl Proteinase K solution were added and incubated for 1 hour at R/T. Then gonads were washed thrice with 2 ml PBST and the supernatant was discarded. 1 ml of *fixation buffer* was added, and then tubes were incubated for 15min at R/T. Gonads were washed twice with 2 ml PBST, and discard supernatant was discarded. Tubes can be kept at 4ºC O/N in PBST. 1 ml PBST / 2mg /ml glycine [20mg/10ml] was added and incubated for 15 minutes at R/T. Gonads were washed thrice in 2 ml PBST and S/N was discarded.

Day 2 to 4. Hybridization

400 µl of 1:1 PBST/*Hybridization buffer* were added and incubated for 5 min at 50°C in a water bath, gonads were collect and SN was discarded. Pre-hybridization was done using 400 µl *Hybridization buffer* for 1 hour at 50°C. Before the previous incubation time was finished, 75 µl of the hybridization probe were mixed with 75 µl Hybridization buffer, and boiled for 5min at 96°C, then immediately cooled to 50°C in a water bath for 2 minutes and finally spun down. Hybridization solution was removed from the gonads and the probe solution was added. Tubes were incubated for ~48hrs (2 O/N) or 63hrs (3 O/N) in a hybridization oven at 48°C.

Day 5 (Monday). Antibody staining

400 µl of pre-warmed *Hybridization buffer* (48°C) were added. Gonads were then washed four times with 400 µl of *Hybridization buffer* (48°C), and incubated for 15 min each time. Then gonads were washed once with 400 µl 1:1 PBST/Hybridization buffer (48°C), and incubated for 10 min each time; then twice with 2 ml PBST (48°C), and incubated for 10 min each time. At the end, gonads were washed once in 2 ml PBST, and incubated 5 min at R/T. Supernatant was discarded, and gonads were blocked by adding 1 ml PBST/BSA, and incubated for 15min at R/T. Supernatant was removed and gonads were incubate in 500 µl antibody solution over night at 4°C.

Day 6 (Tuesday). Detection

All the following steps were conducted at R/T. Gonads were washed twice with 2 ml PBST, and incubated with 2 min each time. Then gonads were washed thrice with 1 ml PBST/BSA, and incubated for 20 min each. Supernatant was removed, and gonads were incubated with 1 ml Staining Buffer, for 5 min. Supernatant was removed and then 1 ml Staining Buffer was added again. In the mean time, gonads were sucked up with a Pasteur pipette and transferred into a watchmaker glass. Using a dissection scope and a micropipette tip adjusted to a Pasteur pipette, fibers and debris were removed from the solution containing the gonads. Most of the liquid was removed and then 500 µl BCIP/NBT/staining buffer were added. The watchmaker glass was placed into a wet chamber and incubated at RT until a dark purple color developed in the antisense-probed samples. The color development could take anywhere from 30 min, hours or O/N. The

reaction was stopped by removing the staining solution, and washing three times in 1 ml PBST. Gonads were carefully transferred into a glass Petri dish with a glass pipette and cut away the remaining body parts with a syringe needle. Gonads were transferred into a PCR tube using a P20 micropipette tip. Gonads were let to settle and supernatant was carefully removed and replaced with 8 µl of mounting media (Vectashield, LINARIS GmbH, H-1000). Solution was transferred onto a 22x22 mm cover glass. When necessary gonads were arranged using an eyelash glued to a glass pipette. Liquid on the cover glass was carefully touched with a slide to form a liquid bed in between the two glasses. Two sides were sealed with nail polish and the other two were let opened. Gonads were analyzed with differential interference contrast microscopy (DIC) using a Zeiss-Axio Observer microscope.

Fixation buffer:

10 ml 16% PFA
(ampoules, EM Sciences #15710 stored at RT – heat to 55ºC before use.
0.53 ml 25% glutaraldehyde
(ampoules, EM Sciences #16220)
25 ml 0.2 M K2HPO4 pH 7.2
(freshly prepared, autoclaved)
15 ml ddH2O
Stored as 5x 10 ml aliquots at -20°C. Heat quickly to 55C and store at RT shortly before use.

Proteinase K solution:

Just before use: add 2 µl Proteinase K (20 mg/ml) to 800 µl PBS-T(0.1%Tween20)

Hybridization buffer: 50 ml total

ml	Solution	[Stock]	[Final]	
12.5	SSC	20 x	5	x
25.0	deionized formamide (FA)	100 %	50	%
0.5	Herring sperm DNA (autoclaved)	10mg/ml	0.1	mg/ml
0.02	Heparin	100mg/ml	50	µg/ml
0.25	Tween 20	20 %	0.1	%
11.73	H2O	0.04 ml	0.04 ml	

Prepared as a 50ml batch and stored in 5x10ml aliquots at -20C
Anti-DIG antibody (Roche, #1093274) was used at 1:10,000 dilution.

Staining buffer: 50ml total

ml	Solution	[Stock]	[Final]	
1.0	NaCl	1 M	100mM	
1.0	Tris pH 9.5 (or Tri-Ethanolamine)	1 M	100mM	
0.2	levamisole	50 mM	1	mM
0.02	MgCl2	1 M	5	mM
0.25	Tween 20	20 %	0.1	%
7.55	H2O	0.04 ml	0.04 ml	

Sigma Fast BCIP/NBT tablets (Sigma #B5655): One tablet / 10 ml staining solution. Pulverize the tablet and dissolve 0.022 g in 1 ml staining solution. Prepare absolutely fresh before use. Pulverized tablet can be stored dry at -20ºC in a 1.5 ml tube protected from light.

PBST / 0.1% Tween 20
500 µl 20% Tween20
100 ml PBS.
Filter solution

PBST/0.02mM levamisole
3.2 µl 0.25 M levamisole
30 ml PBST

PBST / 0.5 mg/ml BSA
500 µl 10 mg/ml BSA
9.5 ml PBST

PBST-glycine 2mg/ml
0.020 g glycine
10 ml PBST
Store aliquotes at -20ºC

4.2.4 RNA EXTRACTION WITH TRIZOL

Harvesting worms

Before staring the harvest, 1.5 ml microfuge tubes were labeled accordingly and kept on ice. From this step onward, tubes and M9 buffer was kept on ice all the time. Plates containing mixed stage worms were washed with chilled M9 buffer and the liquid was transferred into 15 ml tubes. Tubes were spun down at 400 x g at 4ºC for 5 min. Supernatant was eliminated using a Pasteur pipette connected to vacuum. Worm pellets were washed with M9 buffer and spun down. Wash step was repeated twice or more times until the supernatant was clear. 5 volumes of M9/0.01% TX-100 were added to the each worm pellet, and they were gently resuspended using a P1000 micropipette. 500 µl of the suspension were transferred to pre-chilled 1.5 ml microfuge tube, and then they were spun down 500 x *g* for 5 min at 4ºC. All supernatant was carefully collected with a Pasteur pipette. Each tube contained a pellet ~100 µl. Tubes were frozen down immediately in liquid nitrogen and store indefinitely at -80º.

RNA extraction

Before starting the extraction, a thermo shaker was set to 65ºC. Trizol aliquots (1ml in 1.5 ml microfuge tube) were warmed up to 65ºC. Four sets of tubes per condition (genotype, for example) were labeled. The tubes containing the frozen worm pellets were taken out from the freezer and immediately placed in a -20ºC bucket to carry them close to the thermo shaker. 1 ml of pre-warmed Trizol was immediately added to one tube and then incubated at 65ºC for 5 min at maximum shaking. Tubes were individually processed to the corresponding next step. 250 µl (1/5 vol) of chlorophorm added, and each tube was vigorously shacked by hand. Then tubes were let stand for 3 min at R/T to separate phases. Tubes were spun down at 12,000 x *g* for 15 min at 2-8°C. Supernatant was recovered, from top to bottom, using a P200 micropipette. Only 600 µl of the supernatant were recovered (~60% of Trizol volume) and transferred to a new tube. The white interphase was avoided. 600 µl of Iso-propanol were added to the saved supernatant and the tubes were vigorously shook by hand. Tubes were incubated at R/T for 10 min, then spun down at 12000 x *g* for 10 min at 2-8°C.

Pellet was washed with 1 ml of 75% ethanol, spun down at 7,500 x *g* for 5 min at 2-8°C. Pellet was air-dried briefly and then resuspended in 50 µl of DEPC-treated H20. Samples were treated with 1 µl DNAse I (+5 µl 10x buffer) for 10 min at 37ºC. Volume was increased to 250 µl with DEPC H20, then 250 µl (1/5 volume) of Phenol:Chlorophorm were added, and tubes were shook vigorously by hand. Tubes were spun down at 12000 x *g* for 10min at 2-8°C. Supernatant was recovered and 250 µl of Chlorophorm were added and tubes were shaken vigorously by hand. Tubes were spun at 12,000 x *g* for 5 min at 2-8°C. The aqueous phase was recovered, the interphase was avoided. 250 µl of Chlorophorm:Iso-amylic alcohol were added to the supernatant and tubes were shaken vigorously by hand, spun at 12,000 x *g* for 5 min at 2-8°C. The aqueous phase was recovered and 3 volumes of chilled ethanol and 0.4 vol. of 3M sodium acetate (optionally RNA-quality glycogen) were added. To precipitate the RNA, tubes were incubated at -80ºC for 30 min at least. The protocol can be stopped here and the RNA stored in ethanol at -80ºC. The protocol was resumed with 250 µl of ethanol:RNA suspension. To clean the ethanol from the RNA, tubes were spun down for 12,000x *g* for 10 min at 2-8°C. Supernatant was sucked up with a flamed Pasteur pipette and the pellet was washed with 70% ethanol and spun 12,000x *g* for 5 min at 2-8°C. Pellet was resuspended in 15 µl of DEPC-H2O.

TRIZOL:

9.5 g	Guanidiniumthiocyanat (ROTH: # 0017.1)
3.1 g	Ammoniumthiocyanat (ROTH: # 4477.1)
3.5 ml	Na-Acetat solution (3M, pH 5.0) (SERVA: # 39572.01)
5 g	Glycerol
48 ml	Roti-Aqua-Phenol für RNA-Isolierung (pH 4.5) (ROTH: 100ml # A980.2)
2.5mM	EDTA (pH8.0, from 500mM Stock)
2.5mM	EGTA is optional but recommended

Adjust to 100 mL with DEPC-treated H20.

4.2.5 Analysis of RNA on denaturing agarose gel

Preparation of denaturing agarose gel (1% agarose, 3% Formaldehyde)

Spoon and stir bar were flamed before use. 0.8 g agarose were taken with the spoon and weighed in a flask. 66 ml DEPC-ddH2O were added, and agarose was melted by heating in a microwave. The solution was stirred for about 5 min at R/T until it reached ~60°C. While stirring, 8 ml 10x MOPS were added, and then 6.5 ml of 37% Formaldehyde. Gel was poured and let to polymerize, then gel was covered in wrapping plastic and let stand for ~40-60 min, this polymerization time enhances the quality of the gel. The gel was run in 1x MOPS at constant 60 V and 200 mA until the front dye ran off. Per RNA sample the following reagents were assembled every time freshly, a master mix without the RNA was prepared accordingly.

Per one sample:

4.3 µl 37% Formaldehyde
12.5 µl Formamide (deionized, Qbiogene, FORMD002),
2.5 µl 10X MOPS
2.5 µl Orange G Buffer,
0.5 µl ethidium bromide (1% (w/v), SERVA, 21251)
3 µl RNA and 3 µl DEPC-treated ddH2O

The 1.5 ml tube was racked three times to mix, spun down, heated at 96°C for 2 min in a heating block, again racked three times, spun down and loaded immediately.

4.2.6 Northern Blotting

The Whatman Turboblotter System was used (Whatman 10416336). Sealable plastic bags were used for rinsing the gel in the following steps. After the RNA gel running was finished, the gel was transferred to clean plastic tray containing 1X MOPS. To assess the quality of the RNA, the gel was exposed to UV light and a picture was taken. Then, the gel was soaked in 10X SSC twice for 10 min. In the meantime, a nylon membrane (Nytran SuPerCharge 9x11, Whatman 10 416 336) was rinsed in DEPC-H20, and then soaked in 20X SSC for 5 min. Filter paper was assembled from bottom to top as follows:

20 dry thick-ones, 4 dry thin-ones, 1 wet thin-one and the pre-soaked nylon membrane. Agarose gel was placed on top of the membrane making sure that no air bubble stayed in between. When the gel was smaller than blotting membrane, the exciding membrane parts were covered with a thin wrapping plastic. Three presoaked thin filter papers were placed on top of the gel. Buffer tray was filled up with 125 ml 20X SSC. The transfer was started by connecting the buffer wick to the buffer, and placing the plastic wick cover on top (Figure 4.1). Transfer was let O/N at room temperature.

Figure 4.1 TurboBlotter and blotting stack assembly
See text for desription. Image was take from Whatman Turboblotter handbook.

The nylon membrane and one underlying filter paper were taken with metal clamps and transferred to a clean plastic tray, and directly cross-linked using the UV cross-linker (Stratagene, auto-mode). To check the quality of the transfer, membrane was rinsed in 2X SSC, and then incubated in methylene blue solution for 1 minute. Membrane was destained ~5 -10 min with DEPC-H2O inside a plastic box. To document the loading and quality of transfer, membrane was covered in wrapping film and scanned. Membrane was then rinsed twice in 2X SSC. Optionally, after distaining the membrane place on top of aluminum fold and was baked for 30 – 60 min at 120°C. Then membrane was rinsed in once in 2X SSC. Membranes were stored in a plastic bag with 2X SSC at 4°C, or pre-hybridization step was continued.

Pre- and hybridization

68°C is the general recommended hybridization temperature for RNA:RNA, however the temperature can be adjusted to the GC content of the probe. 68°C was used in these experiments. Pre-hybridization, hybridization and further washes were done in glass hybridization bottles containing a plastic mesh inside. 15 ml of DIG Easy Hyb suspension (Roche 11796895001) was pre-heated to hybridization temperature. For pre-hybridization, the membrane was carefully transferred to the hybridization bottles and incubated with 10 ml DIG Easy Hyb suspension 68°C for 30 min with gentle rotation in the Mini Hyb Oven. In the meantime, DIG-labeled RNA probe was diluted 1:10 with DEPC-H20, ~100 ng of probe per ml of hybridization suspension was used. To denature the probe, 400 ng of probe were mixed with 20 µl of DEPC-H20 in a 1.5 ml tube, and boiled for 5 min and then rapidly transferred to iced water. The denatured DIG-labeled probe was added to the remaining pre-heated 4 ml (at least 3.5 ml/100 cm^2 membrane), solution was mixed and bubble formation was prevented. The pre-hybridization solution was poured off, and the probe/DIG Easy Hyb mix was immediately added to the tube containing the membrane. Membranes were incubated in the Mini Hyb oven O/N at 68°C.

Stringency washes

After hybridization, hybridization buffer was poured and membranes were washed in the following order: twice 15 min in 2X SSC/0.1% SDS at R/T, twice 15 min in 2X SSC/0.1% SDS at 68°C, once 15 min in 0.5X SSC/0.1% SDS at 68°C and finally once 1 h in 0.5X SSC/0.1% SDS at 68°C. 25 ml at each step.

Antibody detection

Further steps were done in a sterile sealable plastic. The solution were used here on were form the DIG Wash and Block Buffer Set (Roche 11585762001). Membrane was rinsed in Washing Buffer for 5 min, and then incubated for 30 min with 15 ml Blocking solution (10X blocking solution dissolved with 1x maleic acid). In the meantime, anti-DIG antibody was diluted 1:20,000 in blocking solution, and then membrane was incubated for 30 min with 4 ml of antibody solution in sealed plastic bag at RT. Membrane was then washed twice 15 min with 20 ml of Washing Buffer each.

Membrane was equilibrated for 3 min in 2ml/10cm2 of Detection Buffer. In the meantime, CDP-Star (Roche 1 685 627) (0.25 mM) was diluted 1:100 in Detection Buffer, 700 µl volume was used. After equilibration membrane was placed on a plastic folder, CDP-star mix was immediately added to the membrane, and then covered with the second plastic sheet. Membrane was incubated for 3 min and the excess of liquid was removed. The borders of the plastic folder must be sealed and the membrane must never dry out.

Stripping of RNA blots

Stripping buffer was prepared always fresh, and membranes were stripped the same day after antibody detection.

	for 50 ml
50% formamide	25 ml
50 mM Tris-HCl pH 7,5	2.5 ml
5 % SDS	2.5 g

Membrane was rinsed in DEPC-H20, and incubated twice 1h at 80ºC in stripping buffer in the glass hybridization bottle. Then rinsed twice 5 min in 2X SSC at R/T. Membranes were pre-hybridize for a different probe, or stored in 1X Maleic acid buffer or 2X SSC in a sealed plastic bag at 4ºC.

4.2.7 Reverse transcription and PCR analysis (RT-PCR)

DNase I treatment (for RT-PCR analysis)

RNA was extracted with Trizol as described before. To remove genomic DNA contaminants, the RNA was treated with DNase I (RNase-free, (Roche, 776 785)). Two input samples were pooled and divided into one input sample with and one without DNase I treatment, as a negative control. The components were mixed well, spun down and incubated for 30 minutes at 37°C.

Mixture:

	DNase+	DNase–
10x DNase I buffer	4 µl	4 µl
RNA	20 µl	20 µl
DEPC-H_2O	15 µl	16 µl
DNase I	1 µl	-

Phenol-Chloroform purification of the DNase I-treated RNA

40 µl DNase I-treated RNA were mixed with 360 µl DEPC-H_2O and 30 µl HEPES (DEPC-treated, 50 mM pH 7.5) and extracted once with 350 µl PCI and twice with 350 µl CI. The RNA was precipitated with 1/10 volume 3M NaOAcetate (pH 5.2, DEPC-H20), 2.5x volumes ethanol and 2 µl glycogen (20 mg/ml). Tubes were shook by hand and incubated at -20°C for at least 30 min. Then, RNA was spun 10 minutes at 4°C at 16,000 x g. Supernatant removed with a drawn out Pasteur pipette. Pellet was washed with 1 ml ice-cold 75% ethanol, spun for 5 min at 4°C at 16,000 x *g*. The pellets were air-dried with open lid for 5 min and dissolved in 26 µl DEPC-H_2O.

4.2.7.1 Generation of cDNA by reverse transcription

In a 1.5 ml tube the RNA was heated exactly three minutes at 96°C and put on ice water immediately. The cooled sample was spun down and divided into a RT+ and a RT- sample. The following reaction was assembled on ice in 0.2 ml PCR tubes:

	RT+	RT-
5x AMV buffer	4µl	4µl
dT anchor primer (12.5 µM)	1µL	1µl
dNTPs (10 mM)	1µl	1µl
DEPC-H_2O	-	1µl
RNA	13µl	13µl
AMV Reverse Transcriptase	1µl	-
AMV RT (Promega M510F 17121019 10u/µl)		

The reaction was mixed, spun down, and incubated in a thermocycler for 60 minutes at 55°C, and then 20 minutes at 65°C to inactivate the AMV RT.

4.2.7.2 Gene-specific PCR

To detect the presence of a particular RNA and validate the production of cDNA, gene-specific primer pairs were used to carry out a nested PCR. In order to differentiate genomic DNA from cDNA, primers were chosen to sit out of introns thus genomic DNA (unspliced) amplicons would have a bigger size than cDNA (spliced) amplicons. The primers usually had melting temperatures of 61°C as calculated by the formula [Tm = (4*G + 2*A) – 5]. The following primers were used:

Primers	*gld-1*	*tbg-1*	*nhr-114*
1st pair	CE930/933	CE968/971	CE2367/2366
2nd pair	CE931/932	CE969/970	-
Genomic amplicon:	369 bp	934 bp	1143 bp
cDNA amplicons:	280 bp	378 bp	237 bp

The genomic and cDNA amplicons size corresponds to the 2nd primer pair, except for *nhr-114*. The PCR reaction was assembled as follows:

Template (cDNA)	2 µl
primers (both 5 µM in one mix)	1 µl
dNTPs (10 mM)	0.5 µl
10x PCR buffer	2 µl
HiFi polymerase	0.3 µl
H_2O	14.2 µl

Two input samples were prepared, one with 0.5 µl cDNA and one with 1.5 µl cDNA as templates. The volumes were filled up to 2 µl with H_2O. These two input samples allowed to monitor if the PCR reaction was still in the linear range. The 3-fold difference between the two input samples had to still be visible after the nested PCR for it to be in the linear range. Only if the nested PCR was still in the linear range, the amount of the PCR products reflected the amount of cDNA that was used as an input and therefore allowed to compare the two IP samples. For the IP samples 2 µl cDNA were used as template for the primary PCR.

The following PCR program was run:

1) 95°C for 2 minutes
2) 95°C for 50 seconds
3) 58°C for 50 seconds
4) 72°C for 45 seconds
5) go to step 2) 19 times
6) 72°C for 7 minutes
7) 4°C ∞

The secondary PCR was set up as the primary PCR reaction except that 0.5 µl primary PCR were used as template. The same PCR program as for the primary PCR was run except that at step 5) the cycle was repeated 24 additional times. The complete volume of the secondary PCR was loaded on a 1.2% agarose gel supplemented.

4.2.7.3 Rapid amplification of cDNA end (3' RACE)

The following PCR was setup using the anchor and the *nhr-114* specific primers (CE2367) to a final concentration of 12.5uM. All the PCR volume was run in an agarose gel.

PCR setup:				PCR program	
cDNA	1ul (RT+)	1ul (RT-)		step1	95C, 2min
10xBuffer	5ul	5ul	5ul	step2	95C, 1 min
Anchor primer	1ul	1ul	1ul	step3	59C, 40sec
Specific primer	1ul	1ul	1ul	step4	72C, 1 min
10mM dNTPs	1ul	1ul	1ul	step5	repeat 34x
HiFi Polymerase	1ul	1ul	1ul	step10	72°C, 8min
H2O	40ul	40ul	41ul	step11	20°C, END
50ul	50ul	50ul			

Two products were amplified by the PCR, thus two bands were cut form the agarose gel. Each band was treated independently and they were purified over PCR purification column (Wizard SV Gel and PCR clean-up system #A1460, Promega). DNA was precipitated and sent for automated DNA sequencing using CE2365 primer. Retrieved sequence was compared to predicted *nhr-114* 3'UTR. Both bands corresponded to *nhr-114* isoform 1.a 3'UTR, the difference in size was due to difference a 4 bp difference of adenosine residues. No 3' UTR corresponding to *nhr-114* isoform 1.b was found.

4.3 Worm stainings

4.3.1 Whole mount DAPI staining

A glass Pasteur pipette was flamed and the tip thinned. Young adult animals were picked by hand and transferred into a 1.5 ml tube containing M9+ (M9/0.05% Triton X-100). Worms were chilled for ~1min in ice bath to have no floating worms left behind. Tubes were spun down at 2k rpm for 2 min to collect worms at the bottom. Supernatant was removed and worms were washed twice in the same way as above to get rid of bacteria. 0.5ml -20ºC methanol was added to the worm pellet. Tubes were incubated for incubated for 5 min -20ºC (5 min incubation yielded the best quality staining). 0.5ml M9+ was added methanol, tubes were inverted gently and worm bodies were pellet at 1000rpm for 2 min. 0.5 ml were removed and 0.5ml M9+ were added, pellet bodies were mixed and spun down for 2min at 1000 rpm. All supernatant was removed and worms were washed twice with M9+, and incubated with DAPI (1:2000 diluted in M9). Tubes were covered with aluminum foil and incubated on a rotating wheel for 20-30 min. DAPI was removed and worms were washed twice fast with M9+, and one more time for 5' with M9+. All supernatant were removed except for 200 ul, which were transferred to a PCR tube. Tubes were spun down 1000 rpm for 2 min and most of the carefully removed. Then 10 µl (2x Vol.) of anti-fade mounting solution was added (Vectashield, LINARIS GmbH, H-1000), and tubes were mix well but gently tapping the bottom of the tube. Worms were transferred with a P20 micropipette tip onto a cover slip. 2-8 ul of mounting media was removed to end up with 7-8ul of liquid. A glass slide was used to touch the coverslip. Edges were sealed with nail polish, and slides were observed under a fluorescence microscope.

4.3.2 Antibody staining of extruded germ lines

Subbed glass slides

25 mg Poly-L-Lysine hydrobromide (Sigma: P1524) were dissolved in 50 ml gelatin/chromalum solution and stored at 4°C. To subb glass slides, two drops of poly-L-Lysine/gelation solution were dropped onto a glass slide using a P1000 micropipette. Slide was incubated for 5 min and then the liquid was wicked off. The slides were dried upright until no traces of liquid were left. Then slides were heated for 15 min on a metal heating block at 72°C. Each well was marked with a fat pen (PAP pen, Kisker: MKP-1) to constrict the liquid to the well.

Dissections and stainings

Worms were analyzed 24 hours past the L4 as adults. Dissections were conducted using a stereoscope at 3.2 X magnification. 10 µl of cutting solution were pipetted into a well of the subbed slide. 5 - 10 animals transferred into the cutting solution. Using a syringe needle (25G 1" – Nr.18, 0.5 x 25 mm) the heads or tails of the animals were cut off to allow the gonad and intestine to extrude from the animal. 100 µl 1 % PFA in PBS were added to the cut animals, mixed well by pipetting and incubated for 10 min at room temperature. Slides were kept in a wet chamber. The PFA was removed and the wells were washed once with 50 µl PBST-B and incubated in fresh 50 µl PBST-B for 5 min at room temperature. The PBST-B was removed and the germ lines were blocked in PBS-B for at least 30 min at room temperature. Each well was incubated with 12 µl primary antibody solution over night at 4°C. The wells were washed three times for 10 min with 50 µl PBS-B, and incubated with 50 µl secondary antibody solution for 2 hours at room temperature. The wells were washed 10 minutes in PBS-B, 10 minutes in DAPI-staining solution, and twice 10 minutes PBS-B. All liquid was taken off, 12 µl Vectashield mounting medium (LINARIS GmbH, H-1000) were added to each well. A cover slip was placed on top close the slide, and borders were sealed with nail polish at two sides.

Amounts for 4 wells (2-slides):

PFA 1%
30 µl 16% PFA
450 µl PBS

PBSB-T
10 µl 10% Triton-X100
490 µl PBSB

Cutting solution
2 µl 250 mM levamisole
15 µl 1% PFA
185 µl M9

PBS-B
0.5% BSA
PBS

Secondary antibody solution
Diluted 1:500 in PBS-B, and centrifuged for 5 minutes at full speed and solution was taken from the top.

DAPI staining solution
DAPI 1:1000
PBS-B

Antibodies used:	species	
α-NPC	mo mAb414	used 1:400
α-GLD-1	rb.	used 1:100
α-GLD-4	rb.	used 1: 500
α-anillin-2	rb.	used 1:600
α-HIM-3	SAC38 guinea pig	used 1:200
α-NOS-3	rt.	used 1: 10
α-GLH-1/2	guinea pig SAC47	used 1:200
α-sperm	mouseSP56	used 1:600

The immunostainings using these antibodies were done by Eckmann C. Secondary antibodies: Cy5-, Cy3- or FITC-conjugated AffiniPure donkey anti-rabbit, -rat, -mouse or -guinea pig IgG antibodies (from Jackson ImmunoResearch Laboratories) were used at a concentration of 1.5 µg/ml, (1:500 dilution of a 0.75 mg/ml stock solution).

4.4 WORK WITH YEAST

4.4.1 TRANSFORMATION OF YEAST

To conduct direct yeast two-hybrid assays, *nhr-114,-68, -17,* and *-10* were cloned into pACT (GAL4 Activation domain, AmpR, 7.6 kb, LEU2) and pLex vectors (LexA DBD, pGBKT7 backbone, KanR, 7.3 kb, TRP1). The following protocol was adapted from Gietz lab, (1998). Yeast L40 was streaked out from glycerol stock onto L-agar plate and grew O/N at 30ºC. 20 ml of YPD medium were inoculated with a single yeast colony and grew O/N at 30ºC at 200 rpm shaking. The optical density (OD600) of the O/N culture was measured with a spectrophotometer. O/N culture was diluted to $5x10^6$ cells per ml in 50ml YPD using the formula: 8.3 /OD600 measurement = *x* ml to be added to 50 ml culture. Culture was grown at 30ºC to OD600=0.7-0.9 ($2x10^7$/ml, two cell divisions in ~ 4-5hrs). Cells were harvested by spinning at 4000 rpm for 5 min. Pellet was resuspended in 25 ml H_2O and cells were harvested as before. Supernatant was discarded by inverting the tube. Yeast pellet was resuspended in 1 ml 0.1M Lithium acetate (LioAc) and transferred onto a 1.5 ml tube. Cells were pelleted by spinning at maximum speed for 15 sec in a microfuge. Supernatant was discarded, ~100ul pellet was resuspended in 400 µl 0.1M LioAc total.

Per each transformation, 50 ul of the yeast/LioAc suspension were dispensed into a 1.5 ml tube. Cells were harvested at 8000 rpm for 15sec, and supernatant was discarded. 326 ul of the transformation mix were added to the pellet, and then 34ul of H2O containing 300 ng of each DNA plasmid were added. Tubes were racked thrice vigorously, put on vortex, and then incubated at 30ºC for 25 min in a thermo block without shaking. Then temperature was shifted to 42ºC for 25 min. Cells were harvested at 8000 rpm for 15 sec, supernatant was discarded, and then pellet was resuspended gently in 1 ml H20. 200 ul of this suspension were streaked on the -Leu -Trp SD plates. Plates were incubated at 30ºC for 2-3 days. Plasmids encoding proteins known to interaction, for example GLS-1 and GLD-4, were always included as a positive control. The empty vector was co-transformed with candidate genes and used as negative control.

Transformation mix:	1x	9x	12x
PEG (50% w/v)	240 ul	2160 ul	2880 ul
LiAc (1M)	36 ul	324 ul	432 ul
ssDNA (2mg/ml)	50 ul	450 ul	600 ul

ssDNA was always boiled beforehnad and immediately chilled on ice

4.4.2 ß-GALACTOSIDASE ASSAY

After 2-3 days of transformation, ~10 individual colonies were picked and streaked as a 1 cm lanes into a fresh plate, and incubated at 30ºC for another day or two. A circular nitrocellulose membrane was placed on top of non-cold fresh SD -LEU-TRP. Using a P20 tip, the yeast lanes were streaked on the membrane as lanes of 100 mm x 5 mm each spaced by 70 mm. Plate was incubated for ~4 h. To break the cells, the membrane was carefully removed from the plate and immediately sunk into liquid nitrogen for ~30 sec. In the meantime, using the lid of a plastic petri dish, a circular filter paper was sunk in Z-buffer containing X-gal. Excess of buffer was removed by decanting the liquid. Membrane was taken from the liquid nitrogen using long metal clamps and laid on top of paper avoiding the formation of bubbles in between. Petri dish was closed and sides were sealed with parafilm, and then incubated upside down at 37ºC. Development of blue color was monitored every 30 min for the first two hours and then every hour until seven hours. Petri dish was opened and membrane was scanned every hour.

4.4.3 YEAST PROTEIN EXTRACTION USING TRICHLORIC ACID

The equivalent of a yeast colony was used to inoculate 15 ml of selective media in a glass flask, and culture was grown O/N at 30ºC. OD600 was monitored next day and cells were harvested at OD 600 < 1.5; if OD was higher, cells were diluted to OD 600 of 0.4 and incubated again. 5 OD units were harvested at 4000rpm for 5 min. Yeast pellets were kept at 4ºC. Pellet was washed in 1ml 20% thrichloric acid (TCA) and resuspended, then transferred into a 1.5 ml tube, and then spun for 1 min at maximum speed. Supernatant was discarded, pellet was resuspended in 200 ul 20% TCA and a volume ~200 ul of glass beads were added. Yeast cells were broken using an automatic bead beater for 5' min. Then, tubes were briefly spun and supernatant was saved using long nosed tips, and transferred to a fresh tube.

Extraction was repeated using 200 ul 5% TCA, and 5 min beating. Supernatant was saved and combined with the previous supernatant. To precipitate the proteins, the tubes were spun at 3000 rpm, for 10 min at RT. Supernatant was discarded, then 100 ul of 2X SDS-SB plus 100ul 1M Tris Base were added. Precipitates were resuspended in a thermo block at 95ºC using maximum shaking for 10 min. To precipitate insoluble materials tubes were spun at 3000 rpm for 10 min at R/T. Supernatant was saved in a new tube. 10-15ul were loaded in a SDS-PAGE gel, the remaining was stored at -20ºC. Antibodies used: mouse anti-LexA (SantaCruz) 1:2000, GAL4-AD fusions were detected using anti-HA antibody (1:10000).

4.4 Protein purification from bacteria

4.4.1 Expression and purification of MBP::NHR-114(100-167)

The *nhr-114* sequence encoding amino acids 100-167 was cloned into pMALc2X vector downstream of the sequence that encodes the maltose-binding protein (MBP). *E. coli* BL21 was transformed and six colonies were grown at small scale (2 ml). To test fusion protein production, individual cultures pellets were lysed and resuspended in SDS-SB, resulting insoluble and soluble fractions were independently resolved in an SDS-PAGE gel. The colony with the best profile of fusion protein expression was chosen for large scale expression. An ~51 kDa MBP::NHR-114 fusion protein was found in the soluble fraction. Original culture was stored as a glycerol stock at -80ºC.

For large scale expression, a single colony from a fresh streak-out was used to inoculate 20 ml culture, culture was grown O/N. Using 10 ml of this culture, 6 x 1 liter LB /glucose /Amp were inoculated to an OD600 of ~0.1. Cell were grown cells to 2x108 cells/ml (OD600 ~0.4-6) at 37°C. Protein expression was induced with IPTG at a final conc. of 0.3 mM (BL21). Cells were incubate at 18°C O/N. Cells were harvested by by centrifugation at 6000xg (3500rpm) for 10min (JLA 8.1000 rotor), SN was discarded and cell paste was resuspended in 25 ml column buffer. Resuspension was passed through the Emulsiflex at 17,000 psi. Then homogenate was centrifuged at 12,000 x g for 30 min (JLA 12 rotor).

In the meantime, 2-4 ml bed volume of amylose resin (NEB, cold room) was prepared a in a 50ml tube. Resin was washed in 40ml of Column Buffer and SN was removed. After centrifugation the bacterial extract (SN) was poured into the amylose resin and incubated in the cold room for 15 min on wheel. Beads were spun down (2000rpm, 2min table top centrifuge, remove break at 300rpm when slowing down) and washed twice with 12 x column Vol. of Column Buffer. To eliminate HS-proteins (eg. HSP70, HSP90) the column was treated with ATP-treat (see ATP elution). Resin was transfered to a plastic column with Pasteur pipette. Fusion protein was eluted with Elution Buffer (**+** 10 mM maltose). 10 to 20 fractions of 1 ml each (fraction size = 1/5th column volume) were collected (Figure 4.2. A). The eluted fractions were surveyed using an SDS-PAGE gel for integrity and purity. The protein-containing fractions were pooled and stored at -20°C.

ATP elution:

Beads were mixed with 5x volume of ATP elution buffer w/o ATP. Beads were let to settle and SN was removed completely. 5x bed Vol. of the ATP elution buffer (+ATP) was added, beads were stire with blunted Pasteur pipette and incubated for 15 min at RT. SN was removed and the wash step was repeated and incubated for 10 min. SN was removed and beads were resuspended in Maltose-Elution buffer.

Media & Solutions
1 L LB + 10 ml 20% glucose + 1 ml 100 mg/ml ampicillin
1 M IPTG stock, 1000X protease inhibitor cocktail
1M HEPES pH7.2 can be converted to pH8.0 by adding 2.5ml 4N NaOH

Column Buffer
per liter final conc.
20 ml 1.0 M HEPES pH 7.25 20 mM HEPES
11.7 g NaCl 200 mM NaCl
2.0 ml 0.5 M EDTA 1 mM EDTA
154 mg DTT 1 mM DTT

ATP Elution buffer Maltose Elution buffer
0.1 M HEPES pH 8.0 0.1 M HEPES pH 8.0
0.25 M NaCl 0.5 M NaCl
10 mM MgCl2 10 mM maltose
1-5mM ATP (buffered)

4.4.2 EXPRESSION AND PURIFICATION OF HIS:NHR-114(80-419)

The *nhr-114* sequence encoding amino acids 80-419 was cloned into pRSETa vector upstream of the sequence that encodes the 6x HIS tag. Protein production was verified in a small-scale test as described before. Six 1 L cultures were grown.

Purification under native conditions:

Bacterial pellets were thoroughly resuspended and in 100 ml of PBS/with protease inhibitors (Complete Mini Roche). To lyse the bacteria, the suspension was passed three times using the Emulsiflex at 17000 psi. If the lysis was well done, the color of the suspension will turn darker. Suspension was centrifuged at 4ºC for 30' at 20000 rpm in rotor JA 25.50. Supernatant was discarded, pellets were gently resuspended in 10-15 ml of denaturing lysis buffer. Tubes were placed in the rotating wheel for 30 min at room temperature. Then centrifuged 30 min at 20000 rpm at 4ºC, rotor JA25.50. In the meantime 450 µl of Ni-NTA-beads were pre-washed with denaturing lysis buffer. Lysate supernatants were transferred into a tube and 450 µl of the prewashed Ni-NTA-beads were added and incubated in the rotating wheel for 60 min. Beads were spun down at 800 rpm for 2 min and washed thrice with 10 ml each, with denaturing washing buffer (Save 10ul sample of each wash step).

Colum elutions were initially tried out; however, most of the recombinant protein remained bound to the beads. Therefore, bath elution was then tried out. For this, the washed beads were incubated with 4 ml of elution buffer for 30 minutes. Then supernatant was mixed with 2X-HU-buffer with B-ME and loaded into SDS-PAGE gel, (2.3 mL were loaded per gel). Gel was run overnight at 60V, 30 mA. In some cases, the beads containing the fusion protein were directly mixed with 2X-HU buffer and loaded into the preparative gels. The samples can be stored at -20ºC. to cut out the protein fusion band out of the gel, gels were washed three times the with ddH20. Then gels were stained with Cu^{++} staining solution for 5 min. gel was then washed with desalted water and the predicted size bands were cut out. Gel bands were destained in Cu^{++} destaining solution.

Destained bands were placed in a Petri dish and minced thoroughly with a syringe piston. The volume of the gel pieces was estimated and twice the volume of diffusion elution buffer was added. The gel-buffer mix was distributed in 1.5 ml tubes. Tubes were heat up 10 min at 65ºC on a shaker. Then to 37ºC for 24h or more.

To separate the supernatant containing the protein from gel fragments, the solution containing gel pieces was loaded onto a 20 ml column. Alternatively tubes were centrifuged for 1' at 2000 rpm. The amount of protein was tested in a 10% PAA gel with different amounts 2, 4, 6, 8, 10 µL. To reduce the amount of SDS in the sample without precipitating the protein, the elute was transferred into a dialysis tube and dialyzed stepwise for 2h each at room temperature, using: first, PBS/ 0.25%SDS; then PBS/ 0.1%SDS /0.1% Tween; and finally PBS/ 0.01%SDS/ 0.1% Tween. The solution was transferred out of the dialysis bag into a concentration column with a MW cut-off at least the half the size of the protein of interest. (*i.e.* Vivaspin 10 kDa. Sartorious Stedim VS0201). Columns were centrifuged at room temperature at 4000 x g for 30 min until 50 µl remained in the column. 150 µl of the flowthrough were used to recover the 50 µl. Final protein concentration was estimated using SDS-PAGE gels (Figure 4.2 B).

Elution buffer
8M Urea
0.1 M NaH2PO4
0.01 M Tri-HCl pH 3.8
300 mM Imidazole

Wash buffer
8M Urea
0.1 M NaH2PO4
0.01 M Tri-HCl (pH 6.8-7.0)
20 mM Imidazole
0.5 % NP40

Lysis buffer
8M Urea
0.1 M NaH2PO4
0.01 M Tri-HCl (pH 8.0)
20 mM Imidazole
0.5 % NP40

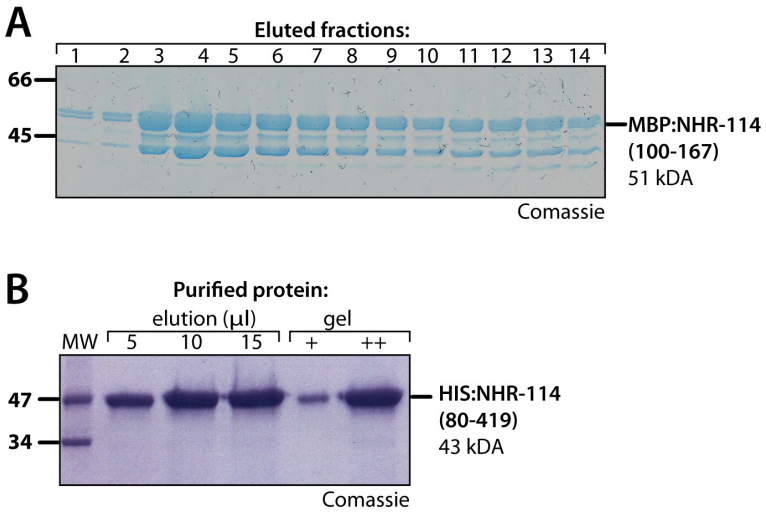

Figure 4.2 Two different NHR-114 recombinant proteins used for antibody production
Representative SDS-PAGE gels stained with Comassie blue staining (Commasie). **A)** Eluted fractions (1-14) of purified MBP::NHR-114 protein. **B)** Different volumes of HIS::NHR-114 protein eluted from cut gel pieces (gel). See main text for details.

4.5 Baculovirus-displayed antigens

Lindley et al. (2000) and Tanaka et al. (2002) reported similar protocols for the production of monoclonal antibodies using recombinant baculovirus displaying fusion proteins at their surface. This method takes advantage of the natural immunogenicity of the virus, and of the display of the fusion protein in its native conformation. In addition, since the baculovirus are produced in eukaryotic cells, (Sf9 insect cells) many eukaryotic posttranslational modifications may be added to the recombinant protein, thus increasing its immunogenicity (Lindley et al. 2000; Tanaka et al. 2005). Furthermore, this protocol has being established for the production of NHRs antibodies (Tanaka et al. 2002). In an attempt to produce efficient antigens for the production of NHR-114 antibodies, I set to establish this protocol to display two different NHR-114 epitopes on the surface of a baculovirus. Briefly, the antigen is produced by placing the coding sequence of interest downstream of the sequence of the surface-glycoprotein gp64 (Lindley et al. 2000; Tanaka et al. 2002). GP64 fusion proteins are produced and exported to the viral surface. Then baculovirus are purified and used for mice immunization.

Baculovirus infected insect cells (BIICs) were produced for two NHR-114 epitopes (K158 and K242) and were used to infect SF9+ insect cells. Expression of recombinant budded viruses was determined at two different viral titers: 0.2 µl BIIC or 8 µl BIIC for 2 million S9+ cells /ml. The higher BIIC concentration was chosen. Time-course assay for the peak of expression of recombinant virus was done as follows: 15 ml of SF9+ culture (2 million/ml) was infected with 120 µl BIIC. A 1.5 ml sample was taken at day 3: 69h, 78h; day 4: 92h, 101h; day 5: at 123h and finally at day 6: at 144 h post infection. Each sample was spun for 5 min 1500 rpm at 4 ºC. 1 ml of the supernatant was carefully taken and saved in a clean centrifuge tube at 4ºC. The pellet was frozen in liquid nitrogen. The supernatant were spun at 80,000 x *g*. Pellet was re-suspended in 20 µl of 2X SDS SB. 10 µl were loaded in a gel (Figure 4.3).

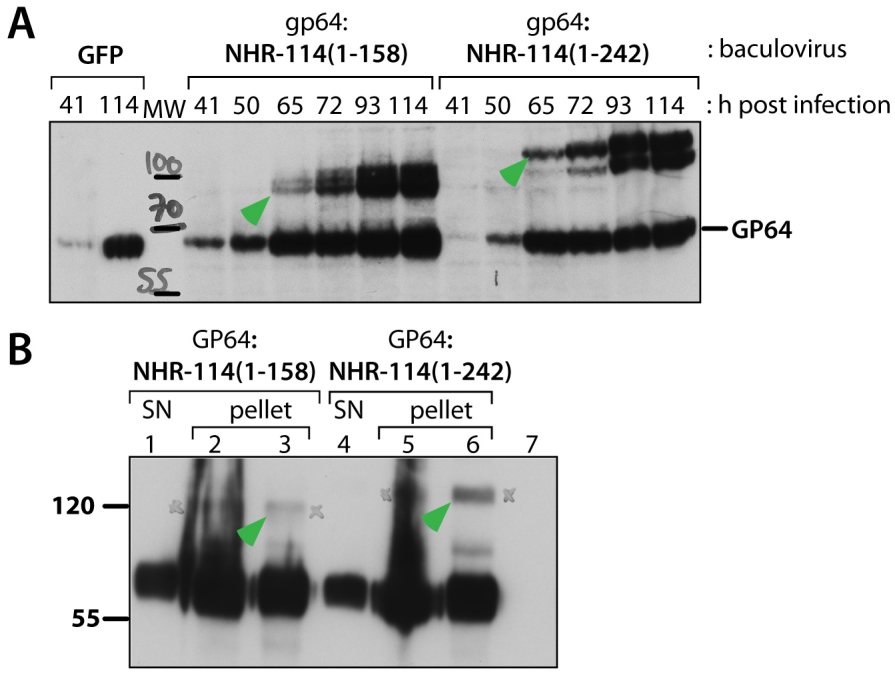

Figure 4.3 Expression of two GP64::NHR-114 fusion proteins
Western blots using anti-GP64 to detect the expression of two different GP64::NHR:114 recombinant proteins (green triangles). **A)** Time-course analysis using total cell lysate of infected Sf9+ cells. Lower band is wild-type GP64. Note the approximate 1:1 ratio between wild-type and recombinant GP64. **B)** Purified viruses used for immunizations. Precipitated viruses (pellet), supernatant (SN). Lane 2 and 5 correspond to filtered precipitated viruses. Note that there is much more wild-type GP64 than recombinant GP64.

500 ml of SF9+ cells at 2 million/ml were infected with 4 ml of the respective BIIC stock. Cells were harvested 94 h post infection. The culture was spun in a conical tube for 5 min at 1500 rpm at 4ºC. Supernatant was transferred to 50 ml tubes and spun for 5 min at 1500 rpm at 4ºC. The second centrifugation step is important to pellet most cells and prevent filter clogging. Cleared supernatant was filtered with 0.45 μm filter pore and kept on ice. The filter was changed every time it got clogged. To isolate the virus, the cleared supernatant was spun at 80,000 x *g* at 4ºC (Table 4.3). Pellets were resuspended 5 ml PBS. 5 ml were spun at 80,000 x *g*. Pellets were re-suspended in 1.5 ml of PBS and stored at 4ºC. Presence of NHR-114 fusion protein was determined by Comassie staining and Western blottin. The fusion protein was not observed as different band above the background by Comassie staining. The fusion protein was seen in WB in a ratio ~1:10 compared to wild type GP64 protein (Fig. 4.3 B). Five Balb/c mice were immunized with 100 μg of NHR-114:GP64 in Freund's Complete Adjuvant. Immunized mice sera were tested for recognition of recombinant and endogenous NHR-114 by western blotting; in both cases there was not immunoreaction. Although recombinant protein was produced, the ratio of recombinant protein versus wild type GP64 was apparently too low to produce an immune response.

Rotor (rpm)	Speed (min)	Time	Volume
Type 19	19000	213	6 x 200 ml
JLA 25.50	25000	93	8 x 40 ml
SW55TI	50000	16	6 x 5 ml
TLA 120.2	80000	5	10 x 1.3 ml

Table 4.3. Centrifugation conversions
Time in different centrifuges to get 80,000 x *g* force. Based on run time conversions using factors.http://www.beckmancoulter.com/
resourcecenter/labresources/centrifuges/runtimecon.asp

5. Abbreviations

AMPK	AMP-activated protein kinase
bp	base pairs
BSA	bovine serum albumin
CARM1	Coactivator-associated arginine methyltransferase 1
CBP	CREB-binding protein
Cy3	Cyanine 3
DAPI	diamidinophenylindole
DEPC	diethyl pyrocarbonate
DNA	deoxyribonucleic acid
dsRNA	double stranded RNA
DTC	distal tip cell
eIF	eukaryotic initiation factor
ER	Endoplasmic reticulum
FBF	*fem-3* binding factor
GLD	germline development defective
Gls	germline survival defecitve
HEPES	(4-(2-hydroxyethyl)-1-piperazineethanesulfonic acid)
HRI	Haem-regulated inhibitor
LB	Luria-Bertani
MAPK	Mitogen activated protein kinase
min	minutes
ml	milliliter

mRNA	messenger RNA
mRNP	mRNA-protein complex
NCoR	Nuclear receptor corepressor
NGM	Nematode Growth Medium
ORF	open reading frame
PABP	poly(A) binding protein
PAGE	polyacrylamide gel electrophoresis
PCI	phenyl:chloroform:isoamylalcohol
PERK	Endoplasmic reticulum kinase
PFA	paraformaldehyde
PKR	Protein kinase activated by double-stranded RNA
PRMT1	Protein arginine N-methyltransferase 1
PUF	Pumilio and FBF
rb	rabbit
RNA	ribonucleic acid
rpm	rounds per minute
RT-PCR	reverse transcrition and PCR
SDS	sodium dodecylsulfate
sec	seconds
SIN3	Switch INdependent = histone deacetylase component homolog
SMRT	Silencing mediator for retinoid or thyroid-hormone receptors
ss	single stranded
ssRNA	single-stranded RNA
µl	microliter

6. ACKNOWLEDGMENTS

I would especially like to thank Christian for trusting in me as a candidate and giving me the opportunity to do my PhD in his lab. I am grateful to him for his enormous input and tireless dedication in educating me for four years. I am thankful to him for patiently teaching me how experiments must be conducted thoroughly, and for his insistence in the importance of solid and rigorous data. Furthermore, I am thankful to him for being an intellectual support, and for being a critical supervisor. I also thank his advices, directions and tips on how to be effective in scientific communication, from how to craft a figure and a slide to how to transmit a clear presentation both visually and orally; and more recently in writing. One of the things I am in debt the most is the many broad advices Christian has shared with me in an informal or sometimes unexpected ways!

I would like to thank David Drechsel and Regis Lemaitre from the MPI-CBG protein expression facility for being open to start the baculovirus antigen display project; and for sharing their knowledge on baculovirus and molecular biology with me. Despite the project did not turn out in our favor, I had the opportunity to work closer with the two of them, which was an enjoyable and dynamic experience. Also, I would like to thank Temo Kurzchalia and every member of his lab for being friendly and helpful sharing their expertise on worm lipids; thanks Sider. I am thankful to Ryuji Minasaki and Marco Nousch for sharing their technical expertise and knowledge that made the start of new endeavors at the bench always easier. In specific, I would like to thank Marco for his support during the preparation of the *Friday Talk*; and Ryuiji for reading and giving feedback on every chapter of the thesis. I am also thankful to Daniel Hampel for helping me with the expression of an NHR-114 epitope, and for troubleshooting and moving forward the *nhr-114* transgene project; and to Valentina Botti, for providing pLex-*gld-4* constructs. Overall, I thank every member of the Eckmann lab for their support and friendship during this years, -in the end, everyone's personality makes of the lab such a peculiar and fun place to work in.

I am grateful to my parents, Francisco and Virginia, for making of education a priority of every aspect in our life as a family; and for being a great support all the time. I take the opportunity to say that I admire both of them for their tenacity and persistence; their effort is a big example for me. *Esta tesis se las dedico a ustedes: Chico y Virgi, me siento realmente afortunado de ser su hijo y del hogar que ustedes dos forjaron. Estoy muy agradecido de que ustedes hayan hecho e insistido en cada momento en la educación como una prioridad de la familia. Creo que Paco, Tuna y yo, fuimos muy privilegiados en crecer en una familia que tiene una manera distinta de ver muchas cosas. Gracias por sus valores, sus enseñansas y sobre todo por ese libre espíritu de los dos.*

I am thankful to my friends in Dresden, those that move out of Dresden early, and those in the other continent, for all being a source of fun and support. I am very thankful to Ofer for his help, discussions and suggestions. I am especially thankful to Edward for his friendship, enormous support, and for being there always. I would also like to thank him for going through the very first draft of the thesis, - I can imagine that was not an easy one. Lastly, I am grateful and thankful to Sara for being supportive, a friend, an example, and much more. I thank Sara for sharing this time in Dresden, and helping me go through; Sara, I thank you for these years.

7. REFERENCES

Adams MD, Celniker SE, Holt RA, Evans CA, Gocayne JD, Amanatides PG, Scherer SE, Li PW, et al. (2000) The genome sequence of Drosophila melanogaster. Science 287:2185–2195

Albanese, A. A., Higgons, R. A., Hyde, G. M., & Orto, L. (1955). Biochemical and nutritional effects of lysine-reinforced diets The American journal of clinical nutrition, 3(2), 121–128.

Albanese, A. A., Higgons, P. A., Hyde, G. M., & Orto, L. (1956). Lysine and tryptophan content of proteins and their utilization for human growth The American journal of clinical nutrition, 4(2), 161–168.

Alberts, B., Johnson, A., Lewis, J., Raff, M., Roberts, K., and Walter, P. (2008). Control of Gene Expression. In Molecular Biology of the Cell, M. Anderson, and S. Granum, eds. (New York, Garland Science, Taylor and Francis Group), pp. 411-499.

Altun, Z.F. and Hall, D.H. (2008). Handbook of C. elegans Anatomy. In WormAtlas. http://www.wormatlas.org/hermaphrodite/hermaphroditehomepage.htm

Amling, M., Priemel, M., Holzmann, T., Chapin, K., Rueger, J. M., Baron, R., & Demay, M. B. (1999). Rescue of the skeletal phenotype of vitamin D receptor-ablated mice in the setting of normal mineral ion homeostasis: formal histomorphometric and biomechanical analyses Endocrinology, 140(11), 4982–4987.

Angelo, G., & Van Gilst, M. R. (2009). Starvation protects germline stem cells and extends reproductive longevity in C. elegans Science (New York, N.Y.), 326(5955), 954–958.

Avery L, Horvitz HR (1990). Effects of starvation and neuroactive drugs on feeding in Caenorhabditis elegans. J Exp Zool. Mar;253(3):263-70.

Antebi, A. (2006). Nuclear hormone receptors in C. elegans. WormBook. doi:10.1895/wormbook.1.64.1

Benoit G, Malewicz M, Perlmann T. (2004). Digging deep into the pockets of orphan nuclear receptors: insights from structural studies. Trends Cell Biol. Jul;14(7):369-76.

Bolz, D. D., Tenor, J. L., & Aballay, A. (2010). A conserved PMK-1/p38 MAPK is required in caenorhabditis elegans tissue-specific immune response to Yersinia pestis infection The Journal of biological chemistry, 285(14), 10832–10840. doi:10.1074/jbc.M109.091629

Bookout, A. L., Jeong, Y., Downes, M., Yu, R. T., Evans, R. M., & Mangelsdorf, D. J. (2006). Anatomical profiling of nuclear receptor expression reveals a hierarchical transcriptional network Cell, 126(4), 789–799. doi:10.1016/j.cell.2006.06.049

Bouillon R, Van Cromphaut S, Carmeliet G. (2003) Intestinal calcium absorption: Molecular vitamin D mediated mechanisms. J Cell Biochem.;88:332–339.

Brenner, S. (1974). The genetics of Caenorhabditis elegans. Genetics 77, 71-94.

Brooks KK, Liang B, Watts JL, 2009 The Influence of Bacterial Diet on Fat Storage in C. elegans. PLoS ONE 4(10): e7545. doi:10.1371/journal.pone.0007545

Bunce CM., Campbell MJ. (2010) Nuclear receptors, an introductory view. Nuclear Receptors, Proteins and Cell Regulation 8, Ed. Bunce CM., Campbell MJ.

Capowski, E. E., Martin, P., Garvin, C., & Strome, S. (1991). Identification of grandchildless loci whose products are required for normal germ-line development in the nematode Caenorhabditis elegans Genetics, 129(4), 1061–1072.

Chawla, A., Repa, J. J., Evans, R. M., & Mangelsdorf, D. J. (2001). Nuclear receptors and lipid physiology: opening the X-files Science (New York, N.Y.), 294(5548), 1866–1870. doi:10.1126/science.294.5548.1866

Chen WS, Manova K, Weinstein DC, Duncan SA, Plump AS, Prezioso VR, Bachvarova RF, Daraell JE Jr (1994) Disruption of the HNF-4 gene, expressed in visceral endoderm, leads to cell death in embryonic ectoderm and impaired gastrulation of mouse embryos. Genes Dev 8:2466–2477

Chitwood DJ (1999) Biochemistry and function of nematode steroids. Crit Rev Biochem Mol Biol 34: 273–284.

Cuppen, E., van der Linden, A. M., Jansen, G., & Plasterk, R. H. A. (2003). Proteins interacting with Caenorhabditis elegans Galpha subunits Comparative and functional genomics, 4(5), 479–491. doi:10.1002/cfg.318

Darby, C. (2005) Interactions with microbial pathogens WormBook, ed. The C. elegans Research Community, WormBook, doi/10.1895/ wormbook.1.21.1, http://www.wormbook.org.

de Haro, C., Méndez, R., & Santoyo, J. (1996). The eIF-2alpha kinases and the control of protein synthesis The FASEB journal : official publication of the Federation of American Societies for Experimental Biology, 10(12), 1378–1387.

Dever, T. E., & Hinnebusch, A. G. (2005). GCN2 whets the appetite for amino acids Molecular cell, 18(2), 141–142. doi:10.1016/j.molcel.2005.03.023

Dey, M., Cao, C., Dar, A. C., Tamura, T., Ozato, K., Sicheri, F., & Dever, T. E. (2005). Mechanistic link between PKR dimerization, autophosphorylation, and eIF2alpha substrate recognition Cell, 122(6), 901–913. doi:10.1016/j.cell.2005.06.041

Drummond-Barbosa, D., & Spradling, A. C. (2001). Stem cells and their progeny respond to nutritional changes during Drosophila oogenesis Developmental biology, 231(1), 265–278. doi:10.1006/dbio.2000.0135

Eckmann, C. R., Kraemer, B., Wickens, M., & Kimble, J. (2002). GLD-3, a bicaudal-C homolog that inhibits FBF to control germline sex determination in C. elegans Developmental cell, 3(5), 697–710.

Eckmann, C. R., Rammelt, C., & Wahle, E. (2010). Control of poly(A) tail length. Wiley Interdisciplinary Reviews: RNA, 2(3), 348–361. doi:10.1002/wrna.56

Finn, R.D, Mistry, J., Tate J., Coggill P., Heger A., J.E. Pollington, O.L. Gavin, P. Gunesekaran, G. Ceric, K. Forslund, L. Holm, E.L. Sonnhammer, Eddy S.R.,Bateman A. (2010). The Pfam protein families database: Nucleic Acids Research Database Issue 38:D211-222

Fox PM, Vought VE, Hanazawa M, Lee MH, Maine EM, Schedl T. (2011). Cyclin E and CDK-2 regulate proliferative cell fate and cell cycle progression in the C. elegans germline. Development. Jun;138(11):2223-34.

Gallo, C. M., Wang, J. T., Motegi, F., & Seydoux, G. (2010). Cytoplasmic partitioning of P granule components is not required to specify the germline in C. elegans Science (New York, N.Y.), 330(6011), 1685–1689. doi:10.1126/science.1193697

Gebauer, F., & Hentze, M. W. (2004). Molecular mechanisms of translational control Nature reviews. Molecular cell biology, 5(10), 827–835. doi:10.1038/nrm1488

Gilbert S. (2006). Developmental Biology. 8th Ed. Sinauer Associates Inc. USA

Ghosh, D., & Seydoux, G. (2008). Inhibition of transcription by the Caenorhabditis elegans germline protein PIE-1: genetic evidence for distinct mechanisms targeting initiation and elongation Genetics, 178(1), 235–243. doi:10.1534/genetics.107.083212

Green RA, Kao HL, Audhya A, Arur S, Mayers JR, Fridolfsson HN, Schulman M, Schloissnig S, Niessen S, Laband K, Wang S, Starr DA, Hyman AA, Schedl T, Desai A, Piano F, Gunsalus KC, Oegema K. (2011) A high-resolution C. elegans essential gene network based on phenotypic profiling of a complex tissue. Cell. Apr 29;145(3):470-82.

Greenstein, D. (2005). Control of oocyte meiotic maturation and fertilization. WormBook, 1-12.

Gruidl, M. E., Smith, P. A., Kuznicki, K. A., McCrone, J. S., Kirchner, J., Roussell, D. L., Strome, S., et al. (1996). Multiple potential germ-line helicases are components of the germ-line-specific P granules of Caenorhabditis elegans Proceedings of the National Academy of Sciences of the United States of America, 93(24), 13837–13842.

Henderson ST, Gao D, Lambie EJ, Kimble J. (1994). lag-2 may encode a signaling ligand for the GLP-1 and LIN-12 receptors of C. elegans. Development 120:2913–24

Hirsh, D., Oppenheim, D., and Klass, M. (1976). Development of the reproductive system of Caenorhabditis elegans. Dev Biol 49, 200-219.

Hieb WF, Rothstein M (1968) Sterol requirement for reproduction of a free- living nematode. Science 160: 778–780.

Horvitz, H. R., Chalfie, M., Trent, C., Sulston, J. E., & Evans, P. D. (1982). Serotonin and octopamine in the nematode Caenorhabditis elegans Science (New York, N.Y.), 216(4549), 1012–1014.

Hubbard, E.J.A., and Greenstein, D. (2005). Introduction to the germ line, Vol September 1, 2005.

Inagaki, T., Moschetta, A., Lee, Y.-K., Peng, L., Zhao, G., Downes, M., Yu, R. T., et al. (2006). Regulation of antibacterial defense in the small intestine by the nuclear bile acid receptor Proceedings of the National Academy of Sciences of the United States of America, 103(10), 3920–3925. doi:10.1073/pnas.0509592103

Jaramillo-Lambert A, Ellefson M, Villeneuve AM, Engebrecht J. (2007) Differential timing of S phases, X chromosome replication, and meiotic prophase in the C. elegans germ line. Dev Biol. Aug 1;308(1):206-21

Johnson, R. W., Liu, L. Y., Hanna-Rose, W., & Chamberlin, H. M. (2009). The Caenorhabditis elegans heterochronic gene lin-14 coordinates temporal progression and maturation in the egg-laying system. (D. Fernig, S. L. Mansour, & D. M. Ornitz, Eds.)Developmental dynamics : an official publication of the American Association of Anatomists, 238(2), 394–404. doi:10.1002/dvdy.21837

Johnstone, O., & Lasko, P. (2001). Translational regulation and RNA localization in Drosophila oocytes and embryos Annual review of genetics, 35, 365–406. doi:10.1146/annurev.genet.35.102401.090756

Jones, A. R., Francis, R., & Schedl, T. (1996). GLD-1, a cytoplasmic protein essential for oocyte differentiation, shows stage- and sex-specific expression during Caenorhabditis elegans germline development Developmental biology, 180(1), 165–183. doi:10.1006/dbio.1996.0293

Juge F, Zaessinger S, Temme C, Wahle E, Simonelig M. Control of poly(A) polymerase level is essential to cytoplasmic polyadenylation and early development in Drosophila. EMBOJ 2002, 21:6603 – 6613.

Jung, S.Y., Malovannaya, A., Wei, J., O'Malley, B.W., and Qin, J. (2005). Proteomic analysis of steady-state nuclear hormone receptor coactivator complexes. Mol. Endocrinol. 19, 2451–2465.

Hara, K., Yonezawa, K., Weng, Q. P., Kozlowski, M. T., Belham, C., & Avruch, J. (1998). Amino acid sufficiency and mTOR regulate p70 S6 kinase and eIF-4E BP1 through a common effector mechanism The Journal of biological chemistry, 273(23), 14484–14494.

Hsu, H.-J., LaFever, L., & Drummond-Barbosa, D. (2008). Diet controls normal and tumorous germline stem cells via insulin-dependent and -independent mechanisms in Drosophila Developmental biology, 313(2), 700–712. doi:10.1016/j.ydbio.2007.11.006

Irazoqui, J. E., Troemel, E. R., Feinbaum, R. L., Luhachack, L. G., Cezairliyan, B. O., & Ausubel, F. M. (2010). Distinct pathogenesis and host responses during infection of C. elegans by P. aeruginosa and S. aureus PLoS pathogens, 6,

Kalogeropoulos N, Christoforou C, Green AJ, Gill S, Ashcroft NR. (2004) chk-1 is an essential gene and is required for an S-M checkpoint during early embryogenesis. Cell Cycle. Sep;3(9):1196-200.

Karashima, T., Sugimoto, A., & Yamamoto, M. (2000). Caenorhabditis elegans homologue of the human azoospermia factor DAZ is required for oogenesis but not for spermatogenesis Development (Cambridge, England), 127(5), 1069–1079.

Kashiwabara S, Noguchi J, Zhuang T, Ohmura K, HondaA, Sugiura S, Miyamoto K, Takahashi S, Inoue K, Ogura A, et al. Regulation of spermatogen- esis by testis-specific, cytoplasmic poly(A) polymerase TPAP. Science 2002, 298:1999–2002.

Keller RW, Ku¨ hn U, Aragon M, Bornikova L, Wahle E,Bear DG. The nuclear poly(A) binding pro- tein, PABP2, forms an oligomeric particle covering the length of the poly(A) tail. J Mol Biol 2000, 297:569 – 583.

Kim D. (2008) Studying host-pathogen interactions and innate immunity in Caenorhabditis elegans. Dis Model Mech. Nov-Dec;1(4-5):205-8.

Kim KW, Nykamp K, Suh N, Bachorik JL, Wang L, Kimble J. (2009). Antagonism between GLD-2 binding partners controls gamete sex. Dev Cell. May;16(5):723-33.

Kimball, S. R. & Jefferson, L. S. (2000). Regulation of initiation by amino acids. Translational control of gene expression. Ed. Sonenberg, N., Hershey, J.W.B., Mathews, B. Cold Spring Harbor Laboratory Press.

Kimble, J., and Crittenden, S.L. (2005). Germline proliferation and its control. WormBook, 1-14.

Kimble, J., and Crittenden, S.L. (2007). Controls of germline stem cells, entry into meiosis, and the sperm/oocyte decision in Caenorhabditis elegans. Annu Rev Cell Dev Biol 23, 405-433.

Kimble, J., and Hirsh, D. (1979). The postembryonic cell lineages of the hermaphrodite and male gonads in Caenorhabditis elegans. Dev Biol 70, 396-417.

Kimble, J.E., and White, J.G. (1981). On the control of germ cell development in Caenorhabditis elegans. Dev Biol 81, 208-219.

Korta, D. Z., & Hubbard, E. J. A. (2010). Soma-germline interactions that influence germline proliferation in Caenorhabditis elegans Developmental dynamics : an official publication of the American Association of Anatomists, 239(5), 1449–1459. doi:10.1002/dvdy.22268

Kraemer, B., Crittenden, S., Gallegos, M., Moulder, G., Barstead, R., Kimble, J. and Wickens, M. (1999). NANOS-3 and FBF proteins physically interact to control the sperm-oocyte switch in Caenorhabditis elegans. Curr Biol 9, 1009-18.

Kuersten, S., & Goodwin, E. B. (2003). The power of the 3' UTR: translational control and development. Nature reviews. Genetics, 4(8), 626–637. doi:10.1038/nrg1125

LaFever, L., & Drummond-Barbosa, D. (2005). Direct control of germline stem cell division and cyst growth by neural insulin in Drosophila Science (New York, N.Y.), 309(5737), 1071–1073. doi:10.1126/science.1111410

Lamont, L. B., Crittenden, S. L., Bernstein, D., Wickens, M., & Kimble, J. (2004). FBF-1 and FBF-2 regulate the size of the mitotic region in the C. elegans germline Developmental cell, 7(5), 697–707. doi:10.1016/j.devcel.2004.09.013

Lindley, K. M., Su, J. L., Hodges, P. K., Wisely, G. B., Bledsoe, R. K., Condreay, J. P., Winegar, D. A., et al. (2000). Production of monoclonal antibodies using recombinant baculovirus displaying gp64-fusion proteins Journal of immunological methods, 234(1-2), 123–135.

Lodish H., Berk A., Zipursky SL, Matsudaira P., Baltimore D., Darnell J. (2000) Molecular Cell Biology, 4th edition. New York: W. H. Freeman; 2000.

Loginova, L. I. Manuilova V. P. and Tolstikov V. P. (1974). Content of free amino acids in peptone and the dynamics of their consumption in the microbiological synthesis of dextran. Pharmaceutical Chemistry Journal Volume 8, Number 4, 249-251

Lonard, D. M., & O'malley, B. W. (2006). The expanding cosmos of nuclear receptor coactivators Cell, 125(3), 411–414. doi:10.1016/j.cell.2006.04.021

Lonard, D. M., & O'malley, B. W. (2007). Nuclear receptor coregulators: judges, juries, and executioners of cellular regulation Molecular cell, 27(5), 691–700. doi:10.1016/j.molcel.2007.08.012

Luitjens, C., Gallegos M., Kraemer B., Kimble J., Wickens M. (2000). CPEB proteins control two key steps in spermatogenesis in C. elegans. Genes & development, 14(20), 2596–2609. doi:10.1101/gad.831700

Mangelsdorf, D. J., Thummel, C., Beato, M., Herrlich, P., Schütz, G., Umesono, K., Blumberg, B., et al. (1995). The nuclear receptor superfamily: the second decade Cell, 83(6), 835–839.

Mangelsdorf DJ, Reiter R, Auwerx J, Hamakubo T, Kodama T. (2002) The generation of monoclonal antibodies against human peroxisome proliferator-activated receptors (PPARs). J Atheroscler Thromb. 2002;9(5):233-42.

Markov G., Bonneton F., Laudet V. (2010) What does evolution teach us about Nuclear Receptors? Nuclear Receptors, Proteins and Cell Regulation 8, Ed. Bunce CM., Campbell MJ.

Mathews, M. B., Sonenberg, N., Hershey, J.W.B. (2007). Origins and principles of translational control. Translational control in Biology and Medicine. Ed. Mathews, M. B., Sonenberg, N., Hershey, J.W.B., Mathews, B. Cold Spring Harbor Laboratory Press.

Matyash, V., Entchev, E. V., Mende, F., Wilsch-Bräuninger, M., Thiele, C., Schmidt, A. W., Knölker, H.-J., et al. (2004). Sterol-derived hormone(s) controls entry into diapause in Caenorhabditis elegans by consecutive activation of DAF-12 and DAF-16 PLoS biology, 2(10), e280. doi:10.1371/journal.pbio.0020280

Meissner, B. (2004). Deletion of the Intestinal Peptide Transporter Affects Insulin and TOR Signaling in Caenorhabditis elegans. Journal of Biological Chemistry, 279(35), 36739–36745. doi:10.1074/jbc.M403415200

Merlet, J., Burger, J., Tavernier, N., Richaudeau, B., Gomes, J.-E., & Pintard, L. (2010). The CRL2LRR-1 ubiquitin ligase regulates cell cycle progression during C. elegans development Development (Cambridge, England), 137(22), 3857–3866. doi:10.1242/dev.054866

Michaelson, D., Korta, D. Z., Capua, Y., & Hubbard, E. J. A. (2010). Insulin signaling promotes germline proliferation in C. elegans Development (Cambridge, England), 137(4), 671–680. doi:10.1242/dev.042523

Narbonne, P., & Roy, R. (2006). Inhibition of germline proliferation during C. elegans dauer development requires PTEN, LKB1 and AMPK signalling Development (Cambridge, England), 133(4), 611–619. doi:10.1242/dev.02232

Prasanth KV, Prasanth SG, Xuan Z, Hearn S, Freier SM, Bennett CF, Zhang MQ, Spector DL. (2005) Regulating gene expression through RNA nuclear retention. Cell. Oct 21;123(2):249-63.

Proud, C. G. (2007). Signalling to translation: how signal transduction pathways control the protein synthetic machinery. The Biochemical journal, 403(2), 217–234. doi:10.1042/BJ20070024

Radford, H. E., Meijer, H. A. and de Moor, C. H. (2008). Translational control by cytoplasmic polyadenylation in Xenopus oocytes. Biochim Biophys Acta 1779, 217-29.

Reinke, S. N., Hu, X., Sykes, B. D., & Lemire, B. D. (2010). Caenorhabditis elegans diet significantly affects metabolic profile, mitochondrial DNA levels, lifespan and brood size Molecular genetics and metabolism, 100(3), 274–282. doi:10.1016/j.ymgme.2010.03.013

Robinson-Rechavi M. and Laudet V. (2003). Bioinformatics of Nuclear Receptors. Methods in Enzymology Vol 364. Nuclear Receptors. Ed. Russell & Mangeldorf DJ.

Robinson-Rechavi, M., Maina, C. V., Gissendanner, C. R., Laudet, V., & Sluder, A. (2005). Explosive lineage-specific expansion of the orphan nuclear receptor HNF4 in nematodes Journal of molecular evolution, 60(5), 577–586. doi:10.1007/s00239-004-0175-8

Rybarska, A., Harterink, M., Jedamzik, B., Kupinski, A. P., Schmid, M., & Eckmann, C. R. (2009). GLS-1, a novel P granule component, modulates a network of conserved RNA regulators to influence germ cell fate decisions PLoS genetics, 5(5), e1000494. doi:10.1371/journal.pgen.1000494

Schmid, M., Küchler, B., & Eckmann, C. R. (2009). Two conserved regulatory cytoplasmic poly(A) polymerases, GLD-4 and GLD-2, regulate meiotic progression in C. elegans Genes & development, 23(7), 824–836. doi:10.1101/gad.494009

Schmidt, D. R., & Mangelsdorf, D. J. (2008). Nuclear receptors of the enteric tract: guarding the frontier Nutrition reviews, 66(10 Suppl 2), S88–97. doi:10.1111/j.1753-4887.2008.00092.

Seydoux, G., & Braun, R. E. (2006). Pathway to totipotency: lessons from germ cells Cell, 127(5), 891–904. doi:10.1016/j.cell.2006.11.016

Shih DQ, Dansky HM, Fleisher M, Assmann G, Fajans SS, Stoffel M (2000) Genotype/phenotype relationships in HNF-4alpha/ MODY1: haploinsufficiency is associated with reduced apoli- poprotein (AII), apolipoprotein (CIII), lipoprotein(a), and tri- glyceride levels. Diabetes 49:832–837

Sijen, T., Fleenor, J., Simmer, F., Thijssen, K. L., Parrish, S., Timmons, L., Plasterk, R. H., et al. (2001). On the role of RNA amplification in dsRNA-triggered gene silencing Cell, 107(4), 465–476.

Sluder, A. E., Mathews, S. W., Hough, D., Yin, V. P., & Maina, C. V. (1999). The nuclear receptor superfamily has undergone extensive proliferation and diversification in nematodes Genome research, 9(2), 103–120.

Strome, S., and Lehmann, R. (2007). Germ versus soma decisions: lessons from flies and worms. Science 316, 392-393.

Strome, S. (2005). Specification of the germ line. WormBook. doi:10.1895/wormbook.1.9.1

Sulston, J.E., Schierenberg, E., White, J.G., and Thomson, J.N. (1983). The embryonic cell lineage of the nematode Caenorhabditis elegans. Dev Biol 100, 64-119.

Sze, J. Y., Victor, M., Loer, C., Shi, Y., & Ruvkun, G. (2000). Food and metabolic signalling defects in a Caenorhabditis elegans serotonin-synthesis mutant Nature, 403(6769), 560–564. doi:10.1038/35000609

Tanaka T, Takeno T, Watanabe Y, Uchiyama Y, Murakami T, Yamashita H, Suzuki A, Aoi R, Iwanari H, Jiang SY, Naito M, Tachibana K, Doi T, Shulman AI,

Tax FE, Yeargers JJ, Thomas JH. (1994). Sequence of C. elegans lag-2 reveals a cell-signaling domain shared with Delta and Serrate of Drosophila. Nature 368:150–54

Thompson, B., Wickens, M., Kimble, J. (2007). Translational control in development. Ed. Mathews, M. B., Sonenberg, N., Hershey, J.W.B., Mathews, B. Cold Spring Harbor Laboratory Press.

Timmons, L., Court, D. L., & Fire, A. (2001). Ingestion of bacterially expressed dsRNAs can produce specific and potent genetic interference in Caenorhabditis elegans Gene, 263(1-2), 103–112.

Taubert S, Ward JD, Yamamoto KR. (2011). Nuclear hormone receptors in nematodes: evolution and function. Mol Cell Endocrinol. Mar 1;334(1-2):49-55.

Troemel, E. R., Chu, S. W., Reinke, V., Lee, S. S., Ausubel, F. M., & Kim, D. H. (2006). p38 MAPK Regulates Expression of Immune Response Genes and Contributes to Longevity in C. elegans. PLoS genetics, 2(11), e183. doi:10.1371/journal.pgen.0020183.st007

Verdaasdonk JS, Bloom K. (2011) Centromeres: unique chromatin structures that drive chromosome segregation. Nat Rev Mol Cell Biol. May;12(5):320-32.

Vanacova S, Wolf J, Martin G, Blank D, Dettwiler S, Friedlein A, Langen H, Keith G, Keller W. A new yeast poly(A) polymerase complex involved in RNA quality control. PLoS Biol 2005, 3:e189.

Vogel BE, Wagner C, Paterson JM, Xu X, Yanowitz JL (2011) An extracellular matrix protein prevents cytokinesis failure and aneuploidy in the C. elegans germline. Cell Cycle. 2011 Jun 15;10(12):1916-20.

Wang, L., Eckmann, C.R., Kadyk, L.C., Wickens, M., and Kimble, J. (2002). A regulatory cytoplasmic poly(A) polymerase in Caenorhabditis elegans. Nature 419, 312-316.

Wisely GB, Miller AB, Davis RG, Thornquest AD Jr, Johnson R, Spitzer T, Sefler A, Shearer B, Moore JT, Miller AB, Willson TM, Williams SP. (2002) Hepatocyte nuclear factor 4 is a transcription factor that constitutively binds fatty acids. Structure. Sep;10(9):1225-34.

Wong D, Bazopoulou D, Pujol N, Tavernarakis N, Ewbank JJ. (2007) Genome-wide investigation reveals pathogen-specific and shared signatures in the response of Caenorhabditis elegans to infection. Genome Biol.;8(9):R194.

Xu X, Vogel BE. (2011) A secreted protein promotes cleavage furrow maturation during cytokinesis. Curr Biol. Jan 25;21(2):114-9.

Zetka, M. C., Kawasaki, I., Strome, S., & Müller, F. (1999). Synapsis and chiasma formation in Caenorhabditis elegans require HIM-3, a meiotic chromosome core component that functions in chromosome segregation Genes & development, 13(17), 2258–2270.

Zhang, B., Gallegos, M., Puoti, A., Durkin, E., Fields, S., Kimble, J. and Wickens, M. P. (1997). A conserved RNA-binding protein that regulates sexual fates in the C. elegans hermaphrodite germ line. Nature 390, 477-84.

Zhang, X.-K. (2007). Targeting Nur77 translocation Expert opinion on therapeutic targets, 11(1), 69–79. doi:10.1517/14728222.11.1.69

Zhang, Z., Burch, P. E., Cooney, A. J., Lanz, R. B., Pereira, F. A., Wu, J., Gibbs, R. A., et al. (2004). Genomic analysis of the nuclear receptor family: new insights into structure, regulation, and evolution from the rat genome Genome research, 14(4), 580–590. doi:10.1101/gr.2160004

8. APPENDIX

1. GENERATION OF ANTI-NHR-114 ANTIBODIES

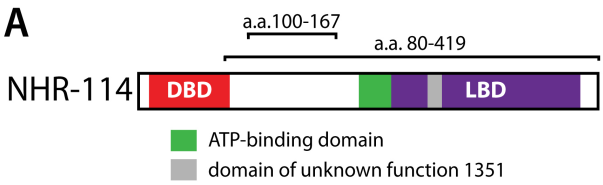

Antigens	Antibodies (sera)	Antigenicity (anti-)
MBP::NHR-114(100-167)	**Rabbit, polyclonal**	
	rb. G5CA	NHR-114
	rb.4FD8	NHR-114
	rb. G5CA affinity purified: AP, AE, BE, HS	NHR-114
HIS::NHR-114(80-419)	**Rabbit, polyclonal**	
	rb. 3250	NHR-17, -68, -114
	rb. 5255	NHR-17, -68, -114
	Mouse, monoclonal	
	C22-1, C22-8, D57-2, D57-1, A23-1, A23-2, A23-3, C48	NHR-114
	B54-1, A67-7-t, B36-6t, A43-5	NHR-17, -114
	D03-1, C52-2, B36-8t	NHR-17, -68, -114

Table 1 Summary of all anti-NHR-114 antibodies produced in this thesis
A) Diagram depicts the amino acids (a.a.) residues used to produce two different NHR-114 antigens. Antigens were expressed and purified from bacteria. Rabitts (rb.) or mice (mo.) were immunized with the respective antigen, see Materials and Methods. Table: Antibodies were tested by western blotting using wild type and *nhr-114(gk849)* worms extracts; and by immunostaining of extruded germ lines of adult hermaphrodites. None of the antibodies recognized endogenous protein in either method. However, different antibodies recognize heterologous expressed NHR-114 protein. Specificity was determined by western blotting using NHR-10, NHR-17, NHR-68 or NHR-114 recombinant proteins expressed in Sf9 insect cells.

2. Preliminary analysis of a germline expressed NHR-114::GFP fusion protein

A fosmid containing the germline specifically expressed *glh-1* gene was used to replace the glh-1 ORF with the *nhr-114* ORF. The gfp ORF containing the nhr-114 3'UTR was cloned downstream of nhr-114 ORF. The resulting fosmid (*glh-1* promoter (Pglh-1):: *nhr-114* ORF::gfp ORF::*nhr-114* 3'UTR) and the selection marker *unc-119* gene were bombarded into *unc-119* mutant animals, which are paralyzed animals. Effectively bombarded animals (moving animals) where then screened live for GFP signal in the germ line. From preliminary analysis: DIC image of germ line (top image), fluorescent image of same germ line (bottom image) shows cytoplasmic GFP signal in all germ cells.

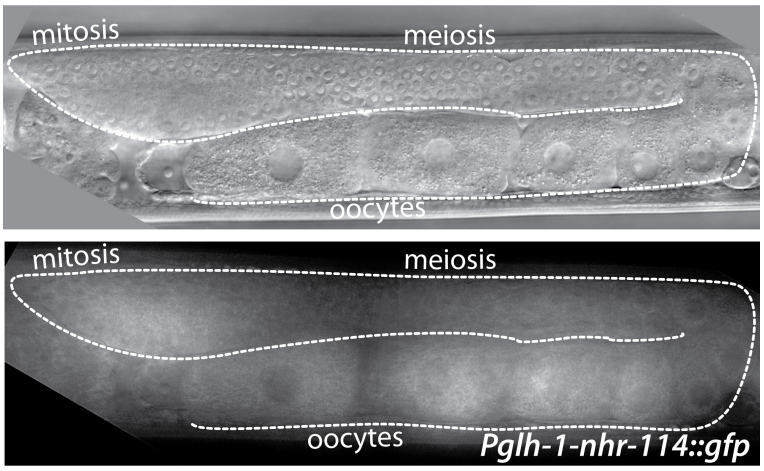

4. *him-8* background and *nhr-114*

This work has shown that male germline development requires *nhr-114* function for proliferation of the mitotic cells and proper germ cell divisions. In addition, this analysis threw an observation: the penetrance of *nhr-114* phenotypes correlates negatively with *him-8* mutant background. Neither *him-8;nhr-114(gk849)* males nor females show *nhr-114* phenotypes or sterility, respectively (n>100), but only mild underproliferation. Consistent with that observation, less than half of *him-8;nhr-114*(RNAi) hermaphrodites are sterile, in contrast to >80% in *nhr-114* (RNAi).

HIM-8 protein is required for meiotic pairing centers of X chromosomes, but not autosomes. In *him-8* absence, autosomes show both RAD-51 foci and excess crossovers, which are indicative of an activated cell cycle checkpoint (HUS-1-independent: not activated by DNA damage) (MacQueen *et al.* 2005). Considering the cell division defects and the aberrant chromatin configurations in *nhr-114* mutants, it raises the question if the activated cell cycle checkpoint in the *him-8* background ameliorate *nhr-114* defects and therefore reduce sterility.

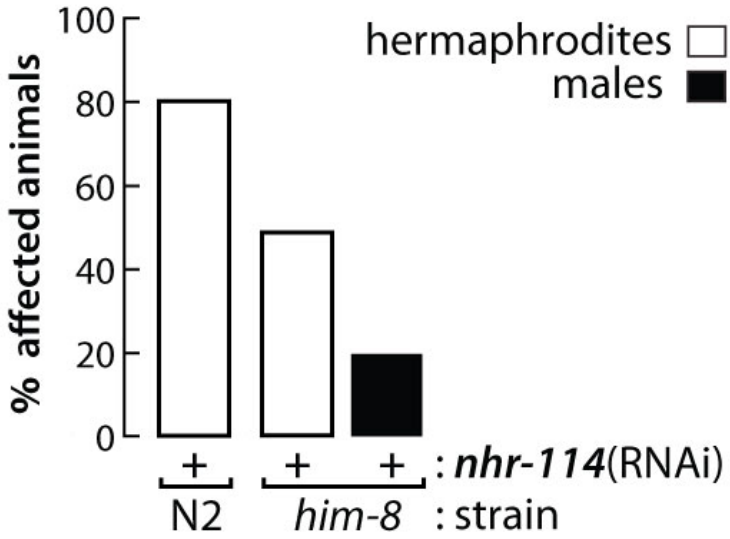

3. Amino acid sequence alignment of the NHR-114 clade and NHR-17

Invariant amino acids are shown in red, highly conserved in blue, and variable in black.

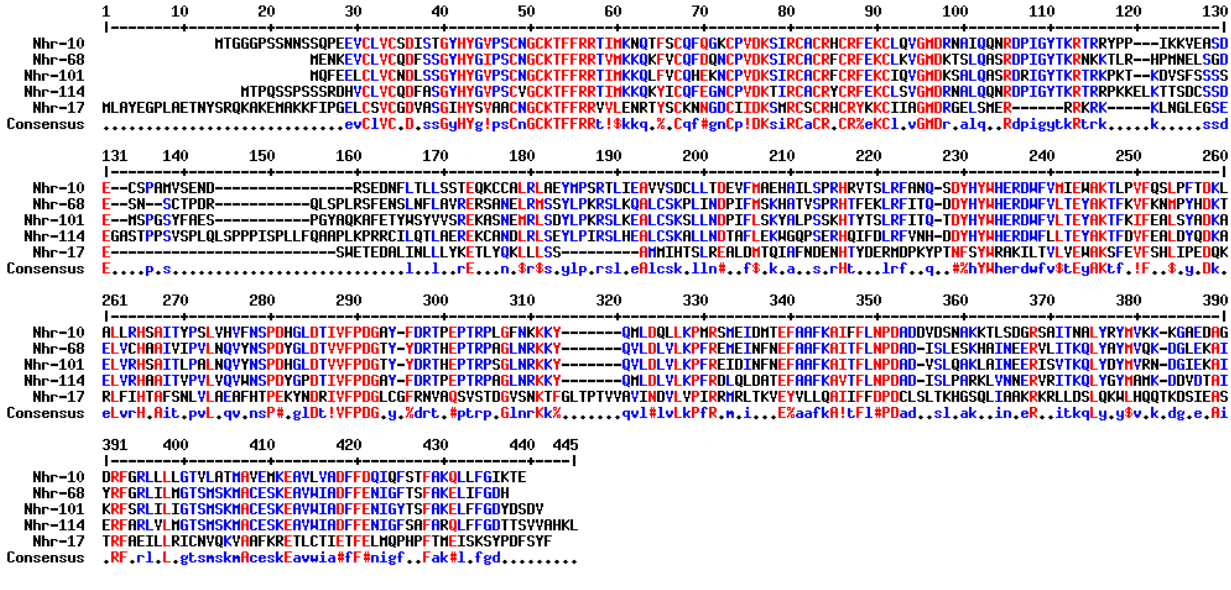

DECLARATION OF OATH

I herewith declare that I have produced this thesis without the prohibited assistance of third parties and without making use of aids other than those specified; notions taken over directly or indirectly from other sources have been identified as such. This thesis has not previously been presented in identical or similar form to any other German or foreign examination board. The thesis work was conducted from October 1st 2007 to September 30th 2011 under the supervision of Christian Eckmann, PhD, at the Max Planck Institute for Molecular Cell Biology and Genetics.

Hiermit versichere ich, dass ich die vorliegende Arbeit ohne unzulässige Hilfe Dritter und ohne Benutzung anderer als der angegebenen Hilfsmittel angefertigt habe; die aus fremden Quellen direkt oder indirekt übernommenen Gedanken sind als solche kenntlich gemacht. Die Arbeit wurde bisher weder im Inland noch im Ausland in gleicher oder ähnlicher Form einer anderen Prüfungsbehörde vorgelegt. Die Dissertation wurde von Dr. Christian R. Eckmann, Max-Planck-Institut für Molekulare Zellbiologie und Genetik (MPI-CBG), Dresden, betreut und im Zeitraum vom 1. Oktober 2007 bis 30. September 2011 verfasst.

Meine Person betreffend erkläre ich hiermit, dass keine früheren erfolglosen Promotionsverfahren stattgefunden haben.

Ich erkenne die Promotionsordnung der Fakultät für Mathematik und Naturwissen-schaften, Technische Universität Dresden an.

Xicotencatl Gracida Canales Dresden, den 24. Oktober 2011